DOCTOR OF PHILOSOPHY

Targeting c-Met for therapy

Wong, Julin

Award date:
2011

DOCTOR OF PHILOSOPHY

Targeting c-Met for therapy

Julin Wong

2011

University of Dundee

TARGETING C-MET FOR THERAPY

Julin Shuxian Wong

P.h.D

University of Dundee

JULY 2011

TABLE OF CONTENTS

ACKNOWLEDGEMENTS

My very first acknowledgment would be to THE BOSS (David Lane). Without David's support, I would never have embarked on this journey. David has given me this opportunity to improve myself as a scientist and to develop myself as an individual. What I am today, the way I think, have all been attributed to this life-changing journey. I had experienced so much, exposed to a variety of cultures, met many outstanding scientists and forged unbelievably strong friendships that would spread all around the world. Thank you David!

I would also like to include in this acknowledgement my supervisor Emma Warbrick. The amount of guidance, support, understanding and patience you have given me was infinite! The numerous blunders, my Singlish-written thesis, the ERK nightmare! Without you, there is no PhD thesis! Emma, no words can express my gratitude and appreciation to you. Thank you so much!

My project would not have be a success if it was not for everyone that helped me along the way. In particular, I would like to express my heartfelt gratitude to Dr. Jeffrey Hills, Dr. Borek Vojtesek, Michael Boylan and Pamela Robertson.

To the people in the Division of Molecular Medicine and DPL lab (Singapore and Dundee), it was a pleasure working together.

To mommy, daddy and the rest of my family members: Thank you for your support, your patience and for enduring me especially during my long periods of absence (which I am so sorry for). I have finally made it!

To my closest friends in Dundee: Helena, Sabine, Becka, Andy, Ashwat and Peter. It will never be Dundee if it was not for all of you! Thank you for all the endless fun, parties and food!

To the climbing gang: Ai Khim, Chai Hong, Dean, Effendy, Esther, Guoli, Kok Hoo and You Keat: Thank you for being there for me during the darkest days of my life. I have been gone for so long, but every time I return, you guys make me feel that I never left at all.

Finally, I would like to thank my ‘rose’ for listening to my endless complains on thesis writing, for being the only person that makes black pudding, seafood spaghetti and the only one that pushes me to write. I enjoyed the times we shared... the times we danced! Thank you.

LIST OF FIGURES

LIST OF TABLES

ABBREVIATIONS

ADCC	Antibody-dependent cell-mediated cytotoxicity
ADCP	Antibody-dependent cellular phagocytosis
α	Alpha
DABCO	1,4- Diazabicyclo-[2.2.2]octane
β	Beta
Bsab	Bispecific antibody
BSA	Bovine serum albumin
CDC	Complement-dependent cytotoxicity
CDR	Complementarily determining region
CEA	Carcinoembryonic antigen
C_{H1}	Constant region of an antibody heavy chain 1
C_{H2}	Constant region of an antibody heavy chain 2
C_{H3}	Constant region of an antibody heavy chain 3
D	Diversity segment of an antibody
DAB	Diaminobenzidine
δ	Delta antibody heavy chain
DMEM	Dulbecco's Modified Essential Medium
HACA	Human anti-chimeric antibody response
HAHA	Human anti-human antibody
HAMA	Human anti-mouse antibody response
HIV	Human immunodeficiency virus
Her2	Human epidermal growth factor receptor 2
HGF	Hepatocyte growth factor
HOS	Human osteogenic sarcoma
HRP	Horseradish peroxidise
ECL	Enhanced chemiluminescence
EFI	Elongation factor I
EGFR	Epidermal growth factor receptor

EMT	Epithelial-mesenchymal transition
ε	Epsilon antibody heavy chain
FDA	Food and Drug Administration
Fab	Fragment antigen binding
Fc	Fragment that crystallises
FCS	Fetal calf serum
FcR	Fc receptor
FDA	Food and Drug Administration
FISH	Fluorescence *in situ* hybridisation
Gab1	Growth factor receptor bound protein 2-Associated Binder 1
γ	Gamma antibody heavy chain
GFP	Green fluorescence protein
HACA	Human anti-chimeric antibody
HAHA	Human anti-human antibody
HAMA	Human anti-mouse antibody
HRP	Horseradish peroxidise
HOS	Human osteogenic sarcoma
IMB	Institute of Medical Biology
IF	Immunofluorescence
Ig	Immunoglobulin
IMAC	Immunobilised metal affinity chromatography
IP	Immunoprecipitate
IPT	Immunoglobulin-like regions in plexin and transcription factors domain
IPTG	Isopropyl-β-D-thio-galactoside
ITAM	Immunoreceptor tyrosine-based activation motif
ITIM	Immunoreceptor tyrosine-based inhibition motif
J	Joining segment of an antibody
κ	Kappa antibody light chain
K	Kringe domain of HGF

λ	Lambda antibody light chain
Mab	Monoclonal antibody
MBS	Met-binding site
MNNG	*N*-Methyl-*N'*-nitro-*N*-nitrosoguanidine
MRS	Met-related sequence domain
μ	Mu antibody heavy chain
N	N-terminal hairpin loop of HGF
OA	One-armed
PCD	Programme cell death
PBS	Phosphate-buffered saline
PDB	Protein data base
PSI	Plexin, semaphorin, integrin domain
PTB	Phospho-tyrosine-binding domain
PTEN	Phosphatase and tensin homolog
RGB	Rosetta-gami B
RG2	Rosetta-gami 2
SBP	Streptavidin binding peptide
scFv	Single chain variable fragment
SCP	Super core promoter
SDS-PAGE	Sodium dodecyl sulfate polyacrylamide gel electrophoresis
SF	Scatter factor
SH2	Src homology 2 domain
SH3	Src homology domain 3
SPH	Serine protease domain
TPR	Translocated promoter region
TPR-MET	Chimeric protein of TPR and c-Met
V	Variable segment of an antibody
VEGFR	Vascular endothelial growth factor receptor
V_H	Variable region of an antibody heavy chain

V_L	Variable region of an antibody light chain
xαβ	Extracellular c-Met alpha-beta chain
xβ	Extracellular c-Met beta chain
X-gal	5-bromo-4-chloro-3-indolyl-β-D-galactoside

DECLARATION

I certify that this thesis is the result of my own work and that I have not been assisted in its production by any other persons, except where acknowledged in the text. No part of this manuscript has been submitted for consideration for any other higher degree, and all references cited have been consulted.

Julin Wong

Phd Student

I certify that Julin Wong is the author of this thesis and has complied with the regulations of the University of Dundee appropriate to its submission.

Sir David P. Lane

Supervisor

March 2011

ABSTRACT

c-Met is a tyrosine receptor kinase which is activated by its only ligand, the hepatocyte growth factor (HGF). Activation of c-Met leads to a wide spectrum of biological activities such as motility, angiogenesis, morphogenesis, cell survival and cell regeneration. c-Met and HGF knock-out mice are embryonic lethal. During embryogenesis, c-Met is required for liver, kidney and skeletal muscles development. In adult tissues, c-Met is involved in wound healing and hepatocyte regeneration.

c-Met is abnormally activated in many tumours types. Aberrant c-Met activation was found to induce tumour development, tumour cell migration and invasion, and the worst and final step in cancer progression, metastasis. In addition, c-Met activation in cells was also shown to confer resistance to apoptosis induced by UV damage or chemotherapeutic drugs. c-Met is thus an attractive target for drug development.

This study describes the development of monoclonal antibodies against c-Met as therapeutic molecules in cancer treatment/diagnostics. Antibodies were raised against the α-chain of c-Met. 21 hybridoma clones were single-cell cloned and subjected to preliminary monoclonal antibody characterisation. 11 monoclonal antibodies were finally selected for ascites production and antibody purification. These purified antibodies were characterised by Western blotting, immunofluorescence staining, functional assays (ERK phosphorylation and cell scatter) and for their ability to recognise native c-Met by flow cytometry. Some of the anti-α-chain c-Met antibodies perform better in Western blotting and immunofluorescence staining than the presently-available commercial antibodies. The Mab 2.1 and 13.1 bind strongly to native c-Met in flow cytometry and may be potential candidates for antibody therapy and cancer diagnostics.

CHAPTER 1: INTRODUCTION

1.1: Tyrosine kinases

Protein phosphorylation is required in signalling transduction pathways to relay messages within the cell. Tyrosine kinases, characterised by their ability to phosphorylate tyrosine residues in cellular proteins, play a role in signalling pathways resulting in the activation of cellular activities such as proliferation, differentiation and motility. Tyrosine kinases are grouped into two groups: cellular tyrosine kinases and receptor tyrosine kinases. Cellular tyrosine kinases, such as c-Src and c-Abl, are soluble intracellular proteins that are activated by ligand binding followed by receptor oligomerisation. Receptor tyrosine kinases contain an extracellular ligand binding domain, a transmembrane domain and an intracellular kinase domain. Similar to the cellular tyrosine kinases, receptor tyrosine kinases are activated upon ligand binding which will result in receptor oligomerisation and activation of catalytic domain. Examples of receptor tyrosine kinases are epidermal growth factor receptor (EGFR), vascular endothelial growth factor receptor (VEGFR) and hepatocyte growth factor receptor (HGFR/c-Met).

Tyrosine kinases are tightly regulated due to their importance in the regulation of cellular processes. Constitutive activation of receptor tyrosine kinases caused by receptor overexpression or mutation often led to cancer progression in human. Tyrosine kinases inhibitors aimed to block abnormal activation of tyrosine kinases have been developed for cancer therapy. The majority of anti-cancer drugs presently approved for therapy are monoclonal antibodies and small molecules inhibitors. Therapeutic monoclonal antibodies have been particularly successful against target receptor tyrosine kinases where the monoclonal antibodies exert their anti-cancer effect by competition

binding to the ligand with the receptor. This is followed by inhibition of receptor oligomerisation. Binding of therapeutic antibodies to the receptor then causes the induction of receptor down-regulation to eliminate receptor signalling or recruitment of host's immune system to eliminate aberrant cells. Herceptin (trastuzumab) is an example of a monoclonal antibody that has been very successful in the treatment of metastatic breast cancer. Herceptin is a humanised murine monoclonal antibody developed against Her2. It binds to the Her2 on the cell surface and results in receptor internalisation (Shawver *et al.*, 2002). Small molecules inhibitors are effective against both receptor and cellular tyrosine kinases. Most small molecule inhibitors are ATP analogs which targets the catalytic domain of tyrosine kinases. Due to the structural similarity among the catalytic domain of kinases, small molecule inhibitors can have an effect on multiple kinases. Imatinib mesylate (STI571) was developed against Bcr-Abl in the treatment of CML while, gefitinib (Iressa) and erlotinib (Tarceva) were developed against EGFR to treat non-small cell lung cancer.

1.2: The c-Met tyrosine kinase receptor

1.2.1: Identification of *c-met* as an oncogene

c-met was first identified as an oncogene nearly two decades ago when a human osteogenic sarcoma (HOS) cell line was treated with the chemical carcinogen *N*-methyl-*N'*-nitro-*N*-nitrosoguanidine (MNNG) (Park *et al.*, 1986; Rong *et al.*, 1992). Hence the name 'Met'. Treatment with MNNG caused a gene rearrangement resulting in the fusion of DNA sequences from translocated promoter region (*tpr*) in chromosome 1 with *c-met* in chromosome 7 (Peruzzi and Bottaro, 2006). This gave rise to a chimeric protein (TPR-Met) consisting of an N-terminal leucine-zipper protein-protein dimerisation motif and a C-terminal kinase domain expressed from *tpr* and *c-met* respectively. TPR-Met was found to have constitutive kinase activity with transforming abilities (Jeffers, 1999). Further work then identified c-Met as a tyrosine kinase receptor that is responsible for a wide spectrum of biological activities in the cell. The c-Met ligand was later identified as a cytokine known as hepatocyte growth factor (HGF) or scatter factor (SF) (Naldini *et al.*, 1991). While c-Met is mostly expressed in cells of epithelial origin like hepatocytes, it is also expressed in endothelial cells and neurons. HGF/SF is expressed in mesenchymal cells. This receptor-ligand pair allows communication between mesenchymal and epithelial cells that is important for regulating the interactions between these two groups of cells. c-Met is required for liver and placental development during embryogenesis. In adult tissues, c-Met is required for tissue repair and hepatocyte regeneration (Birchmeier and Gherardi, 1998).

In vitro experiments show that c-Met activation can cause epithelial cell scattering, proliferation and epithelial tubulogenesis. *In vivo*, c-Met de-regulation induces tumour development, tumour cell migration and invasion, metastasis and angiogenesis

(Birchmeier *et al.*, 2003). c-Met is expressed in a wide variety of human cancers and is believed to play a critical role in the advanced, metastatic phase of the disease (Migliore and Giordano, 2008). Aberrant expression of c-Met correlates with poor disease prognosis (Appendix 1) and recently, has been demonstrated to cause acquired resistance to epidermal growth factor receptor (EGFR) inhibitors (Engelman *et al.*, 2007; Migliore and Giordano, 2008). c-Met's role in a wide spectrum of activities, involvement in tumour progression and main role in tumour metastatic progression makes c-Met an attractive target for the development of cancer therapeutics.

1.2.2: The structure of c-Met

c-Met is a 190 kD tyrosine kinase receptor made up of an extracellular α-chain which is linked by a disulphide bond to a transmembrane β-chain (Figure 1.1). c-Met is synthesised as a 170 kD single polypeptide that is proteolytically cleaved to form the α-chain and the β-chain (Tempest *et al.*, 1988). Cleavage of c-Met occurs in the post-Golgi compartment by the endoprotease, furin (Mondino *et al.*, 1991). The α-chain is 50 kD and constitutes part of the sema domain. The sema domain is a conserved domain shared by semaphorins and plexins. This domain adopts a seven-bladed beta-propeller structure which is important for homo-dimerisation. In c-Met, both the α-chain and the β-chain form the sema domain that is necessary and sufficient for receptor dimerisation and ligand binding (Kong-Beltran *et al.*, 2004).

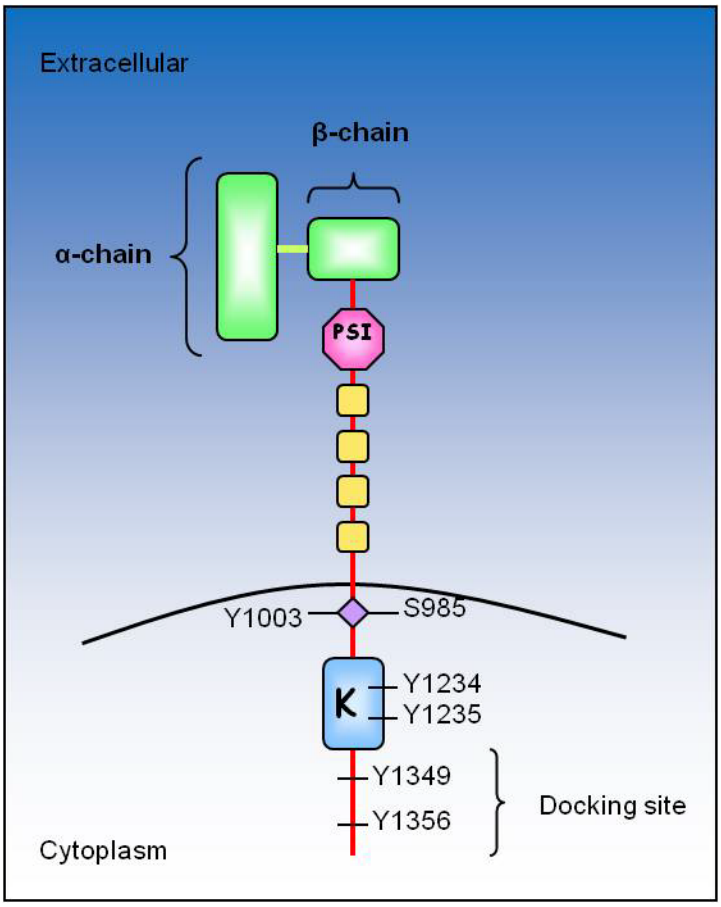

Figure 1.1: Schema of c-Met protein structure.
c-Met is a tyrosine kinase receptor made up of an α-chain and a β-chain. The sema domain (green box), PSI domain (pink octagon) and four IPT domains (orange box) are displayed on the cell surface. The α-chain is disulphide-linked to the β-chain (yellow line). The cytoplasmic domain of c-Met is made up of the juxtamembrane (purple diamond), kinase domain (blue box) and a C-terminal docking site for c-Met downstream signalling. Two negative regulatory sites (S985 and Y1003) are present in the juxtamembrane region. Activation of c-Met leads to autophosphorylation of Y1234 and Y1235. This results in a conformational change which will expose and transphosphorylate Y1349 and Y1356. pY1349 and pY1356 are then available for downstream signalling proteins to bind.

The β-chain is a 140 kD peptide consist of an extracellular domain, a transmembrane domain and a cytoplasmic domain (Figure 1.1). The extracellular portion of the β-chain makes up the reminder of the sema domain. Adjacent to the sema domain, lies the Plexin, Semaphorin, Integrin (PSI) domain, also known as the Met-related sequence (MRS) (Corso *et al.*, 2005; Kong-Beltran *et al.*, 2004). The PSI domain is a cysteine-rich motif made up of 80 amino acids which can also be found in plexins, semaphorins and integrins. Four IPT (Immunoglobulin-like regions in Plexin and Transcription

factors) repeats follow after the PSI domain (Kong-Beltran *et al.*, 2004). It is proposed that the IPT repeats might form a 'stalk' structure that supports the sema domain for ligand binding (Birchmeier *et al.*, 2003). The cytoplasmic portion of c-Met β-chain contains the juxtamembrane region followed by a kinase domain and a carboxyl-terminal tail. The carboxyl-terminal tail is essential for c-Met downstream signalling as it contains the docking site for signalling and adapter proteins that bind to c-Met.

1.2.3: The c-Met ligand

The only known ligand for c-Met is the soluble cytokine hepatocyte growth factor (HGF). HGF was independently identified as a hepatocyte growth factor and a cell motility inducer and has been called both hepatocyte growth factor and scatter factor (SF). Further experiments subsequently proved HGF and SF to be the same molecule (Naldini *et al.*, 1991). HGF is a large glycoprotein that is closely related to the blood protease precursor, plasminogen. HGF is first translated into a 92 kD inactive pro-polypeptide that is secreted into the extracellular environment. Upon secretion, HGF is cleaved to form an active heterodimer made up of an α-chain and a β-chain linked by disulphide bridges (Figure 1.2). Site-directed mutagenesis of amino acid 494 in HGF produces an uncleavable HGF. Interestingly, single chain pro-HGF is still able to bind to c-Met with the same affinity (Hartmann *et al.*, 1992), but is unable to elicit c-Met biological responses (Bardelli *et al.*, 1994; Naka *et al.*, 1992).

The α-chain of HGF contains an N-terminal hair-pin loop (N) followed by four kringle domains (K1 to K4) (Figure 1.2). The α-chain alone, containing the N-terminal hair-pin loop with the first kringle up to the third kringle, is sufficient to bind to the sema domain of c-Met. As mentioned above, the sema domain of c-Met is both necessary and

sufficient for HGF binding and dimerisation of c-Met (Kong-Beltran *et al.*, 2004; Tolbert *et al.*, 2007). HGF β-chain contains a typical serine protease domain (SPH) devoid of serine protease activity due to point mutations in the catalytic domain (Birchmeier and Gherardi, 1998). This smaller β-chain, when expressed separately, is unable to bind to c-Met, but is crucial for optimal c-Met activation (Cao *et al.*, 2001).

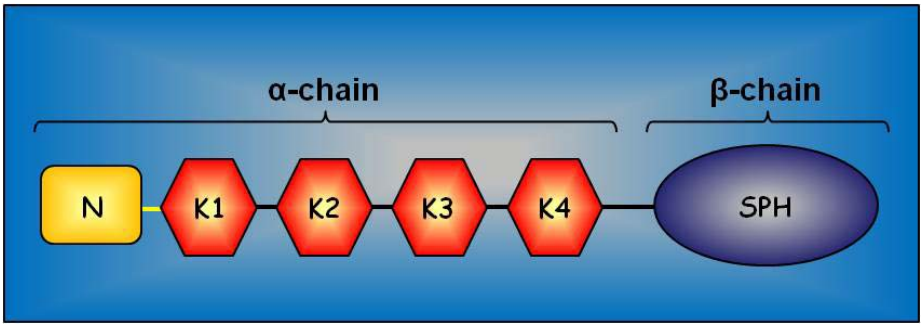

Figure 1.2: Schema of HGF protein structure.
Hepatocyte growth factor (HGF) is the only know ligand for c-Met. Pro-HGF is translated as a single chain molecule and is activated by amino acid cleavage at residue 494. This forms a heterodimer made up of an α-chain and a β-chain linked by disulphide bridges (yellow line). The α-chain is consists of an N-terminal (N) hairpin loop (orange box) and four kringle (K) domains (red octagon). A serine protease domain (SPH) devoid of serine protease activity lies in the β-chain. Adapted from Birchmeier et al., 2003.

Naturally occurring splice variants, NK1 (HGF N-terminal domain with the first kringle domain) and NK2 (HGF N-terminal domain with the first two kringle domain), generated from alternative splicing of the original transcript were found to bind to c-Met (Cioce *et al.*, 1996; Hartmann *et al.*, 1992). These splice variants were shown to partially activate/block c-Met biological activities and further work has been performed to convert these molecules into therapeutic drugs that contained full antagonist activity towards c-Met (Tolbert *et al.*, 2007).

Although the mechanism of HGF binding to c-Met remains unclear, dimerisation of HGF has been thought to promote binding to c-Met and induce c-Met dimerisation on the cell surface leading to the activation of c-Met. Dimerisation of c-Met was reported

to be required, but not sufficient, for c-Met activation by Tolbert *et al.* (2007). *In vitro* studies of the NK1 isoform binding to the sema domain of c-Met suggests that HGF binds to c-Met in a 2:2 stoichiometry, thus forming a uniform dimer complex (Tolbert *et al.*, 2007). Mutations in the four main residues (Y124, K85, D123 and N127) that lie in the NK1-NK1 dimer interface were shown to abolish c-Met dimerisation activity (Tolbert *et al.*, 2007). The details of Met-HGF interaction are still not clear and although the crystal structure has been solved, the structures are of poor quality (low resolution). In addition, the crystal structures only represent part of Met-HGF interaction as truncated proteins were used in the crystallisation. More work is thus required to fully understand the activation of c-Met by HGF.

1.2.4: Activation of c-Met

Binding of HGF/SF to c-Met activates a cascade of downstream signalling events which induce cell motility, metastasis, angiogenesis, morphogenesis, cell survival and cell regeneration. HGF/SF binds to c-Met in the presence of Mg^{2+} ions and ATP (Bardelli *et al.*, 1994; Stella and Comoglio, 1999). Upon ligand binding the c-Met receptor dimerises which results in autophosphorylation of tyrosine residues in the kinase domain (Figure 1.1). Tyrosine residues Y1230, Y1234 and Y1235 are part of a 'three tyrosine motif' that is conserved in other tyrosine kinase receptors (Bardelli *et al.*, 1994). Phosphorylation of Y1234 and Y1235 are essential for full kinase activity. *In vitro* experiments show that substitution of either Y1234 or Y1235 with phenylalanine results in as significant reduction of c-Met kinase activity. Substitution of both tyrosine residues renders the receptor completely incapable of transphosphorylation and

activation. However, substitution of Y1230 alone has no effect on c-Met kinase activity (Bardelli *et al.*, 1994).

Autophosphorylation of Y1234 and Y1235 is thought to induce a conformational change in c-Met, exposing the docking site (Y^{1349}VNVXXXY^{1356}VHV) in the carboxyl-terminal tail of c-Met (Birchmeier *et al.*, 2003). This results in transphosphorylation of tyrosine residues Y1349 and Y1356. The c-Met docking site is both necessary and sufficient to mediate c-Met signal transduction and biological activities (Rosario and Birchmeier, 2003). Mutation of both Y1349 and Y1356 results in loss of c-Met biological functions (Ponzetto *et al.*, 1994). Once Y1349 and Y1356 are phosphorylated, the docking site becomes available for recruitment of adaptor and signalling molecules. Most of these signalling and adaptor proteins contain a SH2 (Src Homology 2) domain that recognises and binds to regions containing either pY1349 or pY1356.

Recruitment of proteins to the c-Met docking site results in the activation of various signalling pathways including the AKT/PI3K, RAS/MAPK and STAT pathways. The AKT/PI3K pathway is activated by the binding of the subunit of p85, a subunit of PI3K, to the docking site of c-Met. This results in a downstream signal that leads to the inhibition of protein molecules like caspase-9 and Bad, promoting cell survival and resistance to apoptosis (Birchmeier *et al.*, 2003). c-Met is also able to induce cell cycle progression and proliferation by signalling through the RAS/MAPK pathway. Activation of the ERK/MAPK pathway occurs via the binding of the adaptor proteins Grb2/SOS complex to the c-Met docking site (Christensen *et al.*, 2003). The Grb2/SOS complex activates Ras and Raf which are part of the MAPK signalling cascade. The ERK/MAPK pathway is also capable of inducing cell migration and invasion by

activating matrix metalloproteinases and urokinase plasminogen activators. Finally, the ERK/MAPK pathway is able to induce alterations in cytoskeleton functions that are essential for cell migration. The invasive properties of c-Met are also induced through the STAT pathway. STAT3 is activated by binding to the docking site of c-Met. Once activated, STAT3 translocates to the nucleus as a transcription factor to initiate transcription of genes involved in cell invasion.

Of the many different proteins that are recruited to the docking site of c-Met, the most crucial and unique protein is the Gab1 (Growth factor receptor bound protein 2-Associated Binder 1). Gab1 null mice display the same phenotypic defects as HGF/SF null and c-Met null mice, demonstrating the importance of Gab1 in c-Met signalling (Rosario and Birchmeier, 2003). Gab1 is an adaptor protein. The direct mode of interaction between c-Met and Gab1 is through the unique Met-binding site (MBS) in Gab1. This 13 amino acid site does not resemble any classical SH2 or phospho-tyrosine-binding (PTB) domains (Birchmeier *et al.*, 2003). The MBS is not shared with other family members of the Gab family and allows direct interaction with c-Met, but not with other receptors. It is thought that the MBS site allows a more stable and prolonged interaction with c-Met, thus resulting in a prolonged Gab1 phosphorylation and activation (Birchmeier *et al*., 2003; Rosario and Birchmeier, 2003). Alternatively, Gab1 activation by c-Met may also occur indirectly by binding to Grb2. Grb2 can only bind to the region containing pY1356 of c-Met through its SH2 domain. Gab1 then binds to the SH3 domain of Grb2 to be activated. Both ways of Gab1 activation (direct or indirect activation) creates multiple binding sites for signalling molecules to bind. Such molecules include PI3K, PLCγ, SHP2 and Shc.

Aberrant c-Met activation causes a normal cell to acquire malignant phenotype. Such cells lose its adheren properties, attain fibroblast-shape and increase its motility – a behaviour characterised as epithelial-mesenchymal transition (EMT). EMT is an important morphological process during embryonic development and is recognised as a mechanism for cancer progression. Given the complex and vast number of cytoplasmic protein recruited to activated c-Met, it is a challenge to dissect the signalling pathways employed by c-Met to induce EMT. Molecular studies have shown that recruitment of PI3K and Src to activated c-Met is necessary for EMT to occur during embryonic development (Thiery, 2002). Activation of PI3K by c-Met activation leads to down regulation of E-cadherin in epithelial cells. E-cadherin is a component of adheren junction complex and is required for stable cell-cell contact. PI3K was found to activate the Rho family GTPase which causes alterations in actin polymerisation and cellular adhesion. Two Rho family GTPase, RacI and Cdc42, are required for adheren junction assembly, lamellipodia formation and cell movement (Rosario and Birchmeier, 2003). Activation of c-Met also phosphorylates β-catenin at the cell membrane. Phosphorylated β-catenin is translocated to the nucleus where it acts as a transcription factor. The Ras-ERK pathway is activated upon HGF stimulation. Activation of Ras via Grb2 (Figure 1.3), which in turn activates the PI3K and MAPK pathways, was also shown to promote cell motility by disassembling adherent junctions.

c-Met activation leads to the induction of a wide array of signalling pathways and a detailed discussion on all the signalling pathways involved is outside the scope of this report. Very often, these complex pathways interact to bring about the pleiotropic functions of c-Met. The final biological outcome of c-Met signalling depends on the

type of cells, duration and strength of signalling and interaction with other proteins on the cell surface.

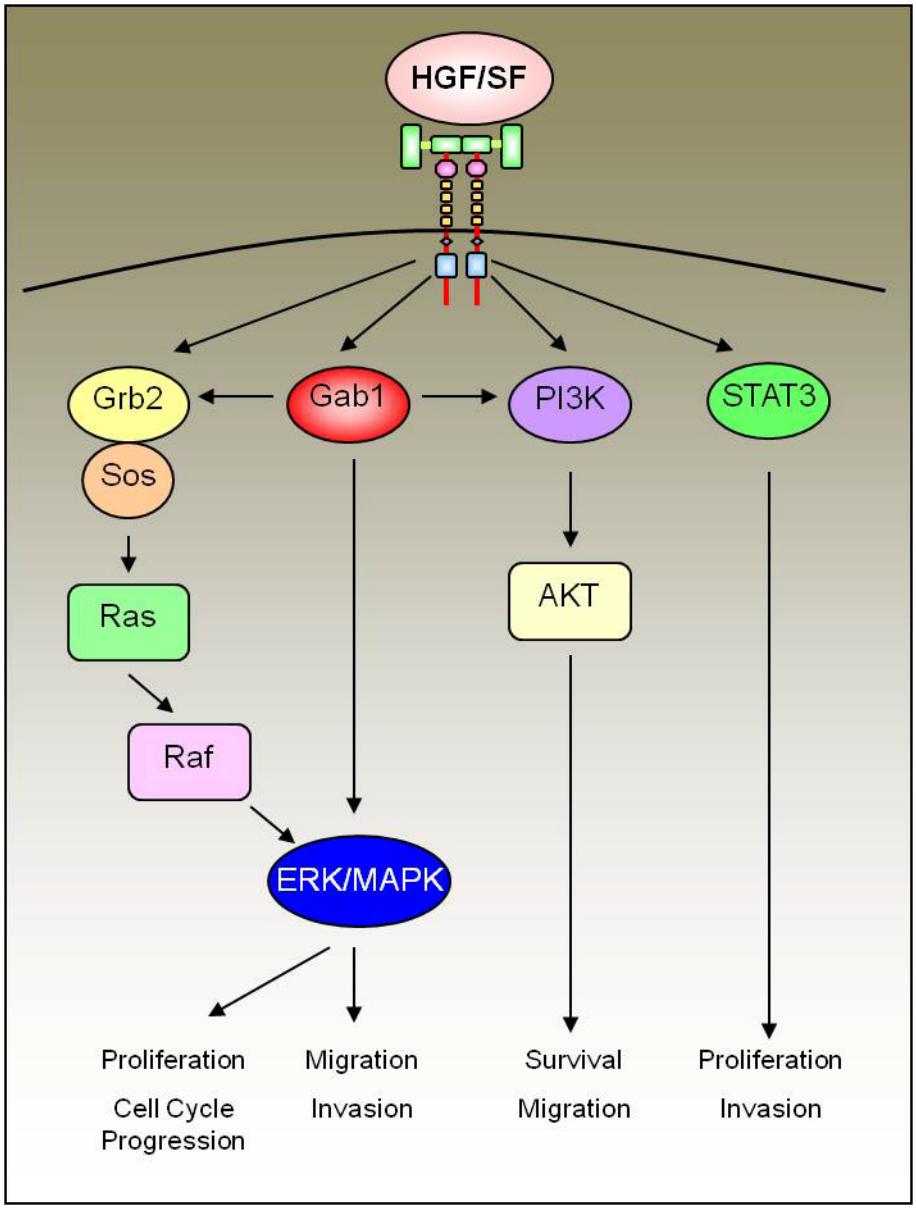

Figure 1.3: Simplified diagram of c-Met induced signalling pathways.
Adapted from Abounader and Laterra (2005).

1.2.5: Negative regulation of c-Met

The juxtamembrane region of c-Met contains two negative regulatory sites for c-Met. Protein kinase C or Ca^{2+}/calmodulin-dependent kinase phosphorylate c-Met at serine residue 985 to inhibit c-Met function (Birchmeier *et al.*, 2003; Corso *et al.*, 2005;

Gandino *et al.,* 1994). The other negative regulatory site lies on tyrosine residue 1003. The E3 ubiquitin ligase, Cbl, recognises and binds to pY1003 (Peschard *et al.,* 2001). Upon HGF/SF binding, c-Met is rapidly poly-ubiquitinated by Cbl. This induces endocytosis of c-Met, followed by transportation to the lysosome for degradation (Hammond *et al.,* 2001). c-Met has also been reported to be degraded via the ubiquitin-proteosomal pathway (Jeffers *et al.,* 1997b) which was verified further by Hammond *et al.* (2001). However, Hammond *et al.* (2001) suggested the c-Met is being degraded by both the lysosomal and proteosomal pathways, with the former being the main route for c-Met degradation. Removal of c-Met from the cell surfaces is thus a mechanism to terminate and control c-Met signalling. The Y1003 regulatory site was found to be absent in the constitutive active c-Met mutant, Tpr-Met.

Recently, shedding of the c-Met extracellular domain has been demonstrated to down regulate c-Met expression. Cells treated with the anti-Met monoclonal antibody, DN30, were reported to shed the c-Met extracellular domain. This results in the loss of the HGF-binding domain of c-Met from the cell surface, thus reducing c-Met signal transduction and releasing a 130 kD fragment into the cell media. This 130 kD c-Met fragment was capable of blocking HGF-induced signal transduction most probably by acting as a decoy to sequester unbound HGF in the extracellular matrix (Petrelli *et al.,* 2006).

1.2.6: c-Met activation in adults and development

During development, c-Met is expressed in epithelial cells of various organs, while HGF/SF is expressed in the adjacent mesenchyme. Through the secretion of HGF/SF,

mesenchymal cells are able to communicate to the epithelial cells which will ‘interpret’ the message to bring about changes in physiological processes, such as cell proliferation, cell migration, tubulogenesis and cell invasion, required for proper embryonic development and tissue organisation. Through such physiological processes, c-Met is involved in muscle development, nervous system formation, hematopoietic differentiation, bone remodelling and angiogenesis.

c-Met and HGF/SF knock-out mice are embryonic lethal (Stella and Comoglio, 1999). Examination of the knock-out mouse embryos shows that they have severe defects in liver and placental development. HGF/SF and c-Met are required during development to control cell survival and proliferation of hepatocytes, as well as the formation of the placenta. Further examination of the mutant embryo showed that the liver is present, but small in size with extensive loss of parachymal cells. However, it is the failure of the developing placenta to support the developing embryo that causes the eventual death of the embryo. The placental labyrinth layer, formed by the epithelial trophoblast, is found to be greatly reduced. The defective placental is thus unable to supply sufficient oxygen and nutrients to the developing embryo. c-Met and HGF/SF null mice also show defects in limb muscle formation. Migration of myoblast precursors from the dermomyotome to the limb, where skeletal muscles are formed, requires c-Met-HGF/SF signalling. c-Met is expressed by the myoblast precursors. Cells adjacent to the dermomyotome and along the route to the limb guide the migrating myoblast precursors to their final destination by expressing HGF/SF (Birchmeier *et al.*, 2003).

c-Met signalling is also crucial for normal establishment of tissue patterning during development (Corso *et al.*, 2005). In the adult, when tissue patterning has been well-established, c-Met function becomes dispensable. c-Met is only required in the adult for

wound healing (Chmielowiec *et al.,* 2007), hepatocyte regeneration and during post-natal physiology. In fact, when c-Met expression is turned off in adult mice containing inducible c-Met expression, the mice have almost no defects except for the inability to regenerate tissue after an injury.

1.2.7: c-Met in Cancer

In normal physiological conditions, c-Met activation is only a transient event. However, in tumour cells, c-Met is often constitutively active. Constitutive activation of c-Met signalling pathways correlates with hyperproliferation, tumour cell invasion, tumour angiogenesis and poor prognosis in various human cancers. In addition, c-Met signalling protects the tumour cell by inhibiting apoptosis and inducing resistance towards cancer therapy, thus hampering the efforts of tumour treatment.

The oncogenic role of c-Met has been documented in numerous cancers and examined in many *in vitro* studies. Xenograft models have also convincingly demonstrated the reduction of tumour size and tumour angiogenesis upon c-Met inhibition (Abounader and Laterra, 2005). A list, containing c-Met and HGF expression levels obtained from human cancer biopsies and the disease prognosis, is available in Appendix 1. Overexpression of c-Met, often discovered in gastric cancers, is the most common cause of aberrant c-Met signalling in human cancers. Linkage analysis revealed that germline activating mutations in the kinase domain of c-Met result in hereditary forms of cancers such as hereditary papillary renal carcinomas, childhood hepatocellular carcinomas and, head and neck squamous-cell carcinomas (Giordano *et al.*, 2005). Autocrine expression

of HGF is often observed in glioblastoma. HGF promotes endothelial cell proliferation, migration and blood vessel formation in glioblastoma (Abounader and Laterra, 2005).

c-Met activation in cancer may be grouped into two categories, ligand-independent and ligand-dependent. In the absence of HGF/SF, overexpression of c-Met leads to spontaneous receptor dimerisation and activation of c-Met. Overexpression of c-Met could be due to gene amplification caused by chromosomal duplication, or by increasing c-Met gene transcription by oncogenes such as Ras and ETS (Furlan *et al.*, 2008). c-Met gene amplification is one of the most common causes of aberrant c-Met expression in cancers. Fluorescence *in situ* hybridisation (FISH) analysis of c-Met gene amplification in gastric cell lines indicates that the c-Met locus is a result of targeted amplification rather than chromosomal aneuploidy (Smolen *et al.*, 2006). Environmental stimuli such as hypoxia may also induce and increase c-Met transcription by acting on the c-Met promoter region. Hypoxia increases c-Met expression by 3-fold which is sufficient to activate c-Met and induce branching morphogenesis (Pennacchietti *et al.*, 2003). Another ligand-independent mechanism of c-Met activation is caused by mutation. Mis-sense mutations in c-Met have been identified in both hereditary and sporadic forms of renal papillary carcinoma (Jeffers *et al.*, 1997a). These activating mutations were mostly in the tyrosine kinase domain of c-Met, which resulted in the constitutive and abnormal activation of c-Met kinase activity leading to tumour malignancies. The fully active c-Met mutant containing both mutations in L1213V and M1268T was found to activate c-Met and cause a full range of c-Met biological changes without autophosphorylation of Y1234, Y1235 and Y1349, Y1356 (Jeffers *et al.*, 1997a). These mutations were thought to alter and stabilise c-Met conformation in the active state thus bypassing the requirements for

autophosphorylating at Y1234 and Y1235. Interestingly, Jeffers *et al.* (1997) demonstrated that dimerisation of mutant c-Met is an absolute necessity for these activating mutations to cause c-Met activation. As mentioned earlier, the Tpr-Met chimeric protein caused by chromosomal translocation *in vitro* contains the N-terminal dimerising motif of TPR gene fused to the C-terminal kinase domain of c-Met. As the regulatory juxtamembrane domain of c-Met was found to be absent in Tpr-Met protein. The lack of a regulatory domain and the effects of the dimerisation motif from TPR, cause Tpr-Met self-dimerisation and a strong constitutive activation of c-Met tyrosine kinase activity. However, Tpr-Met protein in cancers was observed to be very rare (Corso *et al.*, 2005). Finally, Mondino *et al.* reported the activation of c-Met due to defects in the post-translational processing of c-Met. A colon carcinoma cell line (LoVo) lacks the ability to cleave single chain c-Met precursor into the mature α and β chains due to defects in furin activity. Single-chain c-Met is expressed onto the cell surface and is self-activated. The mechanism whereby single-chain c-Met is able to self-induce its tyrosine kinase activity remains unknown (Mondino *et al.*, 1991).

Ligand-dependent activation of c-Met in cancer may occur in an autocrine or paracrine manner. Autocrine activation of c-Met occurs when a cell expresses both HGF/SF and c-Met, thus self-activating c-Met signal transduction resulting in abnormal cellular processes. In certain tumours such as glioblastoma, autocrine activation of c-Met has been found occurring in the tumour cells. Paracrine activation occurs when surrounding stroma cells secrete high levels of HGF/SF constitutively. Abnormal secretion of HGF/SF into the extracellular matrix is detected by normal c-Met expressing cells. The abnormal amount of HGF/SF in the extracellular matrix thus results in abnormal and

constitutive activation of c-Met in the cells, which will lead to enhanced tumourigenicity and malignant progression of the normal cell into a cancer cell.

Recent studies have emerged highlighting c-Met ability to crosstalk with cell surface receptors such as adhesive receptors (CD44 and integrins) and signalling transducing receptors (EGF family, FAS and B plexins). The molecular mechanisms of these interactions are not well-define and the physiological purpose is unclear. Individually, each c-Met crosstalk partner has a role in cancer progression and cooperate with c-Met to promote tumour growth and development (Corso *et al.*, 2005) by reinforcing cMet signalling. CD44v6, an isoform of CD44, was reported to form a complex with c-Met and HGF. While CD44v6 extracellular domain is involved in promoting c-Met and HGF interaction on the cell surface, the intracellular domain acts to amplify c-Met downstream signalling. c-Met anti-apoptotic activity is enhanced by the interaction with the death receptor FAS receptor. In a HGF-independent manner, c-Met binds to FAS receptor and is inhibits its activation. c-Met thus have a dual role by encouraging tumour cell survival through its own activated signalling pathway and inhibiting apoptosis via interaction with FAS. Enhanced cell invasion was observed in c-Met interaction with plexins. Plexins are receptors of semaphorins and are involved in cytoskeleton remodelling and cell adhesion. Both plexins and c-Met interact through their own sema domain which is a protein-protein interaction motif (Gherardi *et al*., 2004). Finally, c-Met was demonstrated to crosstalk with members of the EGFR family to acquire drug resistance against EGFR drugs (e.g. gefitinib) in human cancer. Inhibition of c-Met activity using c-Met specific small molecules inhibitor (PHA-665752) sensitise tumour cells to gefitinib (Engelman *et al.*, 2007) and combine treatment of PHA-665752 and gefitinib showed tumour cell killing.

1.2.8: c-Met and cancer therapy

Aberrant c-Met expression was found in many cancers and the levels of c-Met expression often correlate with tumour aggression. While tumour cell lines containing amplification of c-Met were shown to be sensitive to the small molecule inhibitor PHA-665752, non c-Met amplified tumour cell lines showed no sensitivity (Smolen *et al.*, 2006). This indicates dependence of the cancer cells on c-Met expression and by blocking c-Met activation, tumour cells were sensitised. In addition, c-Met function in adult human is largely dispensable. Results from adult mice that have c-Met gene expression turned off suggested that inactivation of c-Met would have few side effects. These makes c-Met is an attractive target for drug therapy and many groups have employed different strategies in attempts to block c-Met signalling for cancer therapy. They include c-Met/HGF competitive inhibitors, c-Met small molecule inhibitors and antibodies directed against c-Met/HGF.

c-Met/HGF competitors

NK4 molecule and decoy-Met are examples of competitive inhibitors of the Met-HGF interaction. NK4 is a synthetic, truncated variant of HGF α-chain containing the N-terminal hair-pin loop and the four kringle domain. NK4 is able to compete with HGF for c-Met binding, but does not activate c-Met. It was shown to inhibit HGF-induced proliferation and angiogenesis in cell lines and to inhibit tumour growth and metastasis in xenograft models (Brockmann *et al.*, 2003). Another promising molecule is decoy-MET which is a soluble variant of c-Met, consisting of the entire extracellular domain of c-Met. Decoy-Met is able to bind to c-Met to prevent receptor dimerisation as well as to HGF thus preventing HGF from activating c-Met (Michieli *et al.*, 2004). Compared

to NK4 molecule, decoy-Met has a higher affinity towards HGF and was also able to block tumour cell growth and metastasis in mice.

Small molecule inhibitors

Small molecule inhibitors of c-Met were found to be effective in inhibiting the c-Met signalling cascade by competing with ATP for the catalytic domain of c-Met, thus preventing c-Met from activation and phosphorylation of cytoplasmic proteins. AM7, SU11274 and PHA-665752 were separately identified as c-Met small molecule inhibitors, shown to block HGF-induced c-Met activity at nanomolar concentrations (Bellon *et al.*, 2008; Christensen *et al.*, 2003; Sattler *et al.*, 2003; Wang *et al.*, 2003). Interestingly, due to the differential binding of AM7 to c-Met, compared to SU11274, SU11274 was only effective on M1268T and H1112Y c-Met mutants while AM7 showed inhibition against both wild-type and mutant c-Met (Bellon *et al.*, 2008). Small molecules c-Met inhibitors show promising results. However, the likelihood of an ATP inhibitor having complete specificity towards the c-Met kinase is extremely small and there are concerns about the toxicity of these molecules if used as therapeutic molecules (Migliore and Giordano, 2008). XL880 (from Exelixis) and ARQ197 (from ArQule Inc.) are kinase inhibitors that have successfully gone into phase II of clinical trials (Migliore and Giordano, 2008). Other than c-Met, XL880 targets other tyrosine kinases. ARQ197 is a non-ATP-competitive molecule that binds outside of the c-Met ATP binding site. Clinical studies have demonstrated that these drugs have been well tolerated with anti-tumour activity (Migliore and Giordano, 2008).

Monoclonal antibodies and their variants

Monoclonal antibodies have been extremely successful as therapies against receptor protein kinases. The best known examples are Trastuzumab and Rituximab that target

HER-2 and CD20 respectively. Monoclonal antibodies function as receptor inhibitors by blocking the ligand from binding to the receptor or by preventing receptor oligomerisation. Currently, AMG102 from Amgen, is the only therapeutic antibody targeted at the Met-HGF axis that has gone through into clinical trials. AMG102 is a fully human IgG2 monoclonal antibody directed against HGF. It was shown to increase the cell growth inhibition of tumour cells in combination treatment with docetaxel or temozolomide compared with treatments with docetaxl or temozolomide alone (Jun *et al.*, 2007). AMG102 was well tolerated in initial trials and is in the process of entering the second clinical phase.

Other than AMG102, there are reports of other bivalent monoclonal antibodies developed against c-Met/HGF that can successfully block the receptor-ligand interaction. Prat *et al.* (1998) developed two monoclonal antibodies (DO-24 and DN-30) against the extracellular domain of c-Met. Interestingly, both monoclonal antibodies act as an agonist rather than an antagonist and activate c-Met signalling *in vivo*. It is hypothesized that the bivalent binding of an antibody could mimic the dimerising effect of HGF, thus causing c-Met dimerisation upon antibody binding. Attempts to block Met-HGF interaction by developing monoclonal antibodies against HGF were performed by Cao *et al.* (2001). However, none of the antibodies alone were capable of blocking HGF-induced c-Met activation. Only when three different monoclonal antibodies were used in combination, was c-Met activation blocked. Finally, the combination of using two fully human anti-Met antibodies (R13 and R28) was more effective in inhibiting c-Met binding to HGF as compared to using R13 or R28 alone (van der Horst *et al.*, 2009). Binding and activation of c-Met by HGF appears to be a complex interaction as more than one Met-HGF interaction site has to be blocked.

Despite the dimerisation effects of monoclonal antibodies on c-Met, antibodies were able to specifically target c-Met on the cell surface and induce an antagonist/agonist effect on c-Met activation. Other variants of antibodies were thus exploited for targeting c-Met in drug development. Genetech developed a one-armed (OA) variant of the anti-human c-Met antibody 5D5 which showed promising results in orthotopic models. OA-5D5 is a monovalent Fab recombinantly fused to a human Fc region. The heavy and light chains in the Fab region are made up of murine variable domains with human IgG1 constant domains (Martens *et al.*, 2006). OA-5D5 inhibits HGF binding to c-Met and showed inhibition of tumour cell proliferation, migration and angiogenesis with no signs of toxicity (Martens *et al.*, 2006). OA-5D5 has gone into phase I of clinical trials.

Novel strategies

Other strategies have been employed to block Met-HGF interactions. Recently, a Met-binding peptide (YLFSVHWPPLKA) screened from a phage display library was found to compete with HGF for binding to c-Met. Zhao *et al.* (2007) showed that the Met-binding peptide is internalised by Met-expressing cells and is able to inhibit cell proliferation. However, peptides are generally not good therapeutic agents due to instability and protease cleavage. Peptides are usually developed to form peptidomimetic agents by substituting residues with non-naturally occurring amino acids. However, peptides are also useful for forming the starting point for the development of small molecule therapeutic agents. Another strategy employed was to down regulate the mRNA levels of a target by the use of U1snRNA/ribozymes. U1snRNA/ribozyme chimeric molecule is made up of a hammerhead ribozyme, an U1snRNA and an anti-sense mRNA sequence of the target gene. Abounader *et al.* (2001) targeted c-Met and HGF mRNA levels by creating anti-c-Met-U1/ribozyme and anti-HGF-U1/ribozyme respectively. These U1/ribozymes were shown to successfully

inhibit c-Met activation, c-Met-activated biological activities in cell lines as well as inhibit tumour growth in glioma xenograft models. However, this therapeutic strategy requires complex delivery system such as virus or liposomes to efficiently deliver the molecules to the target site *in vivo* (Brockmann *et al.*, 2003).

Although all of these drugs demonstrate anti-tumour activity in xenograft models, their clinical activity still remains unknown. The aim of this project is to produce and screen for conventional and single chain antibodies that will bind c-Met and inhibit c-Met signalling. Promising molecules will be used in xenograft models to determine the effectiveness of these molecules in inhibiting tumour progression, tumour migration and invasion and angiogenesis.

1.3: Antibodies

1.3.1: Introduction to antibodies

Antibodies, also known as immunoglobulins (Ig), are glycosylated proteins secreted by plasma cells as part of the immune defence against foreign molecules in a body. Plasma cells are terminally differentiated B-cells, highly committed to secreting antibodies into the blood stream. Antibodies bind to antigens and facilitate their destruction by recruiting the host's immune effector cells. This can either lead to the phagocytosis of the antibody-coated antigen or to the initiation of the complement system. Each B-cell expresses only one type of antibody that has a unique antigen-binding site. Since B-cells exist as clones, the progeny of a particular B-cell will only produce one type of antibody with a unique epitope.

The basic structure of an immunoglobulin is a 'Y'-shape molecule made up of four polypeptides. Two identical heavy chains and two identical light chains of an immunoglobulin molecule are held together by non-covalent and covalent bonds. Each light chain is paired with a heavy chain, producing a bilaterally symmetric structure. There are two types of light chain: the kappa (κ) and the lambda (λ) light chain. Light chains are approximately 220 amino acid residues long (~25 kD) and are made up of a variable region (V_L) and a constant region (C_L). In contrast, a heavy chain contain approximately 440 amino acid residues (~ 55 kD) and there are five types of heavy chains: mu (μ), alpha (α), gamma (γ), epsilon (ε) and delta (δ). Antibodies are categorised into classes based on the type of heavy chain they possess (IgM, IgA, IgG, IgE and IgD respectively). The different types of heavy chains allow different biological molecules to bind to the antibody, producing different immunological responses. In addition to the major immunoglobulin classes, there are four subclasses of IgG

molecules (IgG1, IgG2, IgG3 and IgG4) based on subtle differences in the γ-heavy chain. The subclasses of IgG will be discussed in Section 1.3.2. The γ-heavy chain of an IgG molecule is made up of one variable region (V_H) and three constant regions (C_{H1}, C_{H2} and C_{H3}). By allelic exclusion, a B-cell expresses only one type of light chain and one type of heavy chain. Table 1.1 summaries the characteristic of the different classes of immunoglobulins.

Table 1.1: Characteristics of immunoglobulin (Ig) classes.

Ig Class	Type of heavy chain	Type of antibody complexes	Antibody valency	Function
IgA	α	Monomer, dimer or trimer	2, 4 or 6	Protects mucous membranes
IgD	δ	Monomer	2	Unknown
IgE	ε	Monomer	2	Protects against parasites
IgG	μ	Monomer	2	Secondary immune response
IgM	γ	Pentamer	10	Primary immune response

Adapted from Harlow and Lane, 1999.

The V_H and V_L regions form the antigen-binding site which can be further restricted to three highly variable domains known as CDR (complementarity determining regions) (Figure 1.4). CDRs are the main antigen binding site of an antibody. As the antibody response matures, somatic hypermutation occurs in the CDR region and fine-tunes the antibody specificity to produce higher affinity antibodies. IgG molecules function as monomers containing two antigen-binding sites. Cleavage of an IgG molecule by the proteolytic enzyme, papain, produces three protein fragments with biological activities: two similar Fab (fragment antigen binding) fragments and one Fc (fragment that crystallises) fragment. The Fab fragments bind to antigens, but fail to evoke an immune response due to the absence of the Fc fragment. The constant regions (C_{H2} and C_{H3}) of the heavy chains make up the Fc fragment (Figure 1.4). The Fc fragment is the main region that determines the class and subclass of an antibody. Different Fc fragments are

recognised by different Fc receptor (FcR) proteins displayed on the surface of cells such as macrophages and neutrophils. Different classes of antibodies are thus able to evoke different immune responses by the binding their Fc fragments to the FcR of different effector cells. FcR are further discussed in Section 1.3.3.

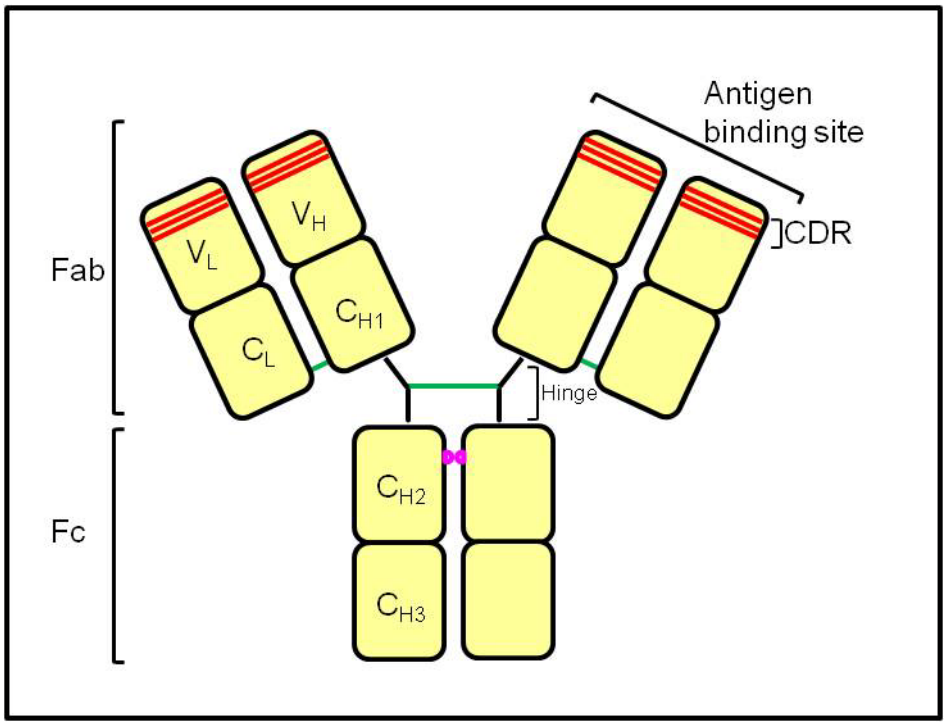

Figure 1.4: Structure of an immunoglobulin (Ig) G molecule.
An IgG molecule is made up of two light chains polypeptides linked to two heavy chain polypeptides by disulphide bonds (in green). The complementarily determining region (CDR) is located in the Fab (fragment antigen binding) region. The variable regions of the heavy and light chains make up the antigen binding site. An antibody's isotype is dependent on the Fc (fragment that crystallises) domain. The C_{H2} region, located within the Fc domain, is glycosylated and is involved in FcR binding. The conserved glycosylation site (asparagine 297) in the C_{H2} region is highlighted in pink. The hinge region determines the flexibility of the IgG molecule and is varied among the different IgG subclasses. V_L: Variable region light chain. V_H: Variable region heavy chain. C_L: Constant region light chain. $C_{H1/2/3}$: Constant region heavy chain 1/2/3.

The κ light chain, λ light chain and the heavy chain of an immunoglobulin are each expressed by a collection of gene segments known as a gene pool. A gene pool typically contains more than four types of gene segments. During B-cell differentiation, the different sets of gene segments, from a gene pool, recombine and are expressed into an antibody polypeptide chain. The V_H and V_L regions of an immunoglobulin are encoded

by genes segments known as the variable (V) segment, diversity (D) segment and joining (J) segment. The V_H region is made up of the V-D-J segments found in the same cluster on chromosome 12 while the V_L region is made up of the V-J segments found in two different gene clusters, the kappa light chain gene cluster on mouse chromosome 6 and the lambda light chain gene cluster on mouse chromosome 16. There are several different copies of each gene segment and only one copy of each gene segment is randomly chosen and combined with other gene segments. This mechanism of recombination results in an enormous repertoire of possible antibodies.

Antibody diversity is not only a result of the random recombination of different copies of gene segments during B-cell differentiation. The recombination process of the gene segments is not precise. Nucleotides are often added on or removed during the process which further increases the antibody diversity. In addition, it is possible to pair any heavy chain polypeptide to any light chain polypeptide. Finally, affinity maturation (as discussed earlier), adds on to this huge antibody repertoire.

1.3.2: IgG subclass

IgG antibodies constitutes the highest percentage (75%) of total immunoglobulin in the blood. In contrast to IgM molecules, IgG antibodies are expressed during secondary antibody response, have longer half-lifes and have higher affinity towards foreign molecules. The four IgG subclasses, designated IgG1, IgG2, IgG3 and IgG4, are enumerated according to their concentration in the blood (Table 1.2). IgG subclasses share 95% homology in the constant domain of the heavy chain and the biggest difference lies in the antibody's hinge region. The hinge region links the antibody's Fab

fragments to the Fc fragment and is responsible for the flexibility of the antibody. Proline and cysteine make up the main residues in the core hinge region (Table 1.3). As length and number of disulphide bonds differs among the IgG subclasses, this in turn influences the antibody's flexibility and ability to bind to serum proteins (Table 1.2).

The IgG subclasses also differ in this ability to recruit effector molecules (by interacting with FcγR displayed on the surface of immune cells), ability to induce CDC (by interacting with C1q component) and serum half-life (by interacting with FcRn), which is mediated through the Fc domain of the IgG. Table 1.2 tabulates the *in vitro* binding properties of IgG subclasses of various effector molecules. Selection of IgG subclasses for antibody therapy is very much dependent on the effector function of the antibody. In cancer therapy, the therapeutic antibody is required to recruit effector functions and destroy the tumour cells, IgG subclasses with strong effector functions is preferred. Although IgG1 and IgG3 share similar biological characteristic that are ideal cancer therapy (Table 1.2), IgG1 are preferred over IgG3 due to the shorter half-life, extensive polymorphism and longer hinge region (thus more susceptible to proteolysis) of IgG3 (Salfeld J.G., 2007, Jefferis R., 2007). Presently, no IgG3 subclasses have been approved for therapy. Both IgG2 and IgG4 are poor mediators of the complement pathway and are usually employed when less aggressive activity is required (i.e. when neutralisation of the antigen is more relevant than the effector function) (Salfeld J.G., 2007). IgG2 antibodies are more resistant to proteolysis due to the shorten hinge region. Recently, IgG2 molecules were shown to form covalent dimers with identical IgG2 molecules and different IgG2 molecules (Correia I.R., 2010). The molecular mechanism of IgG2 dimer formation has yet been understood and the clinical safety implications have not been determined by regulatory bodies. Similar to IgG2, IgG4 subclass have

low affinity to C1q component and were initially chosen as a therapeutic molecule as the recruitment of effector mechanisms is not desirable (Correia I.R., 2010). Natalizumab (Tysabri) is an IgG4 therapeutic molecule used for multiple sclerosis. However, the cytokine storm elicited by the anti-CD28 IgG4 molecule during Phase I clinical trial caused further investigation of using IgG4 subclasses as therapeutic molecules. It was shown that the inter-chain disulphide bonds of IgG4 molecules could be broken to form monovalent half-molecules (one heavy chain and one light chain). The disulphide bonds of the monovalent half-molecules could be re-created again forming a bivalent molecule paired with its original half molecule or a different IgG4 half-molecule.

Table 1.2: Characteristics of IgG subclasses.

	IgG1	**IgG2**	**IgG3**	**IgG4**
Percentage of total IgG concentration (%)	60	25	10	5
Half-life (days)	21	21	7	21
Hinge Length (number of amino acid residues)	15	12	62	12
Inter-heavy chain disulphide bonds (hinge region)	2	4	11	2
Binding properties				
C1q	++	-	+++	-
FcγRI	+++	-	+++	++
FcγRII	+	±	+	?
FcγRIIIa/b	+	-	+	±
FcRn	+	+	+	+

Adapted from Salfeld, J.G. (2007).
IgG subclass binding properties are determined by *in vitro* assays. As every IgG is different, its *in vivo* activity may not correlate to the above table.

Table 1.3: Amino acid sequences of core hinge region of IgG subclasses.

IgG subclasses	Sequence
IgG1	EPKSCDKTHTCPPCP
IgG2	ERKCCVECPPCP
IgG3	ELKTPLGDTTHTCPRCP …… (EPKSCDTPPPCPRCP) x 3
IgG4	ESKYGPPCPSCP

Adapted from Correia, I.R. (2010).

1.3.3: Fc receptors and effector function

Cells of the immune system, such as macrophages, neutrophils and natural killer cells, display Fc receptors on their cell surface which recognises the Fc domain of immunoglobulins. Aggregation of antibodies on an antigen surface is followed by the recognition and binding of FcR to the Fc domain of the immunoglobulin. This triggers the activation of immune effector cells to induce various effector functions such as: 1) antibody-dependent cell-mediated cytotoxicity (ADCC), 2) antibody-dependent cellular phagocytosis (ADCP), and 3) complement-dependent cytotoxicity (CDC) (Chan and Carter, 2010). Binding of FcR to immunoglobulin may also inhibit immune cells from inducing an immune response. Different antibody isotype classes are recognised by specific FcR i.e. FcαR, FcδR, FcεR, FcγR and FcμR which bind to IgA, IgD, IgE, IgG and IgM respectively. Different cell types express different FcR on their cell surface. An immune response raised against an antigen is thus dependent on the cell type, expressing specific FcR that recognises the Fc tail of an antibody class.

There are three different classes of FcγR in human: FcγRI (CD64), FcγRII (CD32), and FcγRIII (CD16). Among the FcγR classes are subclasses (FcγRI, FcγRII and FcγRIII) with different affinity and specificity for the various human IgG isotypes (hIgG1, hIgG2, hIgG3 and hIgG4). Isoforms exist in these subclasses. In humans, the various

FcγR subclasses are encoded from multiple genes: FcγRIA, B and C, FcγRIIA, B and C, and FcγRIIIA and B. Most FcγR are transmembrane proteins and contain a cytoplasmic tail where the immunoreceptor tyrosine-based activation motif (ITAM) or the immunoreceptor tyrosine-based inhibition motif (ITIM) is located. Binding of FcγR to the Fc domain of IgG results in the activation of a signal transduction pathway carried out by the immunoreceptor tyrosine-based motifs (ITAM or ITIM). This eventually leads to the activation or inhibition of the cell immune activity (Schmidt and Gressner, 2005).

Human FcγRI (hFcγRI) is a high affinity receptor. As mentioned earlier, there are three FcγRI genes (FcγRIA, B and C), however only hFcγRIA is being expressed. hFcγRIa is expressed on monocytes and macrophages. hFcγRIa has high affinity for hIgG1 and hIgG3 while its affinity for hIgG4 and hIgG2 is lower, with hIgG2 being the lowest. The murine homologue of human FcγRIa is murine FcγRI (mFcγRI). hFcγRIa binds to murine IgG2a and mIgG3 but not IgG2b (Gessner *et al.*, 1998).

The hFcγRII is a low affinity receptor with affinity for hIgG1 and hIgG3 (Gessner *et al.*, 1998). Members of hFcγRII do not bind to hIgG4 and are widely expressed in various immune cells such as eosinophils, monocytes, leukocytes and macrophages. The ITIM motif only exists in the hFcγRII subclass (namely hFcγRIIb1, hFcγRIIb2 and hFcγRIIb3). FcγRII proteins bind well to mIgG2a and mIgG2b. Like hFcγRII, hFcγRIII is a low affinity receptor. It has affinity for hIgG1 and hIgG3 but low affinity for hIgG4 and hIgG2. hFcγRIII class of FcR are constitutively expressed on macrophages and NK cells. hFcγRIIIa is the human homolog of mFcγRIII (Schmidt and Gessner, 2005).

1.3.4: Antibody therapy

Hybridoma antibody fusion technology, developed by Kohler and Milstein in the mid-1970s, was the main driving force that initiated the use of antibodies for therapy. The fusion of a B-cell to an immortal cell line resulted in a hybrid cell that not only retains its antibody producing ability, but is also immortal. Antibodies produced from a hybridoma clone are called monoclonals, exhibiting specificity to a single epitope. Hybridoma fusion technology has enabled antibodies from different clones to be individually studied and characterised, thus, the most useful and potent antibody could be selected for therapeutic purposes.

With an enormous antibody repertoire and the ability to produce highly specific antibodies, it is possible exploit the antibody-mediated immune system to create an antibody against any cell surface protein, carbohydrate or synthetic molecule. It is thus very attractive to develop antibodies against novel targets for the treatment of human diseases. The first US Food and Drug Administration (FDA) approved therapeutic antibody was Orthclone OKT3, an IgG2a CD3 mouse monoclonal antibody, used as an organ transplant rejection drug in 1986. Antibody therapy has since been very successful in the treatment of human diseases such as inflammation, autoimmune disease and organ transplantation where the antibody interacts and blocks specific cell receptors, ligands and cytokine molecules. Conversely, the use of antibodies for cancer treatment has not been as successful as the other non-cancer illness. This is because the antibody not only has to interact with the cancer cell, it also has to induce the destruction of the cancer cell. The mechanism by which an antibody, upon binding, efficiently targets a cancer cell for destruction is still unclear. While there have been successful therapeutic antibodies (for example Herceptin that targets human epidermal

growth factor 2) in the market, further studies are required to better understand the use of antibodies as cancer therapies, advances in antibody engineering has greatly improved the success of antibodies for clinical purposes. The outlook of using antibodies for cancer treatment is promising.

1.3.5: Antibody engineering

Advances in antibody engineering have allowed the modification and optimisation of an antibody's shape, molecular size, binding affinity, specificity, pharmacokinetics and effector function for the use of antibody in the clinical field. The first generation of antibody therapy used mouse monoclonal antibodies which were not as successful in clinical trials due to their murine origin. The failure was also due to insufficient knowledge required for antibody therapy e.g. the amount of antibodies required to elicit a therapeutic activity (milligrams of antibodies were required) (Glennie and van de Winkel, 2003). Mouse monoclonal antibodies had short half-lifes, failed to efficiently recruit immune effector functions and were highly immunogenic, thus evoking human anti-mouse antibody (HAMA) responses. Binding of human anti-mouse antibodies to murine therapeutic antibodies prevented the antibodies from attaining their therapeutic effectiveness. Attempts were thus made to humanise the murine antibodies which led to the generation of chimeric antibodies. A chimeric antibody is generated by engineering the variable region (containing the epitope binding region) of the mouse monoclonal antibody into the constant regions of a human antibody (V_H and V_L) (Figure 1.5) (Glennie and van de Winkel, 2003). The constant regions were often taken from the kappa light chain and the IgG1 heavy chain subclass. Among the various IgG subclasses, IgG1 have the best ability to recruit effector function in the immune system

as they can efficiently engage receptors on cytotoxic effector cells. This leads to the elimination of the antigen-antibody complex through the activation of the complement cascade or mediation of ADCC. Chimeric antibodies had improved serum half-lifes and reduced immunogenicity, therefore, human anti-chimeric antibody (HACA) responses were still observed in patients (Glennie and van de Winkel, 2003). To further reduce immunogenicity of the chimeric antibodies, humanised antibodies were thus created by engineering the CDR of a murine antibody into a human antibody framework (Figure 1.5). Humanised antibodies greatly reduced the immunogenicity of the antibody molecule, though human anti-human antibody (HAHA) responses could still be elicited. In addition, it was frequently observed that the binding affinity for the target antigen, compared to the parental mouse antibody, was greatly reduced (Glennie and van de Winkel, 2003). Genetic engineering in the CDR region was thus required to improve the binding efficiency. Currently, most of the therapeutic antibodies approved for use in human diseases are chimeric and humanised antibodies. The more successful therapeutic antibodies used in human cancer are bevacizumab (Avastin), cetuximab (Erbitux) and trastuzumab (Herceptin) (Adams and Weiner, 2005).

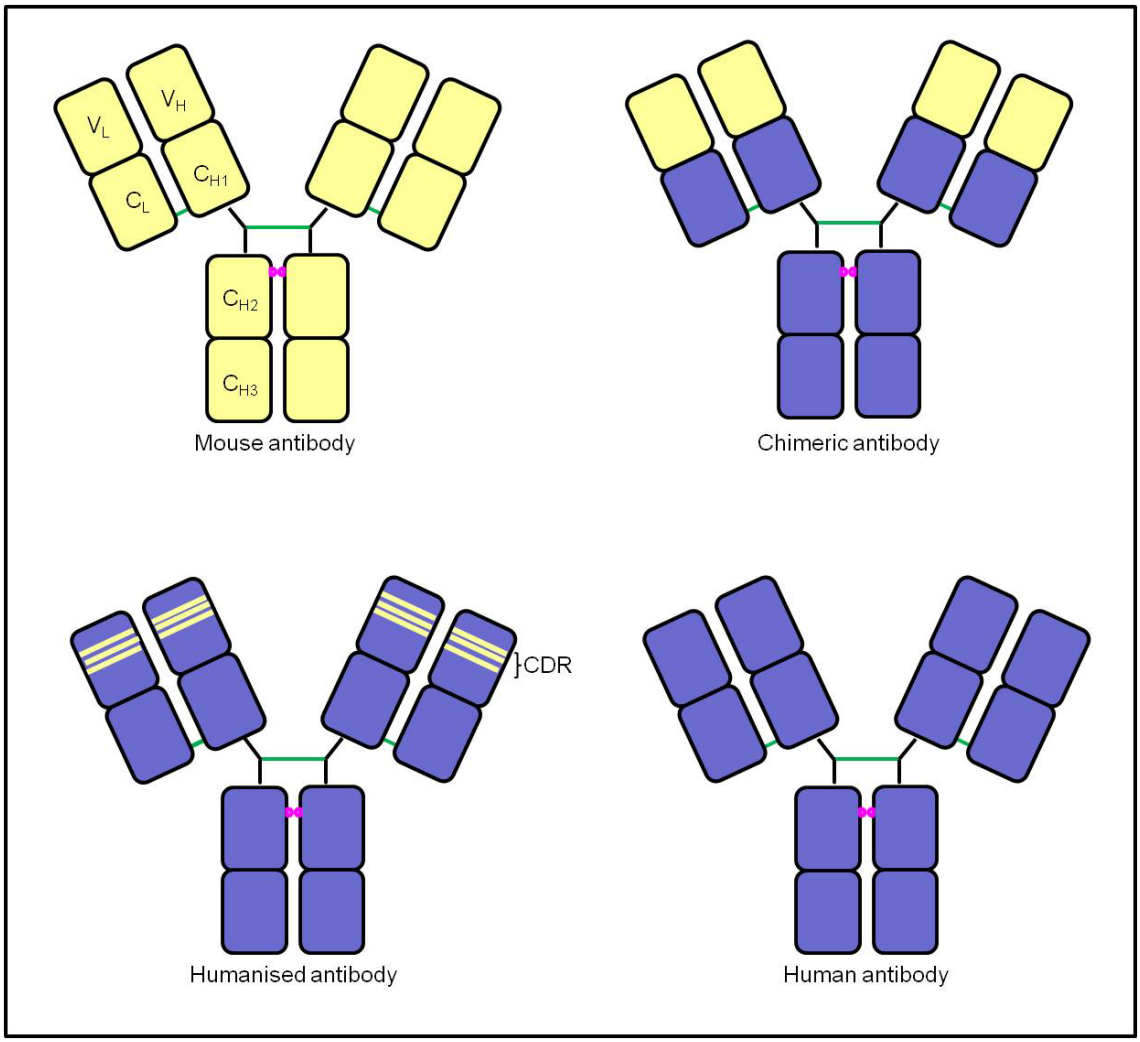

Figure 1.5: Engineering mouse monoclonal antibodies.
Engineering of mouse monoclonal antibodies, for human therapeutic purposes, led to the generation of chimeric and humanised antibodies. Chimeric antibodies contain the variable regions of the mouse monoclonal antibody (in yellow) fused to the constant regions of a human antibody (in blue). The whole framework of a humanised antibody is made of human origin except for the CDR (complementarily determining regions) which is of mouse origin. Disulphide bonds are in green.

Further advances in technology have led to the development of fully human monoclonal antibodies. Human monoclonal antibodies can be generated from transgenic mice which had their murine immunoglobulin genes replaced by the human counterpart (Glennie and van de Winkel, 2003). Panitumumab, a recently approved antibody directed against EGFR, is an example of a fully human monoclonal antibody generated by transgenic mice (Xenomouse by Abgenix). A different approach to generate human monoclonal antibodies is through phage display. Human antibody cDNA libraries cloned into phage

particles are expressed and displayed as fusion proteins on the coat surface of the viruses. One virus will only express and display a single unique cDNA construct and this allows the screening, panning, amplification and isolation of the antibody that binds to the target of interest (Glennie and van de Winkel, 2003). To date, many different variations of human antibody libraries have been created in phage display technology. Naive and immunised libraries were obtained by isolating lymphocytes from non-immunised or immunised individuals respectively. Synthetic human antibody libraries were constructed from random arrangement of the antibody gene segments obtained from germ line cells. Single-chain variable fragment (scFv) and Fab antibody library fragments were also constructed. Successfully selected scFv or Fab fragments could be further engineered to contain a Fc domain that contains appropriate effector functions.

Antibody engineering has also led to the production of various variations of antibody fragments. Depending on the clinical application, antibody fragments can be engineered to be multivalent, smaller in size and have increased stability. Antibody fragments can also be engineered to generate an antibody which can recognise two different epitopes through two distinct Fab arms termed a bispecific antibody (Bsab). With advancing technology and understanding, Bsab molecules are emerging to be promising therapeutic drugs as they have the ability to simultaneously cause dual inhibition (Jain *et al.*, 2007). Other forms of antibody engineering, such as alteration of antibody amino acid sequence, have been focused on enhancing antibody interaction with FcR which led to the improved recruitment of effector functions (Jain *et al.*, 2007). Glycosylation of the antibody's Fc domain also affects the recruitment of effector functions (Figure 1.6). Depending on the type of sugar molecules attached to the core sugar group, the mode and efficacy of the effector function is affected. Sugar moieties, attached to the

single site at asparagine 297, affects the conformation of the IgG Fc domain which in turn, influences the binding of FcγR or C1q to the antibody (Jefferis, 2009). Aglycosylated or deglycosylated antibodies have demonstrated reduced efficacy in the recruitment of effector functions. Additional of certain sugar moieties, such as fucose, to the core sugar group also reduces an antibody's therapeutic activity. Many efforts have thus been focused on engineering cell lines to produce homogenous production of therapeutic antibodies with increased ADCC and CDC (e.g. by engineering CHO cell that add bisecting *N*-acetylglucosamine residues or are deficient in adding fucose residues) (Jefferis R., 2007).

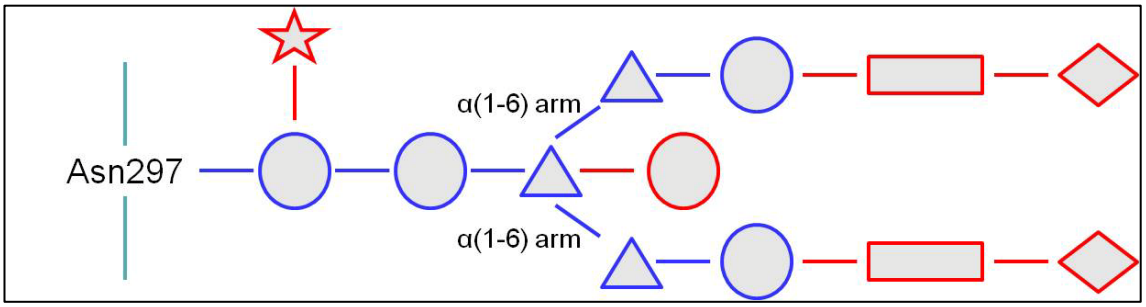

Figure 1.6: Glycosylation on IgG Fc domain.
Glycosylation at asparagine 297, located in the C_{H2} domain, of an IgG molecule is important for the recruitment of effector functions. The core sugar group is shown in blue. Additional sugar molecules could be added to the core group and are shown in red. Circle: *N*-acetylglucosamine. Triangle: mannose. Star: fucose. Rectangle: galactose. Diamond: *N*-acetylneuraminic acid. Adapted from Jefferis R., 2009.

In this work, we describe the development and characterisation of mouse monoclonal antibodies against the α-chain of c-Met. Purified c-Met α-chain was used as an immunogen to raise antibodies in mice. Hybridoma cell lines were created and 39 were identified to stably express antibodies against the α-chain of c-Met. 21 hybridoma cell lines were single cell-cloned and the monoclonal antibodies produced were characterised for their isotype subclass and epitope binding region. Mouse ascites were developed from 11 of these hybridoma clones. Antibodies were purified from the ascites and further characterised by Western blotting, immunofluorescence staining, functional

assays (ERK phosphorylation and cell scatter) and for their ability to recognise native c-Met by flow cytometry.

CHAPTER 2: MATERIALS AND METHODS

Cell lines and reagents

All cells were maintained at 37˚C in 5 % CO_2 humidified incubator. HaCaT, U-87MG and NIH3T3 cells, cultured in Dulbecco's Modified Essential Medium (DMEM) high glucose with sodium pyruvate, were generous gifts from Birgit Lane (Institute of Medical Biology (IMB), Singapore), Nick Leslie (Division of Cell Signalling and Immunology, University of Dundee) and Axel Ullrich (Institute of Medical Biology (IMB), Singapore) laboratories respectively. SNU-5 cells were purchased from Korean Cell Line Bank. T47D and SNU-5 cells were cultured in RPMI 1640 media. DMEM and RPMI were obtained from Invitrogen (Clarlsbad, U.S.A). All tissue culture medium was supplemented with 10% heat-inactivated fetal calf serum (FCS) obtained from HyClone Laboratories/Thermo Scientific (Waltham, U.S.A.). Tissue culture plates and dishes were obtained from TPP (St. Louis, U.S.A).

Recombinant human HGF (#294-HG) and anti-human HGF (#MAB294) were purchased from R&D Systems (Minneapolis, U.S.A.) and were resuspended in phosphate-buffered saline (PBS), according to the manufacturer's instructions. SU11274, the c-Met small molecule inhibitor, was purchased from Calbiochem/Merck (Darmstadt, Germany, #448101) and was dissolved in DMSO to obtain a stock concentration of 5 mM. HGF, anti-HGF and SU11274 were used at a final concentration of 10 ng/ml, 5 μg/ml and 5 μM respectively.

Cloning c-Met for mammalian cell expression

The entry vector, containing full length human c-Met cDNA in pENTR221 vector (#IOH36570), was obtained from Invitrogen. Using the LR clonase II kit (Invitrogen

#11791-020), human c-Met cDNA in pENTR221 was recombined into the following Gateway destination vectors listed on Table 2.1. Briefly, the entry clone was incubated with a destination vector in the presence of LR clonase II at 25^{o}C for an hour. Proteinase K, provided by the kit, was added to the recombination mixture and incubated at 37^{o}C for 10 mins. The recombination mixture was transformed into appropriate strains of commercially-available chemically-competent *E. coli* cells (Invitrogen). Transformed cells were then plated on LB plates (10 g Bacto-tryptone/5 g yeast extract/5 g NaCl /20 g agar per litre) containing antibiotic. Bacteria strains and antibiotic selection used are listed in Table 2.1.

Table 2.1: Mammalian vectors used for transient c-Met expression.

Gateway vectors	Promoter	Tag	Antibiotic selection	Competent cells	Approximate molecular weight	
					Mature c-Met β-chain	c-Met precursor protein
pcDNA3-GW-DEST	CMV TATA	NIL	Ampicillin	TOP10	145 kD	170 kD
pcDNA3-GFPc-GW-DEST	CMV TATA	C-terminal GFP	Ampicillin	TOP10	172 kD	197 kD
pcDNA3-SBPc-GW-DEST	CMV TATA	C-terminal SBP	Ampicillin	TOP10	149 kD	174 kD
pCMV-SCP-EFI-FRT-GW-DEST	Super Core Promoter (SCP)	C-terminal V5	Ampicillin	TOP10	146 kD	171 kD
pLenti6.3-GW-DEST	Super Core Promoter (SCP)	C-terminal V5	Ampicillin & blasticidin	STBL3		
pCMV-SCP-EFI-SBPc-GW-DEST	Super Core Promoter (SCP)	C-terminal SBP	Ampicillin	TOP10	149 kD	174 kD

Blasticidin (Invitrogen) and ampicillin (Sigma-Aldrich), was used at a final concentration of 50 μg/ml and 100 μg/ml respectively.

Cloning c-Met for prokaryotic expression

Four constructs containing different regions of human c-Met (Figure 2.1) were each cloned, without the c-Met membrane localisation signal, into pET19b vector (Novagen/Merck) for prokaryotic expression. The plasmids map of pET19b vector is shown in Figure 2.2. Primer sequences used to amplify the different c-Met regions are listed in Table 2.2. iProof PCR mix (Bio-Rad, Hercules, U.S.A.) which contains proof reading polymerase was used for the amplification. An 'A' tail was added to the 3' end of the PCR product by incubating with Taq polymerase at 72^{o}C for 30 mins. The PCR product was gel purified and cloned into pCR2.1 vector (Invitrogen) using the TOPO TA cloning kit (Invitrogen). Commercially-available TOP10 chemically-competent cells (Invitrogen) was used for bacterial transformation. Transformed cells were plated on LB plates containing ampicillin and X-gal (5-bromo-4-chloro-3-indolyl-β-D-galactoside, from Invitrogen). 40 µl of X-gal (stock concentration of 40 mg/ml) was spread onto each LB plates before use. White colonies were picked for plasmid extraction and these plasmids were screened using restriction enzyme digestion. Restriction enzymes used are listed in Table 2.3. Positive clones were sequenced using M13 forward and M13 reverse primers as well as c-Met internal primers listed in Table 2.4. c-Met encoding regions were then sub-cloned from pCR2.1 into pET19b vectors. c-Met constructs in pET19b were transformed into seven different bacteria strains listed on Table 2.5 for protein expression. All plasmid extraction, gel extraction and PCR product purification protocols were performed using Qiagen (West Sussex, United Kingdom) kits, according to manufacturer's protocol.

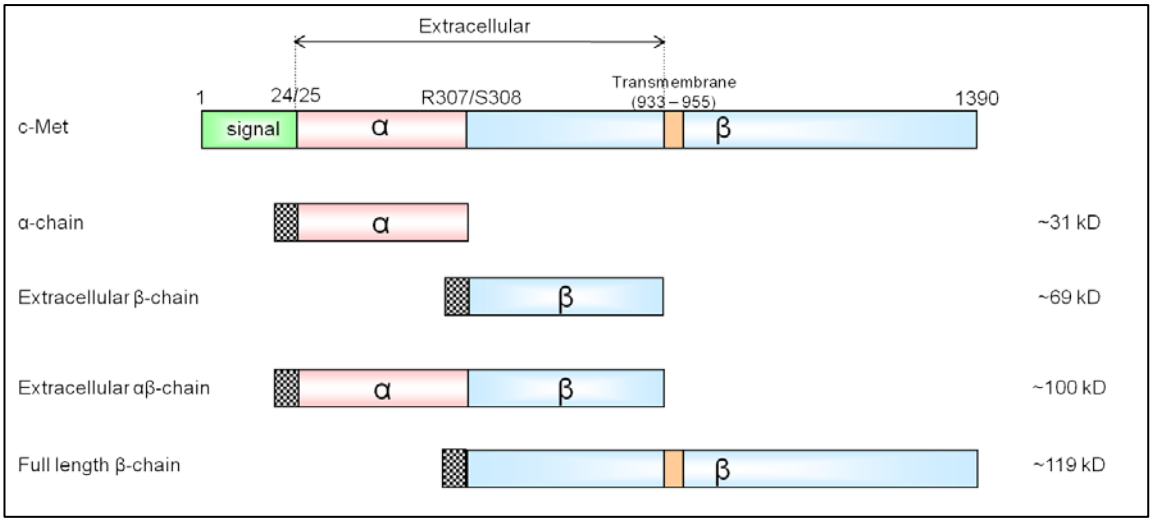

Figure 2.1: Diagram of human c-Met precursor protein and the four c-Met protein expressed in prokaryotes (not drawn to scale).

c-Met precursor is a 1390 amino acid residue protein made up of a membrane localisation signal (green), an alpha chain (pink) and beta chain (blue). The localisation signal, which directs newly synthesised c-Met to the plasma membrane, lies in the first 24 amino acid residues. Furin, an ubiquitous endoprotease, cleaves c-Met precursor at R307/S308 which divides the protein into the α-chain and β-chain. The orange box represents the transmembrane region of c-Met which spans amino acid residues 933 – 955. Four c-Met constructs, with different regions of c-Met, were cloned into pET19b vector for prokaryotic expression. The c-Met proteins were expressed with an N-terminal histidine tag (black-checked box) that that is used for protein purification. The molecular weight of each construct is noted.

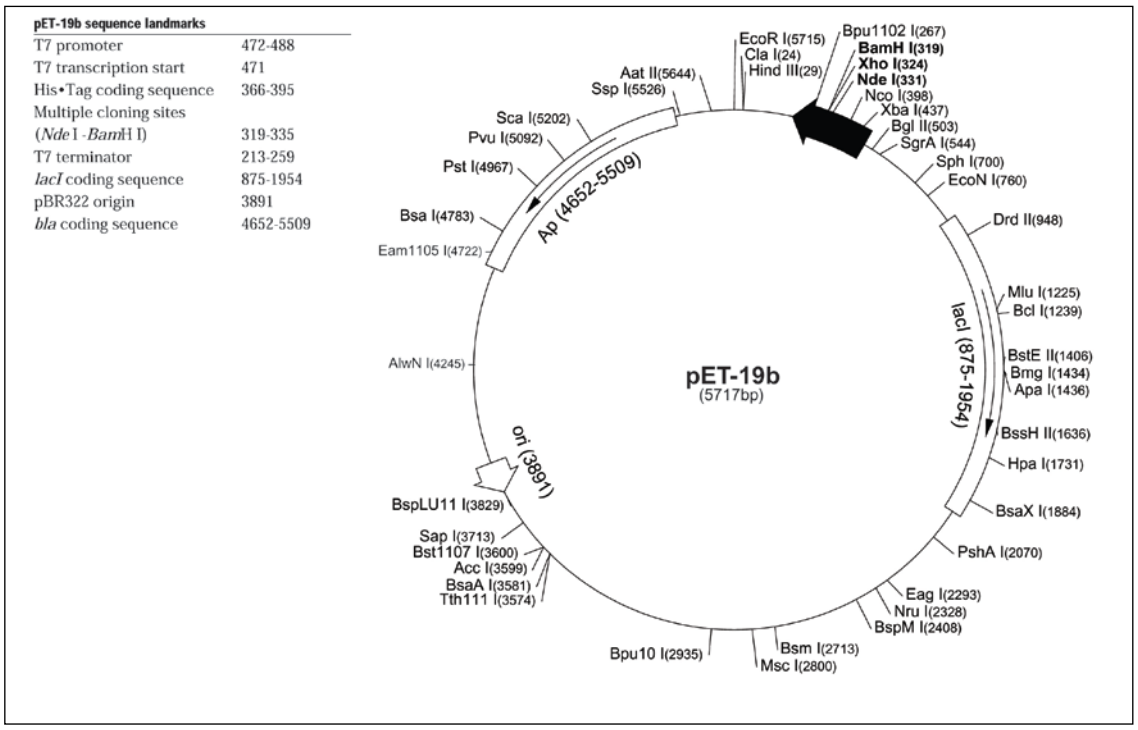

Figure 2.2: Plasmid map of pET19b.

Plasmid map was obtained from Novagen. Proteins expressed from pET19b vector contain an N-terminal histidine tag (10 histidine residues) which could be used for future protein purification or detection by Western blotting.

Table 2.2: Primer sequences used for cloning c-Met into pET19b for prokaryotic protein expression.

Primer	Sequence (5' - 3')	Restriction Sites
Alpha01F	GGAATTCcatatgGAGTGTAAAGAGGCACTAGC	NdeI
Alpha02R	GCggatccCTATCTCTTTTTTCTCTTTTCTGTGAG	BamHI
Beta03F	CCGctcgagTCCACAAAGAAGGAAGTG	XhoI
Beta04R	CCGctcgagCTATGATGTCTCCCAGA	XhoI
Beta05R	ctcgagCTATGTGAAATTCTGATCTGGTTGAACTATTAC	XhoI
AB06F	ctcgagGAGTGTAAAGAGGCACTAGCAAAG	XhoI

Restriction sites are in lower case letters.

Table 2.3: Primers used for c-Met amplification.

c-Met constructs	Forward primer	Reverse primer	Template	Tm (^{o}C)	Restriction enzyme
α-chain	Alpha01F	Alpha02R	IOH36570	65	NdeI / BamHI
Extracellular β-chain	Beta03F	Beta05R		65	XhoI / XhoI
c-Met extracellular αβ-chain	AB06F	Beta05R		65	XhoI / XhoI
Full length β-chain	Beta03F	Beta04R		65	XhoI / XhoI

Table 2.4: c-Met sequencing primers.

No.	Sequence (5’ → 3’)	Nucleotide number
JS01	GATCAACTCATTAGCTGTGGC	382 - 402
JS02	GCGTATGTCAGCAAGCCT	958 - 975
JS03	CTGCAGACATTTCCAGTCC	1557 - 1575
JS04	CAGTTACCGTGAAGATCCCAT	2208 - 2228
JS05	GAGTGGAAGCAAGCAATTTC	2728 – 2747
JS06	GGTTGTGTATATCATGGGACTTTG	3268 – 3291
JS07	GACATGTCGCTGGCAGG	419 - 435 *(c)*
JS08	CGGGTTGTAGGAGTCTTCTC	3897 - 3916 *(c)*
JS11	GAGAAGACTCCTACAACCCG	3897 - 3916

(c): complementary sequence.

Table 2.5: Bacteria characteristic used in this study for protein expression.

Bacteria strain	*lacY* mutation[1]	*Ion*[2] and *ompT*[3] mutations	Rare tRNA codon[4]	*trxB*[5] and *gor*[6] mutations	T7 lysozyme[7]	*rne131* mutation[8]
BL21 DE3		*				
BL21 Star		*				*
BL21 pLysS		*			*	
RG2 DE3			*	*		
RG2 pLysS			*	*	*	
RGB DE3	*	*	*	*		
RGB DE3 pLysS	*	*	*	*	*	

Table was adapted from pET System Manual (11th Edition). Other than BL21 star (Invitrogen), all bacteria strains were obtained from Novagen/Merck.
1) Mutation in *lac* permease provides homogenous uptake of IPTG into all cells in the population, thus facilitating concentration-dependent induction of protein expression.
2) Mutation in cytoplasmic *Ion* protease.
3) Mutation of *ompT* membrane protease prevents cleavage of some membrane proteins during purification.
4) Provides either six or seven tRNAs codons that rarely occur in *E. coli* thus increasing the expression level of proteins limited by codon usage.
5) Mutation in thioredoxin reductase facilitates disulphide bonds formation in the cytoplasm.
6) Mutation in glutathione reductase, when combined with *trxB* mutation, greatly facilitates formation of disulphide bonds in the cytoplasm.
7) Provides T7 lysozyme to reduce basal expression of target genes thus stabilising plasmids that express proteins toxic to *E. coli*.
8) Encodes for defective RNaseE gene thus increasing mRNA stability.

Prokaryotic expression of c-Met constructs

As mentioned earlier, pET19b constructs containing the various c-Met constructs were chemically transformed into seven bacteria strains (gifts from Jeffrey Hill, Experimental Therapeutics Centre, Singapore). The bacteria strains used are BL21 DE3, BL21 star, BL21 pLysS, Rosetta-gami 2 DE3 (RG2 DE3), Rosetta-gami 2 pLysS (RG2 pLysS), Rosetta-gami B DE3 (RGB DE3) and Rosetta-gami B DE3 pLysS (RGB DE3 pLysS) (listed in Table 2.5). BL21 pLysS was used for large-scale protein expression of c-Met α-chain. BL21 star was used for large-scale expression of c-Met extracellular β-chain, extracellular αβ-chain and full length β-chain. Transformed cells were grown in a 500 ml culture until an OD_{600} 0.4 to 0.6 was reached. Protein expression was induced by adding IPTG (isopropyl-β-D-thio-galactoside) to a final concentration of 1 mM.

Cultures were then further allowed to grow for 3 hrs. Cells were recovered by centrifugation at 6,000 xg for 15 mins and resuspended in 12 ml of lysis buffer (0.3 M KCL, 50 mM KH_2PO_4, pH 8.0). Cells were incubated in lysis buffer for 30 mins at 4^oC, with constant swirling before sonication. The resulting cell lysate was centrifuged at maximum speed 33,000 xg for 30 mins. The cell pellet obtained after centrifugation was resuspended in lysis buffer containing 6 M urea and incubated overnight with gentle stirring. The resulting suspension was centrifuged at 33,000 xg for 30 mins and the supernatant (pre-purified supernatant) obtained was used for protein purification.

Protein purification

Various c-Met protein constructs expressed by bacteria was affinity purified on a 1 ml IMAC (immunobilised metal affinity chromatography) Bio-Scale Mini Cartridge (Bio-Rad), using the automated Profinia protein purification system (Bio-Rad). Purified protein was eluted in 4 ml of elution buffer. Purified protein was used to immunise mice for monoclonal antibody production.

Construction of c-Met adenoviral plasmids

Construction of c-Met adenoviral plasmids were performed with reference to AdEasyTM XL Adenoviral Vector System (Stratagene/Agilent Technologies, Santa Clara, U.S.A.) and He *et al*. (1998). c-Met and cMet-SBP were amplified using Expand Long Template PCR System (Roche Applied Science, Mannheim, Germany). An outline of adenoviral plasmid construction is illustrated in Figure 2.3. Primer sequences used for the amplification are listed in Table 2.6. Amplification conditions were performed according to the PCR conditions in Table 2.7 and 2.8. c-Met and cMet-SBP

PCR fragments were ligated into the shuttle vector, pAD.Track.CMV. Ligation mixture was transformed into commercially-available DH5α cells (Invitrogen) and cells were selected on kanamycin (Sigma-Aldrich, St. Louis, U.S.A.) LB plates. Plasmids extracted from these clones were screened using KpnI and HindIII restriction enzyme digest. Positive plasmids were sequenced using c-Met internal primers listed in Table 2.4. pAD.Track.CMV positive constructs were then linearised using PmeI enzyme before phenol/chloroform purification. Purified constructs were electroporated into BJ5183-AD-1 cells (Stratagene) which contained the adenoviral plasmid, pADEasy1. This allows DNA recombination to take place between the linerised pAD.Track.CMV constructs and pADEasy1 vector within BJ5183-AD-1 cells. Transformed cells were plated on LB plates containing kanamycin. Plasmids were extracted from these clones and screened using PacI restriction enzyme digest. Digested plasmids were analysed on 0.8% low melting agarose gels (Invitrogen). Digestion of pADEasy1 constructs, containing c-Met or cMet-SBP, with PacI will produce two DNA bands (one of >10 kb and one ~4 kb).

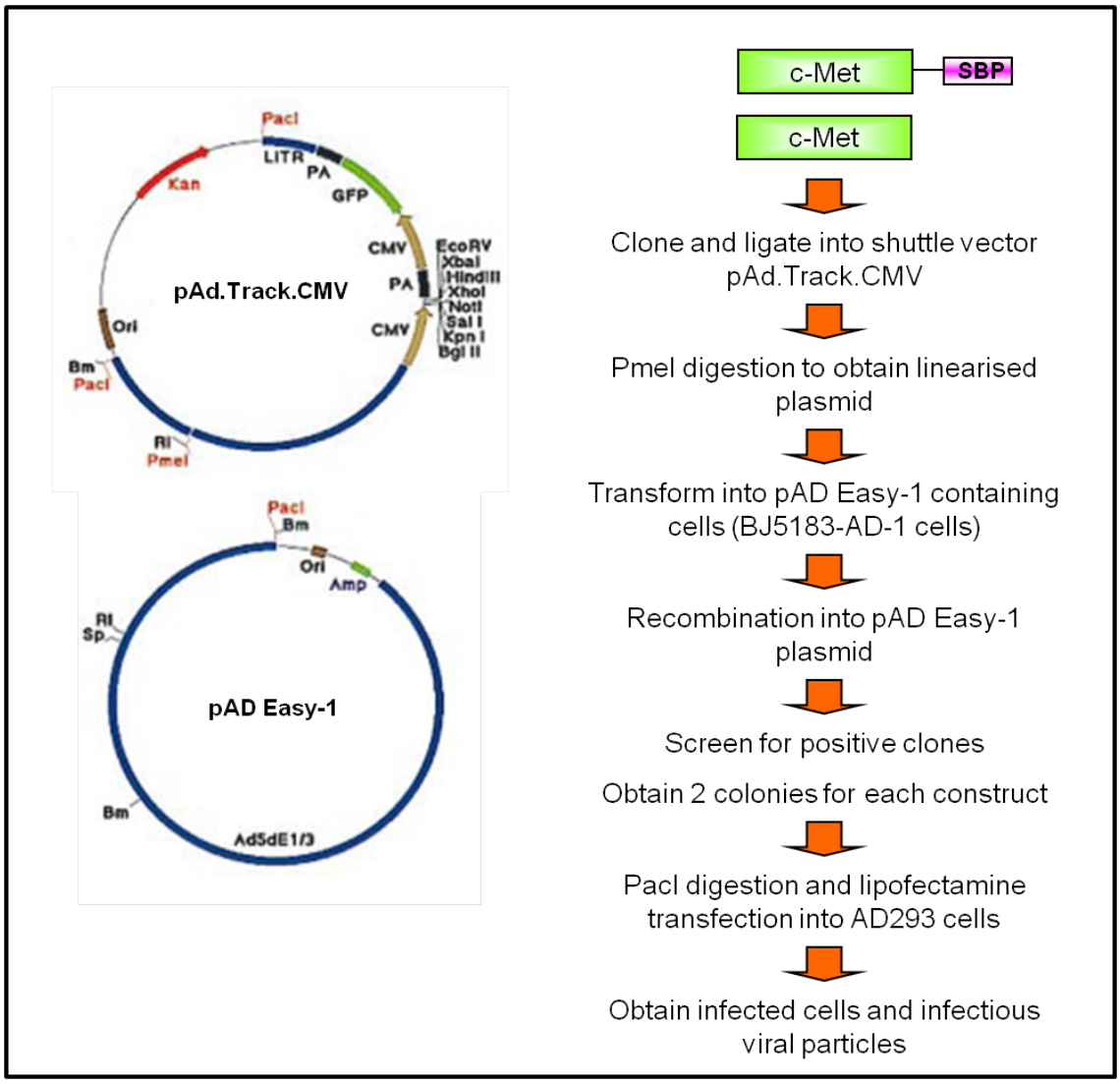

Figure 2.3: An outline of cloning c-Met constructs for adenoviral expression.

Table 2.6: Primer sequences used for cloning c-Met constructs into pAD.Track.CMV vector.

Primer	Sequence (5' - 3')	Restriction Sites
JD09	GggtaccGCCACCATGAAGGCCCCCGCTGTGCTTG	KpnI
JD10	CCCaagcttCTATGATGTCTCCCAGAAGGAGGC	HinDIII
JD11	CCCaagcttTCAGGGTTCACGCTGACCCTGC	HinDIII

Table 2.7: Conditions used for cloning c-Met for adenoviral expression.

c-Met constructs	Forward primer	Reverse primer	Template	Restriction enzyme
c-Met	JD09	JS10	pENTR221-cMet	KpnI / HindIII
cMet-SBP	JD09	JD11	pcDNA3-cMet-SBPc	

Table 2.8: PCR cycle used for c-Met and cMet-SBP amplification.

Step	Tm	Time	No. of cycle
1	92°C	1 min	1
2	92°C	10 sec	10
	60°C	30 sec	
	68°C	2 min 40 sec	
3	92°C	15 sec	15
	60°C	30 sec	
	68°C	2 min 40 sec	
		(Increase 20 sec every cycle)	
4	68°C	7 min	1
5	4°C	-	1

Amplification of functional c-Met viral particles

AD293 cells were grown in DMEM supplemented with 10% heat-inactivated FCS. During the maintenance of AD293 cell culture, care was taken to not allow cell confluence to exceed >50%. To produce viral particles, 1 x 10^5 AD293 cells were seeded in a 6-well plate before transfection. pADEasy1 constructs were linearised with PacI enzyme and transfected into AD293 cells. 2 μg of linearised pADEasy1 constructs were used for the lipofectamine transfection. Cells and media were harvested by centrifugation at 2 krpm for 3 mins at 4°C (Heraeus Accuspin 1R, rotor #3041), once the cells circularise and detach from the plate.

To test if the viral particles are infectious and express c-Met/cMet-SBP, AD293 cells were seeded in 10 cm plates. AD293 cells were allowed to grow to 90% confluence before the viral particle containing extracts (freeze-thawed for three times) were added to the cells. Cells and media were harvested as described above. Half of the cells collected were lysed in RIPA lysis buffer containing complete protease inhibitor (150 mM NaCl, 1% NP40, 0.5% DOC, 0.1% SDS, 50 mM Tris pH 8.0) and probed for c-Met expression by Western blotting. The other half was frozen at -80°C and used for bulk

amplification of viral particles. Bulk amplification of the viral particles was performed by seeding AD293 cells in forty plates of 15 cm dishes. Viral particles collected from the 10 cm plates (described above) were freeze-thawed three times before infecting the cells. Cells and media were harvested as described above. Infected cells were pooled together by centrifugation at 4 krpm for 10 mins at 4^{o}C (Heraeus Accuspin 1R, rotor #3360). Finally, the infected cells were resuspended in 10 mM Tris-Cl, pH 8.0 (0.5 ml of Tris-Cl per every 15 cm dish harvested). Viral particles obtained were freeze-thawed three times. 0.5 ml of viral particles (resuspended in Tris-Cl) was used to infect T47D cells grown to 90% confluence in a 10 cm plate.

Transfection

Lipofectamine 2000 (Invitrogen) was used to transfect NIH3T3 cells. Transfection was performed according to an optimised protocol for NIH3T3 cells. Briefly, 0.9 x 10^{6} cells were seeded on a 10 cm plate. 9 μg of DNA and 45 μl of lipofectamine, both diluted in Optimem Reduced Serum Medium (Invitrogen), were added to cells. Media was replaced after 4 hrs and cells were left to grow for 48 hrs before harvest. Amount of cells, DNA, lipofectamine and Optimem were scaled proportionally according to size of the tissue culture plates/dishes.

Cell harvest and cell lysis

Cell culture plates/dishes were rinsed three times with cold PBS before the cells were scraped off. Cells were collected by spinning in a microcentrifuge for 5 mins at 233 xg, at 4^{o}C. PBS was removed before quick freezing the cell pellet on dry ice. The frozen cell pellet was lysed on ice using NP40 lysis buffer (1% NP40, 150 mM NaCl, 50 mM

Tris-HCL pH 8.0) containing complete protease inhibitor (Roche, West Sussex, United Kingdom, #11 697 498 001) for 30 mins. Cell debris was spun down at 10,000 xg for 10 mins, at 4^{o}C. The supernatant was recovered for analysis. Protein quantification was performed using a BCA kit (Pierce/Thermo Scientific), according to the manufacturer's protocol.

Western blots and antibodies

Protein samples were mixed with 4X LDS sample buffer (Invitrogen) and 10X sample reducing agent (Invitrogen) before analysing on a 4 -12% Bis-Tris gradient gels (Invitrogen) using MOPs buffer (Invitrogen). SeeBlue Plus2 protein ladder (Invitrogen) was used as molecular weight ladder. Transfer of proteins onto a nitrocellulose membrane (0.45 μm pore size, Whatman, Kent, United Kingdom) was performed using Bio-Rad wet transfer system for 2 hrs, at a constant current of 100 V. Transfer buffer contains 25 mM Tris, 192 mM and 20% methanol. Blocking buffer was made up of 5% Marvel in PBST (1% Tween20 in PBS) (w/v). Non-specific sites on the membrane were blocked in blocking buffer for 1 hr before incubating with primary antibodies. The membrane was washed three times and secondary antibodies were added at 1:10 000 dilutions in blocking buffer. The working dilutions and information of primary antibodies can be found in Table 2.9. Secondary antibodies conjugated to horseradish peroxidise (HRP) were obtained from Jacksons Laboratory/Stratech Scientific Ltd. (Suffolk, United Kingdom). Enhanced chemiluminescence (ECL) (Amersham/G.E. Healthcare) was used for the detection of Western blots.

Table 2.9: Primary antibodies used in this study for Western blotting.

Antibody	Company / Catalogue number	Origin	Specificity	Monoclonal / Polyclonal	Incubation time	Working dilution
Anti-cMet (C-12)	Santa Cruz / #SC-10	Rabbit	Peptide located in c-Met cytoplasmic domain	Polyclonal	12 - 24 hrs	1:10 000
Anti-cMet (AF276)	R&D systems / #AF276	Goat	Extracellular domain of c-Met	Polyclonal	12 - 24 hrs	1:10 000
Anti-cMet (EY1454Y)	Abcam / #EY1454Y	Rabbit	N-terminus of c-Met	Monoclonal	12 - 24 hrs	1:10 000
Anti-α-Met (Mab 18.1)	In house	Mouse	α-chain of c-Met	Monoclonal	12 - 24 hrs	1 µg/ml
Anti-phospho-cMet	Invitrogen / #44888G	Rabbit	Phospho-cMet (pYpYpY1230/1234/1235)	Polyclonal	12 - 24 hrs	1:500
Anti-GFP (Clone 7.1 and 13.1)	Roche Diagnostic / #11 814 460 001	Mouse	GFP	Monoclonal	1 hr	1:5 000
Anti-His-Peroxidase (BMG-His-1)	Roche Diagnostic / #11 965 085 001	Mouse	6 constitutive histidine residues	Monoclonal	1 hr	1:5 000
Streptavidin Peroxidase Polymer	Sigma-Aldrich / #S2438	-	Biotinylated biomolecules	-	1 hr	1:2 000
Anti-V5 (Clone 336)	Gift from Dimitri Xirodimas	Mouse	V5 tag	Monoclonal	1hr	1:5 000
Anti-β-actin (AC-15)	Sigma-Aldrich / #A5441	Mouse	β-Actin	Monoclonal	1 hr	1:10 000
Anti-PCNA (PC10)	Moravian Biotechnology	Mouse	PCNA	Monoclonal	1 hr	1:5 000
Anti-α-tublin (B-5-1-2)	Sigma-Aldrich / #T5168	Mouse	α-Tublin	Monoclonal	1 hr	1:8 000
Anti-ERK	Cell Signalling / #9102	Rabbit	ERK 1/2	Polyclonal	12 - 24 hrs	1:1 000
Anti-phospho-ERK	Cell Signalling / #9101	Rabbit	Phospho-ERK 1/2 (Thr 202 / Tyr 204)	Polyclonal	12 - 24 hrs	1:1 000
Anti-AKT	Cell Signalling / #9272	Rabbit	AKT	Polyclonal	12 - 24 hrs	1:1 000
Anti-phospho-AKT Thr308	Cell Signalling / #9275	Rabbit	Phospho-AKT (Thr 308)	Polyclonal	12 - 24 hrs	1:1 000
Anti-phospho-AKT Ser473	Cell Signalling / #9271	Rabbit	Phospho-AKT (Ser 473)	Polyclonal	12 - 24 hrs	1:1 000

Immunoprecipitation

Cells lysates were obtained by lysing cells in NP40 lysis buffer as described above. 1 μg of purified antibody was incubated with cell lysate (200 μg – 500 μg of total protein in approximately 500 μl) at 4^{o}C, overnight. 20 μl of washed protein G beads (Sigma-Aldrich) were added to the cell lysate and incubated for 45 mins at 4^{o}C, with rotation. Beads were collected by spinning at 18,000 xg for 5 mins at 4^{o}C. Beads were washed several times with NP40 lysis buffer. Bound proteins were eluted by adding 60 μl of 2X LDS sample buffer (Invitrogen) and the samples heated at 100^{o}C for 5 mins. Beads were removed from eluate by centrifugating at 10,000 xg for 1 min. The eluate was analysed by SDS-PAGE gel.

SBP pull down experiments

Cells, grown to 90% confluency in a 10 cm plate, were harvested and lysed in NP40 lysis buffer (as described above). Cell lysate was pre-cleared with 10 μl of avidin-conjugated agarose beads (Pierce/Thermo Scientific, #20219). The avidin-conjugated beads were removed from the cell lysate by centrifugation before the addition of 40 μl of streptavidin-conjugated magnetic beads (Dynal/Invitrogen, #112.06). Streptavidin-conjugated beads were incubated with the pre-cleared cell lysate for 2 hrs at 4^{o}C, with rotation. Beads were washed several times with wash buffer (0.1% Tween 20, 150 mM NaCl, 10 mM HEPES) before elution with PBS containing 1 mM of biotin. Eluted proteins were analysed by SDS-PAGE gel.

Antibody production

Antibody production was performed by Dr. Borek Vojtesek from Moravian Biotechnology (Czech Republic). A brief overview of monoclonal antibody production is described in Figure 2.4

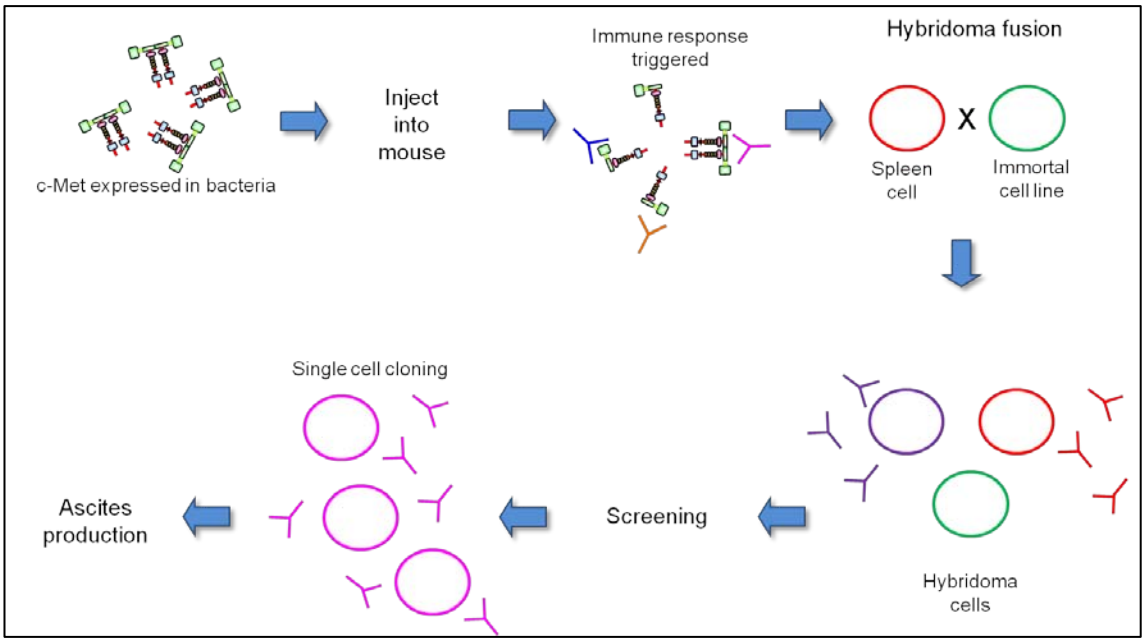

Figure 2.4: Overview of monoclonal antibody production.
Various c-Met constructs were expression in bacteria and purified. The α-chain and the extracellular β-chain were selected for mouse immunisation. Tail bleeds of these mice were obtained to test the immunological response raised against the immunogen. Only mice immunised with the α-chain were sacrificed for hybridoma fusion. Hybridoma cells obtained were grown in selection medium containing hypoxanthine, aminopterin and thymidine. Hybridoma cells that survived in the selection media were screened (primary and secondary screening) for production of anti-α-chain antibodies. Positive hybridoma lines were single-cell cloned and the monoclonal antibodies produced were characterised. Finally, hybridoma clones were selected for ascites production. Antibodies obtained from ascites were purified and characterised further.

Immunisation

Four BALB/c mice were immunised with either purified human c-Met alpha chain or extracellular beta chain. Each injection contained 40 µg of purified protein. The first three injections were done monthly with either complete Freund's Adjuvant (first injection) or incomplete Freund's Adjuvant (second and third injection). Mouse serum was taken after the second injection to test for immunological response against the immunogen. Two mice that gave the highest specific immune response were given the

fourth and fifth injection which was three days and five days, respectively, before the fusion. The fourth and fifth injections did not contain Freund's Adjuvant.

Fusion

Two mice were sacrificed for hybridoma fusion. Spleen cells of the mice were fused with SP2./0-Ag14 cells which are mouse immortal myeloma cells. Hybridoma cells were grown in selection media containing hypoxanthine, aminopterin and thymidine and only hybridoma cells which have been successfully fused between a spleen cell and an immortal cell will survive and grow in the selection media.

Antibody screening

An outline of monoclonal antibody screening is shown in Figure 2.5.

Primary hybridoma screen

Hybridoma cells were screened for anti-α-chain antibody production ten days after cell fusion. This was performed in collaboration with Moravian Biotechnology. Hybridoma supernatants were screened for immunoglobulin (Ig) production and recognition of purified c-Met alpha chain using dot blot technique. Briefly, rabbit anti-mouse antibody (DAKO (Denmark), #Z0109, diluted 1:100), or purified c-Met alpha chain (20 μg/ml) was incubated on nitrocellulose membrane for 2 hrs before rinsing off with PBS. The membrane was blocked in 10% FCS/DMEM then hybridoma supernatants were added. Hybridoma supernatants (~2 μl) were incubated on the nitrocellulose membrane for 1 hr, at room temperature, in a humidity chamber. The supernatants were then rinsed off with PBS and HRP-conjugated anti-mouse antibody (DAKO, P0161, diluted 1:100) was added to the nitrocellulose membrane. The secondary antibody was rinsed off in PBS and a substrate solution was added. This was made up by dissolving a 4-chloro-1-naphthol tablet (Sigma-Aldrich) in 10 ml methanol. 30 ml of PBS was then added and

the solution was filtered. 200 µl of hydrogen peroxide was added before the substrate solution was added onto the dot blot. The reaction was stopped by rinsing the blot in tap water.

Hybridoma supernatants were also screened by Western blotting and cell staining. The Western blotting protocol was mainly performed as described above, except that purified α-chain was resolved on a single well SDS-PAGE gel before the proteins were transferred onto a nitrocellulose membrane. The membrane was cut into strips and neat hybridoma cell supernatant were incubated directly on it. HRP-conjugated anti-mouse secondary antibody (DAKO) was added at 1:1000 dilution for the detection of mouse monoclonal antibodies. For cell staining, NIH3T3 cells were transfected in a 6 cm dish, as described above, with constructs expressing c-Met or Met-V5 (pcDNA3-Met or pCMV-Met-V5). Cells were washed twice with cold PBS and fixed with cold 1:1 acetone/methanol for 6 mins. Acetone/methanol was aspirated off and the plates were left to dry. Grids (0.5 cm x 0.5 cm) were drawn on the opposite side of the tissue culture dish. Approximately 2 µl of supernatant was added in each grid (cell surface side) and incubated in a humidity chamber overnight at 4^{o}C. Cell supernatant was rinsed off three times with PBS and HRP-conjugated anti-mouse secondary antibody, diluted 1:100 in DMEM containing 10% FCS, was added to the fixed cells for 1 hr at room temperature. Cells were rinsed in PBS three times. DAB (Diaminobenzidine, Vector Labs, CA, U.S.A.) substrate was freshly made up and added to cells for approximately 2 mins or until the desired staining intensity develops. The reaction was stopped by rinsing in water (Lane and Lane, 1981). 57 hybridoma cells lines were identified to produce antibodies against c-Met α-chain.

Secondary antibody screening

57 antibodies identified in the primary screen were expanded and tested again for their reactivity against c-Met in the secondary antibody screen. We tested our monoclonal antibodies by Western blotting. Dot blot and cell staining screens were carried out by Moravian Biotechnology. We characterised the ability of our antibodies to detect transfected c-Met and endogenous c-Met from whole cell lysates by Western blot. NIH3T3 cells were transfected with c-Met and Met-GFP (as described above). Whole cell lysate of NIH3T3 transfected cells, U-87MG cells and T47D cells were obtained by directly lysing the cells in boiling 2X LDS. Protein concentration was determined using the BCA kit and 50 μg of whole cell lysates were analysed on SDS-PAGE gel. Western blotting technique was performed as described above with the exception that hybridoma cell supernatants were diluted 1:1 in 5% Marvel/PBST (w/v).

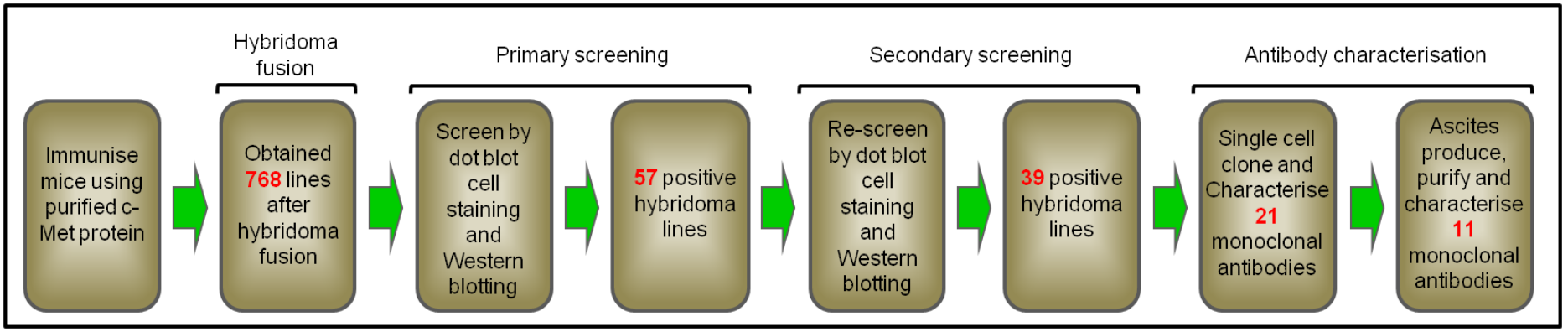

Figure 2.5: Outline of monoclonal antibody screening.
768 cell lines were screened for the production of anti-α-chain antibodies after hybridoma fusion. 57 lines were found to express anti-α-chain antibodies in the primary screen. These lines were expanded and tested again for the production of anti-α-chain antibodies in the secondary screen. 39 lines were observed to stably express anti-α-chain antibodies. 21 lines were selected for single-cell cloning with advice from Moravian Biotechnology. These antibodies were then characterised for region of binding, isotype subclasses, functional assays (ERK phosphorylation and cell scatter), ability to cause cell cluster and functionality on Western blots. Based on these assays, 11 clones were selected for ascites production. Monoclonal antibodies were purified from ascites and characterised further.

Isotyping

Mouse monoclonal antibodies isotype were characterised using the commercially-available IsoQuick™ strips (Sigma-Aldrich). Isotyping strips were incubated in hybridoma cell supernatant for 5 mins. A red test line will develop on the strip. The position of the red test line is dependent on the antibody's isotype, thus by referencing to the manufacturer's isotyping chart, the antibody's isotype is determined.

Pepscan

Peptides that span the entire alpha chain of c-Met was synthesised by Mimotopes (Australia). Peptides were linked to biotin by an SGSG linker sequence at the N-terminus. A total of fifty-five peptides with consecutive, overlapping sequences were synthesised. Each peptide consists of 15 amino acid residues and overlapped the previous peptide by 10 amino acid residues. Streptavidin-coated plates (Pierce/Thermo Scientific, #15520) were blocked with 3% BSA/PBS (w/v) (200 µl per well) for 2 hrs at room temperature. The peptides were dissolved in DMSO and stored according to manufacturer's recommendation. Streptavidin-coated plates were coated with each peptide (5 µg/ml) overnight at room temperature, in a humidity chamber. Wells were washed with 200 µl of 1% NP40/PBS (v/v). 100 µl of hybridoma supernatant (diluted 1:10 in 1% BSA/PBS (w/v)) was added to the each well and the plate was incubated at room temperature for 2 hrs in a humidity chamber. The wells were washed again in 1% NP40/PBS. HRP-conjugated anti-mouse antibody (DAKO, diluted 1:1000 in 1% BSA/PBS) and incubated at room temperature for 2 hrs. The wells were washed again in 1% NP40/PBS. 50 µl of ELISA substrate (Bio-Rad #172-1067) solution was prepared freshly according to the manufacturer's instructions and added to the wells. Colour change was monitored by eye and the reaction was stopped by adding 50 µl of 100 mM

sulphuric acid. Absorbance was read at 450 nM in a microplate reader (SPECTRAmax PLUS^{384}, Molecular Device, CA, U.S.A.). The crystal structure of c-Met extracellular domain, 1SHY, was obtained from Protein Data Base (PDB). Computer imaging of the epitopes were analysed by PyMol (DeLano Scientific LLC, Hamilton Avenue, U.S.A.) software.

Cell cluster assay

0.004 x 10^6 SNU-5 cells/well were seeded in 24-well plates containing the indicated dilution of hybridoma cell supernatant. Hybridoma cell supernatant were diluted in 10% heat-inactivated FCS/RPMI. Cell clumping were observed 24 - 48 hrs later. Cell clumping was observed using Zeiss Axiovert 25 inverted microscope and pictures were taken using Canon EOS 1000 D.

Cell scatter assay

100 - 200 HaCaT cells were seeded in 24-well plates and allowed to grow until small colonies were formed (approximately 7 days). Cells were serum-starved for 24 hrs. Cells were incubated with hybridoma supernatants (dilutions as indicated) or purified monoclonal antibodies (1 μg/ml) for 1 hr before 10 ng/ml of HGF was added. Cells were incubated for 24 hrs before rinsing twice in cold PBS and fixing in ice-cold methanol for 10 mins. Cells were then stained in 1% crystal-violet (w/v) (Sigma-Aldrich) solution for 5 mins. Antibody against HGF, anti-HGF, or SU11274 was used as a control. 5 μg/ml of anti-HGF was pre-incubated with HGF for 1 hr before adding to cells. SU11274 was added to a final concentration of 5 μM for 1 hr before HGF was

added to the cells. Cell staining was observed using Zeiss Axiovert 25 inverted microscope and pictures were taken using a Canon EOS 1000 D camera.

ERK phosphorylation assay

HaCaT cells (0.3 x 10^6 cells/well) were seeded in a 24-well plate and serum starved for 24 hrs. Cells were incubated with hybridoma supernatants (dilutions as indicated) or purified monoclonal antibodies (1 μg/ml) for 1 hr before 10 ng/ml of HGF was added. Cells were incubated with HGF for 30 mins. Antibody against HGF, anti-HGF, or SU11274 was used as a control. 5 μg/ml of anti-HGF was pre-incubated with HGF for 1 hr before adding to cells. SU11274 was added to a final concentration of 5 μM for 1 hr before HGF was added to the cells. Cells were immediately rinsed three times with cold PBS and lysed immediately in 100 μl of boiling 2X LDS loading buffer. The cell lysate was sonicated (three times, 10 sec each) and protein concentrations were determined using Pierce/Thermo Scientific BCA kit. Cell lysates were analysed by Western blotting as described above. The antibodies used for Western blotting are listed in Table 2.9.

Flow cytometry

Flow cytometry was performed with enormous help from Michael Boylan (Flow Cytometry Core Facility, College of Medicine, Dentistry and Nursing, University of Dundee, UK).

T47D were trypsinised to remove them from tissue culture flask. T47D and SNU-5 cells (1 x 10^6 cells) were washed once in cold PBS before blocking in 1% BSA/PBS (w/v) for 15 mins at 4^oC. Cells were then washed twice in cold 1% BSA/PBS before primary antibodies (diluted in 1% BSA/PBS) were added for 30 mins at 4^oC, with rotation.

Primary antibodies, AF276 or c-Met monoclonal antibodies, was used at 1:70 dilution or 1 μg/ml respectively. Cells were washed in cold 1% BSA/PBS before incubating with FITC-conjugated secondary antibodies (diluted 1:500 with 1% BSA/PBS) for 30 mins at 4^{o}C, with rotation. FITC-conjugated secondary antibodies were obtained from Invitrogen: Alexa Fluor 488 donkey anti-goat IgG (#A11055) and goat anti-mouse IgG (#A11029). Cells were finally washed twice in cold 1% BSA/PBS and resuspended in 500 μl of 1% BSA/PBS. Flow cytometry was performed using Becton Dickinson (New Jersey, U.S.A.) FACScan. Cell Quest (Becton Dickinson) and FlowJo (Tree Star Inc., Ashland, U.S.A.) software was used for data analysis.

Immunofluorescence

SNU-5 cells (0.2 x 10^6 cells/slide) were washed once with PBS and deposited onto polylysine-coated slides (Thermo Scientific, #5991056) using the Thermo Shandon Cytospin 3 Cytofuge (Thermo Scientific) at 800 rpm for 5 mins and fixed immediately. T47D cells (0.8 x 10^5 cells/well) were seeded onto 4-well Permanox chamber slides (Nunc/Thermo Scientific, #177429) and were washed three times with PBS before fixation.

Cells were fixed at 4^{o}C for 10 mins in 1:1 cold methanol/acetone. Cells were permeablised and blocked in PBS containing 0.4% Triton X-100 (v/v) and 5% BSA (w/v). Blocking was performed for 30 mins before primary antibody was added and incubated overnight at 4^{o}C. Slides were washed twice in PBS before FITC-conjugated antibody (1:500 dilution) was added and incubated for 1 hr at room temperature. Cells were washed twice again before staining with DAPI (stock concentration of 0.5 μg/ml in PBS) for 5 min at room temperature. Slides were washed once with PBS before mounting with Hydromount (National Diagnostics, Georgia, U.S.A.) containing 2.5% DABCO (1,4- Diazabicyclo-[2.2.2]octane) (Sigma-Aldrich) as an anti-bleaching agent.

Primary antibodies, AF276 or c-Met monoclonal antibodies, was used at 1:70 dilution or 1 μg/ml respectively. FITC-conjugated secondary antibodies were obtained from Invitrogen: Alexa Fluor 488 donkey anti-goat IgG (#A11055) and goat anti-mouse IgG (#A11029). Immunofluorescence was observed using Nikon Eclipse E600 microscope.

CHAPTER 3: RESULTS

3.1: Developing and building bio-tools required for the anti-Met monoclonal antibody screening and development.

3.1.1: Initial analysis of c-Met expression

The original aims of this work were to develop antibodies to native human c-Met by expressing human c-Met in a murine fibroblast cell line, NIH3T3, and using whole live cells as an immunogen in mice. Our initial attempts to study c-Met were difficult due to lack of useful reagents, such as antibodies, and cell lines that are known to be positive or negative for c-Met expression. Therefore, we needed to develop constructs expressing human c-Met and to analyse expression of both transfected and endogenous c-Met in various cell lines.

Full length human c-Met cDNA, commercially obtained from Invitrogen (IOH 36570), came ready-cloned in the Gateway entry plasmid, pENTR221. In order to express human c-Met in NIH3T3 cells, c-Met cDNA was cloned into the mammalian expression vector, pcDNA3-GW-DEST, using the Gateway LR clonase system. This plasmid was then transiently transfected into NIH3T3 cells and cell lysates were prepared for Western blot analysis. To compare c-Met expression levels in human cell lines, whole cell lysates from various cell lines were analysed on a Western blot using the commercial c-Met polyclonal antibodies SC-10 and AF276. These two antibodies were identified from a literature search to be specific to human c-Met and to be the most commonly-used antibodies for c-Met research. SC-10 is a polyclonal antibody that was raised against a peptide within the C-terminal cytoplasmic region of human c-Met and would be expected to recognise c-Met precursor and mature c-Met β-chain on Western blots. AF276 is a polyclonal antibody raised against the extracellular domain of human

c-Met and should recognise c-Met precursor, mature c-Met α-chain and mature c-Met β-chain on Western blots. Whole cell lysate from NIH3T3 cells expressing human c-Met was analysed along with the lysates from the various human cell lines (Figure 3.1).

c-Met would normally give rise to three protein bands on a Western blot: a 170 kD band that represents c-Met precursor, consisting of the α- and β-chain translated together, a 50 kD band that represents c-Met α-chain, and a 145 kD protein band that represents the mature c-Met β-chain. The disulphide bridge between the α-chain and β-chain is predicted to be broken as the samples are prepared under reducing conditions. Analysis of c-Met expression in these cell lines was difficult to interpret due to multiple bands on the Western blot (Figure 3.1). In addition, the rabbit polyclonal commercial antibody, SC-10, weakly recognises a protein band of similar molecular weight to c-Met in untransfected NIH3T3 cells. The AF276 antibody, goat polyclonal, does not recognise the same protein band as SC-10 in the untransfected NIH3T3 sample. Without a cell lines to provide positive and negative controls, it is difficult to interpret if the commercial antibodies recognise human c-Met and/or also the murine homolog of c-Met.

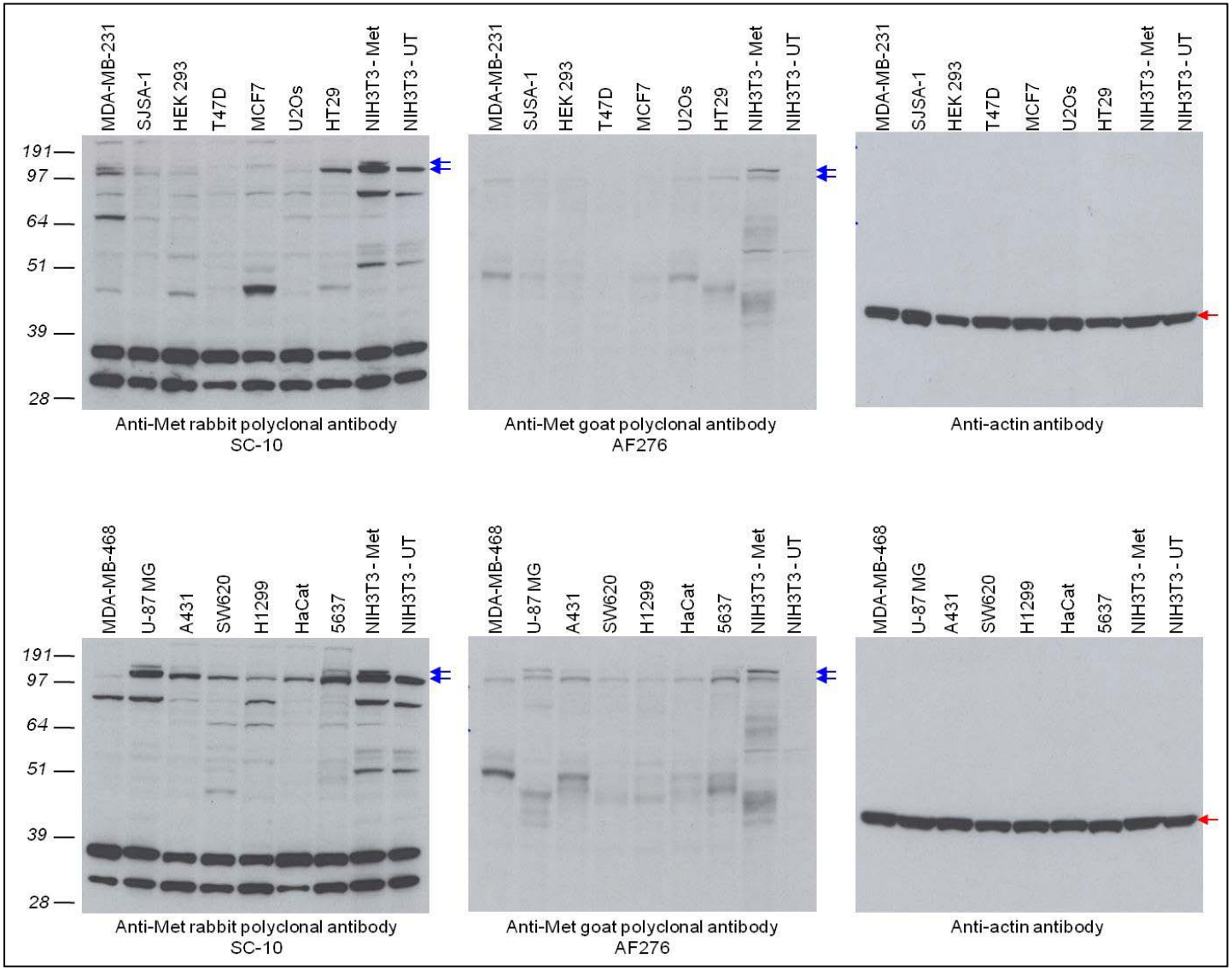

Figure 3.1: Western blot analysis of c-Met from various cell lines.
50 µg of total cell lysate (samples provided by P. Robertson) from various cell lines were analysed for c-Met protein expression. c-Met was detected using the commercial antibodies SC-10 and AF276. NIH3T3 transfected with human c-Met was used as a control. Blue arrows indicate predicted precursor c-Met protein band (top band) and c-Met β-chain (bottom band). Actin was used as a loading control. Red arrows indicate actin band. Molecular weights are noted aside, in kilodaltons. NIH3T3: NIH3T3 cells transfected with human c-Met; UT: Untransfected NIH3T3 cells.

3.1.2: Analysis of c-Met commercial antibodies

SC-10 and AF276 antibodies were identified during a literature search to identify reliable commercial c-Met antibodies used to examine c-Met expression. However, these antibodies gave conflicting results in the analysis of c-Met expression from various cell lines as shown in Figure 3.1. A third commercial antibody, EP1454Y from Abcam, was identified by scanning through commercial c-Met antibodies offered by various biotechnology companies. EP1454Y is an anti-peptide human-specific rabbit monoclonal antibody. The antibody datasheet describes that EP1454Y epitope lies in the N-terminal region of c-Met, but it is not clear if this is the α or β-chain of c-Met. According to the datasheet, this antibody should recognise a single band at approximately 160 kD using 293 cell lysates. To compare these c-Met commercial antibodies (SC-10, AF276 and EP1454Y), endogenous c-Met was immunoprecipitated (IP) from H1299 cell lysate (human lung cancer cell line). H1299 cells were used because they were easily availability in the laboratory and preliminary results suggest that they were positive for c-Met expression (Figure 3.1). Immunoprecipitated proteins were analysed by Western blotting using commercial c-Met antibodies (Figure 3.2).

EP1454Y antibody failed to immunoprecipitate any c-Met (precursor or β-chain) protein of the predicted molecular weight that could be detected by SC-10, AF276 antibodies or by itself. EP1454Y also failed to detect c-Met immunoprecipitated by SC-10 and AF276 on a Western blot, though it detected a single high molecular weight band in the input sample. This protein band is similar to the c-Met protein band shown in EP1454Y datasheet. It is very unlikely that this band represents c-Met as the same band was not detected by EP1454Y in the samples immunoprecipitated by SC-10, AF276 antibodies or by itself. Moreover, the same band was also not immunoprecipitated by EP1454Y shown in the SC-10 and AF276 blots. SC-10 and

AF276 both successfully immunoprecipitated c-Met and successfully detected immunoprecipitated c-Met on a Western blot. EP1454Y was not used for any further analysis.

To investigate further the specificity of SC-10 and AF276 antibodies, the mouse cell line, NIH3T3, was transfected with human c-Met tagged to a C-terminal GFP (Met-GFP). Processing of the full length Met-GFP precursor will result in an un-tagged α-chain and a GFP-β-chain fusion. Met-GFP was immunoprecipitated by either SC-10 or AF276 and the immunoprecipitated proteins were analysed by Western blotting with anti-GFP, SC-10 and AF276 antibodies (Figure 3.3). As observed from the anti-GFP blot, Met-GFP was clearly detectable. Both SC-10 and AF276 antibodies managed to successfully immunoprecipitate Met-GFP from the cell lysate, confirming that these antibodies are able to bind to human c-Met. However, the intense Met-GFP band detected by the anti-GFP antibody (within a relatively short exposure) suggests that this antibody has a much higher affinity for its target that the c-Met commercial antibodies. From Figure 3.3, it is observed that SC-10 and AF276 antibodies successfully immunoprecipitated transfected c-Met (i.e. Met-GFP), but failed to immunoprecipitate and/or detect endogenous murine c-Met. This indicates that either the antibodies do not recognise murine c-Met or that NIH3T3 cells do not express c-Met. Finally, in the anti-GFP antibody blot, it is observed that the protein bands of c-Met in the input samples are smaller than the immunoprecipitated samples. The reason causing the molecular weight difference is unclear, however, it is possible that the process of immunoprecipitating c-Met on a protein bead is similar to the overexpression of c-Met on the cell surface of cancer cells. Clustering of c-Met on a surface leads to self-dimerisation and self-activation of c-Met. c-Met may be phosphorylated which could cause an apparent increase in molecular weight.

The SC-10 antibody blot had high levels of apparently non-specific bands. As observed in the rabbit immunoglobulin sample, non-specific rabbit immunoglobulins which bound to the protein beads were eluted together with immunoprecipitated Met-GFP. The rabbit immunoglobulins are detected by the secondary antibody (anti-rabbit secondary antibody) used in the Western blot analysis, resulting in the protein smear observed. SC-10 antibody was able to detect c-Met immunoprecipitated by SC-10 and AF276 antibodies.

The AF276 blot had fewer non-specific bands compared to the SC-10 antibody blot. AF276 antibody successfully detected Met-GFP immunoprecipitated by SC-10 and AF276 antibodies. The non-specific protein bands observed at approximately 51 kD and 25 kD correspond to the heavy and light chain of the antibody used for immunoprecipitation.

To compare the efficiency of both commercial antibodies (SC-10 and AF276) to immunoprecipitate Met-GFP, cell lysates obtained after immunoprecipitation (depleted cell lysate) were collected and analysed on Western blots using anti-GFP antibodies (Figure 3.4). Clearly, AF276 antibody is more efficient in immunoprecipitating Met-GFP compared to SC-10 antibody. This could be due to the different epitopes that the antibodies recognise. AF276 epitopes lies in the extracellular region of c-Met (α- and β-chain) while SC-10 antibody recognises the C-terminal region of c-Met β-chain. The epitope for SC-10 could be partially obscured by the GFP tag which is constructed in the C-terminus tail of Met-GFP. Finally, AF276 antibody showed stronger band intensity in the c-Met precursor band compared to the mature β-chain. This suggests that either the main epitopes of AF276 antibody (goat polyclonal antibody) lie in the α-chain or that AF276 antibody has a higher affinity to c-Met α-chain compared to the β-chain.

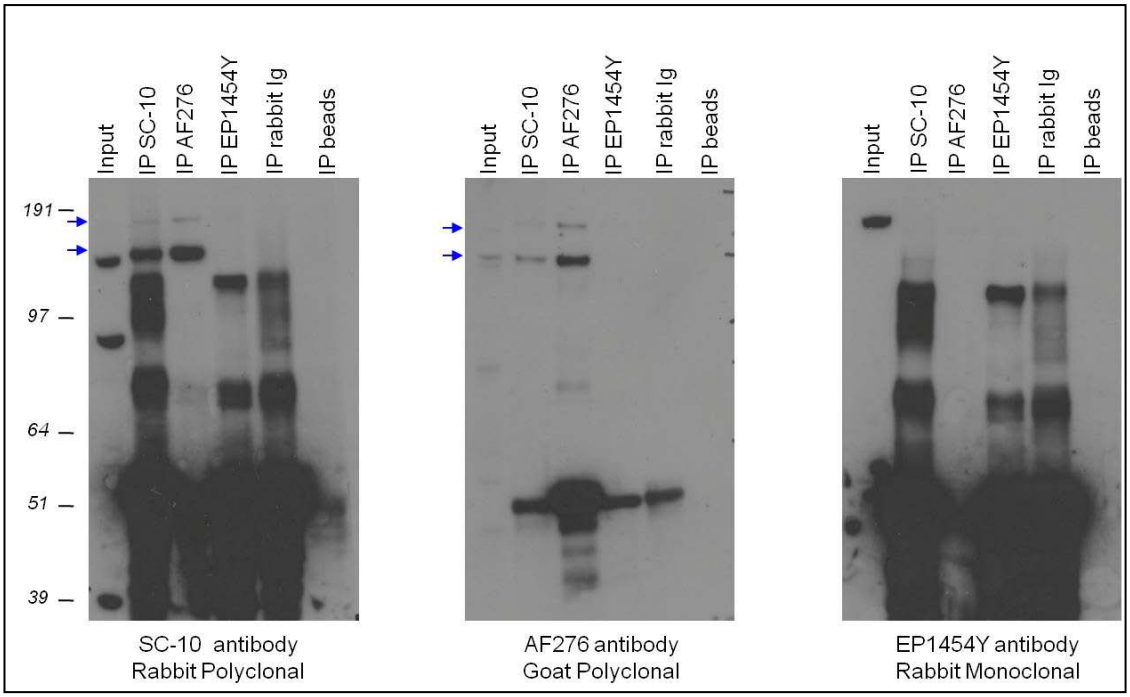

Figure 3.2: Western blot analysis of c-Met immunoprecipitation (IP) with various anti-cMet antibodies.

Proteins were immunoprecipitated from H1299 cell lysate using antibodies as shown and detected with antibodies shown below each panel. Control immunoprecipitations were performed with rabbit immunoglobulin (rabbit Ig) and protein G beads alone. Inputs are whole cell lysate before immunoprecipitation. Input samples contain $1/10^{th}$ of the amount of samples used for immunoprecipitation. Arrows indicate c-Met protein bands at 145 kD and 170 kD. Molecular weights are noted aside, in kilodaltons.

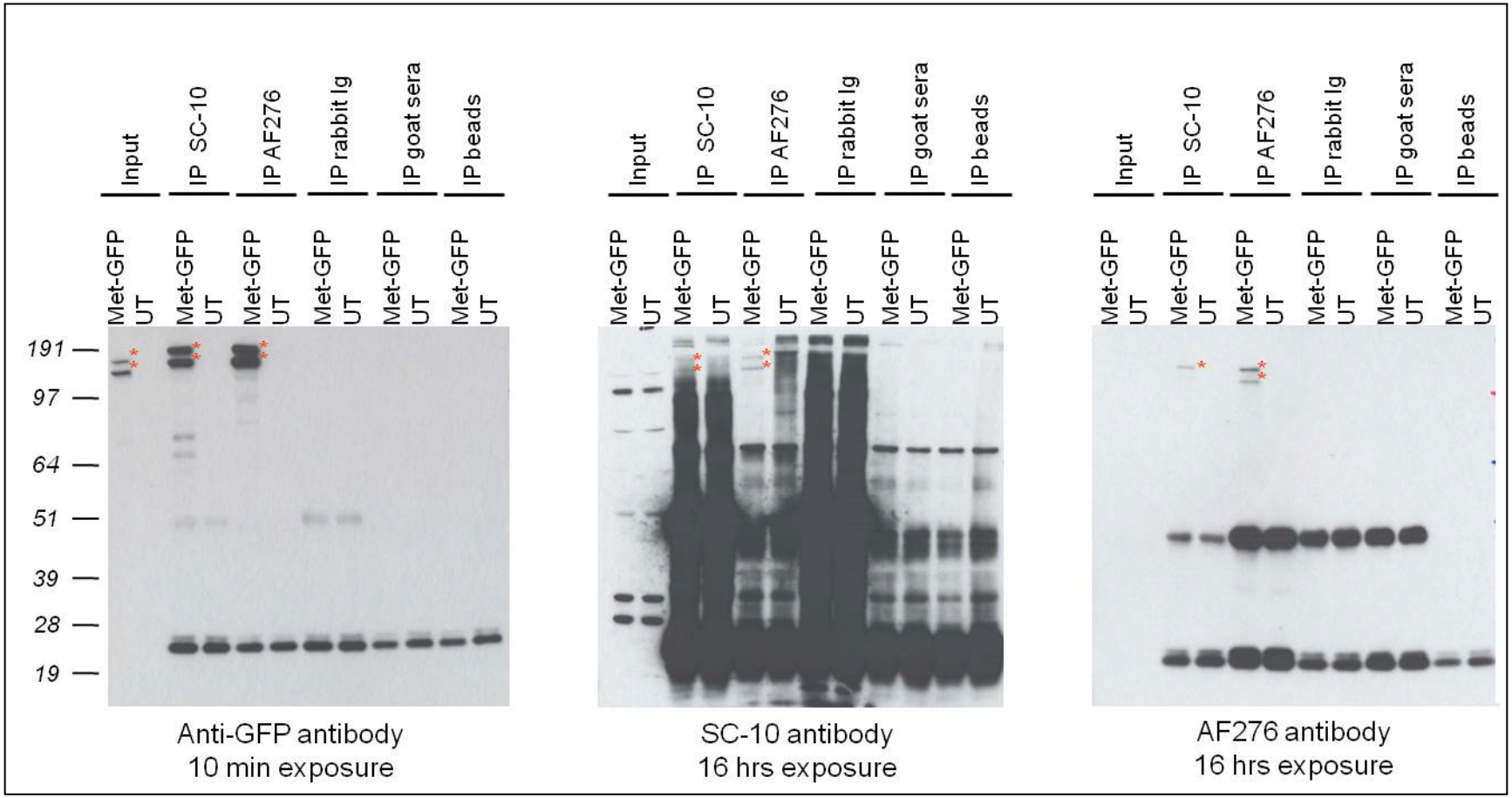

Figure 3.3: Western blot analysis of Met-GFP immunoprecipitation, detected using anti-GFP, SC-10 and AF276 antibodies.
NIH3T3 cells transfected with Met-GFP were lysed and cell lysate were immunoprecipitated using SC-10 and AF276 antibodies. Control immunoprecipitations were performed with rabbit immunoglobulin (rabbit Ig), goat sera and protein G beads alone. Inputs are whole cell lysate before immunoprecipitation. Input samples contain $1/10^{th}$ of the amount of samples used for immunoprecipitation. Red asterisk indicate Met-GFP protein bands at approximately 172 kD and 197 kD. UT: Untransfected. Molecular weights are noted aside, in kilodaltons.

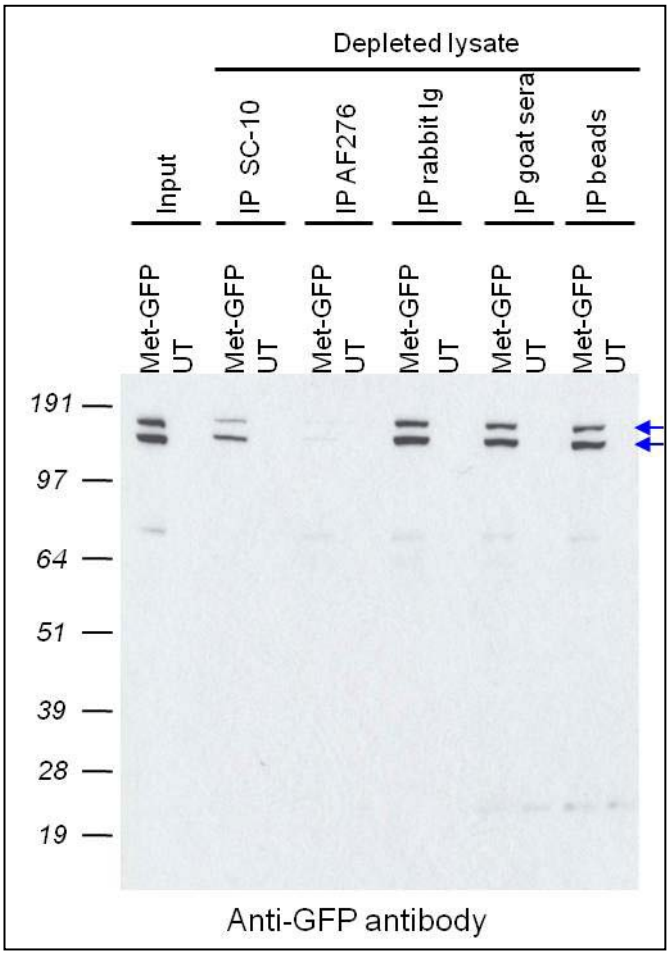

Figure 3.4: Western blotting of Met-GFP depleted cell lysate using anti-GFP antibodies.
NIH3T3 cells transfected with Met-GFP were lysed and cell lysate were immunoprecipitated using SC-10 and AF276 antibodies. Depleted cell lysate (cell lysate left after immunoprecipitation) were collected and analysed by Western blotting. Control immunoprecipitations were performed with rabbit immunoglobulin (rabbit Ig), goat sera and protein G beads alone. Inputs are whole cell lysate before immunoprecipitation. Inputs contain 1/10 of immunoprecipitated proteins. Arrows indicate Met-GFP protein band at approximately 172 kD and 197 kD. UT: Untransfected. Molecular weights are noted aside, in kilodaltons.

3.1.3: Improvement of c-Met expression in NIH3T3

To investigate the possibility of improving c-Met expression in NIH3T3 cells, c-Met full length cDNA (from IOH 36570) was cloned into various vectors and transfected into NIH3T3 cells. The vectors are grouped into two categories, based on the type of promoter they contain. The pcDNA3 vectors (pcDNA3-GW-DEST, pcDNA3-GFPc-GW-DEST and pcDNA3-SBPc-GW-DEST) are pcDNA3-based vectors that contain a CMV TATA promoter and different C-terminal tags i.e. GFP or streptavidin binding peptide (SBP) tag. The SBP is a peptide that binds specifically to streptavidin and can be used for protein purification. The pCMV-SCP-based vectors (pCMV-SCP-EFI-FRT-GW-DEST and pCMV-SCP-EFI-SBPc-GW-DEST) and pLenti vector (pLenti6.3-GW-DEST) contain an improved version of the CMV promoter, termed Super Core Promoter (SCP), which greatly increases gene transcription (Juven-Gershon *et al.*, 2006). In addition, these vectors also contain an intron, located at the 5' end of the gene, which belongs to the first intron of Elongation Factor I (EFI). Although not true for all genes, the presence of introns is reported to help the nuclear export machinery to recognise the mRNA of interest and export it out of the nucleus to be translated (Brinster *et al*., 1988; Dreyfuss *et al*., 2002).

Previously, plasmids used for expressing c-Met (c-Met without tag, Met-GFP and Met-SBP) were from the pcDNA3-based plasmids containing the CMV TATA promoter. Here, we compare c-Met expression from pCMV-SCP-based plasmids, which contains the super core promoter and the additional 5' intron sequences, with and without a C-terminal V5 tag. We also compare c-Met expression, with and without a C-terminal V5 tag, from the pLenti-based plasmid which also shares the same super core promoter and 5' intron sequences as the pCMV-SCP-based plasmids.

Cell lysates obtained from NIH3T3 cells transfected with the various c-Met plasmids were analysed on a Western blot (Figure 3.5). The approximate molecular weight of c-Met and its various constructs are listed in Table 3.1 (below). c-Met protein bands (indicated by red asterisks in Figure 3.5) from the pcDNA3-based plasmids were quite faint, especially in Met-SBP and Met-GFP samples. There is increased c-Met expression in the pCMV-SCP-based and pLenti-based plasmids when compared to the pcDNA3-based plasmids. Other than sharing the same promoter and the additional intron sequences, pCMV-SCP-based plasmids and pLenti-based plasmids are totally different vectors. It is clear that that the increased c-Met expression is due to the effects of the promoter and intron sequences. A non-specific band, close to c-Met protein bands, is observed in every sample. Lastly, it is unclear why only one c-Met band is being observed from the cell extracts. It is uncertain if this c-Met band belongs to the mature β-chain or the precursor protein. However, the staggering bands of tagged and untagged c-Met further confirms that c-Met is being detected in this Western blot.

Table 3.1: Molecular weight of c-Met and constructs.

Constructs	Approximate molecular weight	
	Mature c-Met β-chain	c-Met precursor protein
c-Met	145 kD	170 kD
Met-V5	146 kD	171 kD
Met-SBP	149 kD	174 kD
Met-GFP	172 kD	197 kD

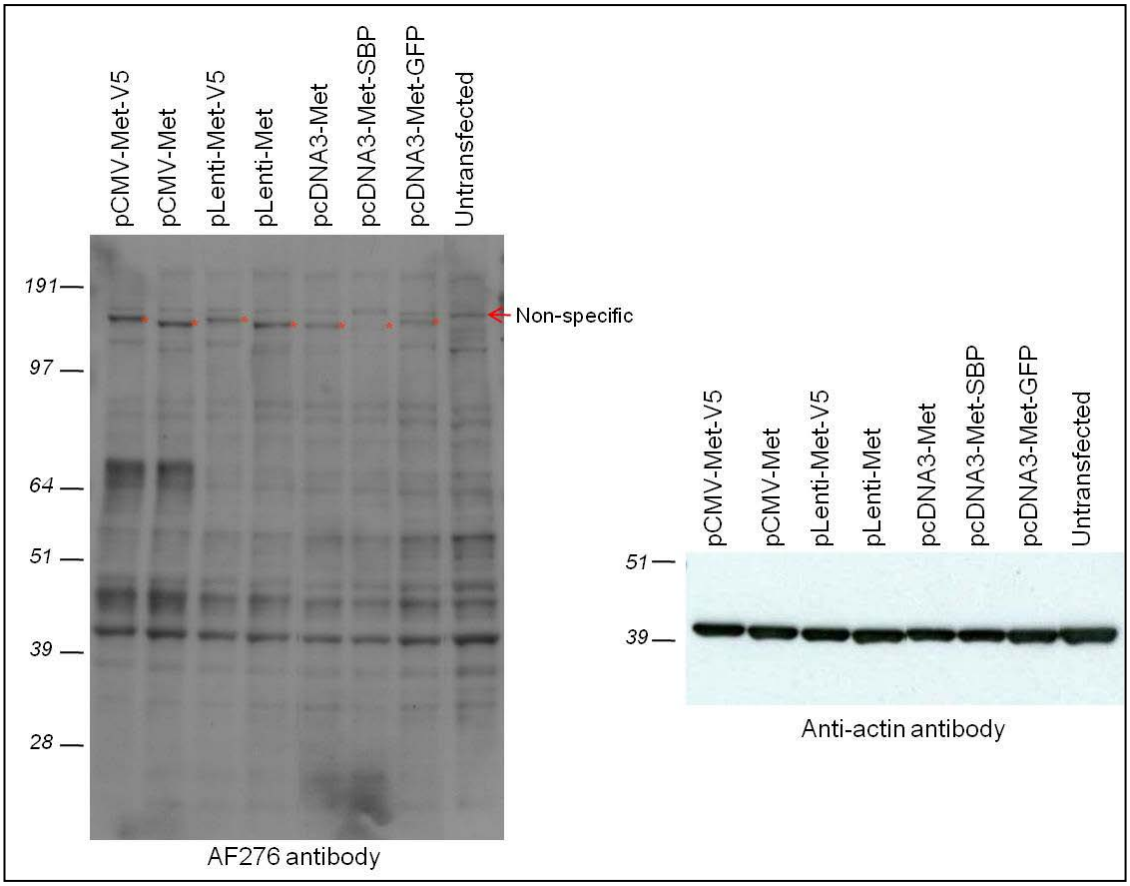

Figure 3.5: Western blot analysis of c-Met expression in NIH3T3 cells using various expression constructs.

Full length c-Met cDNA was cloned into various mammalian cell expression vectors and transfected into NIH3T3 cells. 50 µg of whole cell lysate was analysed for c-Met expression in each sample. c-Met expression was detected using the AF276 antibody. Actin was used as a loading control. Red asterisk indicate c-Met (see text) and its various tagged constructs. Molecular weights are noted aside, in kilodaltons. Various expression constructs were used, as indicated:
pCMV-Met-V5: c-Met with V5 tag in pCMV-SCP-EFI-FRT-GW-DEST
pCMV-Met: c-Met in pCMV-SCP-EFI-FRT-GW-DEST (no tag)
pLenti6.3-Met-V5: c-Met with V5 tag in pLenti6.3-GW-DEST
pLenti6.3-Met: c-Met in pLenti6.3-GW-DEST (no tag)
pcDNA3-Met: c-Met in pcDNA3-GW-DEST (no tag)
pcDNA3-Met-SBP: c-Met with SBP C-terminal tag in pcDNA3-SBPc-GW-DEST
pcDNA3-Met-GFP: c-Met with GFP C-terminal tag in pcDNA3-GFPc-GW-DEST

3.1.4: Further analysis of c-Met expression in selected cell lines

The aim of this project is to produce therapeutic antibodies against c-Met. An understanding of c-Met expression levels in various cell lines is required to develop a good antibody screening protocol to select for anti-cMet antibodies. To determine endogenous c-Met protein levels and phosphorylation/activation status in different cell lines, cell extracts from four cell lines were selected for analysis. U-87MG (human glioblastoma cell line), T47D (human breast cancer cell line) and SNU-5 (human gastric cell line) cells were selected through a literature search while HaCaT cells (human skin keratinocyte cell line) were selected due to their tight colony formation growth characteristics. The growth characteristics of HaCaT cells are required for cell motility assays which will be discussed later in Section 3.3. Cell extracts from U-87MG, T47D, HaCaT and SNU-5 cells were prepared and proteins immunoprecipitated using the AF276 antibody. As a control, goat sera were also used for immunoprecipitation. Immunoprecipitated samples were analysed on Western blots using SC-10 to detect expression of endogenous c-Met. To detect the phosphorylation status of endogenous c-Met, immunoprecipitated samples were also analysed on the Western blot using anti-phospho-tyrosine 4G10 antibody (Figure 3.6).

Consistent with other reports, U-87MG and SNU-5 cells are positive for c-Met protein expression, while T47D cells have undetectable levels of c-Met (Bellon *et al*., 2008; Shen *et al*., 2000; van der Horst *et al*., 2009). HaCaT cells are positive for c-Met protein expression and due to their ability to grow in colonies, they could be used to test our monoclonal antibodies in cell motility assays. SNU-5 cells express the highest amount of c-Met followed by HaCaT cells, U-87MG cells and finally, T47D cells. Interestingly, unlike other cell lines, the precursor band of c-Met (170 kD) from the HaCaT

immunoprecipitated sample is not detected by SC-10 antibody, suggesting that precursor c-Met is not tolerated in the cell and is rapidly processed into the mature form.

c-Met is known to be activated and phosphorylated upon binding to its ligand, hepatocyte growth factor (HGF). Lysates were also analysed from cells treated with HGF. It is difficult to interpret c-Met activation status in SNU-5 cells. Large numbers of protein bands were detected by 4G10 antibody in the SNU-5 samples immunoprecipitated by both AF276 antibody and by control goat sera. Therefore, it is possible that proteins from SNU-5 cell extract were binding non-specifically to the beads or the goat antibodies and these are being detected by 4G10 antibody. However, two bands corresponding to the predicted molecular weight of c-Met precursor and β-chain are detected by 4G10 antibody and these show a similar intensity in the presence and absence of HGF, suggesting that c-Met is constitutively active in this cell line. There is no difference observed in c-Met protein expression levels upon stimulation with HGF in HaCaT and U-87MG cells, though c-Met is phosphorylated in these cell lines in response to HGF. Interestingly, although U-87MG cells are reported to be autocrine (expresses both c-Met and HGF) for c-Met signalling, c-Met is only detectably phosphorylated upon incubation with HGF. This might suggest a mechanism within the cell that inhibits c-Met's constant activation in U-87MG cells.

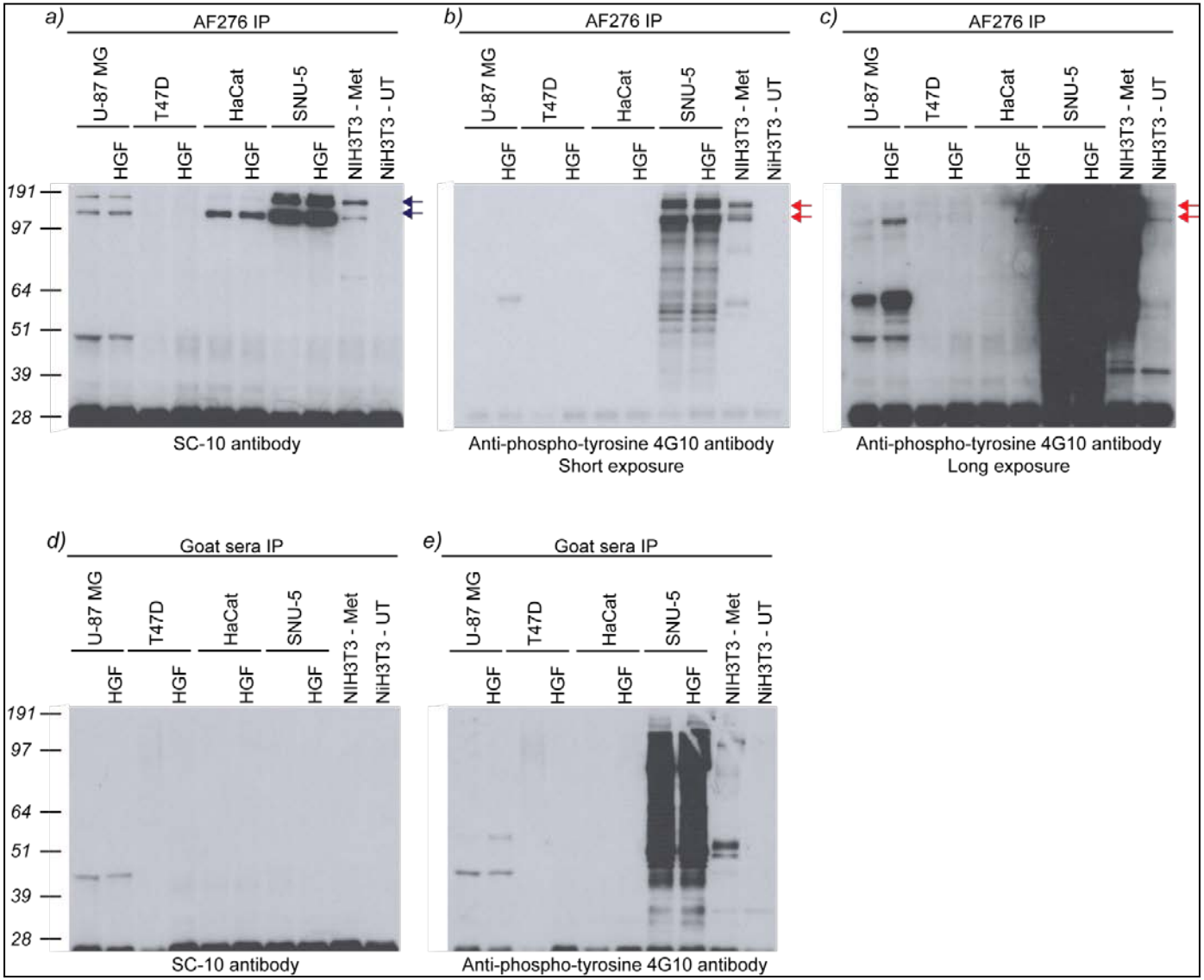

Figure 3.6: Western blot analysis of endogenous c-Met immunoprecipitated with AF276 antibody.
U-87MG, T47D, HaCat and SNU-5 cells were incubated with 10 ng/ml of c-Met ligand (HGF) for 30 mins to induce activation and phosporylation of c-Met. Cells incubated with and without HGF were lysed in NP40 lysis buffer. Proteins were immunoprecipitated using AF276 antibody (*a, b, c*) or goat sera (*d & e*). Immuunoprecipitated samples were detected on Western blots using SC-10 (*a & d*) and 4G10 (*b, c & e*) antibodies. ***b & c)*** Same blots with different exposure time. NIH3T3 cells transfected with human c-Met were controls. Blue arrows indicate endogenous and exogenous c-Met. Red arrows indicate activated/phosporylated endogenous c-Met. HGF: Hepatocyte growth factor. Molecular weights are noted aside, in kilodaltons.

3.1.5: Streptavidin binding peptide

The Streptavidin Binding Peptide (SBP) was reported by Keefe *et al*. in 2001 as a peptide that binds very specifically to streptavidin, but not to avidin. SBP is made up of 38 amino acid residues, has a molecular weight of approximately 4.2 kD, and can be a useful protein purification tag. Protein purified using the SBP tag was shown to be purer than protein purified using maltose-binding protein or histidine tag (Keefe *et al*., 2001). The simplicity of the SBP tag protein purification protocol and the wide range of commercially available streptavidin-associated products in the market (i.e. streptavidin-coated plates) makes the SBP tag a useful tool for high-throughput protein purification.

Proteins previously reported to be purified by SBP tag have been tagged at the N-terminus (Keefe *et al.*, 2001). c-Met contains a plasma membrane localisation signal at the N-terminus (Materials and Methods, Figure 2.1), which is cleaved off during protein maturation, therefore c-Met can only be tagged at the C-terminus. We made constructs expressing GFP tagged with SBP, either at the N- or C-terminus, to determine whether this tag could successfully be used in either context. These constructs were transfected into NIH3T3 cells. Cell lysates were prepared and pre-cleared with avidin-coated beads to remove non-specific proteins. Pull down experiments were then performed with streptavidin-conjugated magnetic beads and bound proteins were eluted with biotin. The beads were boiled to extract any remaining proteins that bound to the beads. Purified proteins were resolved on a SDS-PAGE gel and stained with Coomassie blue dye to determine the purity of the pull down experiment (Figure 3.8). Western blotting, using an anti-GFP antibody and streptavidin-conjugated peroxidase, was also performed (Figure 3.8). Both N-terminally tagged and C-terminally tagged GFP constructs were successfully pulled down with high purity as observed in the Coomassie-stained SDS gel. The pull down is observed to be very efficient and specific as none of GFP-tagged

proteins were observed in the depleted lysate samples or the boiled avidin beads samples. There is a difference in the molecular weight of N-terminal tagged GFP and C-terminal tagged GFP (see shift in molecular weight in Figure 3.8). This difference is due to transfer of C-terminal vector sequences incorporated during the Gateway cloning process. A band of lower molecular weight can also be detected by the anti-GFP antibody in the N-SBP input sample. This band is likely to be untagged GFP which is expressed from an alternate initiation codon, downstream of the tag (Figure 3.7). This is confirmed by the observation that this protein band is not purified by the streptavidin bead pull down and is also not detected by the streptavidin-conjugated peroxidase on the Western blot.

Streptavidin-conjugated peroxidase detects proteins tagged with SBP. Consistent with the protein bands observed on the anti-GFP blot, streptavidin-conjugated peroxidase detected the same GFP constructs. However, three higher molecular weight bands were being purified by the streptavidin-conjugated magnetic beads (in the boiled streptavidin-conjugated magnetic beads samples). It is likely that these proteins bind to the magnetic beads and not streptavidin as these proteins bands are only observed when the beads are boiled and not upon competitive elution by biotin.

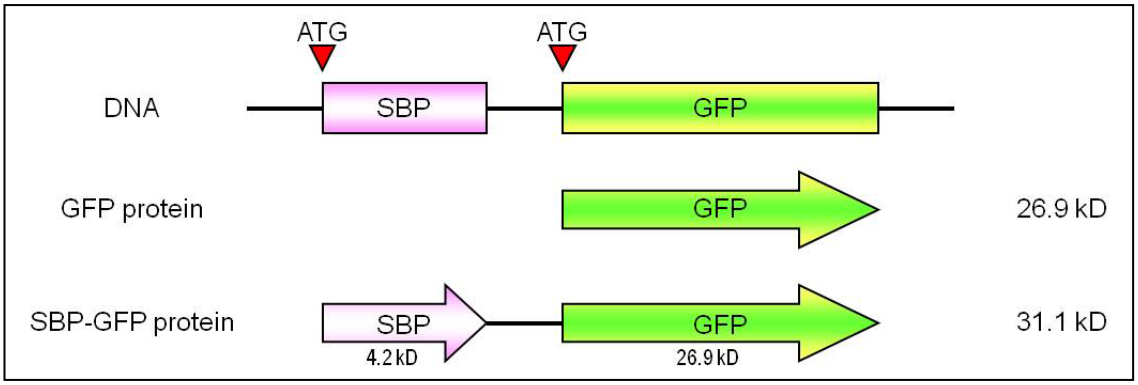

Figure 3.7: Illustration of GFP N-terminally tagged with SBP (SBP-GFP) construct (not drawn to scale).

The SBP tag is a 4.2 kD protein and GFP is a 26.9 kD protein. The SBP tag is cloned 5' of GFP gene, which also contains its own transcription initiation start codon (red arrows, ATG). Transcription may initiate from the SBP tag, producing the 31.1 kD SBP-GFP protein. Alternatively, transcription may also initiate from the GFP gene to produce the 26.9 kD GFP protein.

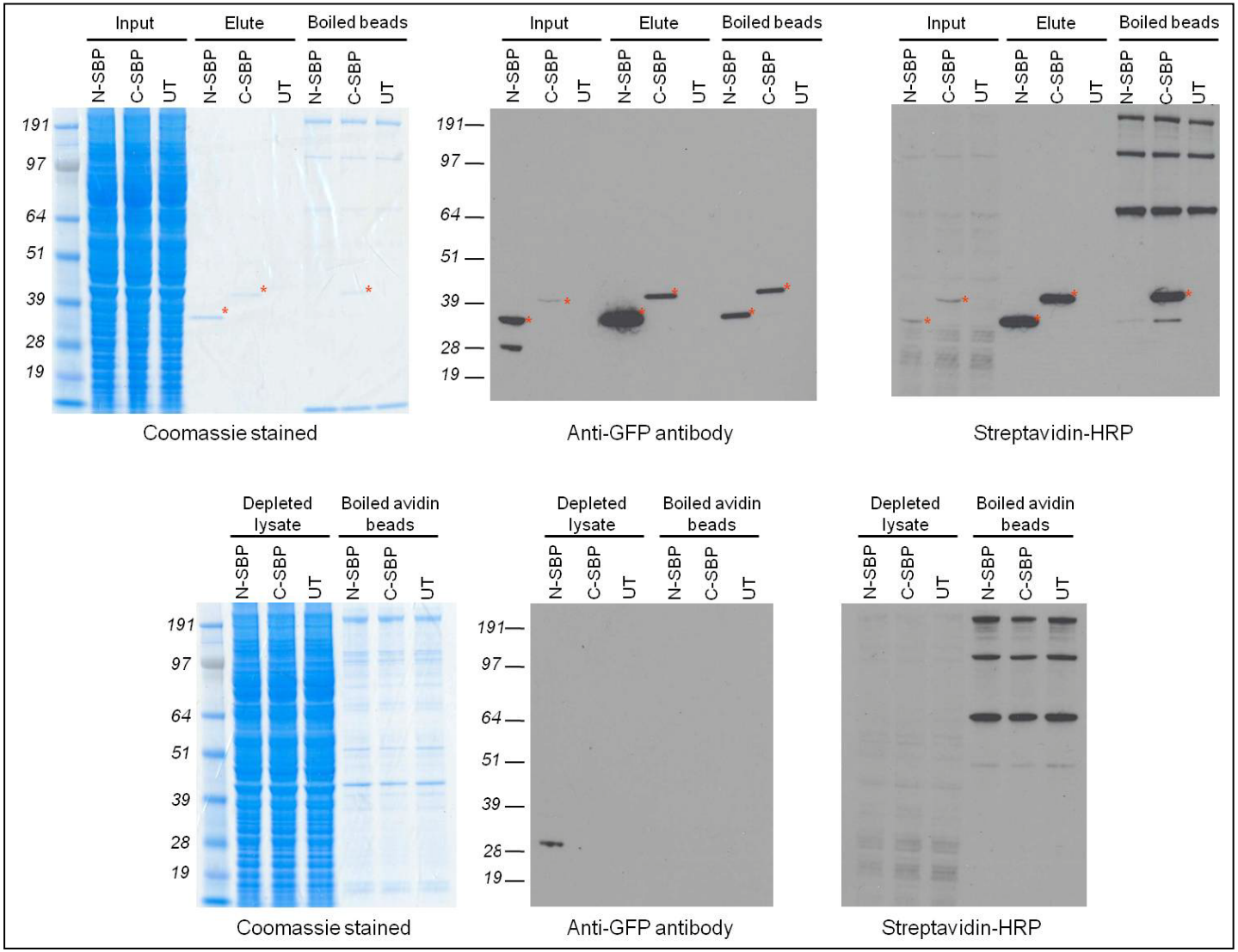

Figure 3.8: Coomassie-stained SDS-PAGE gel and Western blot analysis of GFP-SBP pull down using streptavidin-conjugated magnetic beads.
Plasmids expressing either N- or C-terminally tagged GFP, as indicated, were transfected into NIH3T3 cells. Cell lysate was initially pre-cleared with avidin beads. Proteins binding to streptavidin were purified using streptavidin-conjugated magnetic beads and eluted using biotin. After biotin elution, streptavidin-conjugated magnetic beads were boiled in loading buffer to recover any protein left on the beads. SBP pull down is analysed by Coomassie blue staining of the SDS-PAGE gel and by Western blotting using an anti-GFP antibody and streptavidin-conjugated peroxidase (streptavidin-HRP). Input lanes contain 1/10th of the amount used for purification are shown as controls. Bands representing N- or C-terminally tagged GFP can be seen as indicated by the red asterisk. Elute: Purified protein samples obtained by elution with biotin. Boiled beads: Purified protein samples obtained from boiling streptavidin-conjugated magnetic beads in LDS. N-SBP: GFP N-terminally tagged with SBP. C-SBP: GFP C-terminally tagged with SBP. UT: Untransfected. Molecular weights are noted aside, in kilodaltons.

3.1.6: Purification of c-Met via SBP tag pull down

To test if the C-terminal SBP tag can be used to purify c-Met, full length c-Met cDNA was Gateway cloned into pCMV-SCP-EFI-SBPc-GW-DEST vector and the resulting construct was transfected into NIH3T3 cells. Cell lysate was pre-cleared using avidin-coated beads and proteins pulled down with streptavidin-conjugated magnetic beads. Purified proteins were analysed by Western blotting using AF276 antibody and streptavidin-conjugated peroxidase (Figure 3.9). Using streptavidin-conjugated peroxidise, the very high number of non-specific bands made it impossible to determine if any c-Met proteins were recognised. However, AF276 antibody detected two bands, with molecular weights corresponding to those of the Met-SBP precursor (174 kD) and the β-chain (149 kD). In the AF276 antibody and streptavidin-conjugated peroxidase blots, two protein bands (red asterisks) were observed in the elute lane corresponding to c-Met, indicating that Met-SBP was eluted from streptavidin by competition with biotin. Unlike SBP-tagged GFP constructs (Figure 3.8), Met-SBP was only partially eluted from the beads. The remaining Met-SBP was released by boiling. Finally, two protein bands (blue asterisks) are detected by AF276 antibody in the depleted lysate sample. It is unclear if these bands belong to c-Met as they are slightly smaller than the other c-Met bands. The SBP purification is an excellent method of protein purification which we have shown to efficiently purify large protein such as c-Met from whole cell lysates, produce highly pure proteins, and could potentially yield native protein due to mild elution conditions using biotin.

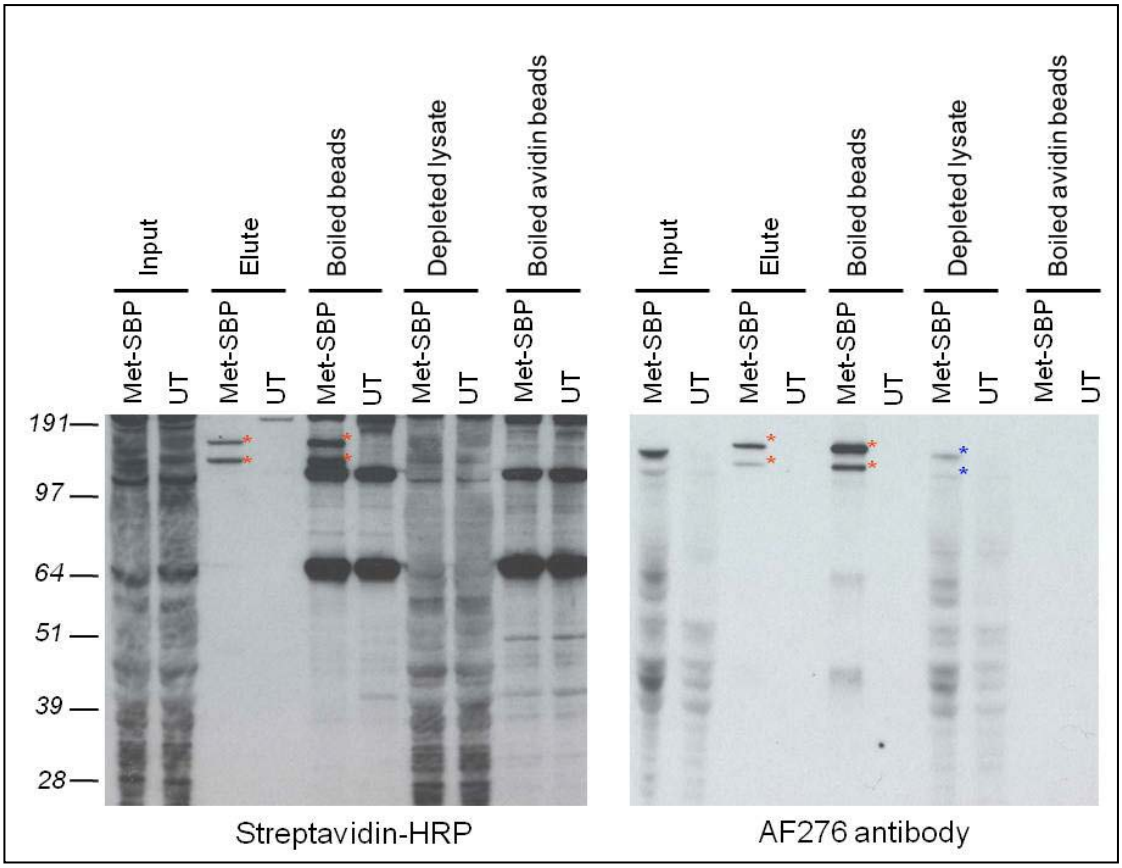

Figure 3.9: Western blot analysis of cMet-SBP purification from NIH3T3 cells.
The plasmid expressing Met-SBP was transfected into NIH3T3. Cell lysate was prepared and pre-cleared using avidin-coated beads. Proteins were purified using streptavidin-conjugated magnetic beads. Purified proteins were eluted using biotin and were analysed on a Western blot using streptavidin-conjugated peroxidase (streptavidin-HRP), or AF276 antibody. Input samples contain $1/10^{th}$ of the amount used for purification. Depleted cell lysate was analysed to determine the efficiency of SBP pull down. Avidin beads used for pre-clearing were boiled and analysed to confirm the specificity of SBP to streptavidin and not avidin. Protein bands representing Met-SBP β-chain (149 kD) and Met-SBP precursor (174 kD) are both indicated by the red asterisk. Elute: Purified protein samples obtained by elution with biotin. Boiled beads: Purified protein samples obtained from boiling streptavidin-conjugated magnetic beads in LDS. Met-SBP: c-Met with C-terminal SBP tag. UT: Untransfected. Molecular weights are noted aside, in kilodaltons.

3.1.7: Adenoviral expression of human c-Met

As shown earlier, human c-Met transient expression in NIH3T3 cells was improved by using pCMV-SCP-based vectors (Figure 3.5). However, c-Met expression levels in these transfected cells were not significantly higher then untransfected cells. To improve expression efficiency, the adenovirus expression system was used to introduce human c-Met cDNA into mammalian cells.

c-Met was successfully purified using the SBP tag (Figure 3.9). SBP purification allows high-throughput protein purification which is useful for antibody screening i.e. high levels of Met-SBP could be easily purified and used to screen for antibodies against c-Met or used as an immunogen. c-Met and Met-SBP were thus cloned into the adenoviral plasmid pADEasy1. Two plasmids, from different bacterial colonies, were selected and purified for each construct. To produce infectious virus particles, plasmids were transfected into AD293 cells. A Western blot analysis was performed on infected AD293 cell lysates to ensure that c-Met was being expressed (Figure 3.10). Two high molecular weight bands were observed from whole cell lysate samples obtained from AD293 cells infected with both c-Met constructs. These protein bands are consistent with the molecular weight of unprocessed and β-chain of c-Met, indicating that adenovirus had successfully infected AD293 cells, and that both constructs were successfully expressed by the cell. Expression of c-Met from plasmid #1 is higher as compared to plasmid #3. Similarly, expression of Met-SBP from plasmid #4 is higher compared to plasmid #5. c-Met #1 and Met-SBP #4 were therefore chosen for bulk virus amplification.

Western blotting of AD293 cells infected with adenovirus was a preliminary test to verify that c-Met constructs were expressed by cells. To ensure that c-Met cDNA

constructs are being expressed by the adenovirus, viruses were used to infect T47D cells (c-Met low expressing cell line). Infected cells were harvested and analysed on a Western blot for c-Met expression using AF276 antibody (Figure 3.10). As a loading control, a Coomassie-stained SDS-PAGE gel was used. c-Met and Met-SBP were expressed, but at very low levels (Figure 3.10). It is unclear why the expressions of the constructs were low. As T47D expresses low levels of c-Met, it is possible that T47D cells harbour some transcription defects or has a strong negative regulation against c-Met expression. The failure to achieve high level expression of c-Met in these experiments caused us to alter our original strategy of immunising with whole cells and led us to pursue the expression of c-Met in prokaryotic system.

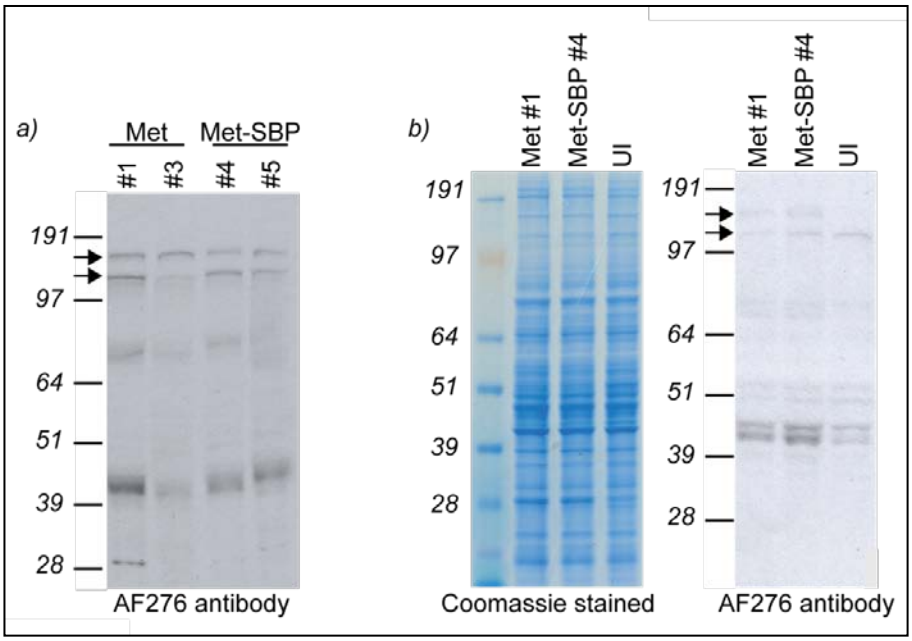

Figure 3.10: Expression of c-Met and Met-SBP in mammalian cells using adenovirus infection.
a) Western blotting of adenovirus expression of c-Met and Met-SBP in Ad293 cells. Two individual plasmid isolates were used for each plasmid construct. Plasmids were transfected into Ad293 cells and whole cell lysate was obtained. Expression of c-Met constructs was analysed on Western blot using AF276 antibody. ***b)*** Analysis of c-Met and Met-SBP in T47D cells. Infectious virus particles carrying c-Met and Met-SBP constructs were used to infect T47D cells. Whole cell lysate was obtained from infected cells and c-Met expression was detected on Western blot using AF276 antibody. Black arrows indicate various c-Met protein constructs. As a loading control, a Coomassie-stained gel was performed. Molecular weights are noted aside, in kilodaltons UI: Uninfected.

3.1.8: Prokaryotic expression of c-Met constructs

We demonstrated that the affinity of c-Met commercial antibodies (SC-10 and AF276) towards human c-Met was poor and EP1454Y antibodies showed undetectable levels human c-Met on Western blots. AF276 antibody was the best commercial antibody tested for detecting c-Met from cell lysates in Western blots. However, to use AF276 antibody to detect c-Met on Western blots, optimisation of blotting protocol, large amount of cell lysate and long exposures were still required. The next stage of this project was to make antibodies that have higher affinity and specificity towards human c-Met than the commercially available ones. These could then be tested for functional activity in either suppressing or inducing c-Met activity.

Monoclonal antibodies against human c-Met were produced by immunising mice with different regions of bacterially expressed, purified, human c-Met. Four regions of human c-Met were cloned into the prokaryotic expression vector, pET19b, for protein expression. The four c-Met constructs are: α-chain (full length), extracellular β-chain, extracellular αβ-chain (the extracellular domain of c-Met) and full length β-chain (Figures 3.11A to D). c-Met constructs were transformed into seven different bacteria strains: BL21 DE3, BL21 star, BL21 pLysS, Rosetta-gami 2 DE3 (RG2 DE3), Rosetta-gami 2 pLysS (RG2 pLysS), Rosetta-gami B DE3 (RGB DE3) and Rosetta-gami B DE3 pLysS (RGB DE3 pLysS). Different bacteria strains have specific characteristics (please refer to Table Materials and Methods), such as increased stability of mRNA, enhanced disulphide bond formation in the bacterial cytoplasm, and enhanced expression of eukaryotic proteins by containing specific tRNA. Any of these characteristics may increase the expression and solubility of c-Met constructs.

To determine if the bacteria strains are able to express the various c-Met constructs, protein expression was induced with IPTG and analysed on a Coomassie blue stained SDS-PAGE gel (Figures 3.11A to D). Among the four different c-Met constructs, c-Met α-chain was most successfully expressed in all seven bacteria stains. This is followed by c-Met extracellular β-chain, full length β-chain and lastly, extracellular αβ-chain. It is observed that as the molecular weight of the c-Met construct increases, the ability to expresses the protein decreases, hence resulting in the faint band observed in the higher molecular weight constructs i.e. full length β-chain (~119 kD) and extracellular αβ-chain (~100 kD) samples. In addition, the presence of other endogenous protein bands near the extracellular αβ-chain protein band on the SDS-PAGE gel made the protein difficult to distinguish. BL21 pLysS was chosen for large scale protein expression of the α-chain. BL21 star was selected to express the extracellular β-chain, extracellular αβ-chain and full length β-chain constructs in larger quantities (Figures 3.12A to D).

Protein expression of the various c-Met constructs was induced for three hours before cells were harvested and lysed in lysis buffer (0.3 M KCL, 50 mM KH_2PO_4, pH 8.0). Bacteria lysate was centrifuged to separate soluble (cell supernatant) and insoluble proteins (cell debris pellet). To determine if the expressed protein resides in the soluble or insoluble fraction after cell lysis, cell supernatant and cell debris pellet samples were resolved on a SDS-PAGE gel (Figures 3.11A to D). Total bacterial cell lysate was used as a control. Despite the use of various bacteria strains in an attempt to increase the solubility of c-Met protein constructs, all four constructs were observed predominantly in the insoluble pellet. The insolubility of c-Met constructs does not pose a problem as denatured protein samples can be used for the immunisation of mice. Insoluble c-Met proteins were extracted from bacterial cell lysate by centrifugation and solubilised in 6M urea before purification.

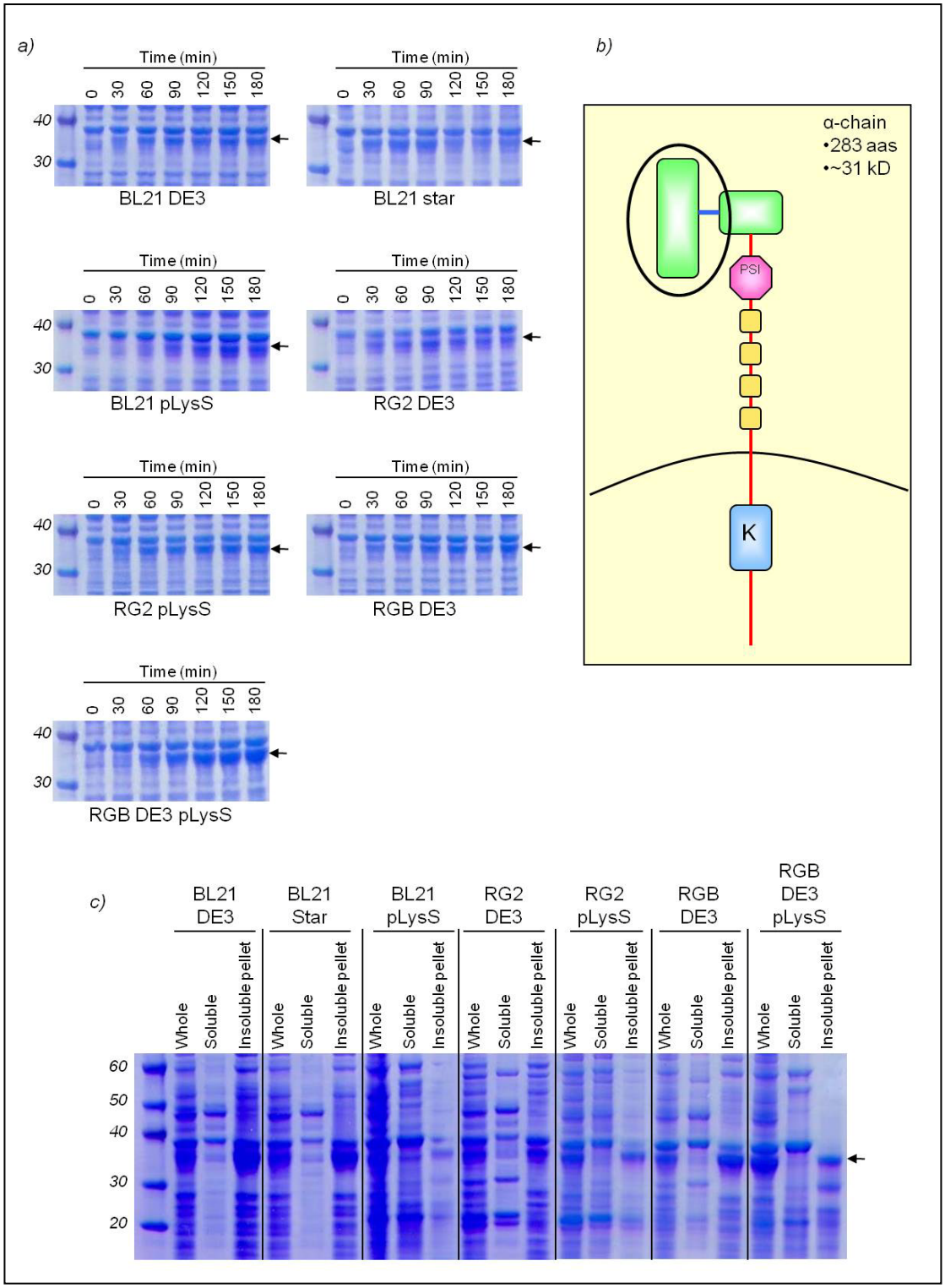

Figure 3.11A: Prokaryotic expression of human c-Met α-chain.
a & c) SDS-PAGE gels stained with Coomassie blue dye. c-Met α-chain is indicated by the arrow. Molecular weights are noted aside, in kilodaltons. ***a)*** Cultures of seven bacteria strains containing c-Met α-chain construct were induced with IPTG for 3 hrs. Cells were harvested at 30 mins intervals to check for the expression of c-Met α-chain. ***b)*** Illustration of c-Met α-chain that is being expressed is highlighted in the black oval (not drawn to scale). Predicted molecular weight and number of amino acid residues of c-Met α-chain are shown. ***c)*** Solubility of c-Met α-chain expressed by the various bacteria strains was tested. c-Met α-chain was induced for 3 hrs before cells were harvested. RG2: Rosetta-gami 2. RGB: Rosetta-gami B. Whole: Bacteria lysate before centrifugation.

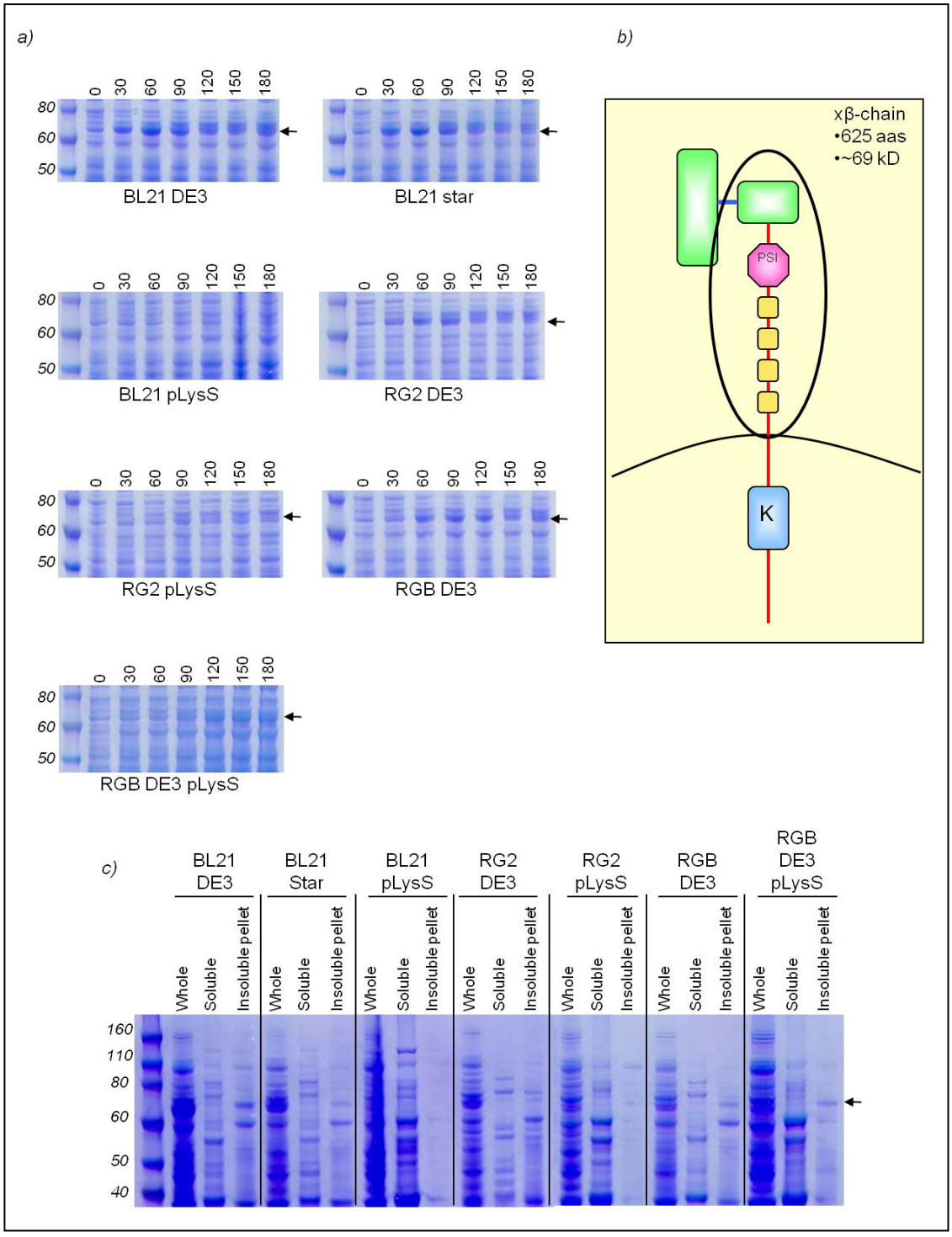

Figure 3.11B: Prokaryotic expression of human c-Met extracellular β-chain.
a & c) SDS-PAGE gels stained with Coomassie blue dye. c-Met extracellular β-chain is indicated by the arrow. Molecular weights are noted aside, in kilodaltons. ***a)*** Cultures of seven bacteria strains containing c-Met extracellular β-chain construct were induced with IPTG for 3 hrs. Cells were harvested at 30 mins intervals to check for the expression of c-Met extracellular β-chain. ***b)*** Illustration of c-Met extracellular β-chain that is being expressed is highlighted in the black oval (not drawn to scale). Predicted molecular weight and number of amino acid residues of c-Met extracellular β-chain are shown. ***c)*** Solubility of c-Met extracellular β-chain expressed by the various bacteria strains was tested. c-Met extracellular β-chain was induced for 3 hrs before cells were harvested. RG2: Rosetta-gami 2. RGB: Rosetta-gami B. Whole: Bacteria lysate before centrifugation.

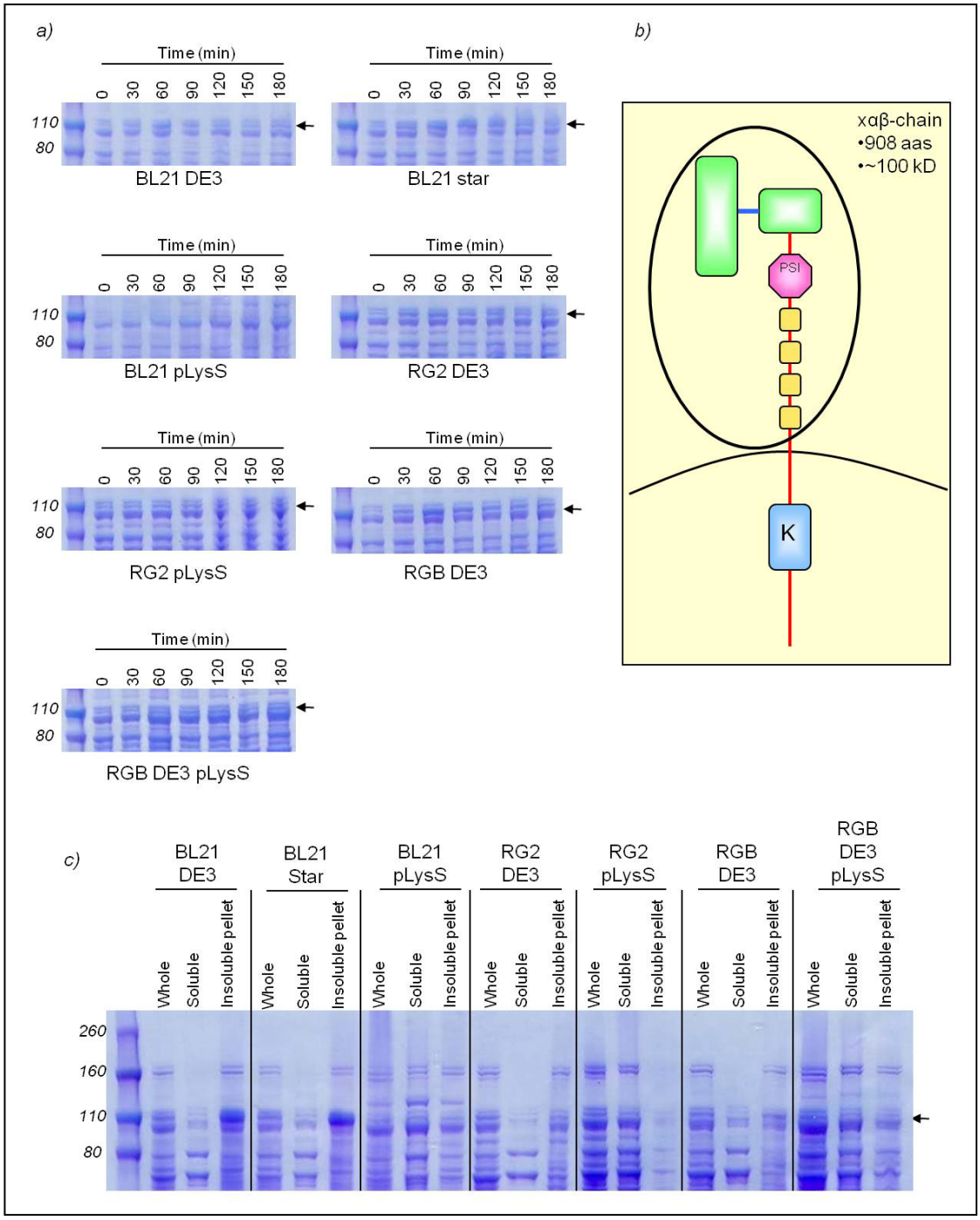

Figure 3.11C: Prokaryotic expression of human c-Met extracellular αβ-chain (or extracellular domain of c-Met).

a & c) SDS-PAGE gels stained with Coomassie blue dye. c-Met extracellular αβ-chain is indicated by the arrow. Molecular weights are noted aside, in kilodaltons. ***a)*** Cultures of seven bacteria strains containing c-Met extracellular αβ-chain construct were induced with IPTG for 3 hrs. Cells were harvested at 30 mins intervals to check for the expression of c-Met extracellular αβ-chain. ***b)*** Illustration of c-Met extracellular αβ-chain that is being expressed is highlighted in the black oval (not drawn to scale). Predicted molecular weight and number of amino acid residues of c-Met extracellular αβ-chain are shown. ***c)*** Solubility of c-Met extracellular αβ-chain expressed by the various bacteria strains was tested. c-Met extracellular αβ-chain was induced for 3 hrs before cells were harvested. RG2: Rosetta-gami 2. RGB: Rosetta-gami B. Whole: Bacteria lysate before centrifugation.

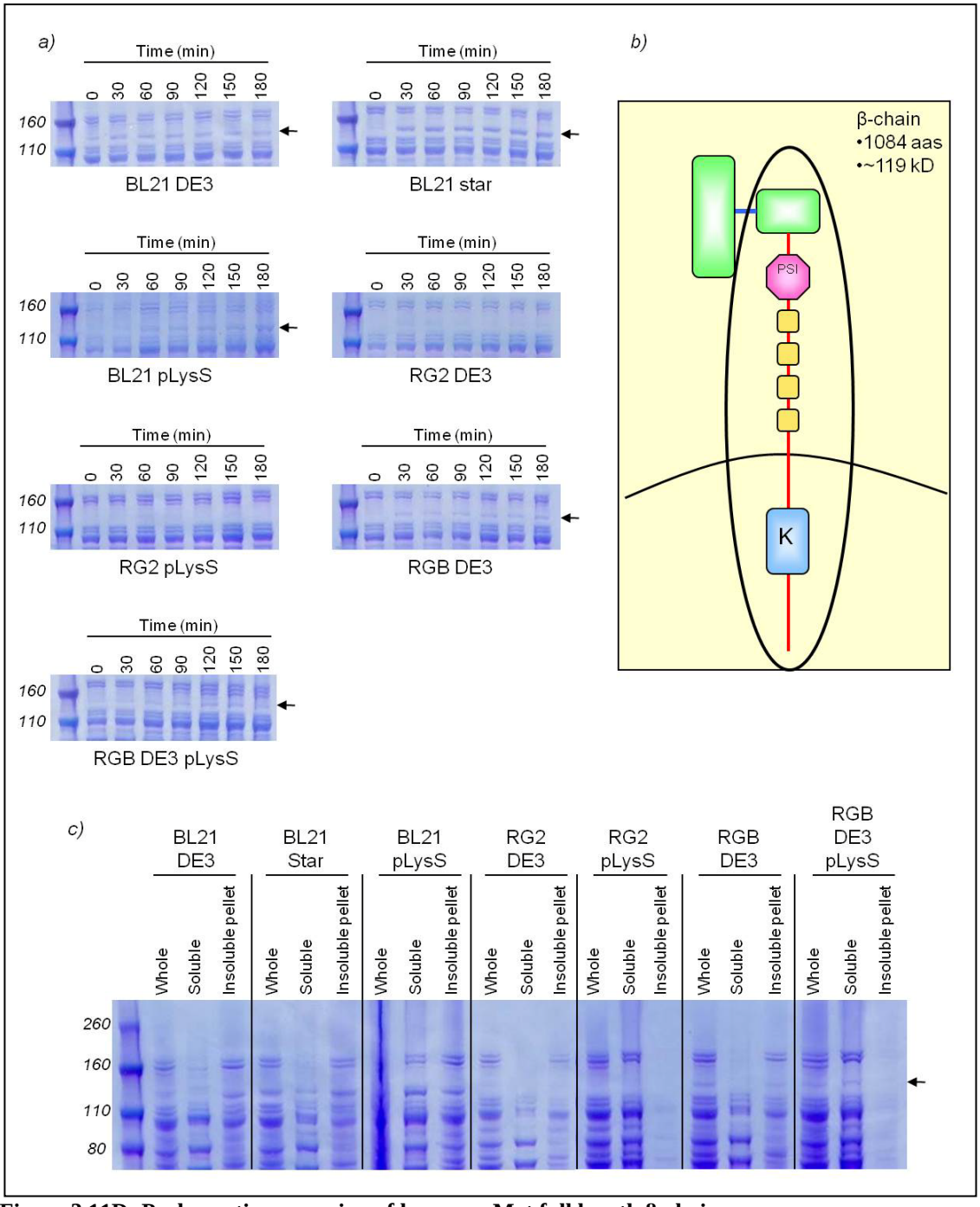

Figure 3.11D: Prokaryotic expression of human c-Met full length β-chain.
a & c) SDS-PAGE gels stained with Coomassie blue dye. c-Met full length β-chain is indicated by the arrow. Molecular weights are noted aside, in kilodaltons. ***a)*** Cultures of seven bacteria strains containing c-Met full length β-chain construct were induced with IPTG for 3 hrs. Cells were harvested at 30 mins intervals to check for the expression of c-Met full length β-chain. ***b)*** Illustration of c-Met full length β-chain that is being expressed is highlighted in the black oval (not drawn to scale). Predicted molecular weight and number of amino acid residues of c-Met full length β-chain are shown. ***c)*** Solubility of c-Met full length β-chain expressed by the various bacteria strains was tested. c-Met full length β-chain was induced for 3 hrs before cells were harvested. RG2: Rosetta-gami 2. RGB: Rosetta-gami B. Whole: Bacteria lysate before centrifugation.

3.1.9: Purification of c-Met protein

Cloning into pET19b expression vector allowed the expression of c-Met constructs tagged at the N-terminal by ten residues of histidine (Materials and Method, Figure 1). c-Met constructs were expressed in large volume bacterial cultures. Bacterial lysates were centrifuged to obtain the insoluble c-Met constructs. Insoluble c-Met proteins were then re-solubilised in 6M urea before affinity purification using commercially-obtained nickel columns (IMAC Bio-scale mini profinity cartridges). Purified proteins were resolved on a SDS-PAGE gel and Coomassie stained. Western blot analysis using anti-Histidine-peroxidase was performed to validate the protein bands seen on the Coomassie-stained SDS-PAGE gel (Figures 3.12A to D). All c-Met constructs were successfully purified. However, contaminating bands were observed in the purified sample of all proteins. It could be that these contaminating bands are degraded or truncated products of the c-Met protein constructs. We have obtained sufficient purified proteins for immunising the mouse for monoclonal antibody production. The α-chain of c-Met and the extracellular β-chain of c-Met were chosen for immunisation as they were the most highly expressed compared to the other two c-Met constructs. Antibody production in mice was done in collaboration with Moravian Biotechnology. Purified protein samples were sent to them as immunogens for the mice.

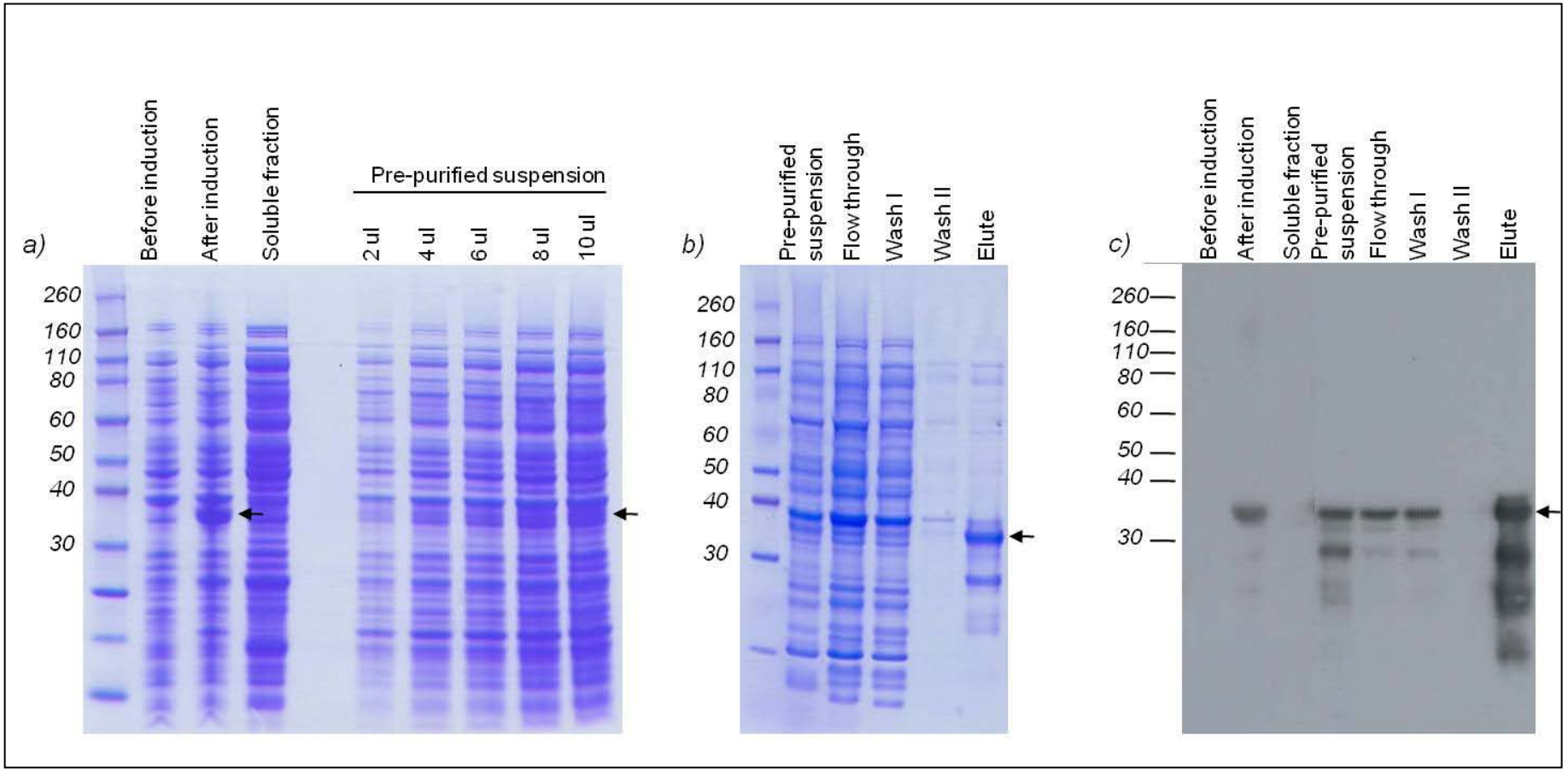

Figure 3.12A: SDS-PAGE gel and Western blot analysis of human c-Met α-chain expression in BL21 pLysS bacteria strain.
a &b) SDS-PAGE gels stained with Commassie blue dye. ***a)*** Bacteria cells containing c-Met α-chain construct were induced with IPTG for 3 hrs. Expression of c-Met α-chain can be seen (as indicated by the arrow). The insoluble fraction of bacterial lysate was solubilised in 6M urea before purification and loaded in increasing amounts to visualize c-Met α-chain (pre-purified suspension). ***b)*** c-Met α-chain was affinity purified using a 1 ml Bio-Scale mini cartridge. The flow through, washes (wash I and wash II), and elute were collected and analysed on a SDS-PAGE gel. c-Met α-chain has a predicted molecular weight of 31 kD although it runs at a higher molecular weight. Arrow indicates purified c-Met α-chain. ***c)*** Western blot analysis of c-Met α-chain expression. Half the amount of protein used in *a)* and *b)* was used in this Western blot. The presence of purified c-Met α-chain was confirmed by detecting the N-terminal histidine tag using an anti-Histidine-peroxidase antibody.

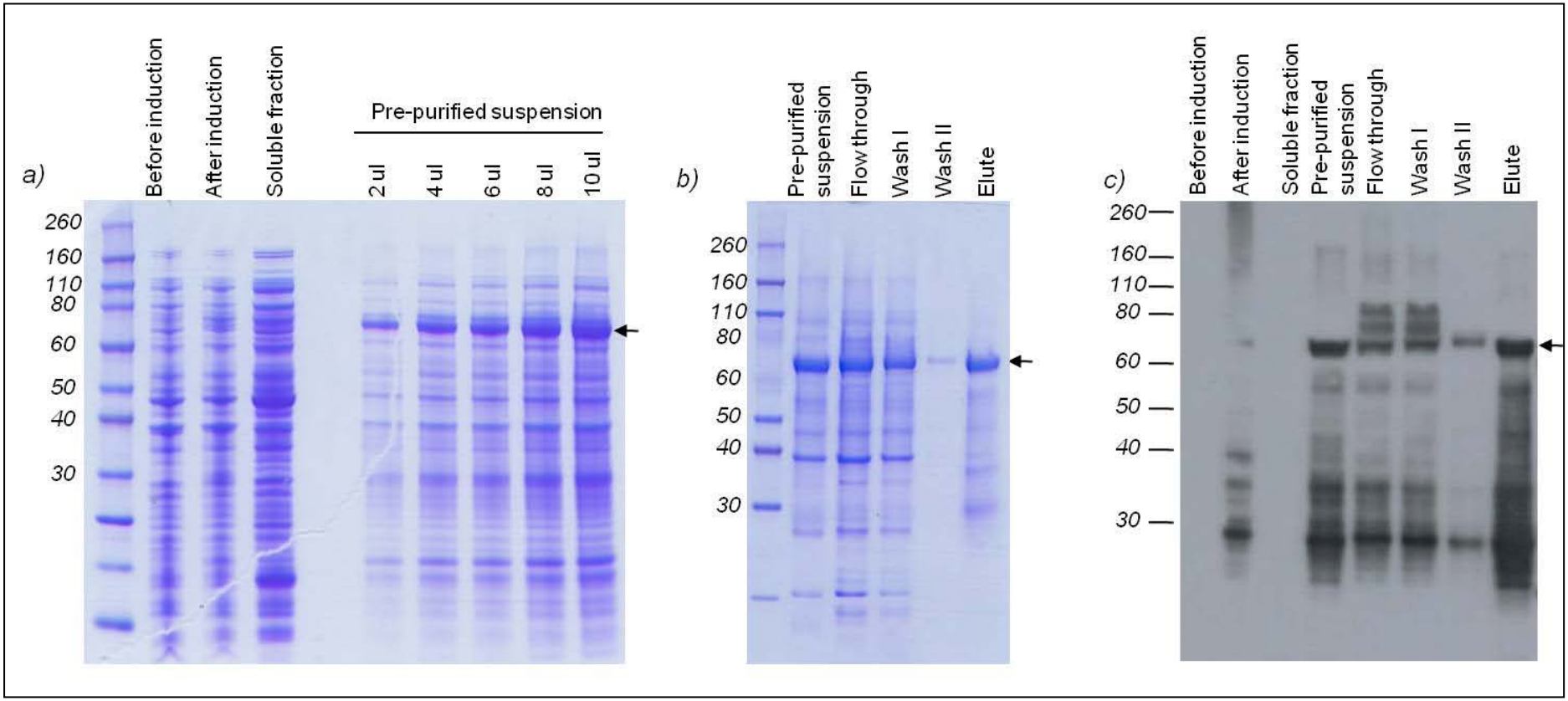

Figure 3.12B: SDS-PAGE gel and Western blot analysis of human c-Met extracellular β-chain expression in BL21 star bacteria strain.
a & b) SDS-PAGE gels stained with Commassie blue dye. ***a)*** Bacteria cells containing c-Met extracellular β-chain construct were induced with IPTG for 3 hrs. Expression of c-Met extracellular β-chain can be seen (as indicated by the arrow). The insoluble fraction of bacterial lysate was solubilised in 6M urea before purification and loaded in increasing amounts to visualize c-Met α-chain (pre-purified suspension). ***b)*** c-Met extracellular β-chain was affinity purified using a 1 ml Bio-Scale mini cartridge. The flow through, washes (wash I and wash II), and elute were collected and analysed on a SDS-PAGE gel. Arrow indicates purified c-Met extracellular β-chain that has a predicted molecular weight of 69 kD. ***c)*** Western blot analysis of c-Met extracellular β-chain expression. Half the amounts of protein used in *a)* and *b)* was used in this Western blot. The presence of purified c-Met extracellular β-chain was confirmed by detecting the N-terminal histidine tag using an anti-Histidine-peroxidase antibody.

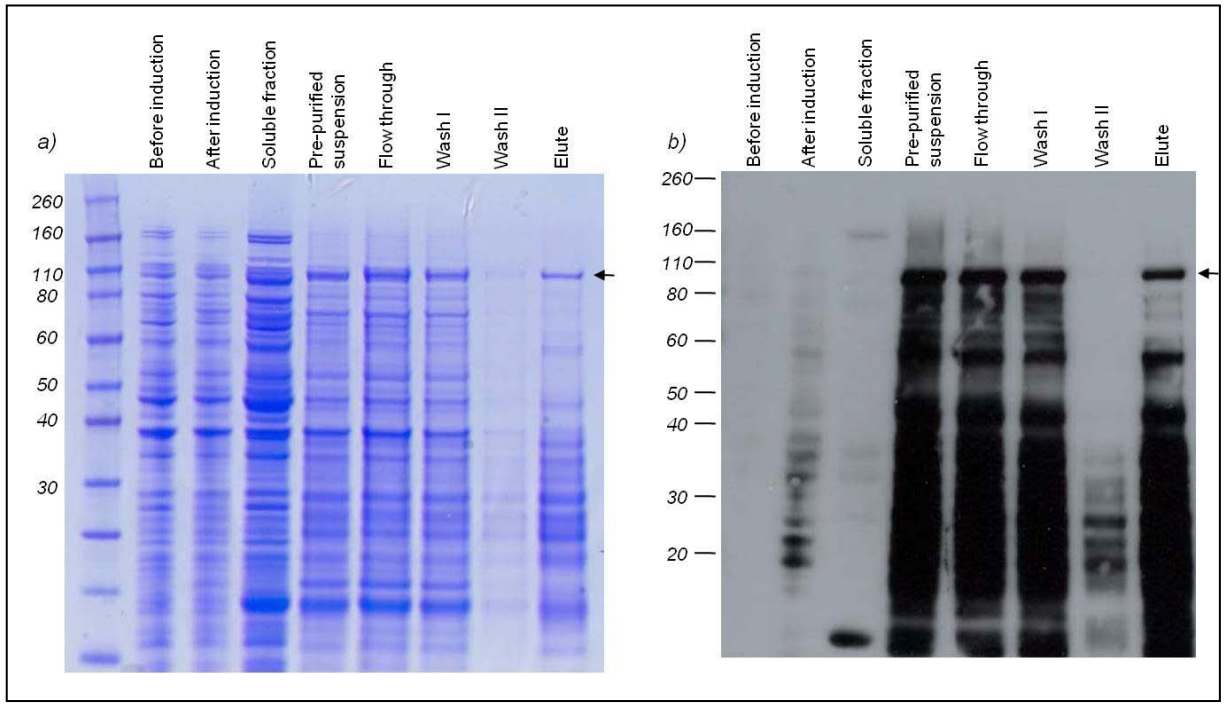

Figure 3.12C: SDS-PAGE gel and Western blot analysis of human c-Met extracellular αβ-chain expression in BL21 star bacteria strain.
a) Commassie-stained SDS-PAGE gel. Bacteria cells containing c-Met extracellular αβ-chain construct were induced with IPTG for 3 hrs. Expression of c-Met extracellular αβ-chain can be seen (as indicated by the arrow). Whole cell lysate before and after induction were analysed. Insoluble fraction of bacterial lysate before purification (pre-purified suspension) was solubilised in 6M urea before analysis. c-Met extracellular αβ-chain was affinity purified using a 1 ml Bio-Scale mini cartridge. The flow through, washes (wash I and wash II), and elute were collected and analysed on a SDS-PAGE gel. Arrow indicates purified c-Met extracellular αβ-chain that has a predicted molecular weight of 100 kD. ***b)*** Western blot analysis of a similar gel to that shown in *a)*. Half the amounts of protein used in *a)* were used in this Western blot. The presence of purified c-Met extracellular αβ-chain was confirmed by detecting the N-terminal histidine tag using an anti-Histidine-peroxidase antibody.

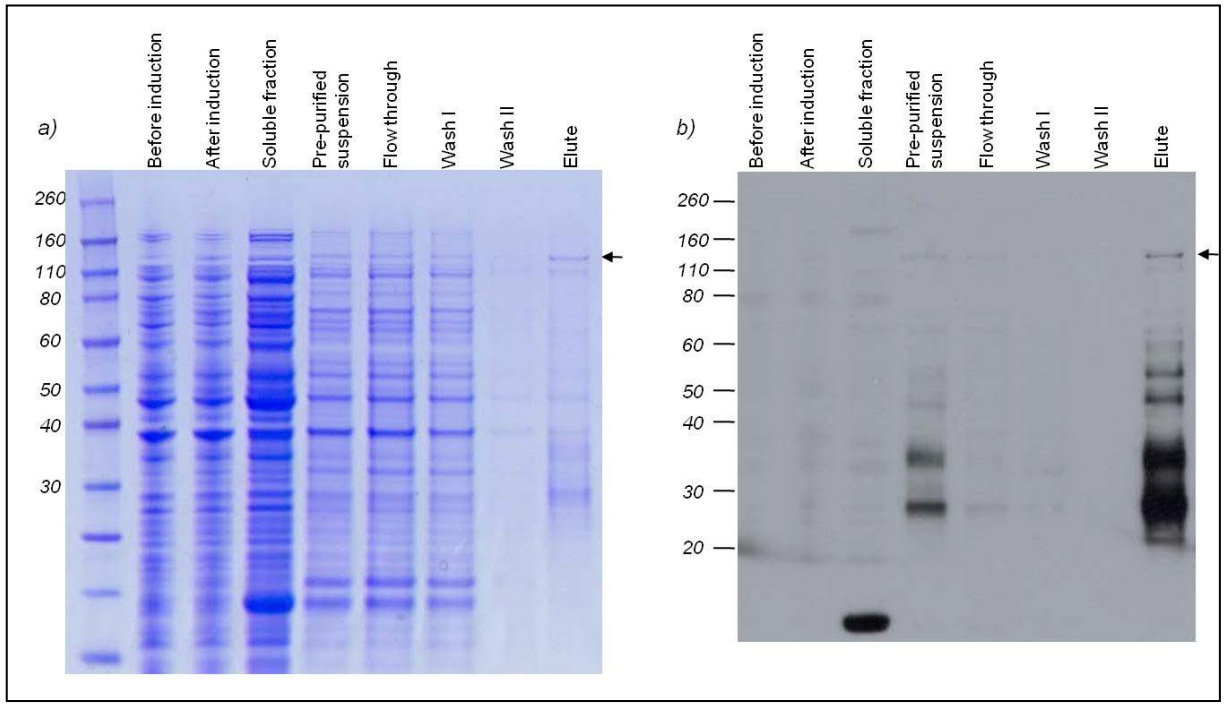

Figure 3.12D: SDS-PAGE gel and Western blot analysis of human c-Met full length β-chain expression in BL21 star bacteria strain.
a) Commassie-stained SDS-PAGE gel. Bacteria cells containing c-Met full length β-chain construct were induced with IPTG for 3 hrs. Expression of c-Met β-chain can be seen (as indicated by the arrow). Whole cell lysate before and after induction were analysed. Insoluble fraction of bacterial lysate before purification (pre-purified suspension) was solubilised in 6M urea before analysis. c-Met β-chain was affinity purified using a 1 ml Bio-Scale mini cartridge. The flow through, washes (wash I and wash II), and elute were collected and analysed on a SDS-PAGE gel. Arrow indicates purified c-Met β-chain that has a predicted molecular weight of 119 kD. ***b)*** Western blot analysis of a similar gel to that shown in *a)*. Half the amounts of protein used in *a)* were used in this Western blot. The presence of purified c-Met β-chain was confirmed by detecting the N-terminal histidine tag using an anti-Histidine-peroxidase antibody.

3.1.10: Summary of Section 3.1

This project aims to produce therapeutic monoclonal antibodies against the tyrosine kinase receptor, c-Met. At the beginning of this project, there were limited resources and biological reagents to allow us to study c-Met. However, in this section, we have: 1) verified the use of AF276 antibody as a positive control antibody, 2) determined the expression levels of endogenous c-Met in various mammalian cell lines, thus enabling us to have c-Met expressing and low c-Met expressing cells lines for antibody screening, 3) improved c-Met expression levels in mammalian cells by using various vectors as well as utilising the adenoviral system, and 4) investigated the use of SBP tag for c-Met purification. Armed with these useful tools, we are now able to design an antibody screening protocol to select for therapeutic monoclonal antibodies directed against c-Met.

Various c-Met constructs were successfully expressed in prokaryotes and purified. Purified c-Met α-chain and c-Met extracellular β-chain were sent to Moravian Biotechnology as immunogens for antibody production in mice. Antibody production and screening will be described in Section 3.2.

3.2: Production, screening and initial characterisation of monoclonal hybridoma supernatant

3.2.1: Screening of immunised mice by Western blotting

The aim of this project was to produce therapeutic mouse monoclonal antibodies against c-Met. In Section 3.1, c-Met α-chain and extracellular β-chain proteins were successfully expressed in bacteria, affinity purified and sent to Moravian Biotechnology for mouse immunisation. Four mice were immunised with each protein preparation. After several rounds of immunisation, tail-bleeds (blood sera) were collected and screened for an immunological response against c-Met. To determine if an immune response was evoked, serum obtained from each mouse was diluted successively and tested on Western blots for reactivity against the purified protein used for immunisation and transiently transfected full length human c-Met from NIH3T3 whole cell lysate (Figures 3.13A to B and 3.14A to B).

All four mice immunised with the α-chain of c-Met developed good immunological responses against purified α-chain as shown by Western blotting (Figure 3.13A). Since the α-chain of human c-Met was used as an immunogen, the mice sera should theoretically detect the 170 kD c-Met precursor and the mature 50 kD c-Met α-chain in cell lysates. However, AF276 failed to detect the α-chain in samples from transfected NIH3T3 cells, it is not known if the α-chain is being stably expressed. Sera from these mice successfully detected full length c-Met precursor immunoprecipitated from NIH3T3 transfected cells (Figure 3.13B), but failed to detect mature c-Met α-chain in the same sample. The mice sera also failed to detect full length c-Met from U-87MG and T47D cell lysates which are c-Met expressing and low c-Met expressing cells lines respectively. Protein bands, observed at the approximate predicted molecular weights of

c-Met, are present at equal intensity in samples from both U-87MG and T47D. This suggests that they are non-specific protein bands. Anti-α-chain serum 3 detected two bands of approximately 55 kD specifically in U-87MG samples, suggesting that they could be modified versions of c-Met α-chain. Serum is a crude mixture containing various types of antibodies and proteins. It is possible that the antibodies produced against human c-Met were present at a low concentration within the serum, resulting in the failure to detect full length endogenous human c-Met in cell lysates.

Despite going through the same immunisation and screening procedure as with the α-chain, mice immunised with c-Met extracellular β-chain did not develop good immune responses. Only the tail-bleeds obtained from the first and second mice were able to detect purified c-Met β-chain by Western blotting (Figure 3.14A). Theoretically, anti-β-chain chain blood sera should be able to detect c-Met precursor and mature c-Met β-chain (170 kD and 145 kD respectively) on Western blots using whole cell extracts. Consistent with this, the tail-bleed from the first mouse successfully detected both precursor and mature c-Met β-chain from immunoprecipitated c-Met protein in NIH3T3 transfected cells as well as endogenous c-Met from U-87MG cells (Figure 3.14B). However, there was a strong cross reactivity band at 170 kD (Figure 3.14B). The second mouse immunised with the β-chain developed no response as it failed to detect immunoprecipitated c-Met and endogenous c-Met on Western blots. Finally, the last two mice developed poor or no response towards purified β-chain.

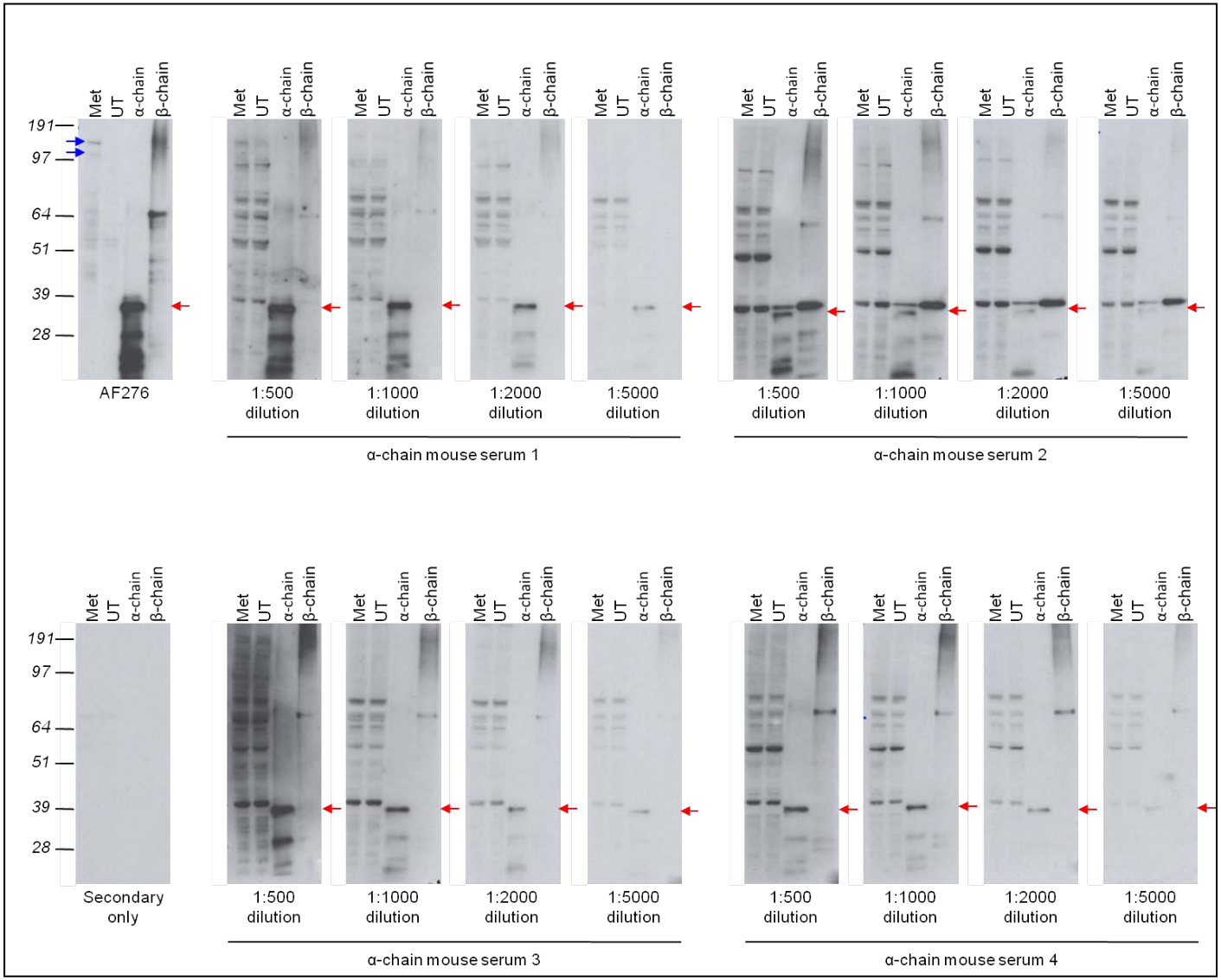

Figure 3.13A: Screening of mouse tail-bleeds against c-Met α-chain by Western blotting.
Four mice were immunised with purified c-Met α-chain. Tail-bleeds (blood sera) obtained from these mice (mouse serum 1 to 4) were diluted 1:500, 1:1000 1:2000 and 1:5000, and tested for reactivity against purified c-Met α-chain and c-Met in lysates of NIH3T3 cells transfected with plasmid DNA expressing full length human c-Met (Met). Lysates from untransfected cells and purified extracellular β-chain protein were used as controls. 20 µg of cell lysate, 50 ng of purified α-chain and 200 ng of purified β-chain was used in each case. AF276 antibody and secondary antibody only (secondary only) were used as controls. Blue arrows indicate c-Met β-chain (145 kD) and precursor c-Met (170 kD). Red arrows indicate purified c-Met α-chain which was predicted to be 31 kD. The observed increase in molecular weight may have been due its secondary structure. UT: Untransfected NIHT3 cells. α-chain: Purified α-chain used for immunisation. β-chain: Purified extracellular β-chain. Molecular weights are noted aside, in kilodaltons.

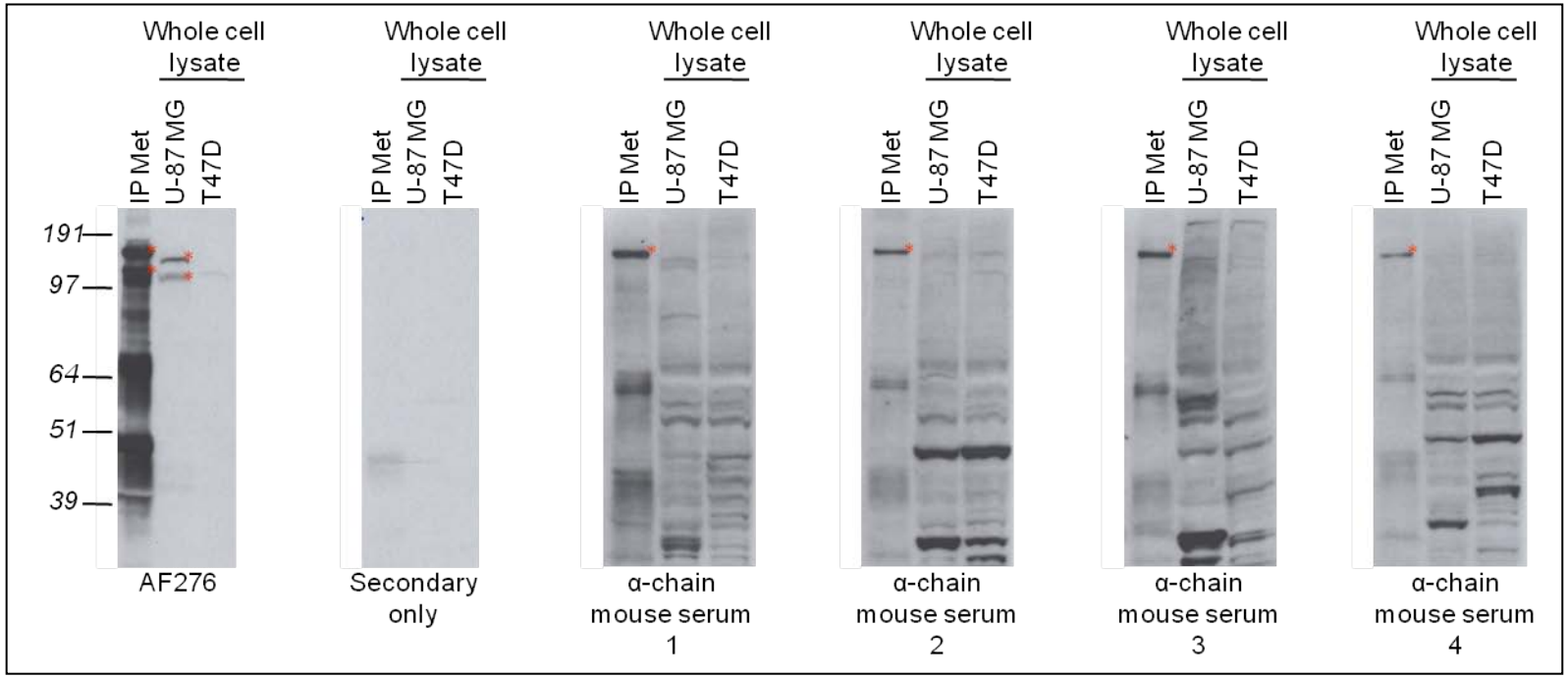

Figure 3.13B: Screening of anti-α-chain mouse tail-bleeds against endogenous c-Met by Western blotting.
Tail-bleeds (blood sera) obtained from α-chain immunised mice were tested for their reactivity towards immunoprecipitated and endogenous c-Met. 50 µg of whole cell lysates were analysed from U-87MG and T47D samples. U-87MG expresses human c-Met while T47D expresses very low levels of human c-Met. c-Met immunoprecipitated using AF276 antibody from 500 µg of cell lysate (obtained from NIH3T3 transiently expressing human c-Met) was used as a positive control (IP Met). Since the antibodies are directed against the α-chain of c-Met, they should recognise c-Met at 50 kD and 170 kD, but not at 145 kD. Tail-bleeds are used at 1:500 dilutions. AF276 antibody was used a positive control. Red asterisks indicate precursor c-Met protein band (top band) and c-Met β-chain (bottom band). IP: Immunoprecipitated. Molecular weights are noted aside, in kilodaltons.

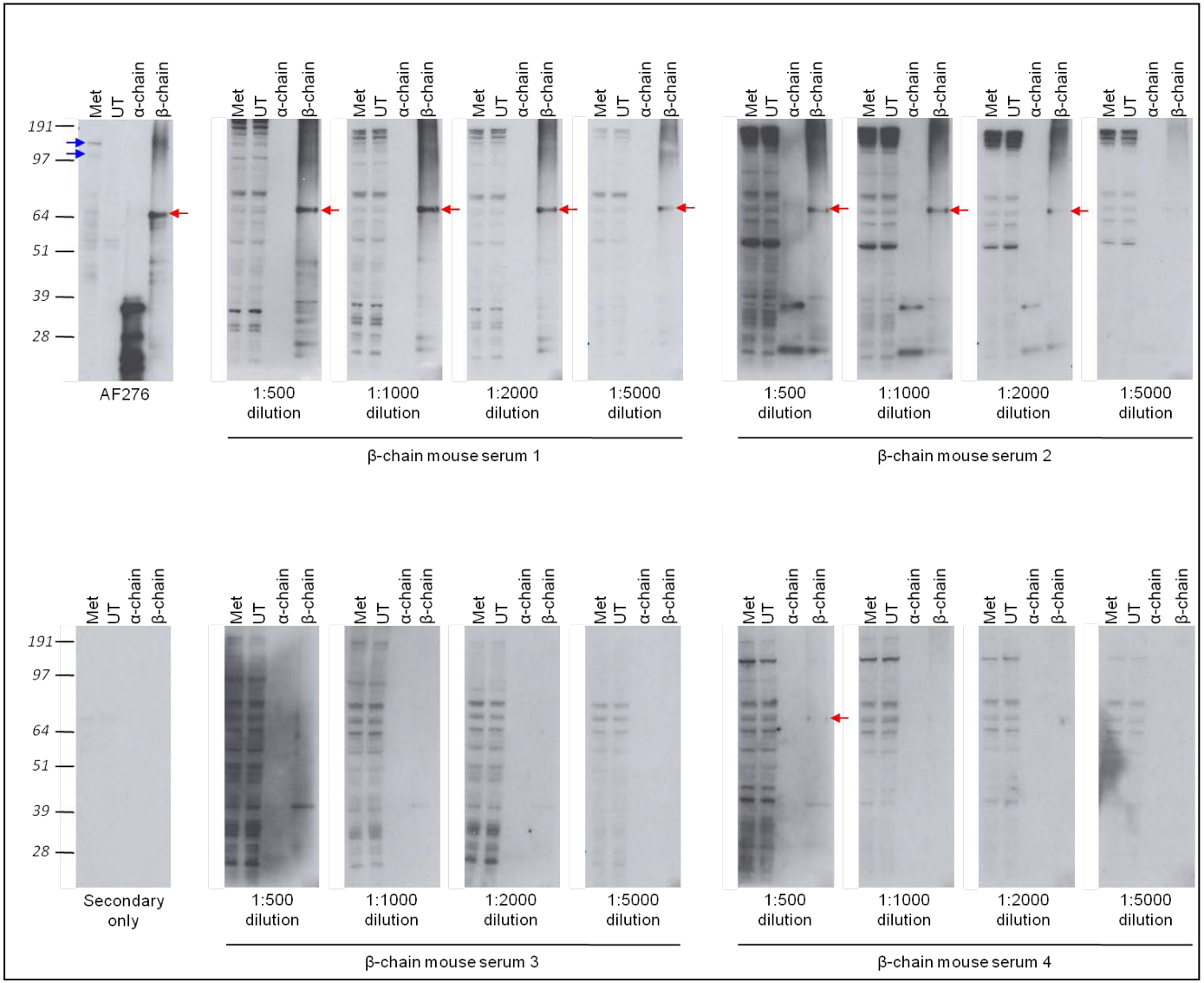

Figure 3.14A: Screening of mouse tail-bleeds against c-Met extracellular β-chain by Western blotting.
Four mice were immunised with purified c-Met extracellular β-chain. Tail-bleeds (blood sera) obtained from these mice (mouse serum 1 to 4) were diluted 1:500, 1:1000 1:2000 and 1:5000, and tested for reactivity against purified c-Met β-chain and c-Met in lysates of NIH3T3 cells transfected with plasmid DNA expressing full length human c-Met (Met). Lysates from untransfected cells and purified extracellular β-chain protein were used as controls. 20 µg of cell lysate, 50 ng of purified α-chain and 200 ng of purified β-chain was used in each case. AF276 antibody and secondary antibody only (secondary only) were used as controls. Blue arrows indicate c-Met β-chain and precursor c-Met (145 kD and 170 kD respectively) while red arrows indicate purified c-Met β-chain. The predicted molecular weight of extracellular β-chain was 69 kD. UT: Untransfected NIH3T3 cells. α-chain: Purified α-chain used for immunisation. β-chain: Purified extracellular β-chain. Molecular weights are noted aside, in kilodaltons

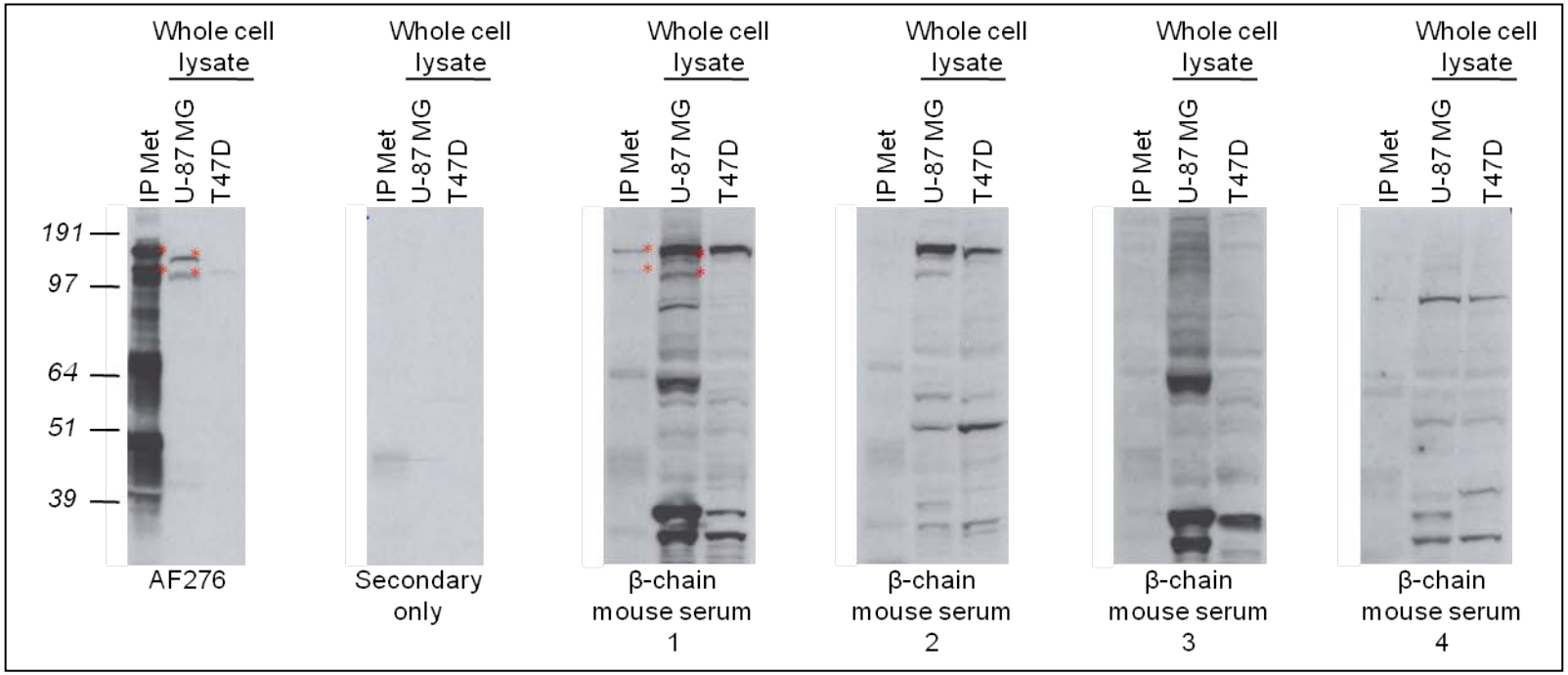

Figure 3.14B: Screening of anti-β-chain mouse tail-bleeds against endogenous c-Met by Western blotting.
Tail-bleeds (blood sera) obtained from extracellular β-chain immunised mice were tested for their reactivity towards immunoprecipitated and endogenous c-Met. 50 µg of whole cell lysates were analysed from U-87MG and T47D samples. U-87MG expresses human c-Met while T47D expresses very low levels of human c-Met. c-Met immunoprecipitated using A276 antibody from 500 µg of cell lysate (obtained from NIH3T3 transiently expressing human c-Met) was used as a positive control (IP Met). Since the antibodies are directed against the extracellular β-chain of c-Met, they should recognise c-Met at 145 kD and 170 kD. Tail-bleeds are used at 1:500 dilutions. AF276 antibody was used a positive control. Red asterisks indicate precursor c-Met protein band (top band) and c-Met β-chain (bottom band). IP: Immunoprecipitated. Molecular weights are noted aside, in kilodaltons.

3.2.2: Screening of sera from immunised mice by cell staining

The immunological responses of immunised mice were also screened by cell staining of untransfected NIH3T3 cells, or NIH3T3 cells transiently transfected with either full length human c-Met or full length human c-Met tagged with V5 (Met-V5). Sera from all α-chain immunised mice were able to detect both c-Met and Met-V5 in cell staining, but with low intensity (Figures 3.15A and B). This was probably due to the low levels of antibodies present in the mice sera. Consistent with the Western blotting analysis, only the first mouse immunised with the β-chain of c-Met showed reactivity against c-Met in cell staining. The β-chain of c-Met therefore appears to be a poor immunogen. Only mice producing antibodies directed against c-Met α-chain were used for hybridoma fusions directed towards making anti-Met monoclonal antibodies.

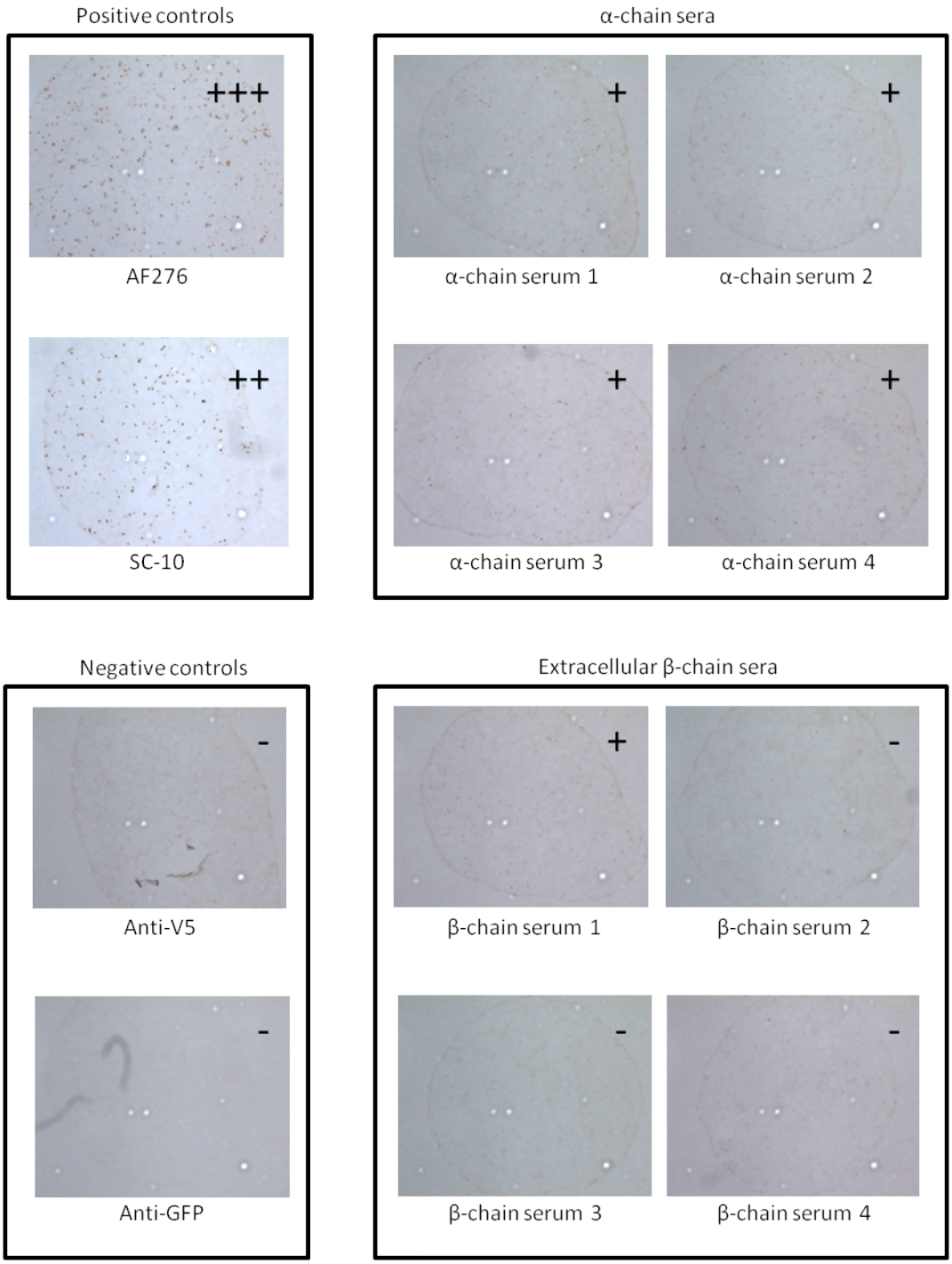

Figure 3.15A: Screening of immunised mouse tail-bleeds by cell staining of NIH3T3 cells transfected with human c-Met.

Tail-bleeds obtained from mice immunised with either c-Met α-chain or extracellular β-chain were used to detect c-Met protein in NIH3T3 cells transiently transfected with full length human c-Met. Mouse sera were used at a 1:500 dilution. AF276 and SC-10 antibodies were used as positive controls while anti-V5 and anti-GFP antibodies were used as negative controls. A score, located at the top right of each picture, indicates the staining intensity of each antibody. (-): no staining; (+): slight staining; (++): intermediate staining; (+++): intense staining.

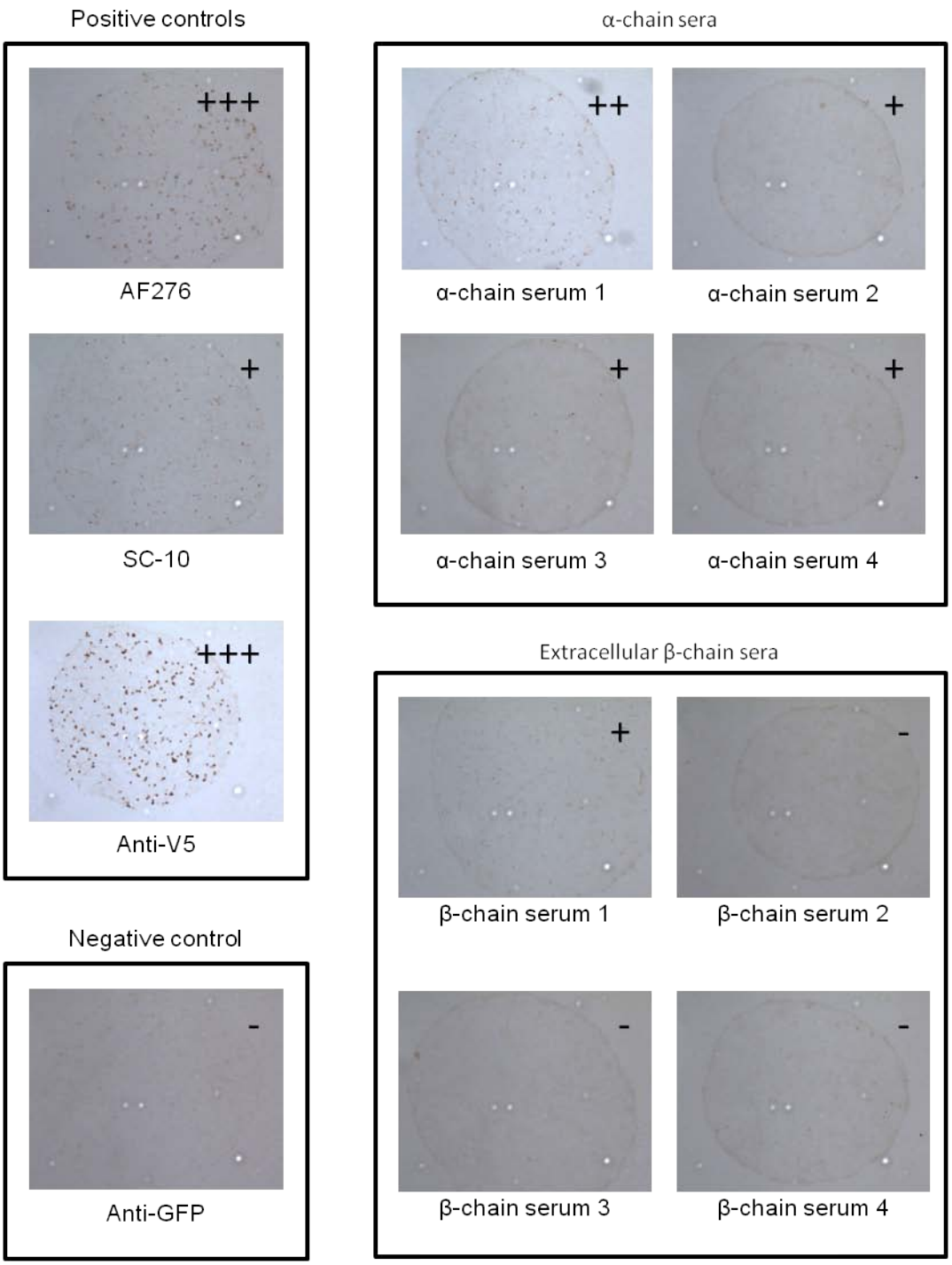

Figure 3.15B: Screening of immunised mouse tail-bleeds by cell staining of NIH3T3 cells transfected with human c-Met tagged with V5.

Tail-bleeds obtained from mice immunised with either c-Met α-chain or extracellular β-chain were used to detect c-Met protein in NIH3T3 cells transiently transfected with full length human c-Met with C-terminus V5 tag. Mouse sera were used at a 1:500 dilution. AF276, SC-10 and anti-V5 antibodies were used as positive controls while anti-GFP antibodies were used as a negative control. A score, located at the top right of each picture, indicates the staining intensity of each antibody. (-): no staining; (+): slight staining; (++): intermediate staining; (+++): intense staining.

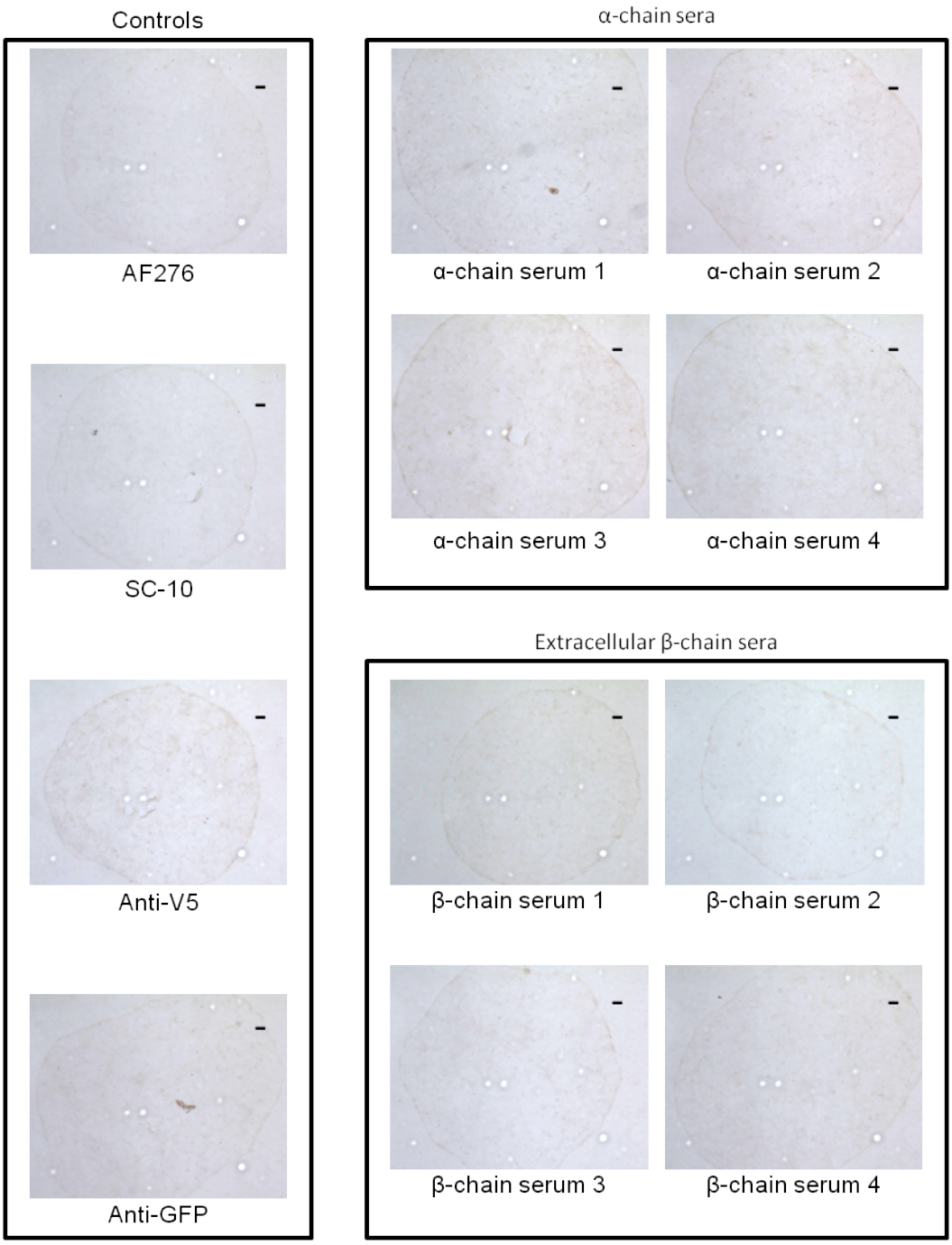

Figure 3.15C: Screening of immunised mouse tail-bleeds by cell staining of untransfected NIH3T3 cells.

Tail-bleeds obtained from mice immunised with either c-Met α-chain or extracellular β-chain were tested on untransfected NIH3T3 cells as a negative control. Mouse sera were used at a 1:500 dilution. A score, located at the top right of each picture, indicates the staining intensity of each antibody. (-): no staining; (+): slight staining; (++): intermediate staining; (+++): intense staining.

3.2.3: Hybridoma cell fusion and primary hybridoma supernatant screening

In order to develop an immortal cell line that secretes a monoclonal antibody, the spleen cells of an immunised mouse are fused to the mouse cell line Sp2/0-Ag14. This can result in a hybrid cell that contains both the antibody secreting properties of the spleen cell and the growth characteristics of the immortal cell line. Antibodies produced from a single hybridoma clone are termed monoclonal antibodies. By single cell cloning hybridoma cells, cell lines secreting a single monoclonal antibody are created. Due to the high specificity of monoclonal antibodies, hybridoma cells and their secreted antibodies are extremely useful tools in biomedical science research and have the potential to be developed into therapeutic agents.

Hybridoma cell fusion and monoclonal antibody production were performed by Moravian Biotechnology. Briefly, two mice immunised with c-Met α-chain were sacrificed and had their spleens removed. Spleen cells obtained from these mice were fused with the mouse immortal cell line, SP2/0-Ag14. Immediately after fusion, the cell mixture was plated into 96-well plates and fused cells were grown in selection media containing hypoxanthine, aminopterin and thymidine. Hypoxanthine and thymidine are intermediates in the DNA synthesis pathway. Aminopterin blocks the *de novo* synthesis of DNA causing cells to rely on the salvage pathway for DNA synthesis. Sp2/0-Ag14 cells are defective in the DNA salvage pathway, therefore are unable to survive in aminopterin selection media due to the blockage of both DNA synthesis pathways. Spleen cells are functional in both DNA synthesis pathways, however, due to their limited propagation capacity under tissue culture conditions, spleens cells fail to survive. Only hybridoma cells which have been successfully fused between a spleen cell and an immortal cell will survive and grow in the selection media. This is because the immortal-spleen hybrid cell will contain the ability of the immortal cell line to

proliferate under tissue culture conditions and the functional DNA salvage pathway of the spleen cell. To screen for anti-cMet antibody producing hybridoma clones, cell supernatant were taken from individual 96-wells (referred here as hybridoma lines to avoid confusion) that contained growing hybridoma cells. A flow chart of hybridoma screening is shown in Materials and Methods section (Figure 2.5).

To screen for hybridoma lines secreting immunoglobulin (Ig) antibodies against the α-chain of human c-Met, we took cell supernatants from growing hybridoma cells and tested separately for Ig production (data not shown) and for antibody reactivity against c-Met α-chain by dot blot technique. An example of dot blot analysis which was used to screen for antibodies against c-Met α-chain is shown in Figure 3.16*a*. From two separate dot blot analyses, 82 hybridoma lines were identified to be both positive for Ig and for reactivity against c-Met α-chain. These lines were then screened for their reactivity towards purified c-Met α-chain by Western blotting and for their ability to recognise full length c-Met by cell staining. Figure 3.16*b* shows an example of hybridoma cell supernatant screening by Western blotting. Antibodies identified from dot blot analysis were found to be variable in their reactivity towards c-Met in Western blotting and cell staining. This may be due to the varying methods of fixation which can lead to differing epitope presentation. For example, antibodies from the 12A12 line detected purified α-chain in Western blotting, but failed to detect full length human c-Met in cell staining (Figure 3.17). Based on the results of the screening procedure using dot blot, Western blotting and cell staining, hybridoma cells lines that successfully detected c-Met in the screening assays were selected for clonal expansion and further screening. In total, 58 hybridoma lines were identified.

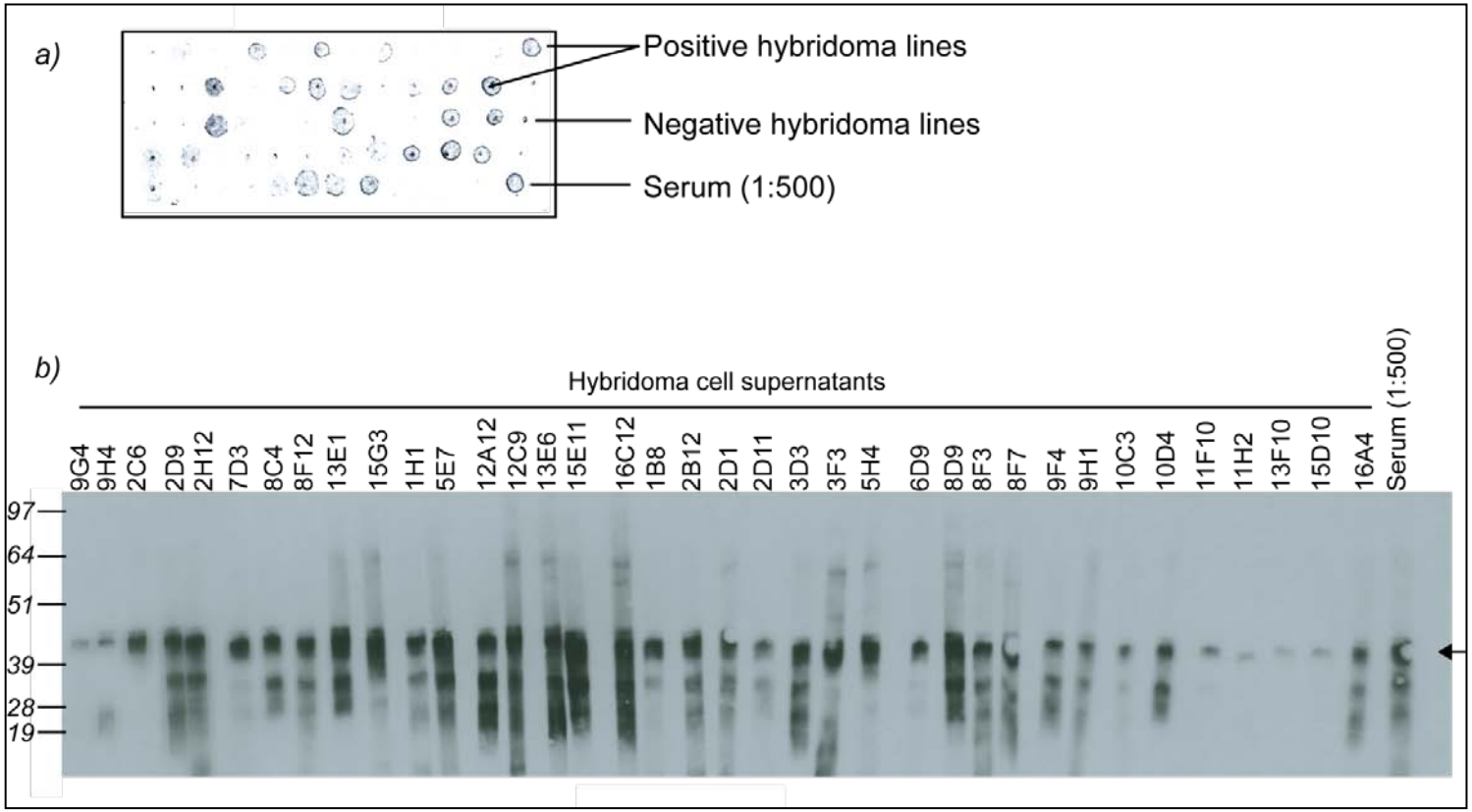

Figure 3.16: An example of hybridoma cell supernatant screening by dot blot and Western blotting.
a) Dot blot analysis of hybridoma cell supernatant reactivity against purified α-chain. Purified α-chain was coated onto a nitrocellulose membrane. Approximately 2 µl of undiluted hybridoma cell supernatant were spotted onto the nitrocellulose membrane, forming a circular droplet. Hybridoma cell supernatant was rinsed away before anti-mouse secondary antibody conjugated to HRP was added onto the nitrocellulose membrane. HRP activity was detected using 4-chloro-1-naphthol and hydrogen peroxide which resulted in a colourmetric reaction. Positive hybridoma lines were identified by the dark purple/black circles developed on the nitrocellulose membrane. Serum taken from the mouse before it was sacrificed was the positive control. Dots on the nitrocellulose membrane are pencil marks to indicate the position of the supernatant sample on the membrane. ***b)*** A panel of hybridoma lines were tested for the ability to detect purified c-Met α-chain on Western blotting. Purified α-chain was resolved on a single well SDS-PAGE gel and proteins were transferred onto a nitrocellulose membrane. Membrane was cut into strips and neat hybridoma cell supernatant were incubated directly on it. Again, serum taken from the mouse was used as positive control. Black arrow indicates the α-chain. Molecular weights are noted aside, in kilodaltons. Preparation of dot blots in *a)* and Western blot strips in *b)* was done in collaboration with Moravian Biotechnology.

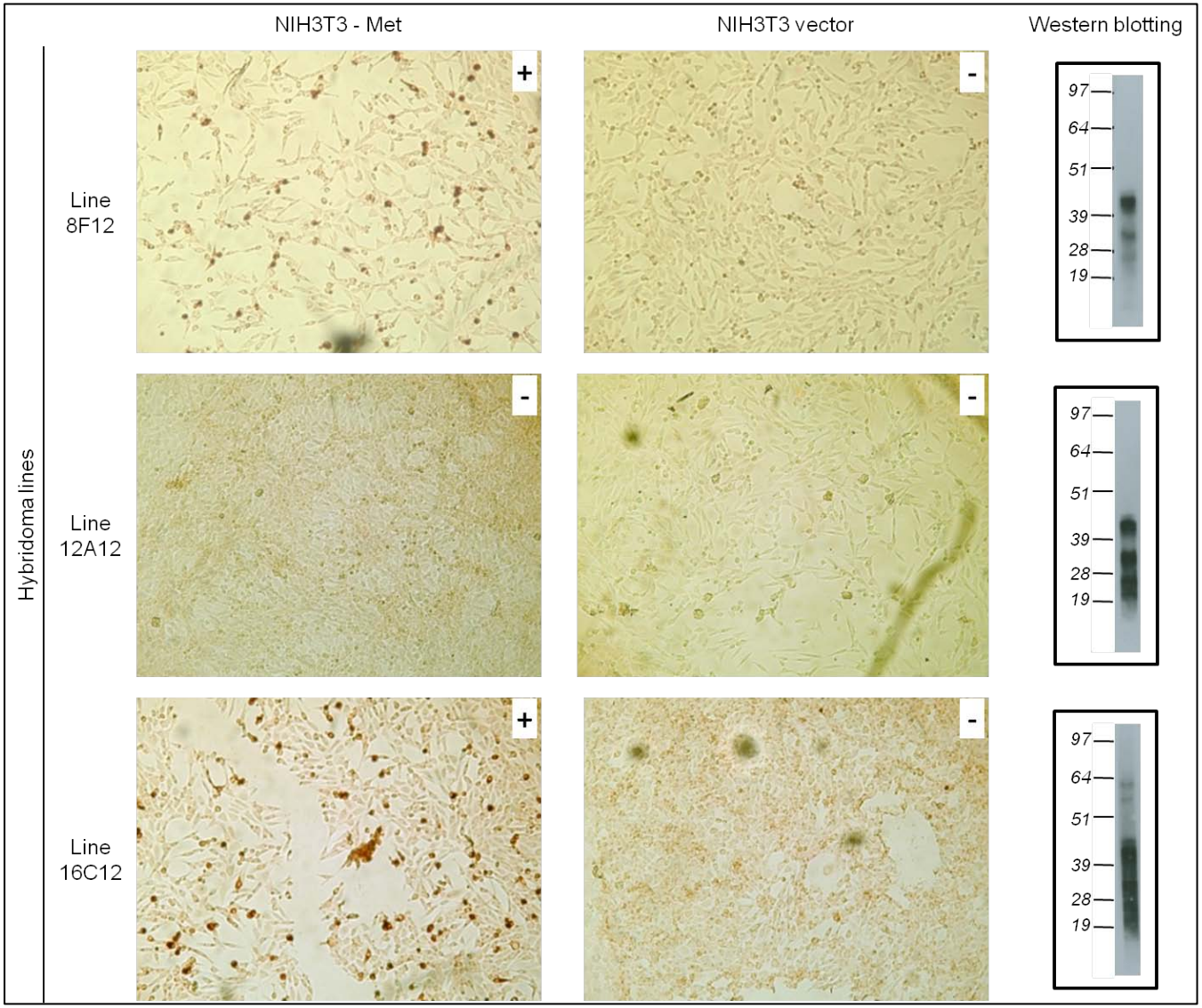

Figure 3.17: Examples of hybridoma lines screening by cell staining and Western blotting.
Hybridoma lines were screened for antibody production against c-Met by cell staining and Western blotting. Cell supernatants were taken from hybridoma cells and used to stain NIH3T3 cells transfected with full length human c-Met and vector alone. A score, located at the top right of each picture, indicates the staining intensity of each antibody. Hybridoma cell supernatants were also screened for their reactivity against the immunogen, purified α-chain, by Western blotting. Blue arrow indicates α-chain. (-): no staining; (+): staining. Molecular weights are noted aside, in kilodaltons.

3.2.4: Secondary hybridoma supernatant screening

To ensure that the hybridoma lines are stably expressing antibodies against c-Met, the 58 hybridoma lines were expanded and re-tested by dot blot, Western blotting and cell staining in a secondary screen. Secondary screen was performed entirely by Moravian Biotechnology, thus only an example of the data is shown. Dot blot and cell staining screening was performed using the same methods as the primary screening. Hybridoma supernatants were analysed on Western blot for the detection of purified α-chain and full length human c-Met in cell lysates derived from NIH3T3 transfected cells. Examples of this analysis are shown in Figure 3.18*a*. The ability of these antibodies to recognise endogenous human c-Met in extracts from U-87MG cells were also tested by Western blotting (Figure 3.18*b*).

The hybridoma cell lines used in this screening process were derived from surviving cells in a 96-well during hybridoma fusion selection, not from a single cell clone. Therefore at this stage, it remained a possibility that they might contain a mixture of hybridoma cells secreting two or possibly more antibodies. In addition, it was not possible to standardise the antibody concentration in the hybridoma supernatant due to the presence of fetal calf serum (FCS). Variation in antibody concentration might affect the results obtained in the screen. Although these points must be borne in mind when analysing the results shown, the primary screen was designed to identify promising clones for further analysis. In the secondary screen, 39 hybridoma lines were observed to be stably producing anti-α-chain antibodies and were successful in detecting c-Met by dot blotting, Western blotting and cell staining to varying extents (Table 3.2).

21 cell lines, identified from the secondary screen, were chosen to be single cell cloned for monoclonal antibody production following consultation with Moravian Biotechnology (refer to Table 3.2).

Figure 3.18: Secondary screening of hybridoma lines by Western blotting.
a) 58 hybridoma lines identified from primary screening were re-tested for their ability to recognise human c-Met in cell lysates derived from NIH3T3 cells transfected with either c-Met or Met-GFP fusion construct. ***a & b)*** 50 μg of whole cell lysates was used in the case of untransfected (UT) NIH3T3 cells, and NIH3T3 cells transfected with constructs expressing c-Met or Met-GFP as shown. 50 μg of cell lysates dervied from U-87MG or T47D cells was used. 100 ng and 10 ng of purified c-Met α-chain protein was analysed in *a)* and *b)* respectively. Hybridoma supernatants were diluted 1:1 with 5% milk in PBST. AF276 antibody was used as a positive control. Hybridoma supernatants should be tested against murine c-Met to determine the cross-species reactivity of the antibodies. Blue arrows indicate c-Met precursor or c-Met tagged to GFP. Red arrows indicate purified α-chain. Molecular weights are noted aside, in kilodaltons.

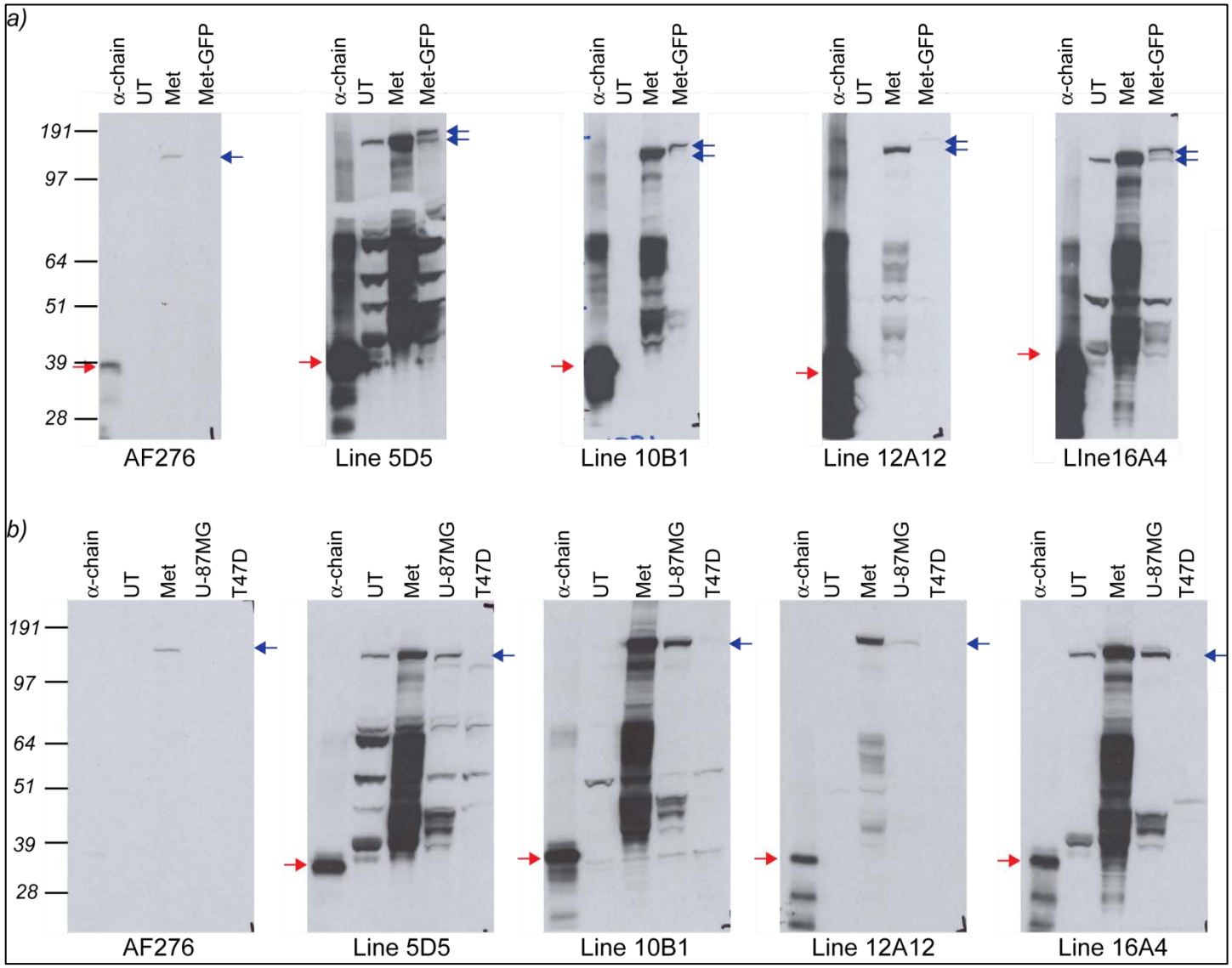
a)
α-chain
UT
Met
Met-GFP
191
97
64
51
39
28
AF276
Line 5D5
Line 10B1
Line 12A12
LIne16A4
b)
α-chain
UT
Met
U-87MG
T47D
191
97
64
51
39
28
AF276
Line 5D5
Line 10B1
Line 12A12
Line 16A4

Table 3.2: Screening results of the 21 hybridoma lines selected for monoclonal antibody production.

Line	Cell staining		Western blot				Dot blot	
	Met transf.	Met-V5 transf.	α-chain	Met transf.	U-87MG	T47D	Ig	α-chain
2C6	++	+++	+++	+++	+++	NS	+++	+++
2H8	+++	+++	+++	+++	+	-	+++	+++
3E6	+	+	++++	+++	+++	-	+++	+++
5D5	++	+++	+++	+++	++	NS	+++	+++
5E7	+++	+++	+++	+++	+++	-	++	+++
5G12	+++	+++	+++	+++	+++	-	++	+++
5H4	-/+	+	++	+/++	-/+	-	+++	+++
6D9	-/+	+	++	++	+	-	+++	+++
9H1	+	++	+++	+++	+	-	+++	+++
9H4	++	+++	+++	+++	++	-	+++	+++
13E1	++	+++	++++	+++	++	-	+++	+++
10B1	+++	+++	+++	+++	++	NS	+++	+++
12A12	_	-	++++	++	-/+	-	++	+++
12C9	++	+++	++++	+++	+++	-	++	+++
12D10	+++	++	++++	++	+	NS	+++	+++
15E11	++	+++	+++	+++	++	-	+++	+++
15G3	+	+++	+++	++	++	-	++	+++
16A4	-/+	+	++++	+++	++	-	+++	+++
16C11	+	++	++++	+++	+++	NS	+	++
16F6	++	++	++++	+++	+	-	++	+++
16H3	+++	++	++++	++++	+++	NS	+++	+++

Cell staining was performed using NIH3T3 cells transfected with constructs expressing c-Met or Met-V5. Recognition of purified c-Met α-chain and full length human c-Met (from whole cell extract of NIH3T3 transfected with c-Met plasmid, U-87MG and T47D cells) by the antibodies were analysed by Western blotting. NS refers to recognition of non-specific bands observed in T47D samples. Ig production by the hybridoma cell lines and antibody reactivity to α-chain were analysed by dot blot. Transf.: Transfected. NS: Non-specific binding. Ig: Immunoglobulin. Antibody screening results were graded accordingly: (-): no reactivity; (+): slight reactivity; (++): intermediate reactivity; (+++): strong reactivity.

3.2.5: Monoclonal antibody production and screening

21 hybridoma clones were selected from the secondary hybridoma screen and were single-cell cloned to obtain cell lines expressing single monoclonal antibodies by Moravian Biotechnology. Monoclonal antibodies (Mab) were renamed for convenience and to avoid confusion. Reference to the original hybridoma clone names could be found in Table 3.4 at the end of this section. Cell supernatants were harvested from single-cell cloned cells and were re-tested their reactivity against c-Met to ensure they retained their anti-α-chain antibody producing capability (Figures 3.19A and B).

As mentioned, antibodies produced from a single hybridoma clone are monoclonal and thus it is assumed that the results observed are caused by a single antibody, specific to a single epitope. Consistent with the previous screening results, all monoclonal antibodies successfully detected both transfected and endogenous c-Met precursor from whole cell lysates in Western blots (Figures 3.19A and B). None of the anti-α-chain monoclonal antibodies were able to detect mature c-Met α-chain at its predicted molecular weight of 50 kD in cell lysates. The commercial AF276 antibody, which was raised against the extracellular domain of human c-Met, should be able to detect the mature α-chain of c-Met. From Figures 3.19, AF276 detected purified α-chain weakly but failed to detect endogenous and transfected α-chain from cell extracts. SC-10 was raised against a peptide in the C-terminal tail of c-Met and therefore, it did not recognise the α-chain. Due to the lack of antibodies that recognise the α-chain in cell lysates, there is no positive control to compare the protein bands observed in our anti-α-chain blots. It is difficult to conclude if the 40-70 kD protein bands observed, is genuinely representing the α-chain on Western blots. It is unclear why mature α-chain could not be detected on Western blots. Differential glycosylation of the α-chain could result in various sizes of α-chain observed on a Western blot. The mature α-chain could be rapidly degraded

upon cell lysis. In addition, the presence of non-specific protein bands observed on some of the Western blots probed with the monoclonal antibodies, could also obscure the faint mature c-Met α-chain. Several protein bands observed on the Western blots could be explained by: 1) antibodies present in the FCS from cell media, 2) genuine recognition of the antibodies to its epitope which is present in other proteins, 3) high antibody concentration in the cell supernatants, and 4) degradation or processing of c-Met protein.

Finally, it is observed that the band profile produced by a group of monoclonal antibodies (Mab 6.1, 9.1, 10.1, 11.1, 12.1, 14.1, 20.1 and 21.1) on Western blots are highly similar. Mab 17.1, 18.1 and 19.1, also make up another group of antibodies that share a very similar band profile to this large group of antibodies. Mab 8.1 also shares a similar band profile to the large group of antibodies except for the presence of some non-specific bands. In contrast, Mab 13.1 recognises precursor c-Met and β-chain but also recognises a range of protein bands throughout the blot. This suggests that Mab 13.1 does not work well on Western blotting as it detects many non-specific bands. Western blot band profiles are dependent on an antibody recognising its epitope. Monoclonal antibodies that share the same band profile could be recognising the same epitope while antibodies with different band profile will most probably recognise a different epitope. More assays are required to further characterise the monoclonal antibodies and allow us to select the appropriate antibody to be used in human therapy. A more detailed comparison of the Western blot band profiles will be discussed in the later part of this section.

Figure 3.19A: Screening of monoclonal antibodies following single cell cloning of hybridoma cell lines (Mab 1.1 to Mab 10.1) by Western blotting.
21 hybridoma clones were selected for monoclonal antibody production and tested again for reactivity against full length c-Met in whole cell lysates. Monoclonal antibodies (Mab) were renamed to avoid confusion. 50 μg of whole cell lysates were obtained from untransfected NIH3T3 cells (UT), NIH3T3 cells transfected with full length human c-Met (Met) construct, U-87 MG cell lines and T47D cell lines. Hybridoma supernatants were diluted 1:1. 10 ng of purified α-chain and AF276 antibody were controls. Upper blue arrows indicate c-Met precursor. Lower blue arrows indicate β-chain detected in AF276 and SC-10 blots. Red arrows indicate purified α-chain. Mab: Monoclonal antibody. Molecular weights are noted aside, in kilodaltons.

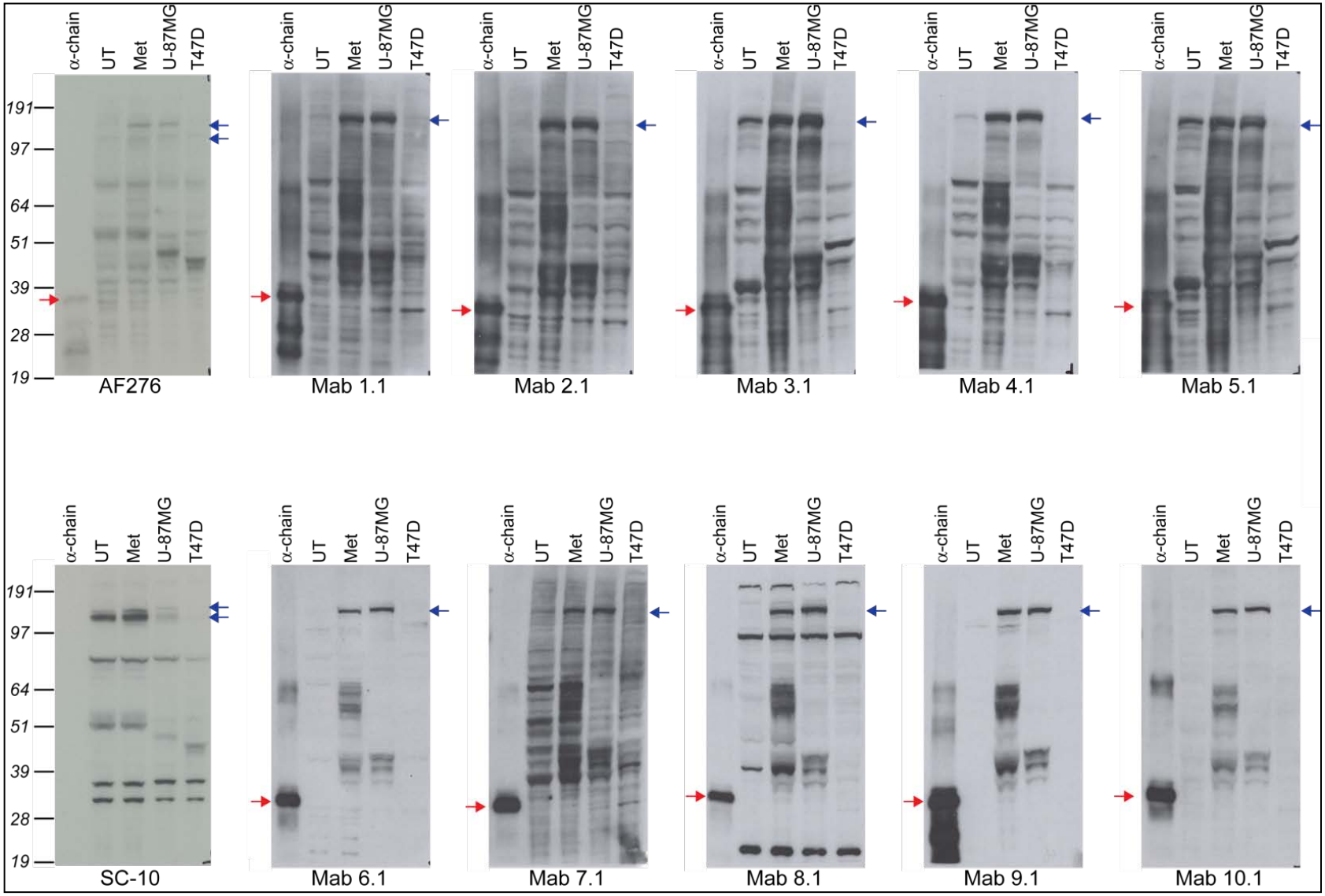
α-chain
UT
Met
U-87MG
T47D
191
97
64
51
39
28
19
AF276
Mab 1.1
Mab 2.1
Mab 3.1
Mab 4.1
Mab 5.1
SC-10
Mab 6.1
Mab 7.1
Mab 8.1
Mab 9.1
Mab 10.1

Figure 3.19B: Screening of monoclonal antibodies (Mab 11.1 to Mab 21.1) by Western blotting.
21 hybridoma clones were selected for monoclonal antibody production and tested again for reactivity against full length c-Met in whole cell lysates. Monoclonal antibodies (Mab) were renamed to avoid confusion. 50 μg of whole cell lysate were obtained from untransfected NIH3T3 cells (UT), NIH3T3 cells transfected with full length human c-Met (Met) construct, U-87 MG cell lines and T47D cell lines. Hybridoma supernatants were diluted 1:1. 10 ng of purified α-chain and AF276 antibody were controls. Upper blue arrows indicate c-Met precursor. Lower blue arrows indicate β-chain detected in AF276 blot. Red arrows indicate purified α-chain. Mab: Monoclonal antibody. Molecular weights are noted aside, in kilodaltons.

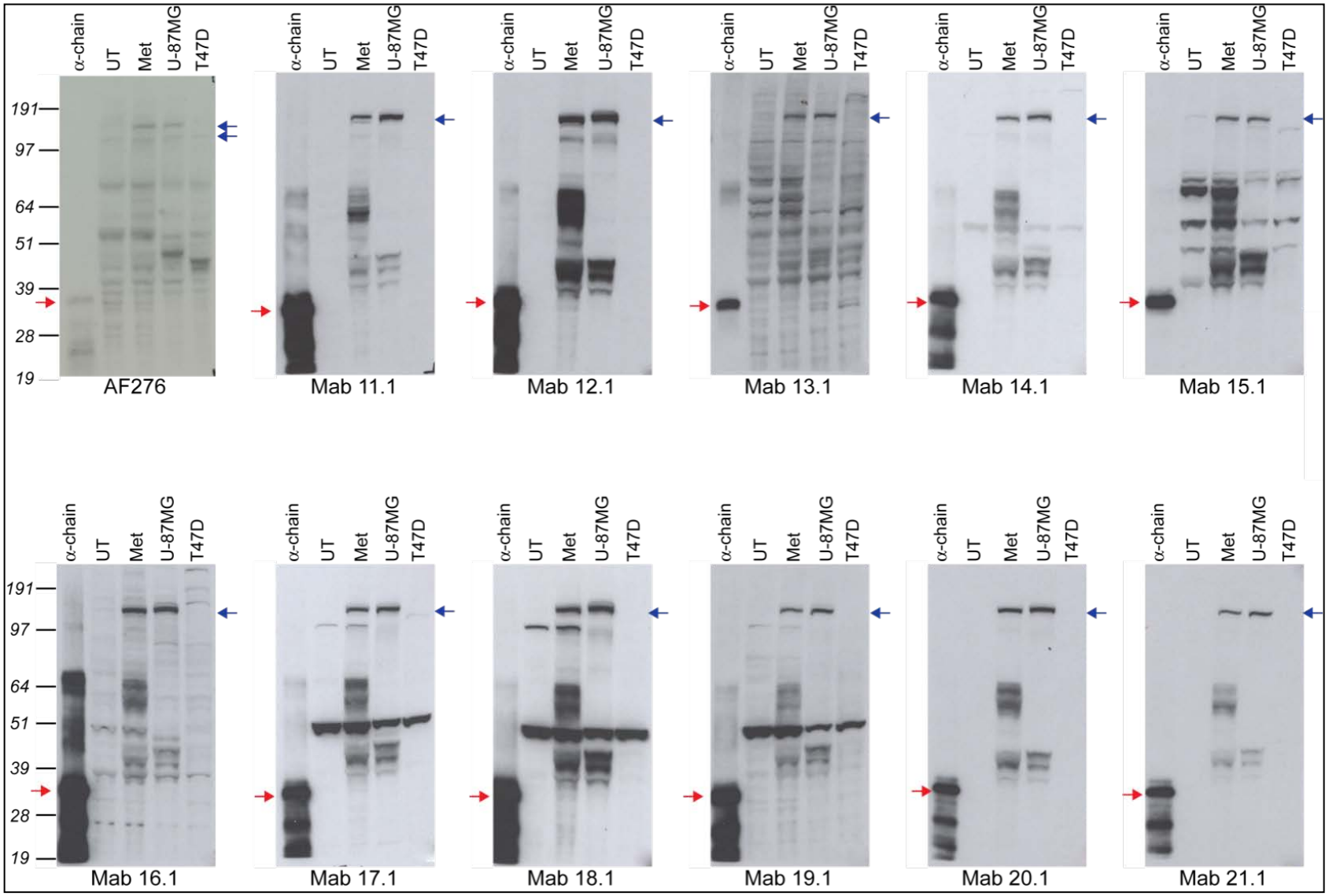
α-chain
UT
Met
U-87MG
T47D
191
97
64
51
39
28
19
AF276
Mab 11.1
Mab 12.1
Mab 13.1
Mab 14.1
Mab 15.1
Mab 16.1
Mab 17.1
Mab 18.1
Mab 19.1
Mab 20.1
Mab 21.1

3.2.6: Monoclonal antibody isotyping

Antibody isotype determines both antibody purification technique and ability of the antibody to recruit effector functions. Antibody isotyping was performed by dipping commercially available isotyping strips into cell supernatant. These strips can differentiate between IgG subclasses and antibody light chain subclasses (examples shown in Figure 3.20). A test line will develop on the strip specific to the antibody isotype. The appearance of several test lines indicates the presence of other antibodies in the cell supernatant.

All 21 monoclonal antibodies contain the IgG class and a single test line was observed for each antibody tested. This is an indication that the monoclonal antibodies are obtained from a single hybridoma clone. IgG subclass antibodies form dimers, are bivalent molecules and play an important role in antibody-dependent cell-mediated cytotoxicity (ADCC). Not all the antibodies share the same IgG subclass. 19 monoclonal antibodies were IgG1. Mab 4.1 and 16.1 were IgG2A while Mab 19.1 was IgG2B. All 21 monoclonal antibodies contain the kappa light chain and these results are summarised in Table 3.4 at the end of this section.

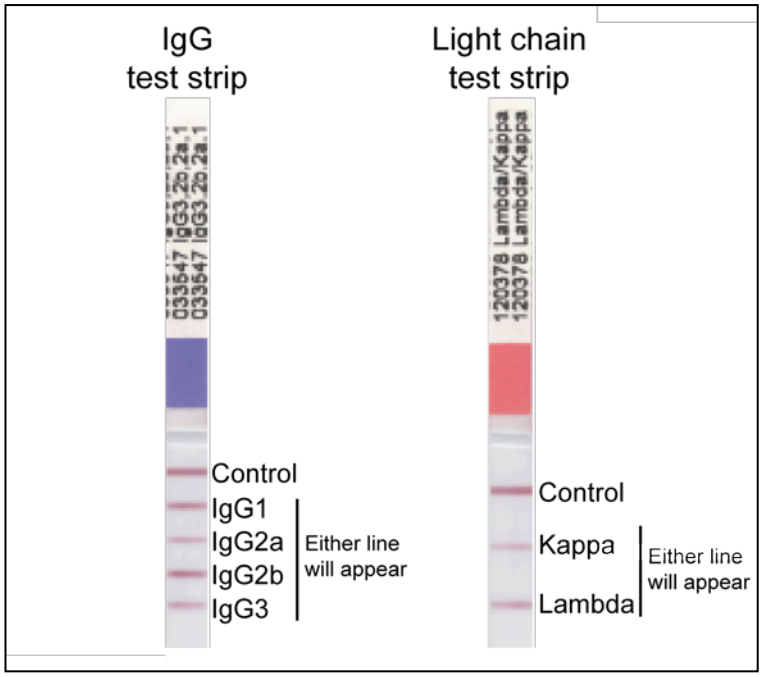

Figure 3.20: Examples of monoclonal antibody isotyping strips.
Commercially isotyping strips are individually available for characterising an antibody's IgG subclass and light chain. Isotyping strips are dipped in cell supernatant containing monoclonal antibodies. A red band would appear which corresponds to the type of IgG subclass and light chain present in the cell supernatant. Control band ensures that the test strips are functional. If no IgG subclass or light chain is present in the cell supernatant, only the control band will appear. Figure is adapted from Sigma-Aldrich.

3.2.7: Mapping of monoclonal antibody binding regions

Monoclonal antibodies were further characterised by mapping the region of their epitope by pepscan. Identifying the region of c-Met bound by the antibody is important in determining whether the antibody might be able to block c-Met from binding to its ligand, HGF. Consecutive overlapping peptides that span the entire α-chain were synthesised *in vitro* (Mimotopes). Each peptide, made up of 15 amino acid residues, overlaps each neighbouring peptide by 10 amino acids. These peptides were tagged with biotin at the N-terminus through an SGSG linker sequence. Peptides were added to individual wells in a 96-well plate and unbound peptides were removed by extensive washing. To determine the region of antibody binding on the α-chain, hybridoma cell supernatants were added to each peptide. Binding of the antibody was detected by colorimetric assay and analysed by absorbance reading at 450 nM. The region of antibody binding was then mapped to a crystal structure of the c-Met extracellular domain binding to the β-chain of HGF which contains full length α-chain and partial β-chain (Figure 3.24). This crystal structure was obtained from Protein Data Base, accession number 1SHY. In total, 10 different regions from the α-chain were identified from the 21 monoclonal cell supernatants tested, indicating that this is no one main region that is highly immunogenic. To avoid confusion, the regions identified were labelled 1 to 10 according to their position on the α-chain. Region 1 is closest to the N-terminus while region 10 is the most C-terminal region. A simplified diagram of the antibody binding domain on c-Met α-chain is shown in Figure 3.21 and the amino acid sequence is shown in Figure 3.22.

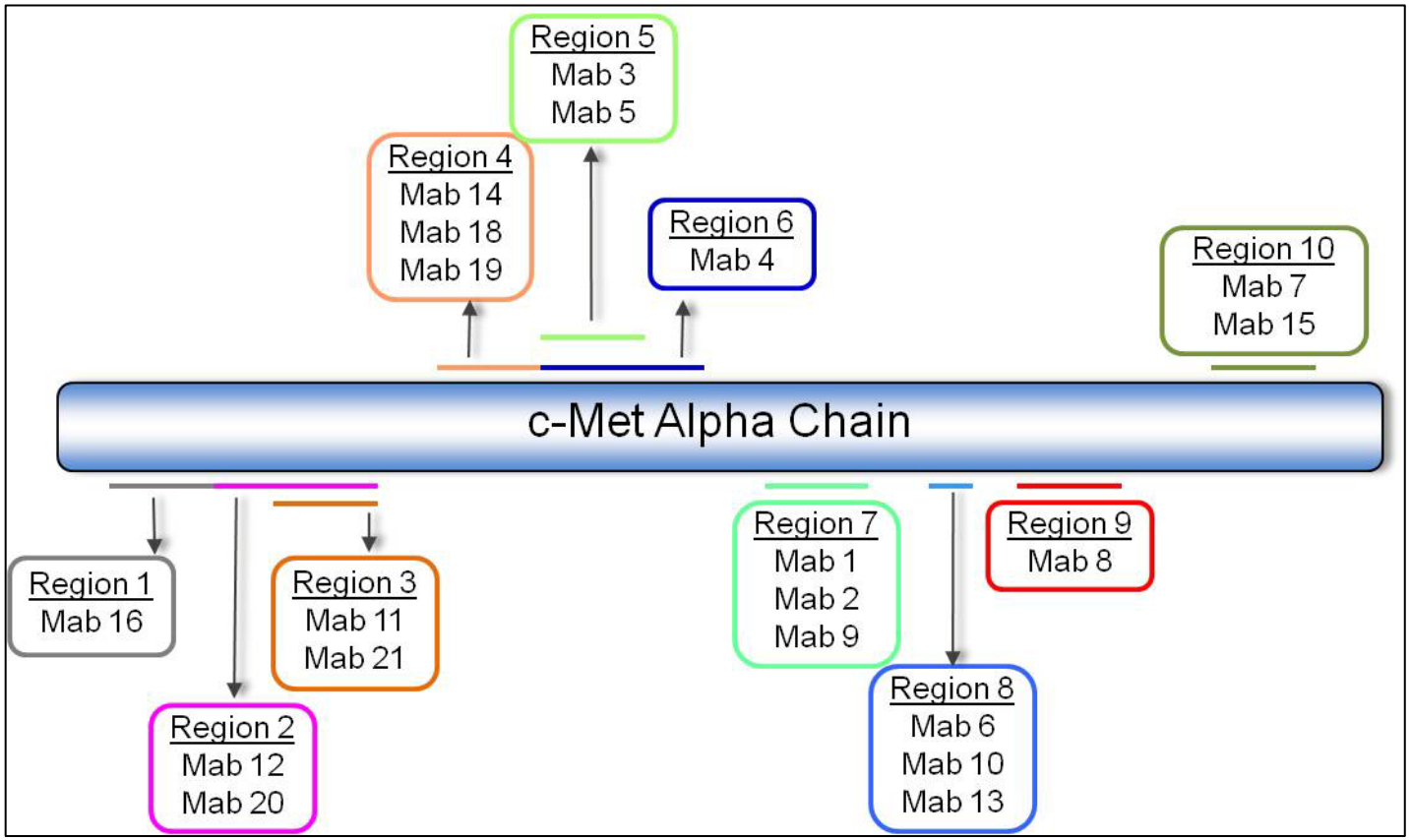

Figure 3.21: Schema of antibody binding regions.
Pepscan was used to determine the binding region of 21 monoclonal supernatants. Consecutive overlapping peptides that span the entire α-chain were synthesised *in vitro*. Each peptide, made up of 15 amino acid residues, overlaps each neighbouring peptide by 10 amino acids. To determine the region of antibody binding on the α-chain, monoclonal cell supernatants were added to each peptide. Binding of the antibody was detected by colorimetric assay and analysed by absorbance reading at 450 nM. The epitope of the antibodies were categorised into regions. Region 1 is closest to the N-terminus while region 10 is the most C-terminal region. Antibodies that share the same binding region are indicated. The peptide sequence of the binding regions, in reference to the full length α-chain sequence, is shown in Figure 3.22. Figure not drawn to scale.

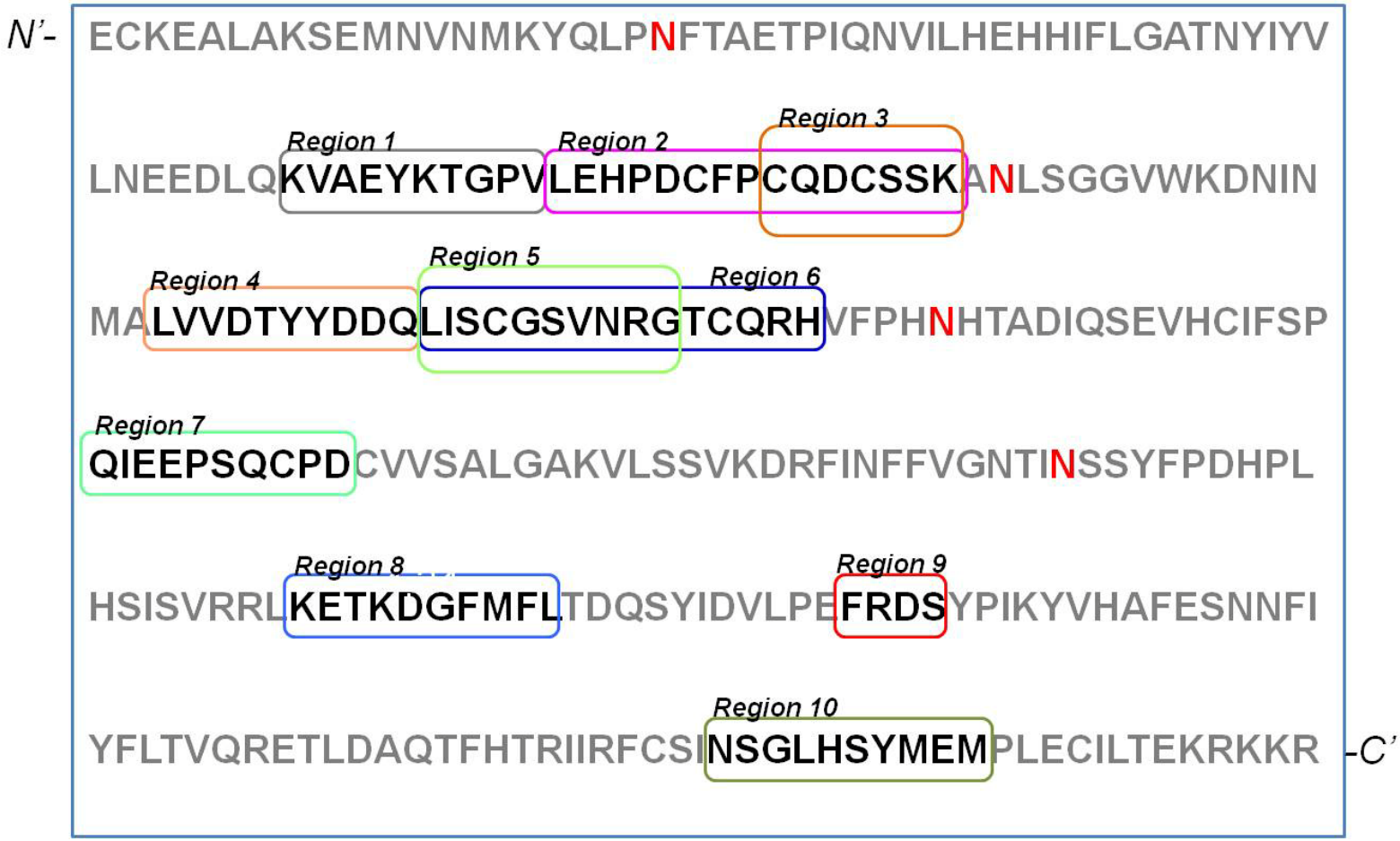

Figure 3.22: Antibody binding regions highlighted in the amino acid sequence of c-Met α-chain.
10 binding region were identified among 21 monoclonal antibody developed against the α-chain of c-Met. The full length amino acid sequence of c-Met α-chain, excluding the N-terminal signalling peptide, is indicated above. This sequence was expressed in bacteria and purified for mouse immunisation. Antibody binding regions are indicated. Predicted glycosylation sites on asparagines (N) are highlighted in red. Region 1 is closest to the N-terminus while region 10 is the most C-terminal region. N'-: N-terminus of the protein sequence. –C': C-terminus of the protein sequence.

Region 1

Mab 16.1 binds to both peptides 11 and 12 (Figure 3.23A). The epitope of Mab16.1 must therefore reside within the overlapping 10 amino acid residues of these peptides. This region is labelled as region 1. Peptide 12 developed a stronger colorimetric reaction compared to peptide 11. It is probable that the last five amino acid residues in peptide 12 contribute to the antibody-antigen interaction. Finally, it is observed that the epitope of Mab 16.1 does not lie within the region of the α-chain which interacts directly with HGF.

Region 2

Mab 12.1 and 20.1 bind only to one peptide, peptide 14 (Figure 3.23B). This indicates that residues on both sides of the central five amino acid region (amino acid residues 'CFPCQ') must be essential for epitope recognition (amino acid residues 'LEHPD' and 'DCSSK'). It is likely that the central five amino acids (amino acid residues 'CFPCQ') are required. Alternatively, the main epitope could be a discontinuous sequence that is made up amino acids flanking the central region at peptide 14. Therefore, only one peptide is being detected. Alanine scan analysis would be required to define the specific residues more clearly.

The epitopes of Mab 12.1 and 20.1 are mapped to region 2, suggesting that both epitopes could be the same. This is consistent that both of these antibodies were observed to produce similar Western blot band profiles (Figure 3.23B). Alternatively, it is possible that Mab 12.1 and 20.1 are different antibodies that bind to different epitopes within region 2. Further analysis, using techniques such as phage display, could be performed to verify this issue. Finally, it is observed that region 2 does not lie within the region of the α-chain which interacts directly with HGF.

Region 3

The epitopes of Mab 11.1 and 21.1 (region 3) lie within a similar region to region 2 (recognised by Mab 12.1 and 20.1), though a smaller region of 10 amino acid residues is required for antibody recognition. Mab 11.1 and 21.1 bind to peptide 14 and 15 (Figure 3.23C), indicating that the main epitope is located within the overlapping residues 'CFPCQDCSSK'. Similarly to Mab 16.1, one peptide (peptide 14) developed a stronger colorimetric reaction then the other (peptide 15), indicating that the residues outside this region may contribute to antibody-antigen binding.

As region 2 and 3 overlap each other, the Western blotting analysed by Mab 11.1, 12.1, 20.1 and 21.1 are being compared. All four antibodies produced very similar Western blot band profiles although the epitopes for these antibodies might be quite distinct from each other. Mab 16.1 recognises region 1 of c-Met (Figure 3.23A) and clearly, its epitope is distinct from Mab 11.1, 12.1, 20.1 and 21.1. Interestingly, Mab 16.1 shares similar band profiles with this group of antibodies suggesting that the bands observed on the Western blots are various sizes c-Met. These bands could be degradation products of c-Met or c-Met α-chain.

Region 4

Region 4 contains the epitopes of 14.1, 18.1 and 19.1, which is located in the overlapping residues of peptide 19 and 20 (Figure 3.23D). Both peptides show similar antibody binding intensity demonstrating that both peptides contain the essential residues that make up the epitope. Region 4 lies within the region of the α-chain which interacts directly with HGF.

Mab 18.1 and 19.1 produced identical Western blots while Mab 14.1 produced a slightly different blot. This suggests that Mab 14.1 do not recognise the same epitope as

Mab 18.1 and 19.1, although they share the same binding region. Mab 17.1 also binds to region 8 which will be discussed below.

Region 5 and 6

Mab 3.1 and 5.1 bind to peptides 21 and 22 showing a similar intensity indicating that they bind to the overlapping region of these peptides (Figure 3.23E). Region 5 is tucked inside c-Met so would not be available for antibody binding to the native protein. It is not surprising that the epitopes of Mab 3.1 and 5.1 lie inside c-Met because denatured α-chain was used as immunogen. Mab 4.1 bound only to peptide 22, here referred as region 6 (Figure 3.23F). Similar to region 5, region 6 is tucked inside c-Met and is unlikely to be involved in receptor-ligand binding. Mab 3.1, 4.1 and 5.1 bind within the same region, but may not necessarily recognise the same epitope. However, comparison of their Western blots profiles suggests that they do recognise similar epitopes.

Region 7

The epitopes of Mab 1.1, 2.1 and 9.1 are located within peptides 28 and 29 (Figure 3.23G). Since both peptides have similar colour intensity, the overlapping amino acid residues (region 7) must contain the binding regions for these antibodies. Antibodies binding to region 7 might be capable of blocking receptor-ligand binding as this region lies on the surface of the c-Met extracellular domain, close to the binding region of the HGF β-chain.

Mab 9.1 was observed to have different Western blot band profiles compared to Mab 1.1 and 2.1. Although the antibodies share the same binding region, it is likely that they recognise different epitopes. High background and non-specific bands were observed in Mab 1.1 and 2.1. Lowering the antibody concentration for Mab 1.1 and 2.1 on Western blot could help reduce the non-specificity and produce a clearer blot.

Region 8

The pepscan analysis of Mab 6.1, 10.1 and 13.1 yielded surprising results. Unlike other monoclonal antibodies that bound only a maximum of two peptides, these antibodies bound four peptides: peptide 36, 42, 43 and 44 (Figure 3.23H). Peptides 42, 43 and 44 share the sequence 'EFRDS', but have no shared sequence with peptide 36. Various explanations are possible for the observed binding to peptide 36: 1) non-specific antibody binding, 2) contamination of the monoclonal antibody with other antibodies, 3) antibodies were not produced from a single hybridoma clone, 4) the paratope (antibody's antigen binding site) of monoclonal antibodies bind to discontinuous epitopes, or 5) the antibodies are polyreactive antibodies (an antibody molecule recognising two epitope). Interestingly, peptide 36 contains a sequence 'FPDH' which is similar to the 'FRDS' sequence within the shared region of peptides 42, 43 and 44. Therefore 'FxDx', whereby x means any amino acid residue, could be the main epitope. If this is true, many proteins do contain the 'FxDx' sequence which will be recognised by these antibodies by Western blotting. Consistent with this theory, Mab 13.1 detected numerous protein band on Western blotting (Figure 3.23H panel *c*), suggesting that its epitope could be 'FxDx'. Amino acid point mutations could be performed to confirm this hypothesis. Mab 6.1 and 10.1 produced identical band profile when Western blotting for c-Met, which is different from Mab 13.1 (Figure 3.23H). Fewer protein bands were observed on Mab 6.1 and 10.1 blots compared to Mab 13.1 suggesting that the Mab 6.1 and 10.1 epitopes are not 'FxDx'. Mab 6.1 and 10.1 may share the same epitope within region 8 however, further analysis is required to determine the exact epitope.

Region 9

Mab 8.1 was the only monoclonal antibody that bound to region 9 defined by the overlap of peptides 39 and 40 (Figure 3.23I). Interestingly, region 9 lies in the

interacting surface of c-Met extracellular domain and HGF β-chain. It would be interesting to test if Mab 8.1 would be able to block c-Met from binding to HGF *in vivo*. The Western blot profile of Mab 8.1 shares some similarities with other antibodies, however, it also recognises a set of non-specific protein bands (Figure 3.19A).

Region 10

Lastly, the epitopes for Mab 7.1 and 15.1 lie in region 10. Both antibodies bound to peptides 52 and 53 with equal affinity (Figure 3.23J). Region 10 lies on the surface of the c-Met extracellular domain, close to the binding domain of the HGF β-chain. Mab 7.1 and 15.1 may be capable of disrupting receptor-ligand interactions. The Western blot band profile of Mab 7.1 is different from Mab 15.1. This suggests that Mab 7.1 and 15.1 have different epitopes that both lie within region 10.

Mab 17.1

To our surprise, Mab 17.1 bound to six peptides, peptide 19, 20, 36, 42, 43 and 44, simultaneously (Figure 3.23K). No common peptide sequence was observed among these six peptides. In addition, these peptides are not in proximity to each other when mapped on the c-Met α-chain crystal structure. Peptides 19 and 20 contain the epitope of Mab 14.1, 18.1 and 19.1 (region 4) while peptides 36, 42, 43 and 44 contain the epitope Mab 6.1, 10.1 and 13.1 (region 8). It is highly possible that Mab 17.1 is not produced from a single clone i.e. there is more than one hybridoma clone in the pool of cells producing IgG1 antibodies. One clone could be producing antibodies against region 4 while the other could be producing antibodies against region 8. Interestingly, the Western blot band profile of Mab 17.1 was highly similar to Mab 18.1 and 19.1 (Figure 3.23D). Mab 18.1 and 19.1 recognise region 4 which is one of the regions that Mab 17.1 recognises. Although Mab 17.1 also recognises region 8, the band profile suggest that its epitope is more similar to region 4 than to region 8.

To investigate whether Mab 17.1 is produced from a single clone, hybridoma clone 2H8 was single cell cloned again. Eleven colonies were obtained. Cell supernatants were harvested and analysed by pepscan. Pepscan results for the Mab 17.1 re-cloned lines are tabulated in Table 3.3. Interestingly, seven clones bound to both regions 4 and 8, four clones bound to region 4 specifically and none bound to region 8 specifically. It is unclear why the majority of the clones still bound to both regions despite being single-cell cloned for the second time. One explanation is that Mab 17.1 is a polyreactive antibody. Normally, an IgG antibody molecule contains two similar antigen binding sites which recognise and bind to the same epitope (homotypic bivalent binding). Homotypic bivalent binding can only occur when the antigen is in abundance i.e. when epitopes are in close proximity. This is, however, not possible when the antigens are scarce such as in the case of the gp140 glycoprotein displayed on the surface of the human immunodeficiency virus (HIV). Mouquet *et al.* (2010) reported the production of anti-HIV polyreactive antibodies in humans. Polyreactive antibodies have two different antigen binding sites thus allowing the antibody to recognise two epitopes in the same antigen molecule (bivalent heteroligomerisation). This allows antibodies to bind foreign molecules in situations whereby the antigen is scarce, and homotypic bivalent binding is not possible. Mab 17.1 could be a polyreactive monoclonal antibody, binding to two different regions of c-Met. Nonetheless, the results from Table 3.3 suggest that the original Mab 17.1 clone could contain a mixture of poly-reactive monoclonal antibodies and monoclonal antibodies that recognises region 4. Since the results of Mab 17.1 re-clones are not interpretable, and it would be interesting to test the effect of blocking two regions of c-Met in functional assays, future experiments were performed with the parental Mab 17.1 clone.

It should be noted that we have only narrowed down the monoclonal antibody binding region and not identified the actual epitopes. As mentioned earlier, although some monoclonal antibodies share the same region of binding, it does not necessarily mean that they share the same epitope. In addition, although most of the antibody binding regions do not coincide with the region of c-Met interaction with HGF β-chain, does not mean that the antibodies would not be able to block the receptor-ligand interaction. 1SHY is the crystal structure of a partial extracellular c-Met domain binding to the β-chain of HGF. The crystal structure of full length c-Met (or at least full length c-Met extracellular domain) binding to full length HGF has not been solved. Our monoclonal antibodies binding to c-Met might block the HGF α-chain interaction with c-Met, prevent c-Met dimerisation or affect global protein conformation (Figure 3.24). The antibodies might also block other protein interactions, such as α6β4 integrin and CD44 (Trusolino *et al.*, 2001; van der Voort *et al.*, 1999) which have been reported to interact with c-Met.

A list of monoclonal antibody names, clone names, region of binding, sequence of binding region and isotype group can be found in Table 3.4. In the same table, is the comparison of the sequence of antibody binding region on human c-Met to its mouse homologue. The full length sequence alignment of human and mouse c-Met can be found in Appendix 2. The mapping of the epitope binding regions on the sequence alignment of human and mouse c-Met α-chain is shown in Figure 3.25. The alignment of the human and mouse c-Met sequences implies that it should be possible to raise antibodies that are both species specific- and cross-reactive (Table 3.4). As self-tolerance to low abundance proteins is held in the T cell compartment, immunisation with the human protein can be predicted to induce antibodies that are human specific and are cross-reactive between the mouse and human proteins. Our results confirm this

completely (epitope mapping regions 5 and 6). Notably a single amino acid difference in an epitope is sufficient to define complete species specificity (Table 3.4). In a well-studied example, the anti-p53 antibody recognises the DLW motif in the TFSDLW sequence at the N terminus of human p53. The same antibody is completely unreactive with the mouse p53 protein which has the sequence TFSGLW at this site. Thus the G to D substitution defines the species specificity of this very potent antibody. Interestingly in phage display peptide mapping all DO-1 binding phage peptide sequences contained the DLW motif (Lane, D.P. *et al.*, 1996).

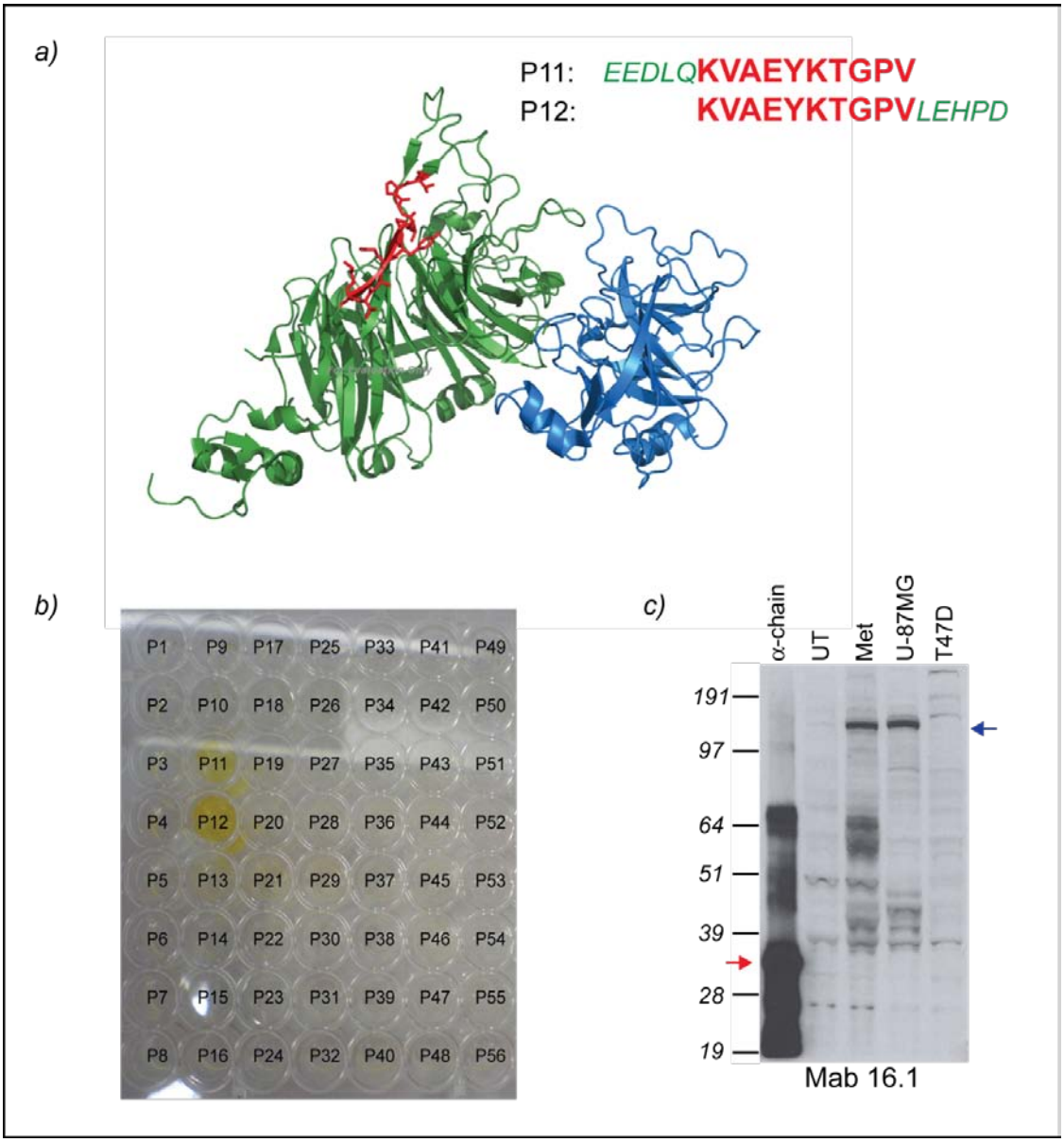

Figure 3.23A: Region 1 contains the epitope of Mab 16.1.
a) Crystal structure of c-Met extracellular domain (amino acid residues 25 – 567), binding to HGF β-chain. Crystal structure was obtained from Protein Data Bank (PDB), accession number 1SHY. c-Met is highlighted in green, HGF in blue and region 1 in red. The sequence of region 1 is also noted in red. ***b)*** Pepscan of Mab 16.1. Cell supernatant was added to wells coated with various peptides (peptide 1 to 55) as shown. Binding of monoclonal antibodies to their epitope will produce a yellow colorimetric reaction. Sequence of peptide 11 and 12, and region 1 (overlapping region of both peptides) is noted in *a)*. P56 (no peptide) is the negative control. ***c)*** Mab 16.1 Western blot analysis of c-Met in cell extracts obtained from untransfected (UT) NIH3T3 cells, NIH3T3 cells transiently expressing human c-Met (Met), U-87MG cells and T47D cells. Western blots are shown for comparison and are the same as those in Figures 3.19. Blue arrows and red arrows indicate c-Met precursor and c-Met purified α-chain respectively. Molecular weights are noted aside, in kilodaltons. P: Peptide (example P1 = Peptide 1).

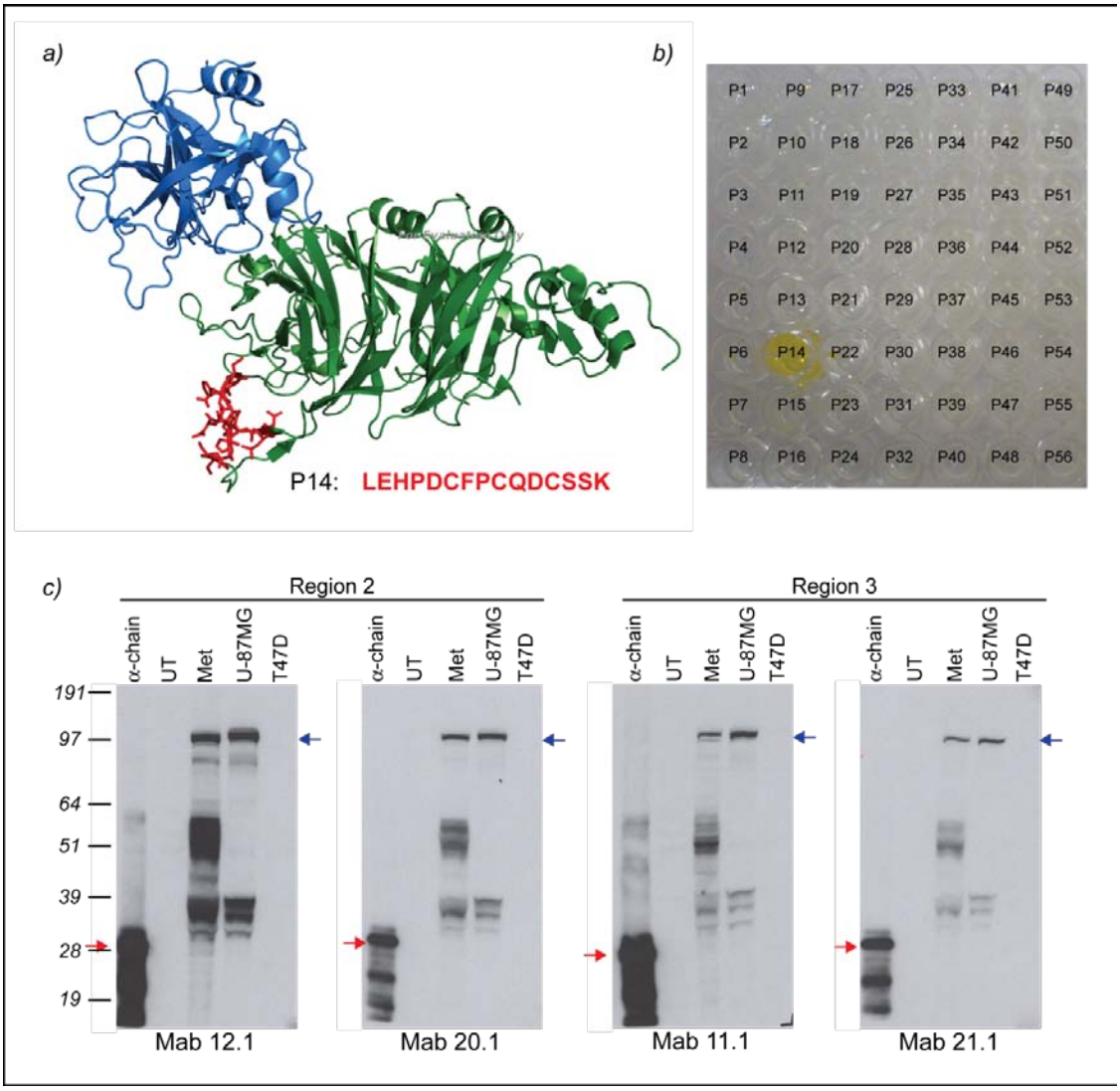

Figure 3.23B: Region 2 contains the epitope of Mab 12.1 and 20.1.
a) Crystal structure of c-Met extracellular domain (amino acid residues 25 – 567), binding to HGF β-chain. Crystal structure was obtained from Protein Data Bank (PDB), accession number 1SHY. c-Met is highlighted in green, HGF in blue and region 2 in red. The sequence of region 2 is also noted in red. ***b)*** A pepscan example of Mab 12.1 and 20.1. Cell supernatants were added to wells coated with various peptides (peptide 1 to 55) as shown. Binding of monoclonal antibodies to their epitope will produce a yellow colorimetric reaction. Sequence of peptide 14/region 2 is noted in *a)*. P56 (no peptide) is the negative control. ***c)*** Western blot analysis of c-Met in cell extracts obtained from untransfected (UT) NIH3T3 cells, NIH3T3 cells transiently expressing human c-Met (Met), U-87MG cells and T47D cells. Western blots were individually analysed by Mab 11.1, 12.1, 20.1 and 21.1. Western blots were grouped according to the binding region the antibody recognises, thus allowing the comparison of Western blot band profile among antibodies that bind within the same region. Antibodies from region 2 (Mab 12.1 and 21.1) and 3 (Mab 11.1 and 20.1) were grouped together as their binding region are overlapping. Western blots are the same as those in Figures 3.19. Blue arrows and red arrows indicate c-Met precursor and c-Met purified α-chain respectively. Molecular weights are noted aside, in kilodaltons. P: Peptide (example P1 = Peptide 1).

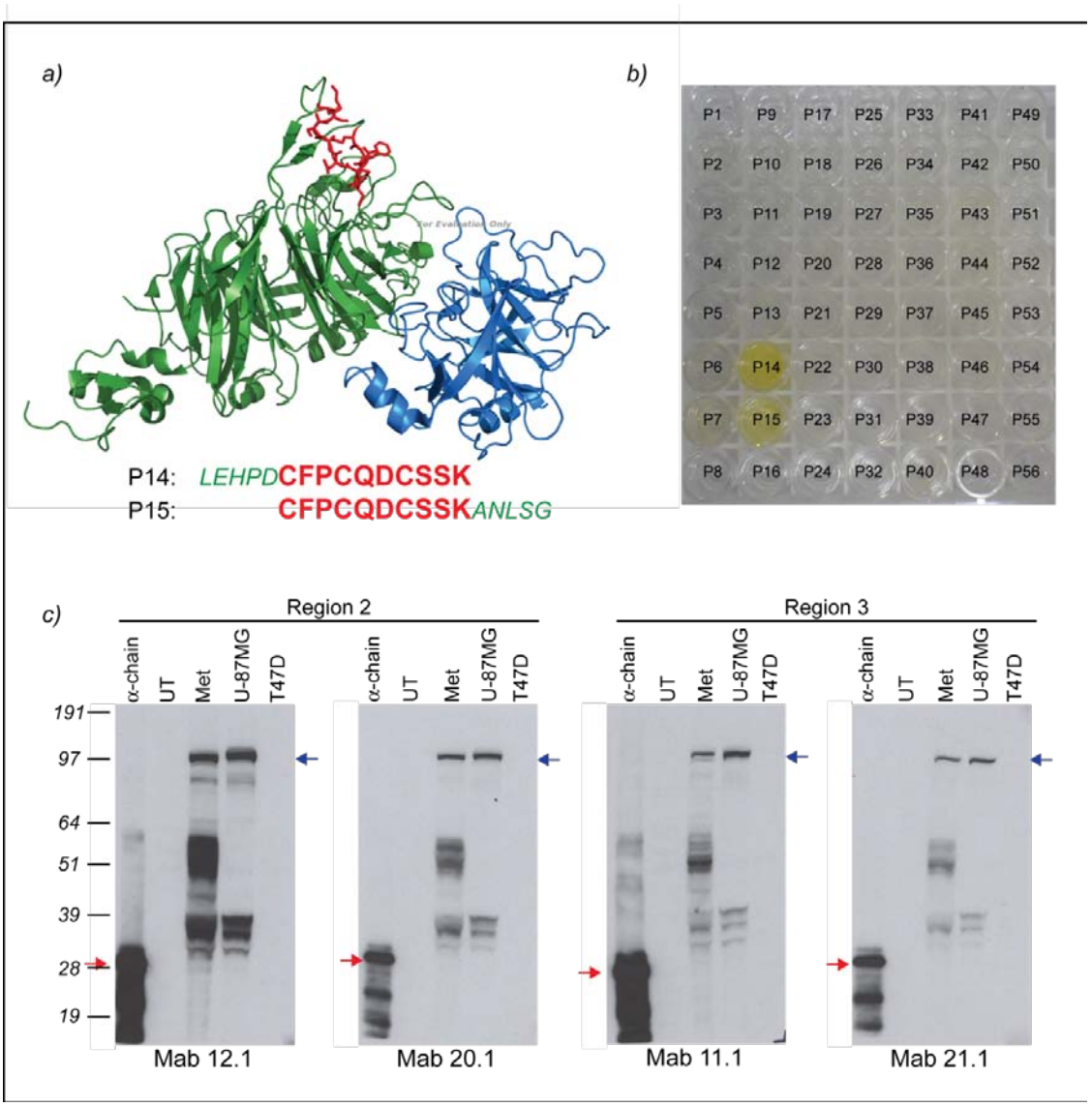

Figure 3.23C: Region 3 contains the epitope of Mab 11.1 and 21.1.
a) Crystal structure of c-Met extracellular domain (amino acid residues 25 – 567), binding to HGF β-chain. Crystal structure was obtained from Protein Data Bank (PDB), accession number 1SHY. c-Met is highlighted in green, HGF in blue and region 3 in red. The sequence of region 3 is also noted in red. ***b)*** A pepscan example of Mab 11.1 and 21.1. Cell supernatants were added to wells coated with various peptides (peptide 1 to 55) as shown. Binding of monoclonal antibodies to their epitope will produce a yellow colorimetric reaction. Sequence of peptide 14 and 15, and region 3 (overlapping region of both peptides) is noted in *a)*. P56 (no peptide) is the negative control. ***c)*** Western blot analysis of c-Met in cell extracts obtained from untransfected (UT) NIH3T3 cells, NIH3T3 cells transiently expressing human c-Met (Met), U-87MG cells and T47D cells. Western blots were individually analysed by Mab 11.1, 12.1, 20.1 and 21.1. Western blots were grouped according to the binding region the antibody recognises, thus allowing the comparison of Western blot band profile among antibodies that bind within the same region. Antibodies from region 2 (Mab 12.1 and 21.1) and 3 (Mab 11.1 and 20.1) were grouped together as their binding region are overlapping. Western blots are the same as those in Figures 3.19. Blue arrows and red arrows indicate c-Met precursor and c-Met purified α-chain respectively. Molecular weights are noted aside, in kilodaltons. P: Peptide (example P1 = Peptide 1).

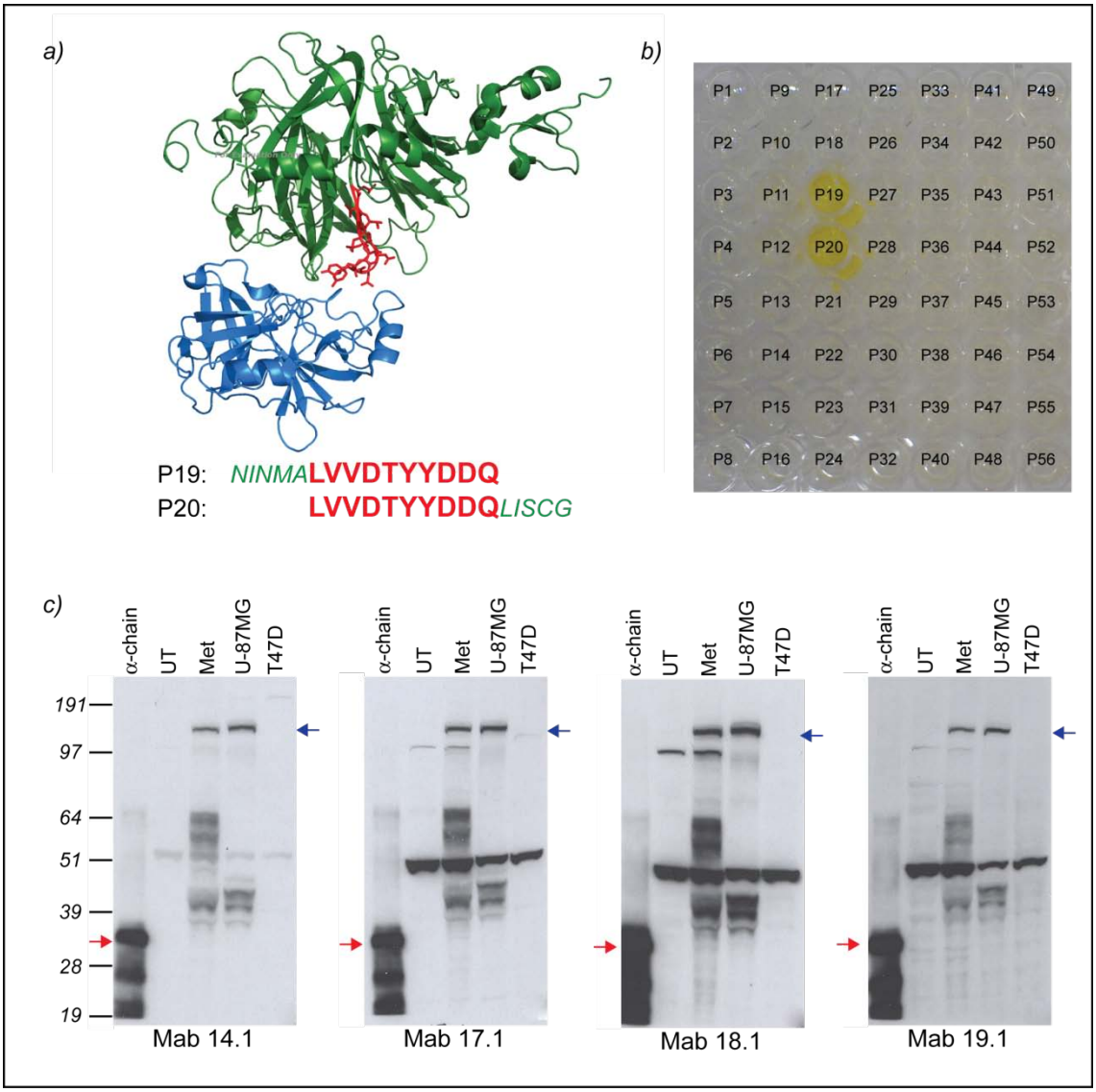

Figure 3.23D: Region 4 contains the epitope of Mab 14.1, 18.1 and 19.1.
a) Crystal structure of c-Met extracellular domain (amino acid residues 25 – 567), binding to HGF β-chain. Crystal structure was obtained from Protein Data Bank (PDB), accession number 1SHY. c-Met is highlighted in green, HGF in blue and region 4 in red. The sequence of region 4 is also noted in red. ***b)*** A pepscan example of Mab 14.1, 18.1 and 19.1. Cell supernatants were added to wells coated with various peptides (peptide 1 to 55) as shown. Binding of monoclonal antibodies to their epitope will produce a yellow colorimetric reaction. Sequence of peptide 19 and 20, and region 4 (overlapping region of both peptides) is noted in *a)*. P56 (no peptide) is the negative control. ***c)*** Western blot analysis of c-Met in cell extracts obtained from untransfected (UT) NIH3T3 cells, NIH3T3 cells transiently expressing human c-Met (Met), U-87MG cells and T47D cells. Western blots were individually analysed by Mab 14.1, 17.1, 18.1 and 19.1. Western blots were grouped according to the binding region the antibodies recognises, thus allowing the comparison of Western blot band profile among antibodies that bind within the same region. Mab 17.1 recognises regions 4 and 8. Western blots are the same as those in Figures 3.19. Blue arrows and red arrows indicate c-Met precursor and c-Met purified α-chain respectively. Molecular weights are noted aside, in kilodaltons. P: Peptide (example P1 = Peptide 1).

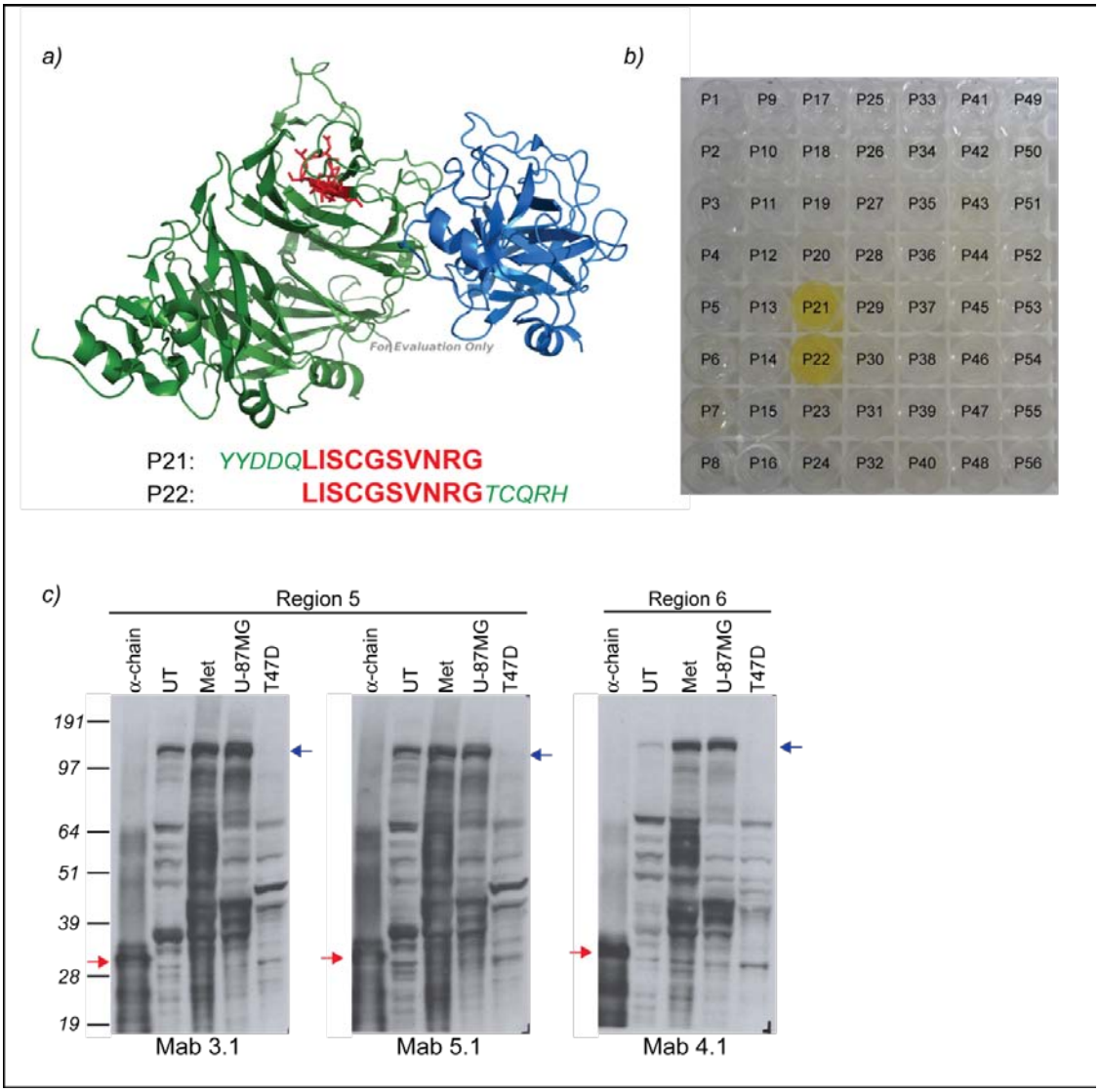

Figure 3.23E: Region 5 contains the epitope of Mab 3.1 and 5.1.
a) Crystal structure of c-Met extracellular domain (amino acid residues 25 – 567), binding to HGF β-chain. Crystal structure was obtained from Protein Data Bank (PDB), accession number 1SHY. c-Met is highlighted in green, HGF in blue and region 5 in red. The sequence of region 5 is also noted in red. ***b)*** A pepscan example of Mab 3.1 and 5.1. Cell supernatants were added to wells coated with various peptides (peptide 1 to 55) as shown. Binding of monoclonal antibodies to their epitope will produce a yellow colorimetric reaction. Sequence of peptide 21 and 22, and region 5 (overlapping region of both peptides) is noted in *a)*. P56 (no peptide) is the negative control. ***c)*** Western blot analysis of c-Met in cell extracts obtained from untransfected (UT) NIH3T3 cells, NIH3T3 cells transiently expressing human c-Met (Met), U-87MG cells and T47D cells. Western blots were individually analysed by Mab 3.1, 4.1 and 5.1. Western blots were grouped according to the binding region the antibody recognises, thus allowing the comparison of Western blot band profile among antibodies that bind within the same region. Antibodies from region 5 (Mab 3.1 and 5.1) and 6 (Mab 4.1) were grouped together as their binding region are overlapping. Western blots are the same as those in Figures 3.19. Blue arrows and red arrows indicate c-Met precursor and c-Met purified α-chain respectively. Molecular weights are noted aside, in kilodaltons. P: Peptide (example P1 = Peptide 1).

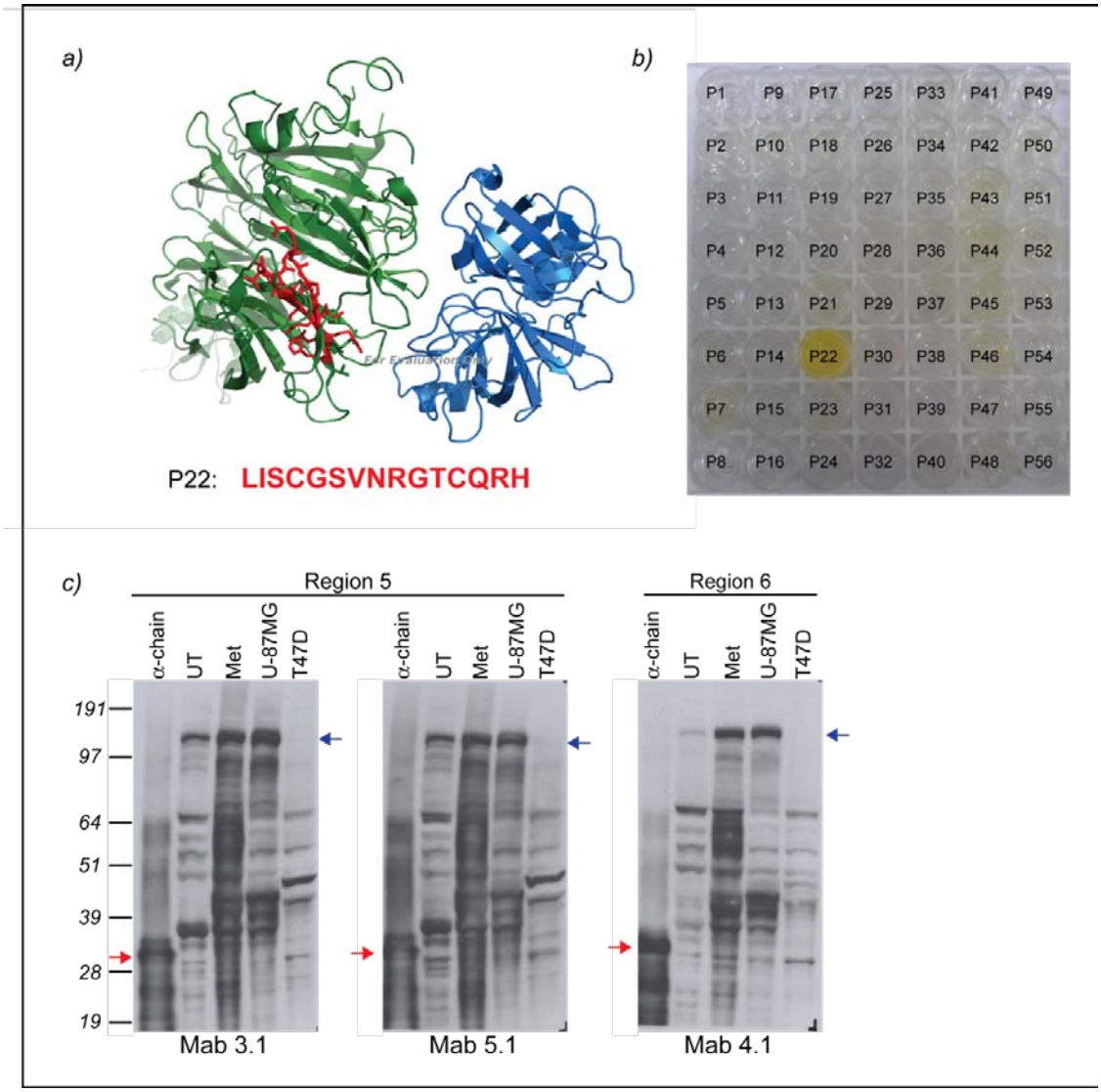

Figure 3.23F: Region 6 contains the epitope of Mab 4.1.
a) Crystal structure of c-Met extracellular domain (amino acid residues 25 – 567), binding to HGF β-chain. Crystal structure was obtained from Protein Data Bank (PDB), accession number 1SHY. c-Met is highlighted in green, HGF in blue and region 6 in red. The sequence of region 6 is also noted in red. ***b)*** Pepscan of Mab 41. Cell supernatant was added to wells coated with various peptides (peptide 1 to 55) as shown. Binding of monoclonal antibodies to their epitope will produce a yellow colorimetric reaction. Sequence of peptide 22/region 6 is noted in *a)*. P56 (no peptide) is the negative control. ***c)*** Western blot analysis of c-Met in cell extracts obtained from untransfected (UT) NIH3T3 cells, NIH3T3 cells transiently expressing human c-Met (Met), U-87MG cells and T47D cells. Western blots were individually analysed by Mab 3.1, 4.1 and 5.1. Western blots were grouped according to the binding region the antibody recognises, thus allowing the comparison of Western blot band profile among antibodies that bind within the same region. Antibodies from region 5 (Mab 3.1 and 5.1) and 6 (Mab 4.1) were grouped together as their binding region are overlapping. Western blots are the same as those in Figures 3.19. Blue arrows and red arrows indicate c-Met precursor and c-Met purified α-chain respectively. Molecular weights are noted aside, in kilodaltons. P: Peptide (example P1 = Peptide 1).

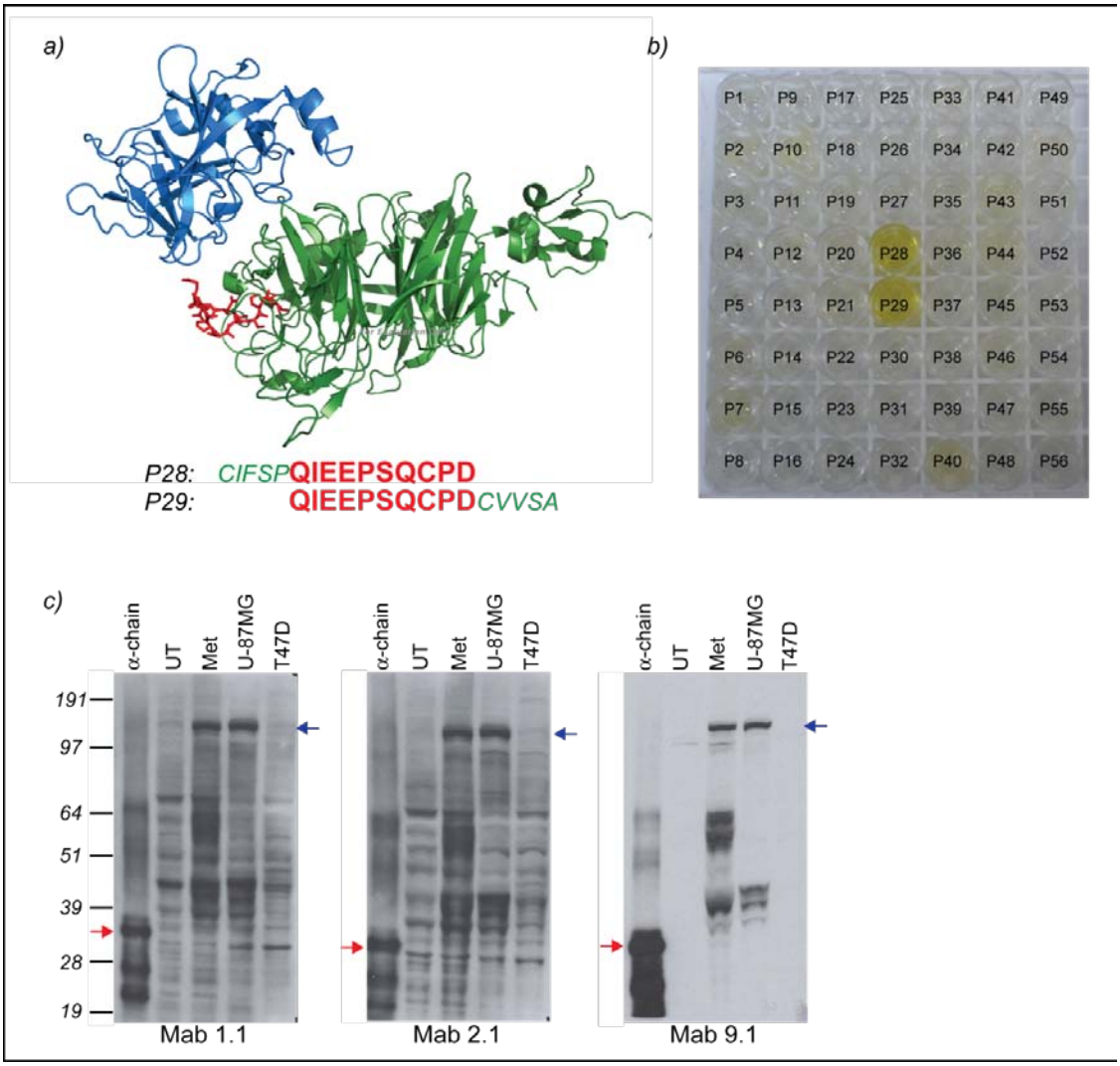

Figure 3.23G: Region 7 contains the epitope of Mab 1.1, 2.1 and 9.1.
a) Crystal structure of c-Met extracellular domain (amino acid residues 25 – 567), binding to HGF β-chain. Crystal structure was obtained from Protein Data Bank (PDB), accession number 1SHY. c-Met is highlighted in green, HGF in blue and region 7 in red. The sequence of region 7 is also noted in red. ***b)*** A pepscan example of Mab 1.1, 2.1 and 9.1. Cell supernatants were added to wells coated with various peptides (peptide 1 to 55) as shown. Binding of monoclonal antibodies to their epitope will produce a yellow colorimetric reaction. Sequence of peptide 28 and 29, and region 7 (overlapping region of both peptides) is noted in *a)*. P56 (no peptide) is the negative control. ***c)*** Western blot analysis of c-Met in cell extracts obtained from untransfected (UT) NIH3T3 cells, NIH3T3 cells transiently expressing human c-Met (Met), U-87MG cells and T47D cells. Western blots were individually analysed by Mab 1.1, 2.1 and 9.1. Western blots were grouped according to the binding region the antibody recognises, thus allowing the comparison of Western blot band profile among antibodies that bind within the same region. Western blots are the same as those in Figures 3.19. Blue arrows and red arrows indicate c-Met precursor and c-Met purified α-chain respectively. Molecular weights are noted aside, in kilodaltons. P: Peptide (example P1 = Peptide 1).

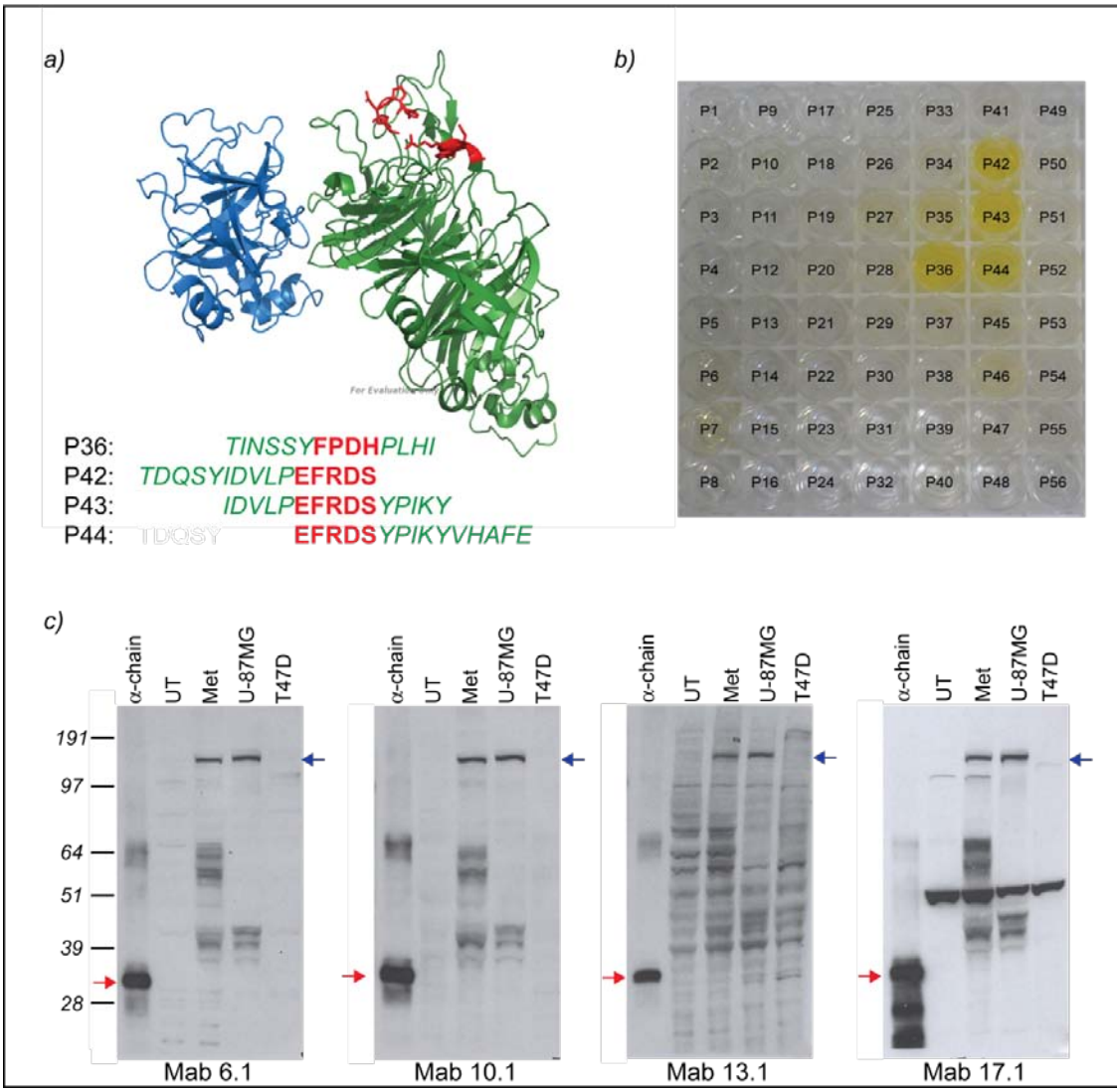

Figure 3.23H: Region 8 contains the epitope of Mab 6.1, 10.1 and 13.1.

a) Crystal structure of c-Met extracellular domain (amino acid residues 25 – 567), binding to HGF β-chain. Crystal structure was obtained from Protein Data Bank (PDB), accession number 1SHY. c-Met is highlighted in green, HGF in blue and region 8 in red. The sequence of region 8 is also noted in red. ***b)*** A pepscan example of Mab 6.1, 10.1 and 13.1. Cell supernatants were added to wells coated with various peptides (peptide 1 to 55) as shown. Binding of monoclonal antibodies to their epitope will produce a yellow colorimetric reaction. Sequence of peptide 36, 42, 43 and 44, and region 8 (overlapping region of both peptides) is noted in *a)*. P56 (no peptide) is the negative control. ***c)*** Western blot analysis of c-Met in cell extracts obtained from untransfected (UT) NIH3T3 cells, NIH3T3 cells transiently expressing human c-Met (Met), U-87MG cells and T47D cells. Western blots were individually analysed by Mab 6.1, 10.1, 13.1 and 17.1. Western blots were grouped according to the binding region the antibodies recognises, thus allowing the comparison of Western blot band profile among antibodies that bind within the same region. Mab 17.1 recognises regions 4 and 8. Western blots are the same as those in Figures 3.19. Blue arrows and red arrows indicate c-Met precursor and c-Met purified α-chain respectively. Molecular weights are noted aside, in kilodaltons. P: Peptide (example P1 = Peptide 1).

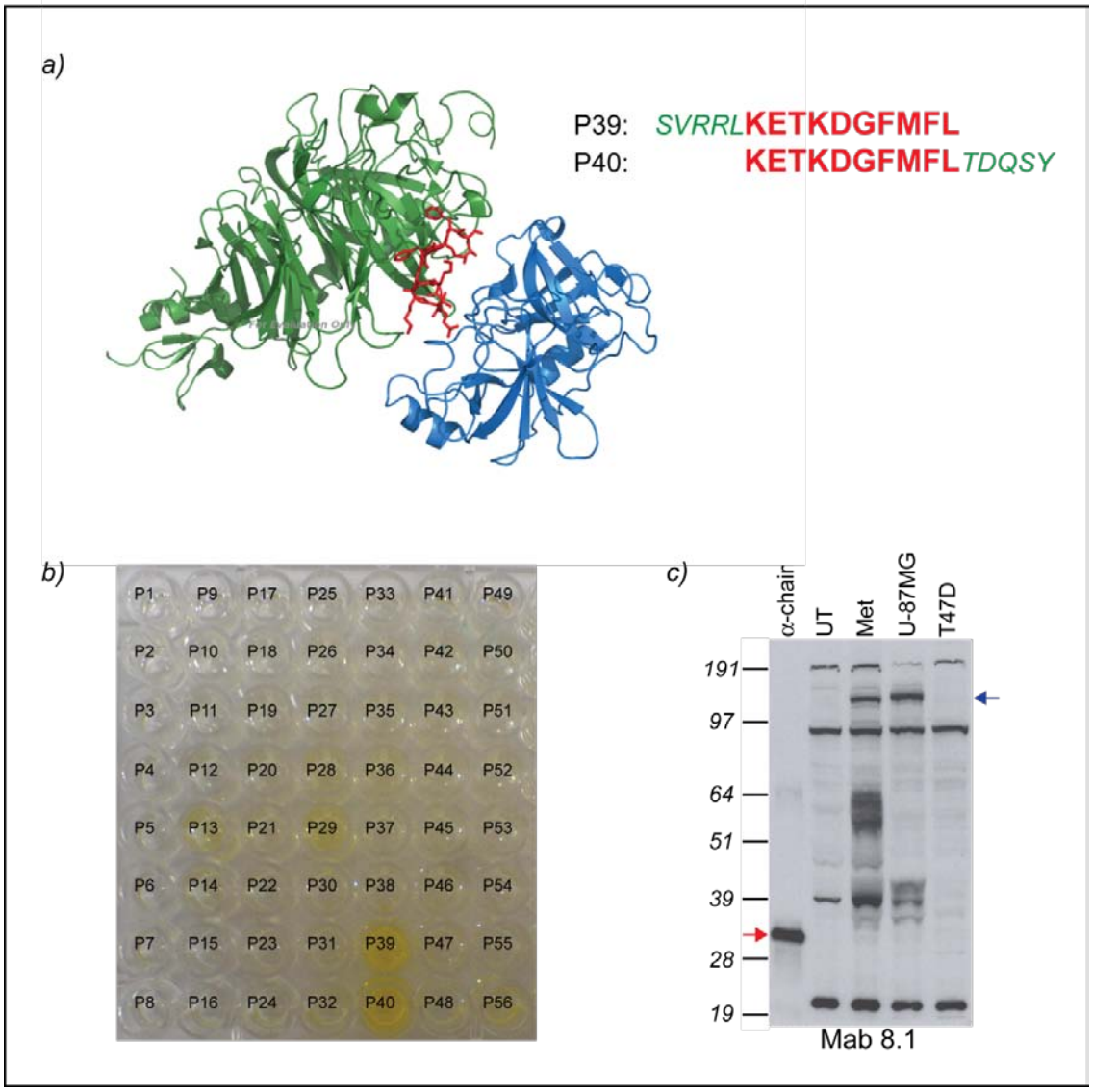

Figure 3.23I: Region 9 contains the epitope of Mab 8.1.

a) Crystal structure of c-Met extracellular domain (amino acid residues 25 – 567), binding to HGF β-chain. Crystal structure was obtained from Protein Data Bank (PDB), accession number 1SHY. c-Met is highlighted in green, HGF in blue and region 9 in red. The sequence of region 9 is also noted in red. ***b)*** Pepscan of Mab 8.1. Cell supernatant was added to wells coated with various peptides (peptide 1 to 55) as shown. Binding of monoclonal antibodies to their epitope will produce a yellow colorimetric reaction. Sequence of peptide 39 and 40, and region 9 (overlapping region of both peptides) is noted in *a)*. P56 (no peptide) is the negative control. ***c)*** Mab 8.1 Western blot analysis of c-Met in cell extracts obtained from untransfected (UT) NIH3T3 cells, NIH3T3 cells transiently expressing human c-Met (Met), U-87MG cells and T47D cells. Western blots are shown for comparison and are the same as those in Figures 3.19. Blue arrows and red arrows indicate c-Met precursor and c-Met purified α-chain respectively. Molecular weights are noted aside, in kilodaltons. P: Peptide (example P1 = Peptide 1).

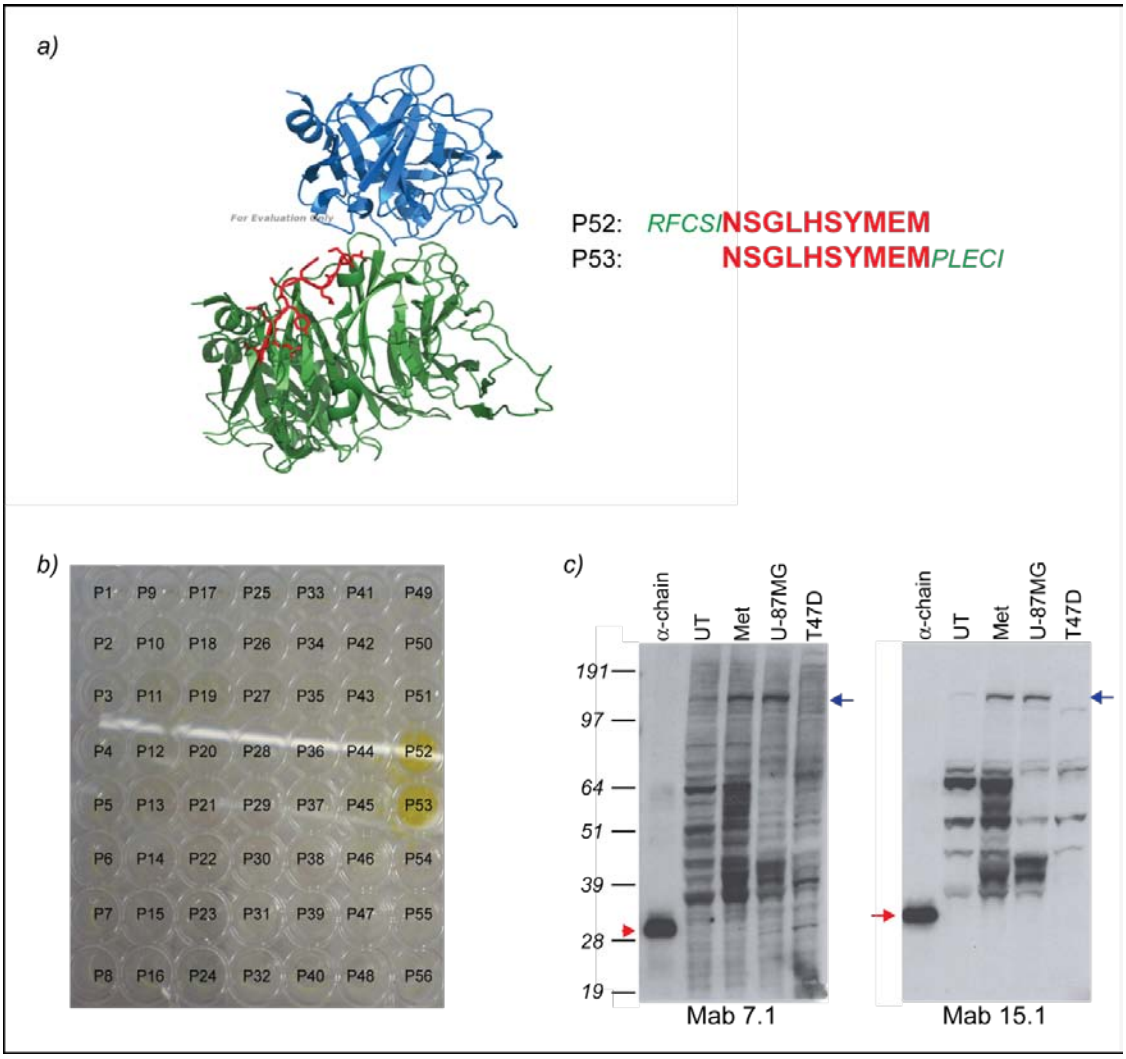

Figure 3.23J: Region 10 contains the epitope of Mab 7.1 and 15.1.
a) Crystal structure of c-Met extracellular domain (amino acid residues 25 – 567), binding to HGF β-chain. Crystal structure was obtained from Protein Data Bank (PDB), accession number 1SHY. c-Met is highlighted in green, HGF in blue and region 10 in red. The sequence of region 10 is also noted in red. ***b)*** A pepscan example of Mab 7.1 and 15.1. Cell supernatants were added to wells coated with various peptides (peptide 1 to 55) as shown. Binding of monoclonal antibodies to their epitope will produce a yellow colorimetric reaction. Sequence of peptide 52 and 53, and region 10 (overlapping region of both peptides) is noted in *a)*. P56 (no peptide) is the negative control. ***c)*** Western blot analysis of c-Met in cell extracts obtained from untransfected (UT) NIH3T3 cells, NIH3T3 cells transiently expressing human c-Met (Met), U-87MG cells and T47D cells. Western blots were individually analysed by Mab 7.1 and 15.1. Western blots were grouped according to the binding region the antibody recognises, thus allowing the comparison of Western blot band profile among antibodies that bind within the same region. Western blots are the same as those in Figures 3.19. Blue arrows and red arrows indicate c-Met precursor and c-Met purified α-chain respectively. Molecular weights are noted aside, in kilodaltons. P: Peptide (example P1 = Peptide 1).

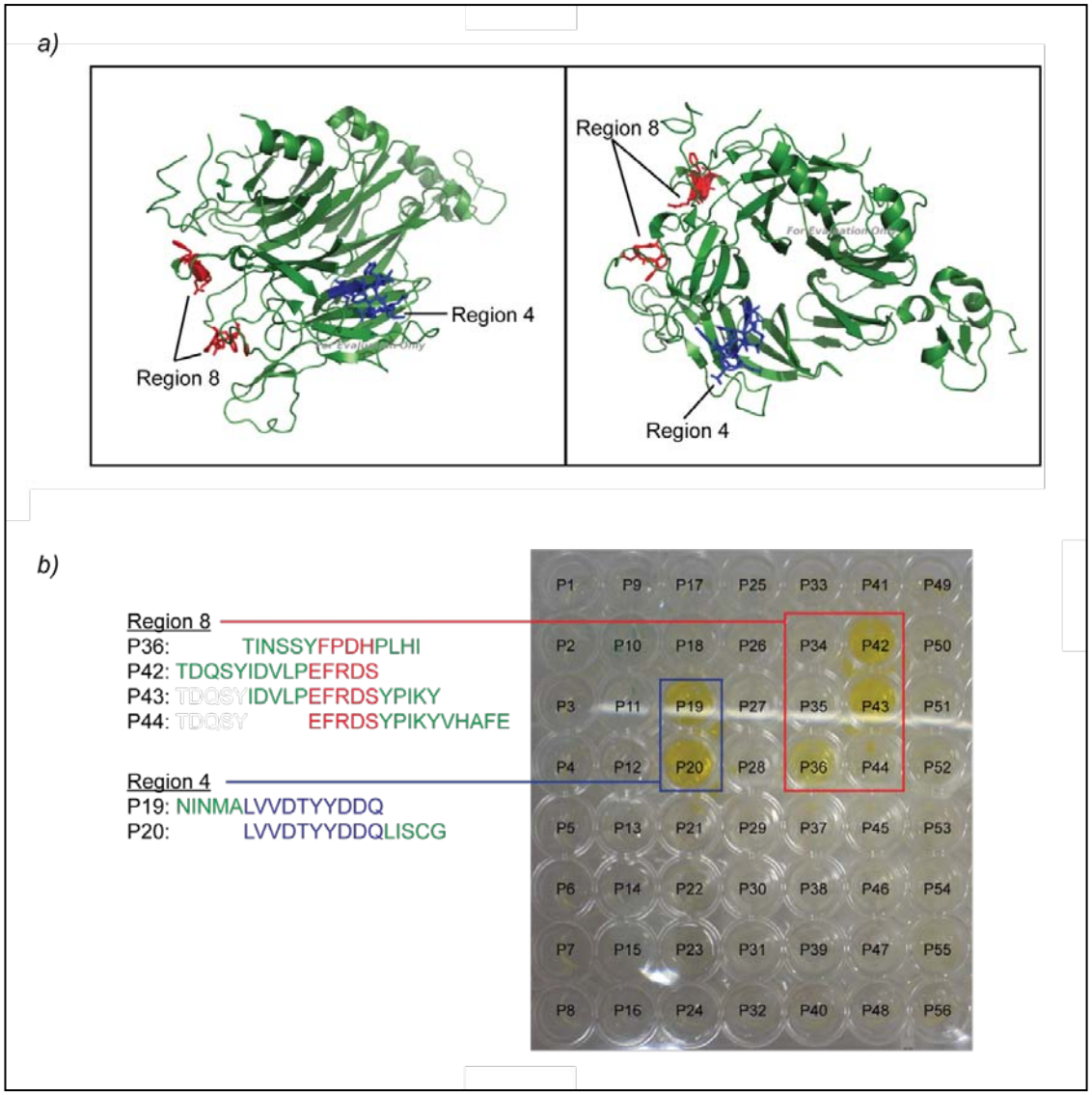

Figure 3.23K: Pepscan analysis of Mab 17.1.
a) Crystal structure of c-Met extracellular domain (amino acid residues 25 – 567) with Mab 17.1 binding regions highlighted. Crystal structure was obtained from Protein Data Bank (PDB), accession number 1SHY. Mab 17.1 binds to region 4 (in red) and region 8 (in blue). The protein complex is shown from two different viewpoints to allow visualisation of both regions. ***b)*** Pepscan of Mab 17.1. Monoclonal cell supernatant were added to wells coated with various peptides (peptide 1 to 55) as shown. Binding of monoclonal antibodies to their epitope will produce a yellow colorimetric reaction. Mab 17.1 binds to both regions 4 and 8. The sequence of region 4 and 8 are noted. The sequences of region 4 and region 8 are in blue and red respectively. P56 (no peptide) is the negative control. P: Peptide (example P1 = Peptide 1).

Table 3.3: Pepscan results of Mab 17.1 re-clones

Antibody 17.1 clones	Region	
	4	8
E1	X	
E2	X	x
F1	X	x
F2	X	x
F3	X	x
F4	X	x
F6	X	
H2	X	
H3	X	
G2	X	x
G12	X	x
Parental 17.1 clone	X	x

(x) indicate region of binding

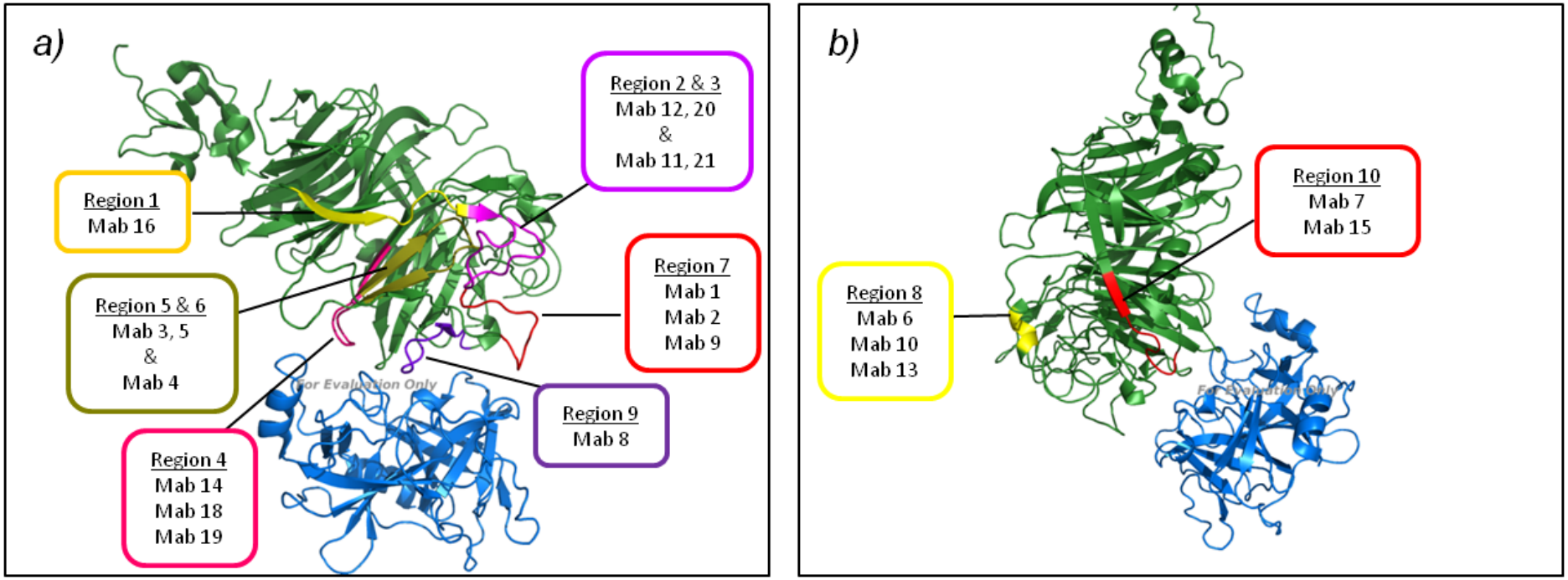

Figure 3.24: Mapping of antibody binding regions to the crystal structure of c-Met.
Crystal structure of c-Met extracellular domain (amino acid residues 25 – 567), binding to HGF β-chain. Crystal structure was obtained from Protein Data Bank (PDB), accession number 1SHY. c-Met is highlighted in green and HGF in blue. The protein complex is shown from two different viewpoints (*a)* and *b)*) to allow visualisation of the different antibody binding regions in relation to ligand-receptor interaction site.

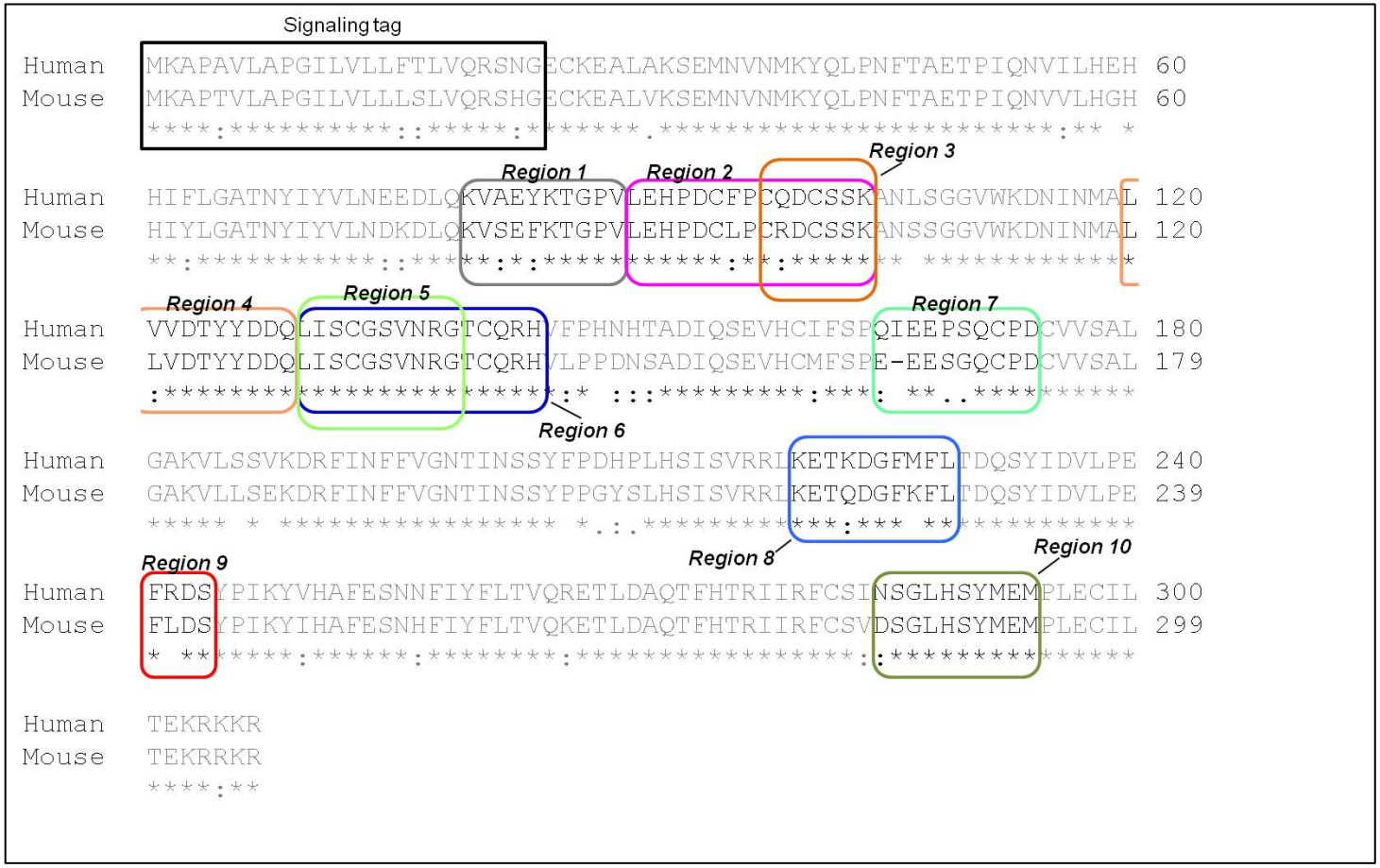

Figure 3.25: Alignment of human and mouse c-Met α-chain.
The sequence alignment of human and mouse c-Met, Swiss-Prot number P08581 and P16056 respectively, was performed and the α-chain sequence is shown only. The regions of antibody binding were mapped on to the sequence alignment to identify conserved residues. Detailed information on the antibody and its corresponding binding region is listed in Table 3.4. (*): residues identical in the alignment. (:): conserved residues subsitutions. (.): semi-conserved residues substitutions.
Sequence alignment was performed with the Clustal series of programs. (2003)
Chenna, Ramu, Sugawara, Hideaki, Koike,Tadashi, Lopez, Rodrigo, Gibson, Toby J, Higgins, Desmond G, Thompson, Julie D.
Nucleic Acids Res 31 (13):3497-500 PubMedID: 12824352

Table 3.4: Characterisation of monoclonal antibodies

Binding region	Antibody	Clone number	IgG subclass	Light chain	Protein sequence of region	Alignment* (human / mouse)
1	16.1	12D10	IgG2A	Kappa	KVAEYKTGPV	KV**A**E**Y**KTGPV KV**S**E**F**KTGPV
2	12.1 20.1	5E7 5G12	IgG1	Kappa	LEHPDCFPCQDCSSK	LEHPDC**F**PC**Q**DCSSK LEHPDC**L**PC**R**DCSSK
3	11.1 21.1	9H1 12C9	IgG1	Kappa	CFPCQDCSSK	C**F**PC**Q**DCSSK C**L**PC**R**DCSSK
4	14.1 18.1 17.1 19.1	3E6 16H3 2H8 12A12	IgG1 IgG2B	Kappa	LVVDTYYDDQ	L**V**VDTYYDDQ L**L**VDTYYDDQ
5	3.1 5.1	9H4 16A4	IgG1	Kappa	LISCGSVNRG	LISCGSVNRG LISCGSVNRG
6	4.1	15E11	IgG2A	Kappa	LISCGSVNRGTCQRH	LISCGSVNRGTCQRH LISCGSVNRGTCQRH
7	1.1 2.1 9.1	13E1 16F6 16C11	IgG1	Kappa	QIEEPSQCPD	**Q**IEE**PS**QCPD **E-**EE**SG**QCPD
8	6.1 10.1 13.1 17.1	10B1 15G3 5H4 2H8	IgG1	Kappa	FRDS	F**R**DS F**L**DS
9	8.1	2C6	IgG1	Kappa	KETKDGFMFL	KET**K**DGFMFL KET**Q**DGFKFL
10	7.1 15.1	6D9 5D5	IgG1	Kappa	NSGLHSYMEM	**N**SGLHSYMEM **D**SGLHSYMEM

*Top sequence: Human c-Met protein sequence. Bottom sequence: Murine c-Met protein sequence. Red: Differences in amino acid sequences.

3.3: Further characterisation of monoclonal hybridoma supernatant

3.3.1: Activation of endogenous c-Met by recombinant HGF

HGF is the only known ligand for c-Met. Upon ligand binding, c-Met dimerises and undergoes autophosphorylation. c-Met is then activated and phosphorylates cytoplasmic proteins involved in signalling pathways, leading to activation of various signalling cascades such as the ERK and AKT pathways. Previously, we have single-cell cloned 21 hybridoma clones to obtain cell supernatant containing monoclonal antibodies. The monoclonal antibody's isotype and binding region on c-Met were characterised. In this Section, we characterise the functional activity of the monoclonal antibodies by analysing the effects of the monoclonal antibodies were analysed on HGF-induced ERK phosphorylation and cell scatter.

Before characterising the functional activity of the monoclonal antibodies, appropriate cell lines and experimental setups were required. In Section 3.1.4, we demonstrated that U-87MG, HaCaT and SNU-5 cells were positive for c-Met expression while T47D cells were negative for c-Met expression. Here, we test the experimental setup on these cell lines by analysing the effects of recombinant HGF (purchased from R&D Systems) on activation of c-Met, ERK and AKT. SNU-5 cells were not tested due to their high levels of phosphorylated c-Met, in the absence of added HGF (Figure 3.6).

Cells were grown to 90% confluency and were then subjected to serum starvation for 24 hrs to switch off growth signalling pathways. Recombinant HGF was then added to the cells for 30 mins and the cells were immediately harvested in hot sample loading buffer. U-87MG cells are a human glioblastoma cell line that expresses both c-Met and HGF, thus is it autocrine for c-Met activation (Martens *et al.*, 2006). In serum-free media containing no added HGF, c-Met was observed to be phosphorylated (Figure 3.26),

which is consistent with the observation that U-87MG cells are autocrine for c-Met signalling. Interestingly, both c-Met precursor and mature β-chain were observed to be phosphorylated. Phosphorylation of c-Met correlates with increasing concentration of HGF, while the levels of total c-Met protein remained constant. Total levels of AKT protein remained constant with increasing HGF concentration. Increasing phosphorylation of AKT at threonine 308 (T308) correlated with increasing concentration of HGF, however, AKT phosphorylation at serine 473 (S473) was observed to remain constant. T308 and S473 lies in the kinase domain and C-terminal tail of AKT respectively. Activation of AKT results in the phosphorylation of T308 in the kinase domain. However, for full kinase activity, phosphorylation at a second site, S472, is required (Fresno Vara *et al.*, 2004). Similarly to c-Met, ERK phosphorylation correlated with increasing HGF concentration while total ERK protein levels stayed the same. Activation of c-Met has been reported to lead to ERK and AKT phosphorylation (Bellon *et al.*, 2008; Birchmeier *et al.*, 2003; Smolen *et al.*, 2006). It is not surprising that both ERK and AKT are phosphorylated with no added HGF because U-87MG cells are PTEN (phosphatase and tensin homolog) null cells. PTEN is a tumour suppressor protein that is a negative regulator of the AKT signalling pathway. AKT is thus constantly phosphorylated in U-87MG cells, even in the absence of added HGF.

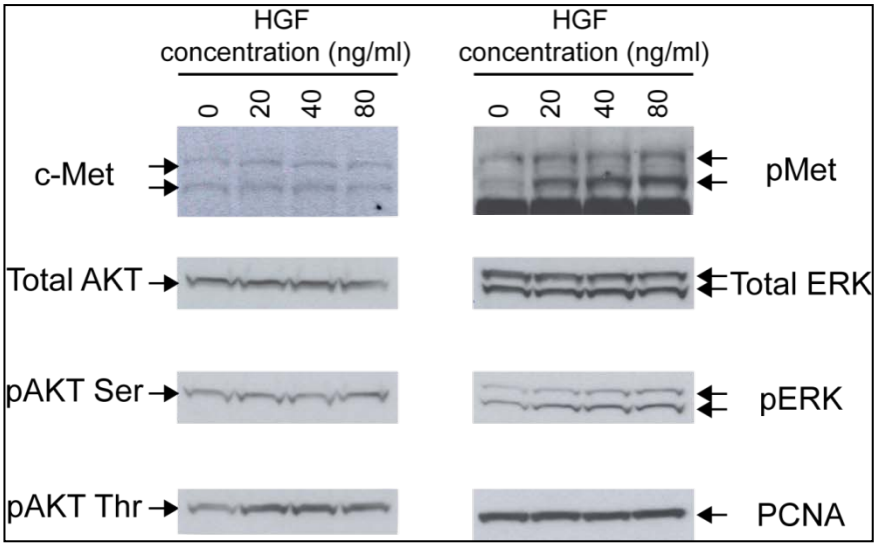

Figure 3.26: Activation of endogenous c-Met by recombinant HGF in U-87MG cells.
Western blotting of U-87MG cell extracts from cells treated with 0, 20, 40 and 80 ng/ml of recombinant HGF. Cells were serum-starved for 24 hrs. HGF was added to the cells, in serum-free media, for 30 mins before harvesting in sample buffer. 40 µg of total cell lysate was analysed in each sample. Activation of c-Met was examined by detecting phosphorylated c-Met (pMet). Arrows on the pMet blot indicate phosphorylated c-Met precursor (170 kD) and phosphorylated c-Met β-chain (145 kD). Activation of ERK and AKT signalling pathways were also examined by detecting phosphorylated ERK and AKT (at either S473 or T308). Anti-ERK and anti-phospho ERK antibodies detected 2 bands at 44 kD and 42 kD, which correspond to ERK1 and ERK2 respectively. PCNA was used as loading control. pERK: Phosphorylated ERK. pAKT: Phosphorylated AKT.

HaCaT are derived from human keratinocyte cells and were shown to express c-Met in Figure 3.6. In this cell line, phosphorylation of c-Met was found to correlate with HGF concentration (Figure 3.27). In contrast to U-87MG cells, only c-Met mature β-chain was phosphorylated. HaCaT cells could not be grown to very high densities, therefore production of sufficient cell lysate to load 40 µg protein per well would have required prohibitive amounts of commercially bought HGF. As commercially available antibodies (AF276 and SC-10 antibodies) failed to detect total levels of c-Met analysed in 10 µg of cell lysates, the anti-α-chain antibody Mab 18.1, developed in this project, was used to detect precursor c-Met. An increase in c-Met precursor protein was detected when 20 and 40 ng/ml of HGF was added to the cells. A decrease of c-Met precursor levels was observed when 80 ng/ml of HGF was added, but due to time constraints, it

was not possible to show if this was a reproducible result. Interestingly, HGF resulted in an increase of total ERK levels in HaCaT cell but not in U-87MG cells.

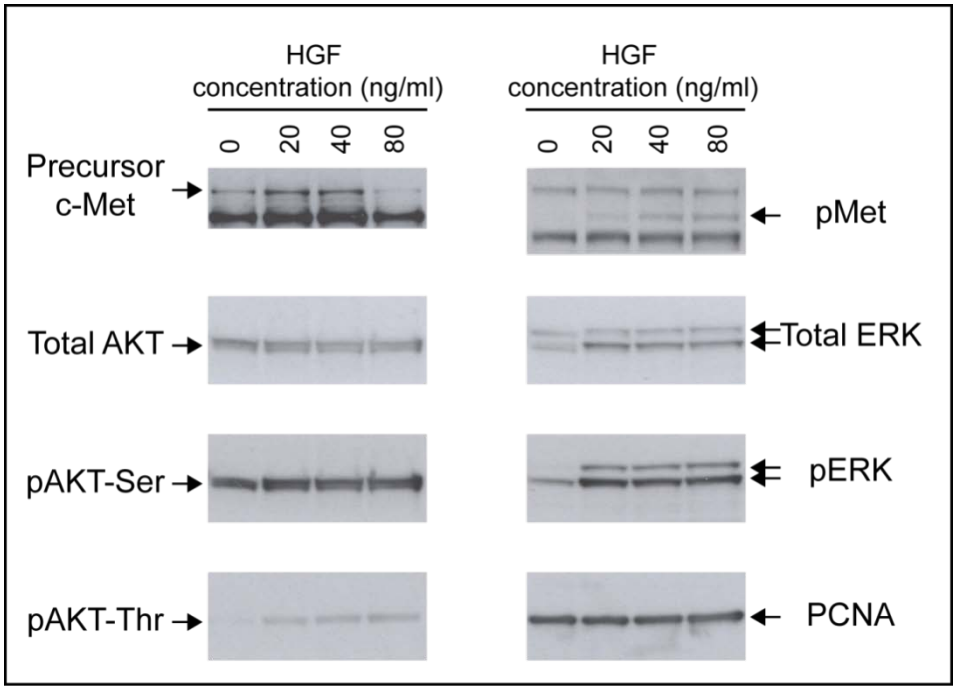

Figure 3.27: Activation of endogenous c-Met by recombinant HGF in HaCaT cells.
Western blotting of HaCaT cell extracts treated with 0, 20, 40 and 80 ng/ml of recombinant HGF. Cells were serum-starved for 24 hrs. HGF was added to the cells, from cells in serum-free media, for 30 mins before harvesting in sample buffer. 10 μg of total cell lysate was analysed in each sample. Activation of c-Met was examined by detecting phosphorylated c-Met (pMet). Arrows on pMet blot indicate phosphorylated c-Met β-chain (145 kD). Activation of ERK and AKT signalling pathways were also examined by detecting phosphorylated ERK and AKT (at either S473 or T308) respectively. Anti-ERK and anti-phospho-ERK antibodies detected 2 bands at 44 kD and 42 kD, which correspond to ERK1 and ERK2 respectively. PCNA was used as loading control. pERK: Phosphorylated ERK. pAKT: Phosphorylated AKT.

Increased phosphorylation of AKT S473 should have been observed in HaCaT cells treated with increasing HGF concentrations as the cells were presumed to not produce HGF. Interestingly, increased HGF concentration did not affect total AKT protein levels or phosphorylation of AKT at S473. Constant levels of AKT phosphorylation at S473 is also observed in U-87MG cells treated with increasing HGF concentrations. U-87MG cells, which are HGF self-producing, are thus constantly phosphorylated at AKT S473, and added HGF would not have caused further increase in phosphorylation. As phosphorylation of AKT S473 indicates full AKT activation (Nicholson and Anderson,

2002), it is probable that the increased HGF concentrations were not sufficient to induce full AKT activation or a longer time point is required for full AKT activation i.e. HGF-induced phosphorylation of AKT at S473 occurs after 30 mins. Finally, AKT phosphorylation at T308, ERK phosphorylation and total protein levels of ERK, correlated with increased HGF concentration in HaCaT cells.

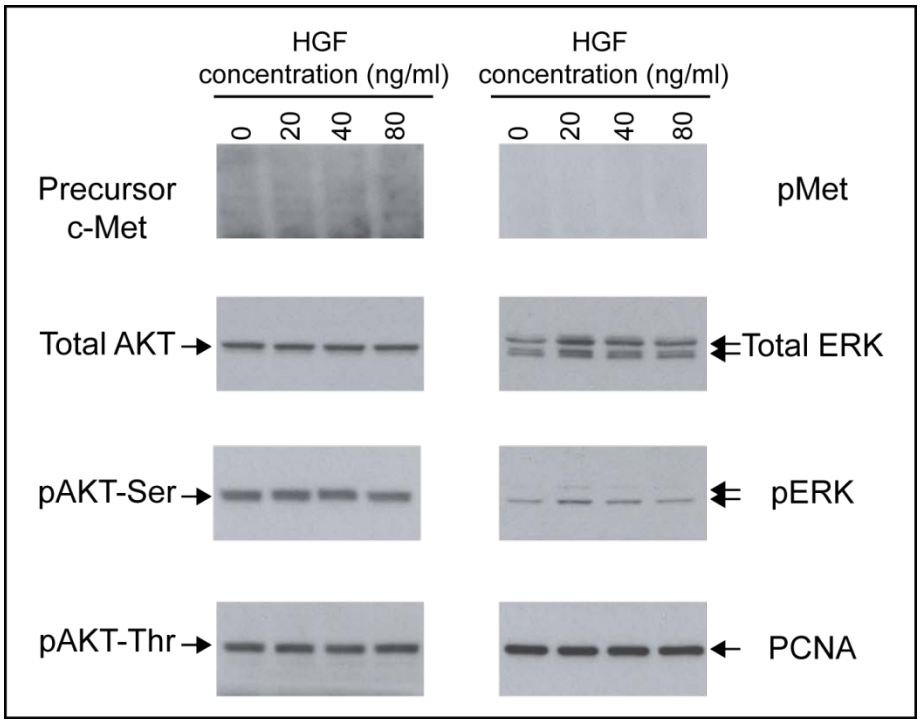

Figure 3.28: Activation of ERK and AKT signalling pathways by recombinant HGF in T47D cells. Western blotting of T47D cell extract from cells treated with 0, 20, 40, 80 ng/ml of recombinant HGF. T47D cells express very low levels of c-Met. Cells were serum-starved for 24 hrs. HGF was added to the cells for 30 mins before harvesting in sample buffer. 10 μg of total cell lysate was analysed in each sample. Activation of c-Met was examined by detecting for phosphorylated c-Met (pMet). c-Met and phosphorylated c-Met protein band were absent in the precursor c-Met and pMet blot. Activation of ERK and AKT signalling pathways determined by examining phosphorylation of ERK and AKT (at either S473 or T308) respectively. Anti-ERK and anti-phospho-ERK antibodies detected 2 bands at 44 kD and 42 kD, which correspond to ERK1 and ERK2 respectively. PCNA was used as loading control. pERK: Phosphorylated ERK. pAKT: Phosphorylated AKT.

As a control to determine if HGF has non-specific effects, ERK and AKT phosphorylation were examined in T47D cells. T47D cells are human breast cancer cells that were reported to express very low levels of c-Met protein (Shen *et al.*, 2000) and we have conclusively shown that endogenous c-Met could not be immunoprecipitated from these cells (Figure 3.6). As expected, Mab 18.1 and anti-

phospho-Met antibodies failed to detect total c-Met protein levels and phosphorylated c-Met, respectively, by Western blotting (Figure 3.28). There were also no changes in AKT phosphorylation upon treatment with HGF. Interestingly, a slight increase in total ERK was observed across all levels of HGF, but mainly in samples treated with 20 ng/ml of HGF. At this level, an increase in ERK phosphorylation was also observed. It should be noted that the increased ERK phosphorylation could be due to the increased levels of total ERK, rather than increased phosphorylation of ERK. This result is unexpected and could be due to the low level of c-Met activation in T47D cells.

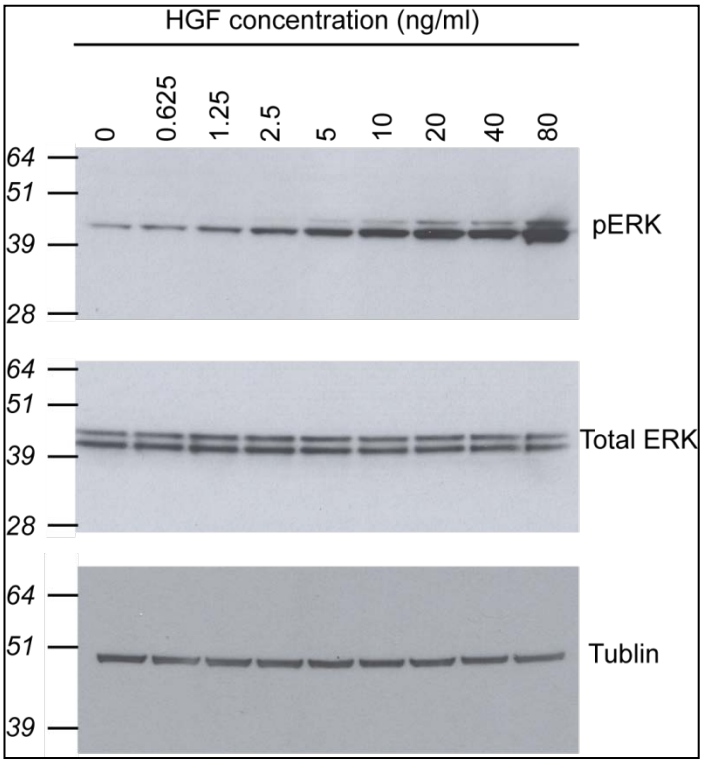

Figure 3.29: Activation of ERK pathway by increasing concentration of HGF in HaCaT cells.
Western blotting of HaCaT cell extracts treated with increasing concentration of recombinant HGF. Cells were serum-starved for 24 hrs. Indicated concentrations of HGF were added to the cells and then they were incubated for 30 mins before harvesting in sample buffer. 10 µg of total cell lysate was analysed in each sample. Phosphorylation of ERK is used as an indicator of c-Met activation by HGF. Anti-ERK and anti-phospho-ERK antibodies detected 2 bands at 44 kD and 42 kD, which correspond to ERK1 and ERK2 respectively. Tubulin was used as loading control. pERK: Phosphorylated ERK. Molecular weights are noted aside, in kilodaltons.

Comparing the activation of ERK and AKT pathways in U-87MG cells and HaCaT cells through activation of c-Met by HGF, ERK phosphorylation in HaCaT cells was the

most distinct and obvious. We therefore chose to examine ERK phosphorylation in HaCaT cells as an indicator of c-Met activation in our functional assays. To determine the minimum concentration of HGF required to induce activation of endogenous c-Met, recombinant HGF was added to HaCaT cells in gradually increasing concentrations. Cells were harvested and analysed for ERK phosphorylation by Western blotting. ERK phosphorylation correlated with increased HGF concentration while total ERK protein levels remained constant (Figure 3.29). 10 ng/ml of HGF was the minimum concentration required to activate c-Met in HaCaT cells. In our antibody functional assay, 10 ng/ml of HGF was thus used to compete with the monoclonal antibodies for binding to c-Met.

3.3.2: Preliminary analysis of the effect of treatment with monoclonal antibodies on ERK phosphorylation

The overall aim of this project was to produce and screen for therapeutic antibodies against c-Met. Section 3.1 and 3.2 of this report have: 1) described the production of monoclonal antibodies against c-Met, 2) shown that the antibodies recognise denatured protein on Western blots, 3) identified the isotype of each antibody and 4) delineated the region of antibody binding on human c-Met. We now examine whether these 21 monoclonal antibodies are functionally active by analysing the effects of the antibodies on HGF-induced ERK phosphorylation. Structural analysis of antibody binding regions in Section 3.2.7 suggests that some of the antibodies (Mab 1.1, 2.1, 7.1, 8.1, 9.1 and 15.1) may be able to compete with HGF for c-Met binding, thus inhibiting c-Met activation by ligand binding.

HaCaT cells were grown to approximately 90% confluency and then grown in serum-free medium for 24 hrs. Hybridoma cell supernatants were then diluted in serum-free media and incubated with the cells for 1 hr. 10 ng/ml of HGF was added to the cells and incubated for 30 mins. Cells were immediately harvested in hot sample loading buffer and 10 μg of total cell lysate were analysed by Western blotting. It should be noted that hybridoma cell supernatants are being tested and not purified antibodies. FCS contains growth factors, antibodies and other various proteins. Therefore, due to the presence of FCS in hybridoma cell supernatant, it is not possible to measure antibody concentration. Each hybridoma clone has an individual rate of antibody secretion and so antibody concentration is different in each hybridoma supernatant sample. In addition, it is also not possible to determine how much FCS remains in the media. Due to the various issues mentioned above, it is difficult to standardise this assay. Varying antibody concentrations were therefore tested by diluting cell supernatant in 1:10, 1:5 and 1:1

with serum-free media. It is assumed that the cell supernatant contained 10% FCS and the amount of growth factors in each batch of FCS, between Moravian Biotechnology and our lab, is identical but this assay should be seen as a preliminary screening test designed to help prioritise antibodies for further study.

As mentioned earlier, activation of c-Met by HGF results in activation of intracellular signalling pathways, one of which is the ERK pathway (Figure 3.27). HaCaT cells were used in this study due to their low basal level of ERK phosphorylation after serum starvation (Figure 3.27). Cells were serum-starved to switch off growth signalling pathways. Activation of c-Met, induced by HGF or by our monoclonal antibodies, after serum starvation would result in phosphorylation of ERK. Inhibition of HGF-induced c-Met activation, by commercial inhibitors or our monoclonal antibodies, would result in very low basal levels of ERK phosphorylation.

Due to the presence of FCS in antibody containing cell supernatant, various controls were carried out to determine the effect of FCS on ERK phosphorylation (Figure 3.30). Without serum starvation, untreated cells were harvested to determine the basal level of ERK phosphorylation. Only ERK2 (lower band, 42 kD) was detectably phosphorylated. Following serum starvation, and in the absence of FCS, added HGF resulted in increased ERK protein levels and an increased phosphorylation of both ERK1 and ERK2. In order to mimic the effects of adding hybridoma cell supernatant (containing FCS) at 1:1 dilution to serum-starved cells, media containing final concentrations of 5% FCS was used as control. Adding media containing 5% FCS to serum-starved cells was sufficient to induce an increase in total ERK levels as well as an increase in phosphorylation of both ERK1 and ERK2. This indicates that the levels of FCS proteins in the cell supernatant would have an effect on the outcome of this assay. Serum-starved cells treated with HGF, in the presence of 5% FCS, produced similar increased in total

ERK levels and phosphorylated ERK as compared to serum-starved cells treated with HGF, in the absence of FCS. This indicates that HGF alone was capable of increasing total ERK levels and inducing ERK phosphorylation without FCS. As a control to block HGF from binding to c-Met, an anti-HGF antibody was incubated with HGF for an hour prior its addition to serum-starved cells, at a final concentration of 5 μg/ml (from Jiao *et al.* (2005) and Somlen *et al.* (2006)), in media containing 5% FCS. In the presence of the anti-HGF antibody, the addition of HGF did not affect the levels of ERK protein or levels of ERK phosphorylation. These levels of total ERK and ERK phosphorylation were similar to serum-starved cells treated with media containing 5% FCS. This suggests that anti-HGF antibody completely inhibits the ability of HGF to activate the ERK pathway through c-Met and the constituents of FCS are evidently acting to activate the ERK pathway.

Prat *et al.* (1998) reported work aimed at developing inhibitory monoclonal antibodies against c-Met. These anti-Met antibodies turned out to be agonistic instead of antagonist. It was thus hypothesised that bivalent binding of an antibody molecule is capable of dimerising c-Met molecules which leads to c-Met activation. Martens *et al.* (2006) developed a one-armed anti-Met antibody that consists of only one epitope binding site. This one-arm antibody was reported to successfully block tumour growth in mouse models. Anti-α-chain antibodies developed here were thus tested for their ability activate c-Met or block HGF binding to c-Met. Due to the presence of FCS in the hybridoma cell supernatant, which also caused ERK phosphorylation, it was difficult to interpret these results.

Hybridoma cell supernatants were diluted 1:1 in serum-free media. Total ERK levels and phosphorylated ERK levels were analysed from cells treated with hybridoma cell supernatant and either with or without HGF (Figure 3.30). Results were compared to

control cells treated in media containing 5% FCS, and tabulated in Table 3.5. Any decreases in ERK phosphorylation levels suggest that these antibodies are inhibiting HGF-induced activation of c-Met. Based on the results on Table 3.5, the effects of monoclonal antibodies on total ERK levels and ERK phosphorylation could be classified into several groups. The majority of antibodies (highlighted in green) fell into a group in which a decrease of total ERK and phosphorylated ERK were observed in both HGF induced and un-induced samples. It is likely that the treatment with these antibodies caused a reduction in total ERK levels, resulting in a reduction in the observed levels of phosphorylated ERK. Alternatively, serum levels or the ERK-inducer present in the serum is reduced, thus resulting in the reduced ERK levels. Mab 1.1, 2.1 and 13.1 together fell into another distinct group (highlighted in red). In this group, an increase in total ERK levels was observed in the absence of HGF and there was no change in phosphorylated ERK compared to the no-antibody control. No changes in total ERK levels and phosphorylated ERK levels were observed in HGF-induced samples. These results suggest that Mab 1.1, 2.1 and 13.1 do not have an effect on ERK phosphorylation but are affecting ERK levels by an unknown mechanism. Total ERK levels were observed to remain constant in HGF-induced and un-induced samples treated with either Mab 3.1, 7.1 or 8.1 (highlighted in purple). Interestingly, although total ERK levels remained constant, a decrease in ERK phosphorylation levels was observed in these samples. These antibodies are of interest as the results suggest that these antibodies have the ability to inhibit c-Met activation thus resulting in the decrease of ERK phosphorylation observed. With Mab 14.1 and 15.1, total ERK levels and ERK phosphorylation levels remained constant in the different treatments tested indicating that these antibodies do not have any effect on c-Met. Finally, Mab 9.1 was the only antibody whose total ERK levels and phosphorylated ERK levels stayed the same upon

HGF induction but decreased in un-induced samples. It is possible that Mab 9.1 is able to reduce total ERK and phosphorylated ERK levels in the absence of HGF. However, in the presence of HGF, the reduced effect of Mab 9.1 is being cancelled out by HGF-induction resulting in the constant levels of ERK and phosphorylated ERK observed. The ERK pathway clearly plays a role in the biological changes, such as cell proliferation and cell motility, induced by c-Met activation (Birchmeier et al., 2003; Li et al., 2005; Rosario and Birchmeier, 2003). However, the mechanism by which c-Met or anti-Met antibodies affect ERK levels is still unclear. The observed changes in ERK levels within one hour of antibody incubation, followed by 30 mins of HGF treatment, could possibility be due to the effects of antibody treatment or FCS effects.

The results of antibody binding regions in Section 3.2.7 suggested that the epitopes of Mab 1.1, 2.1, 7.1, 8.1, 9.1 and 15.1 lie within Met-HGF interaction site. Competition binding of these antibodies to c-Met would disrupt the receptor-ligand interaction, prevent c-Met activation and activation of the ERK pathway. Consistent with the structural analysis, reduced ERK phosphorylation was observed in Mab 7.1 and 8.1 treated samples suggesting that these antibodies are inhibiting c-Met activation by competing with HGF for c-Met.

Hybridoma cell supernatant tested at 1:10 dilution (data not shown) failed to produce significant ERK responses. Subtle differences in ERK responses were observed in samples treated with hybridoma supernatant diluted 1:5 in serum-free media (Appendix 3). In this assay, some effects of monoclonal antibody on ERK levels and phosphorylation levels were observed. However, the presence of FCS makes it difficult to differentiate the effects of the monoclonal antibodies and the effect of FCS. Purified monoclonal antibodies, which will be discuss in the next section, will be required to eliminate this FCS issue.

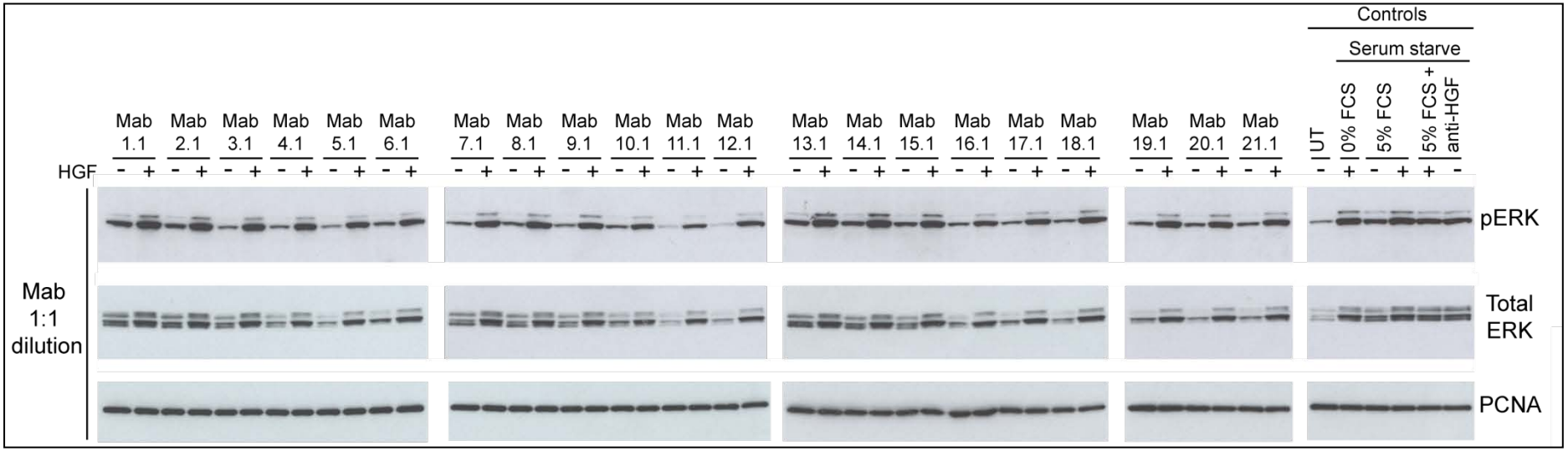

Figure 3.30: Mab (diluted 1:1) effects on ERK phosphorylation in HaCaT cells.

HaCaT cells were treated with anti-α-chain c-Met antibodies. HaCaT cells were grown to 90% confluency before serum starvation. Monoclonal antibody cell supernatants were diluted 1:1 in serum-free media and incubated with HaCaT cells for an hour. 10 ng/ml of HGF was added to the cells for 30 mins before harvesting in hot sample buffer. 10 µg of total cell lysate was analysed in each sample by SDS-PAGE. Western blotting was performed using anti-phospho-ERK, anti-ERK and PC10 antibodies to detect phosphorylated ERK, total ERK and PCNA levels respectively. Activation of c-Met was determined by phosphorylation of ERK. PCNA levels were used as loading control. All controls were serum-starved, except for untreated (UT) samples. Controls with media containing 0% and 5% FCS were performed to examine the effect of FCS on ERK phosphorylation. Antibody against HGF (5 µg/ml) was used as a control to block HGF from binding to c-Met. pERK: Phosphorylated ERK. Anti-HGF: Antibody against HGF.

Table 3.5: Mab effects on total ERK and phosphorylated ERK levels.

Mab	Total ERK		Phosphorylated ERK	
	No HGF	HGF	No HGF	HGF
1.1	↑	S	S	S
2.1	↑	S	S	S
3.1	S	S	↓	↓
4.1	↓	↓	↓	↓
5.1	↓	↓	↓	↓
6.1	↓	↓	↓	↓
7.1	S	S	↓	↓
8.1	S	S	↓	↓
9.1	↓	S	↓	S
10.1	↓	↓	↓	↓
11.1	↓	↓	↓	↓
12.1	↓	↓	↓	↓
13.1	↑	S	S	S
14.1	S	S	S	S
15.1	S	S	S	S
16.1	↓	↓	↓	↓
17.1	↓	↓	↓	↓
18.1	↓	↓	↓	↓
19.1	↓	↓	↓	↓
20.1	↓	↓	↓	↓
21.1	↓	↓	↓	↓

Summary of results from Figure 3.30. Levels of ERK and phosphorylated ERK from HaCaT cells treated with monoclonal antibody supernatant, in the presence or absence of HGF. Results were compared to control cells treated in 5% FCS and tabulated. Hybridoma cell supernatant that have the same effects on ERK levels are highlighted in the same colour. (↑): increased levels compared to control; (↓): decreased levels compared to control; (S): levels remain the same as control.

3.3.3: Preliminary analysis of monoclonal antibodies effects on cell scattering

The activation/inhibition effects of monoclonal antibodies on ERK phosphorylation do not necessary induce the same effects on other hallmarks of c-Met activation (Prat *et al.*, 1998). We thus investigated the effects of the antibodies on HGF-induced changes in cell motility or scattering. Cell scattering is one of the biological effects of c-Met activation upon HGF stimulation (Birchmeier *et al.*, 2003). HaCaT cells are cuboidal-shaped cells that form tight circular colonies under normal tissue culture growth conditions. In the presence of HGF, HaCaT cells become spindle-shape cells and scatter, which is a hallmark of the epithelial-mesenchymal transition (EMT).

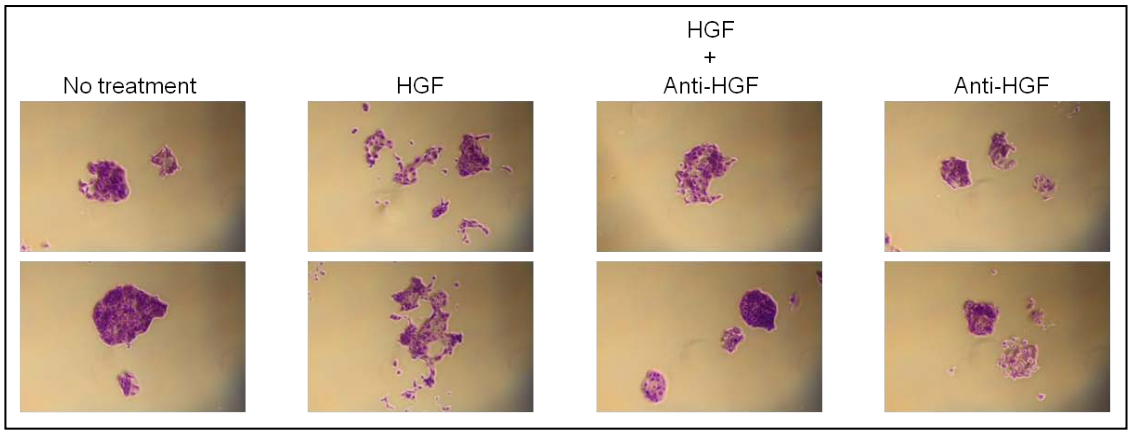

Figure 3.31: HGF induction causes cell scattering in HaCaT cells.
Crystal violet staining of HaCaT cells. Un-induced HaCaT cells form tight, circular colonies. However, upon HGF stimulation, HaCaT cells change shape and spread out (scatter), no longer retaining their tight, circular colonies. Scattering of HaCaT cells by HGF induction could be blocked by anti-HGF antibodies. HaCaT cells were seeded at low cell density and allowed to grow until colonies formed. HGF and anti-HGF antibody were used at a final concentration of 10 ng/ml and 5 µg/ml respectively. Anti-HGF antibody was pre-incubated with HGF, in media containing 2% FCS, for 1 hr before adding to the cells. Cells were treated, as indicated in media containing 2% FCS, for 24 hrs before fixing in methanol and staining with crystal violet. Results were shown in duplicates for each set of conditions.

HaCaT cells were seeded at low cell density and allowed to grow until colonies were formed. Cells were serum-starved for 24 hrs following which, hybridoma cell supernatants containing monoclonal antibodies were added to the cells for 1 hr. HGF was then added and the cells incubated for 24 hrs. Cells were then fixed with methanol and stained with crystal violet for easy visualisation of cell colonies (Figures 3.31 and

3.28). Percentage of cell scatter is not available. Magnitude of cell scatter was observed by eye. Pictures of cell colonies taken represent the majority phenotype observed for each indicated treatment. It is assumed that the hybridoma supernatants contained 10% FCS and as a rough guide, a final concentration of 2% of FCS was used in controls (Figure 3.31). As observed, HaCaT cells only scatter in the presence of HGF. HaCaT cells failed to scatter under normal conditions (no treatment control), treatment with a combination of HGF and anti-HGF antibody and with anti-HGF antibody alone. Failure to scatter under the combination of HGF and anti-HGF antibody is due to anti-HGF antibody competition binding with c-Met for HGF, thus preventing c-Met activation by added HGF.

To test whether our anti-α-chain antibodies were capable of blocking the effects of HGF on HaCaT cells, varying antibody concentrations were tested by diluting cell supernatant in 1:10, 1:5 and 1:1 with serum-free media. The anti-α-chain antibodies did not induce cell scattering in the absence of HGF (Figure 3.32). The one exception was Mab 6.1, which induced a slight scattering effect, suggesting that Mab 6.1 has an activating effect on c-Met-induced cell scatter. In the presence of added HGF, Mab 4.1, 8.1, 11.1, 14.1 and 17.1 showed discernable inhibition of cell scatter, indicating that these antibodies are inhibitory towards HGF-induced cell motility. The inhibitory effect of cell scatter by the remaining antibodies is not obvious as the colonies were observed to scatter less than the HGF control and were not as tight at the combination of HGF and anti-HGF antibody control.

The effects of the hybridoma monoclonal antibodies in functional assays (ERK phosphorylation and cell scatter) are compiled in Table 3.6. From this table, it is observed that Mab 4.1, 8.1, 11.1, 14.1 and 17.1 are able to inhibit cell scatter and reduce/remain ERK phosphorylation levels. The next stage is to analyse the effects of

the antibodies without the presence of FCS to confirm their effect on ERK phosphorylation and cell scatter.

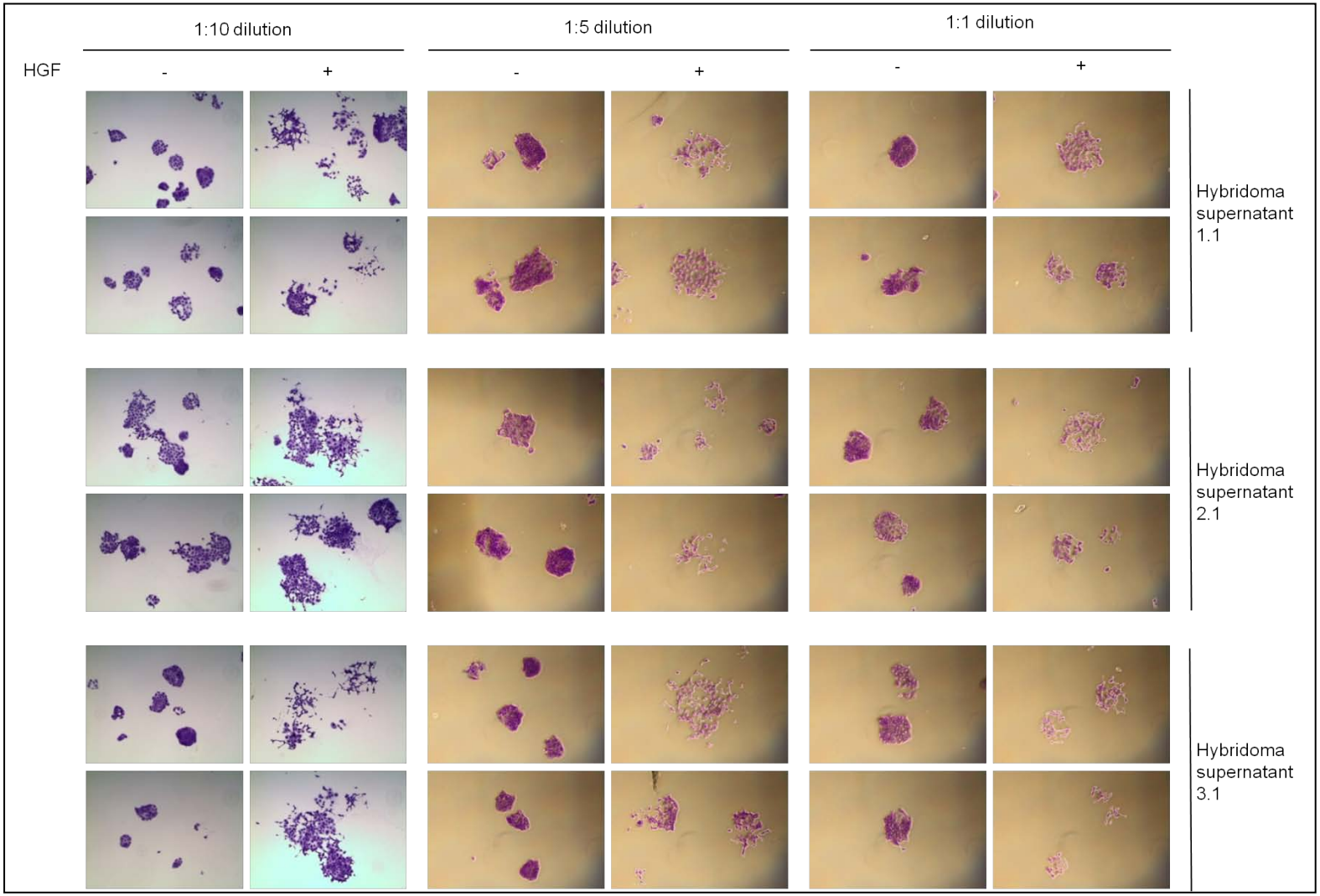

Figure 3.32A: Mab 1.1, 2.1 and 3.1 effects on cell scattering in HaCaT cells.
Crystal violet staining of HaCaT cells. HaCatTcells were seeded at low cell density and allowed to grow until colonies were formed. Cells were serum-starved for 24 hrs before incubating with cell supernatant containing monoclonal antibodies for an hour. Cell supernatants were diluted 1:10, 1:5 and 1:1 in serum-free media. HGF was added to the cells for 24 hrs before fixation in methanol and staining in crystal violet. Two fields are shown for each cell treatment condition.

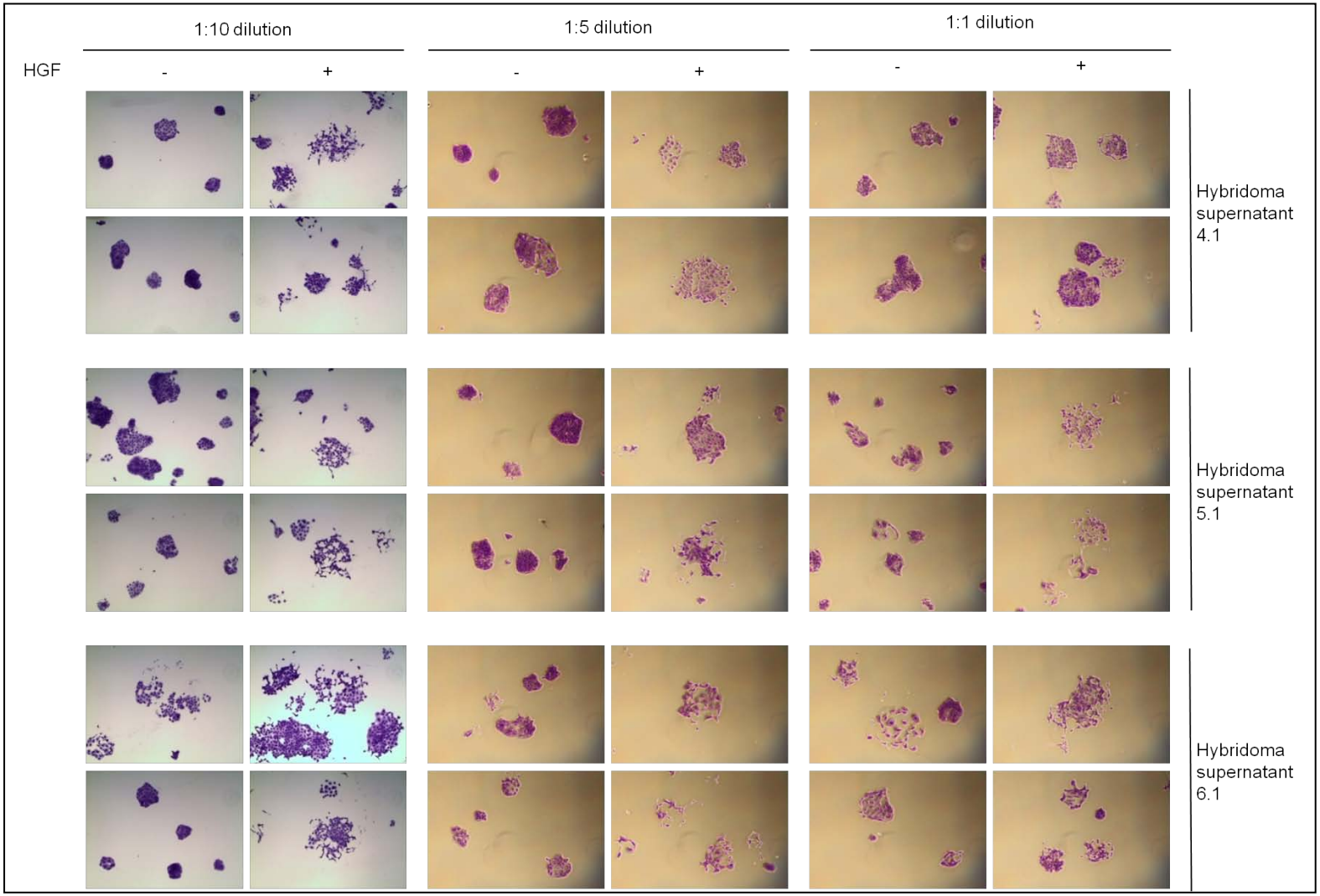

Figure 3.32B: Mab 4.1, 5.1 and 6.1 effects on cell scattering in HaCaT cells.

Crystal violet staining of HaCaT cells. HaCaT cells were seeded at low cell density and allowed to grow until colonies were formed. Cells were serum-starved for 24 hrs before incubating with cell supernatant containing monoclonal antibodies for an hour. Cell supernatants were diluted 1:10, 1:5 and 1:1 in serum-free media. HGF was added to the cells for 24 hrs before fixation in methanol and staining in crystal violet. Two fields are shown for each cell treatment condition.

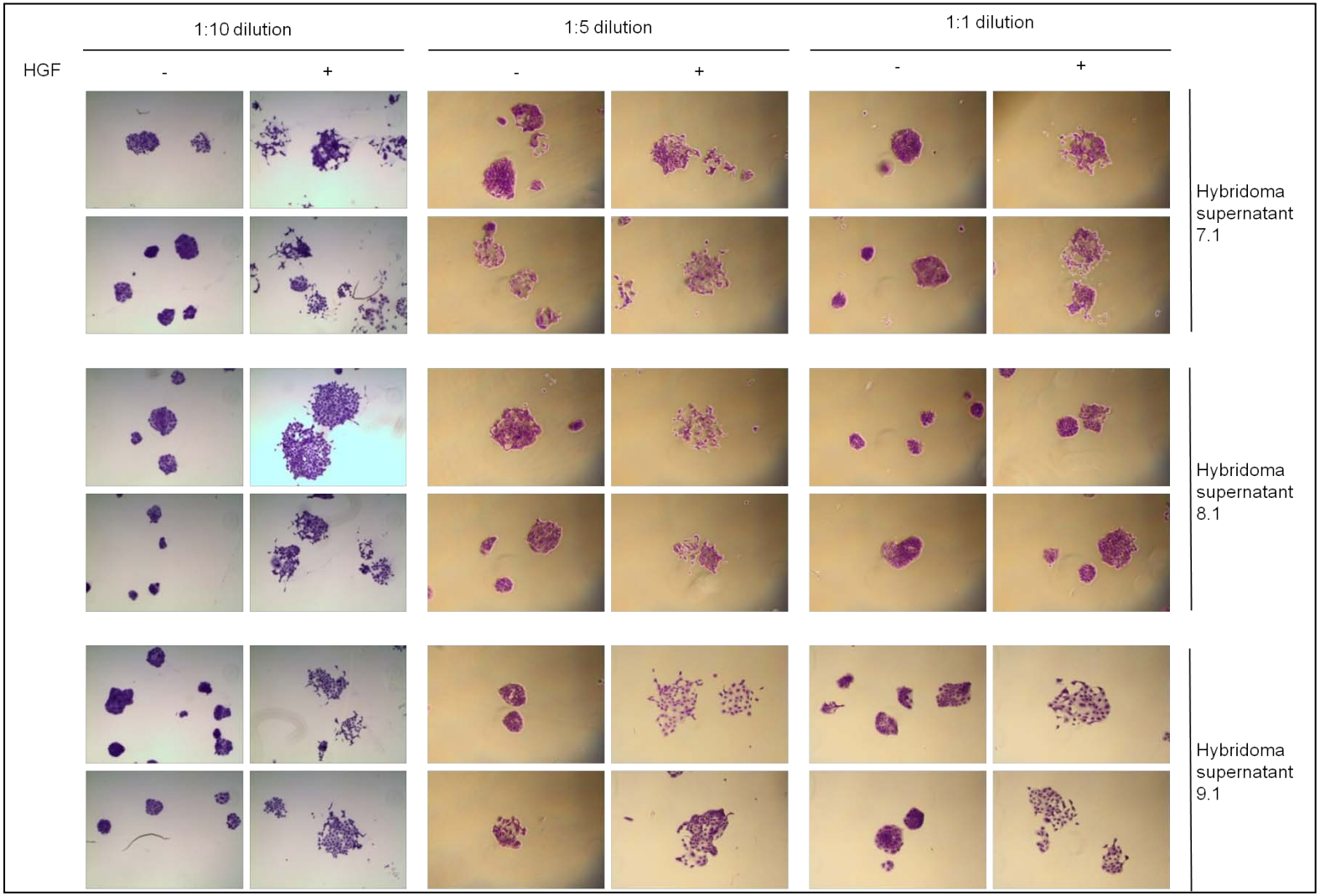

Figure 3.32C: Mab 7.1, 8.1 and 9.1 effects on cell scattering in HaCaT cells.
Crystal violet staining of HaCaT cells. HaCaT cells were seeded at low cell density and allowed to grow until colonies were formed. Cells were serum-starved for 24 hrs before incubating with cell supernatant containing monoclonal antibodies for an hour. Cell supernatants were diluted 1:10, 1:5 and 1:1 in serum-free media. HGF was added to the cells for 24 hrs before fixation in methanol and staining in crystal violet. Two fields are shown for each cell treatment condition.

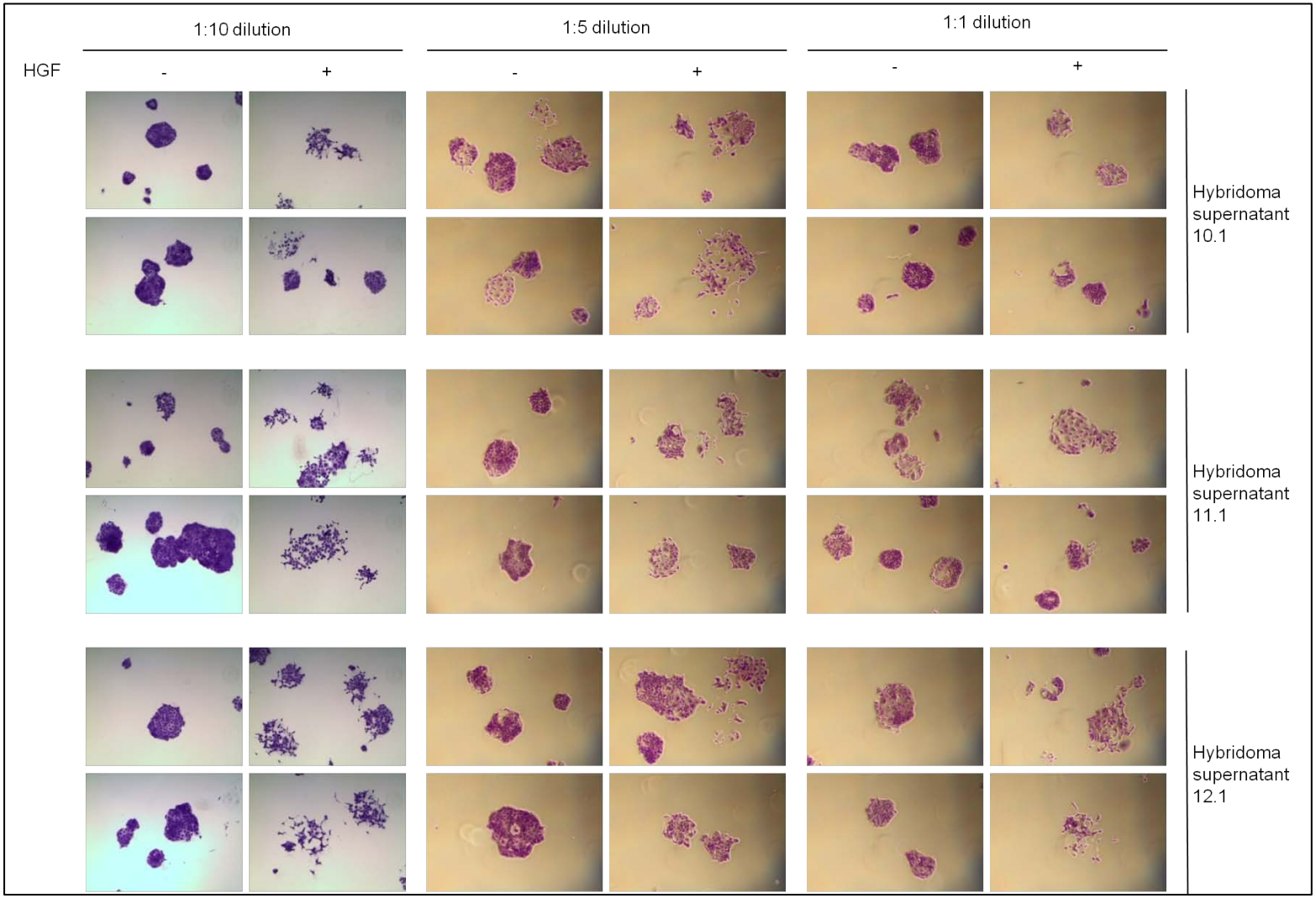

Figure 3.32D: Mab 10.1, 11.1 and 12.1 effects on cell scattering in HaCatTcells.
Crystal violet staining of HaCaT cells. HaCatTcells were seeded at low cell density and allowed to grow until colonies were formed. Cells were serum-starved for 24 hrs before incubating with cell supernatant containing monoclonal antibodies for an hour. Cell supernatants were diluted 1:10, 1:5 and 1:1 in serum-free media. HGF was added to the cells for 24 hrs before fixation in methanol and staining in crystal violet. Two fields are shown for each cell treatment condition.

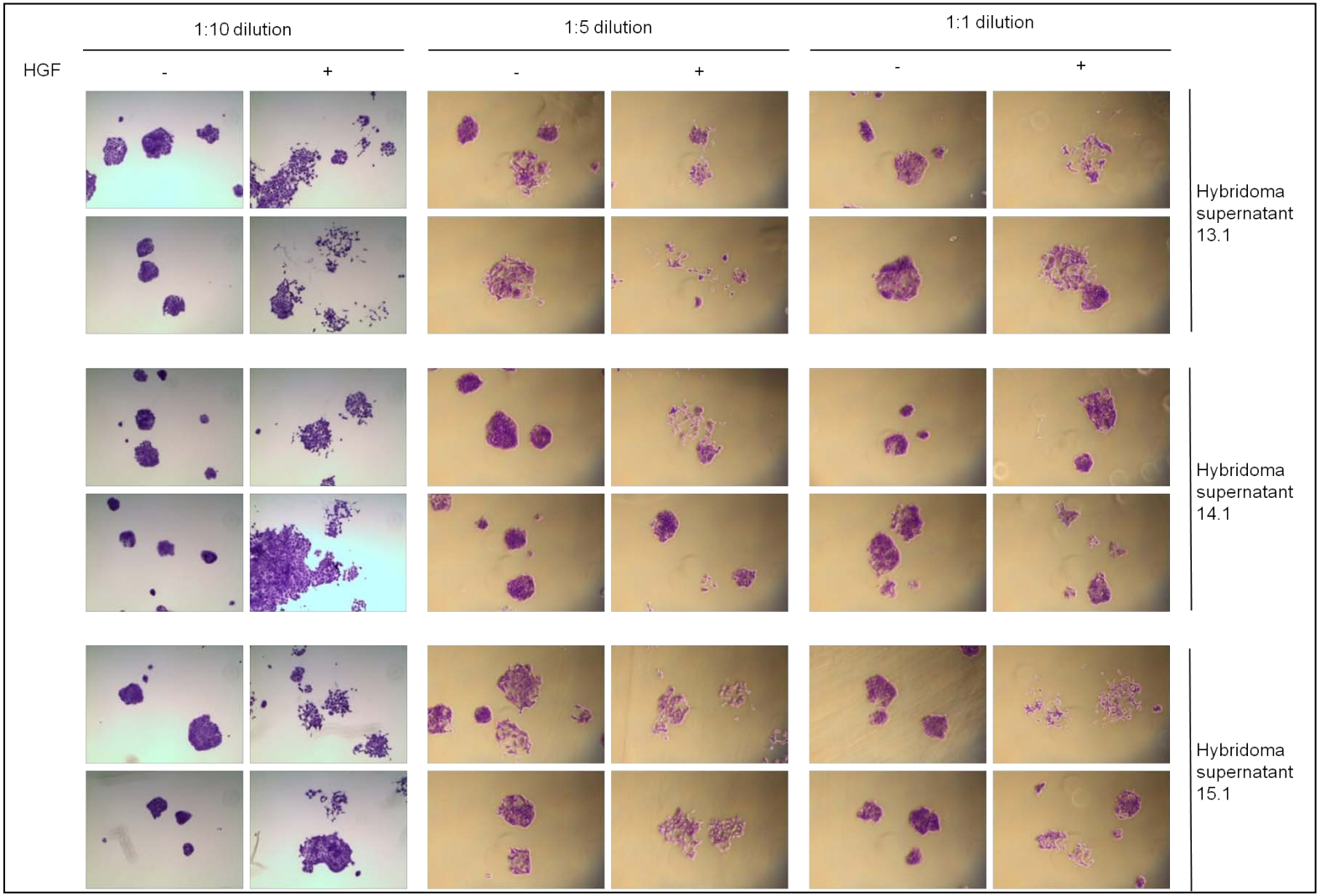

Figure 3.32E: Mab 13.1, 14.1 and 15.1 effects on cell scattering in HaCaT cells.
Crystal violet staining of HaCaT cells. HaCatTcells were seeded at low cell density and allowed to grow until colonies were formed. Cells were serum-starved for 24 hrs before incubating with cell supernatant containing monoclonal antibodies for an hour. Cell supernatants were diluted 1:10, 1:5 and 1:1 in serum-free media. HGF was added to the cells for 24 hrs before fixation in methanol and staining in crystal violet. Two fields are shown for each cell treatment condition.

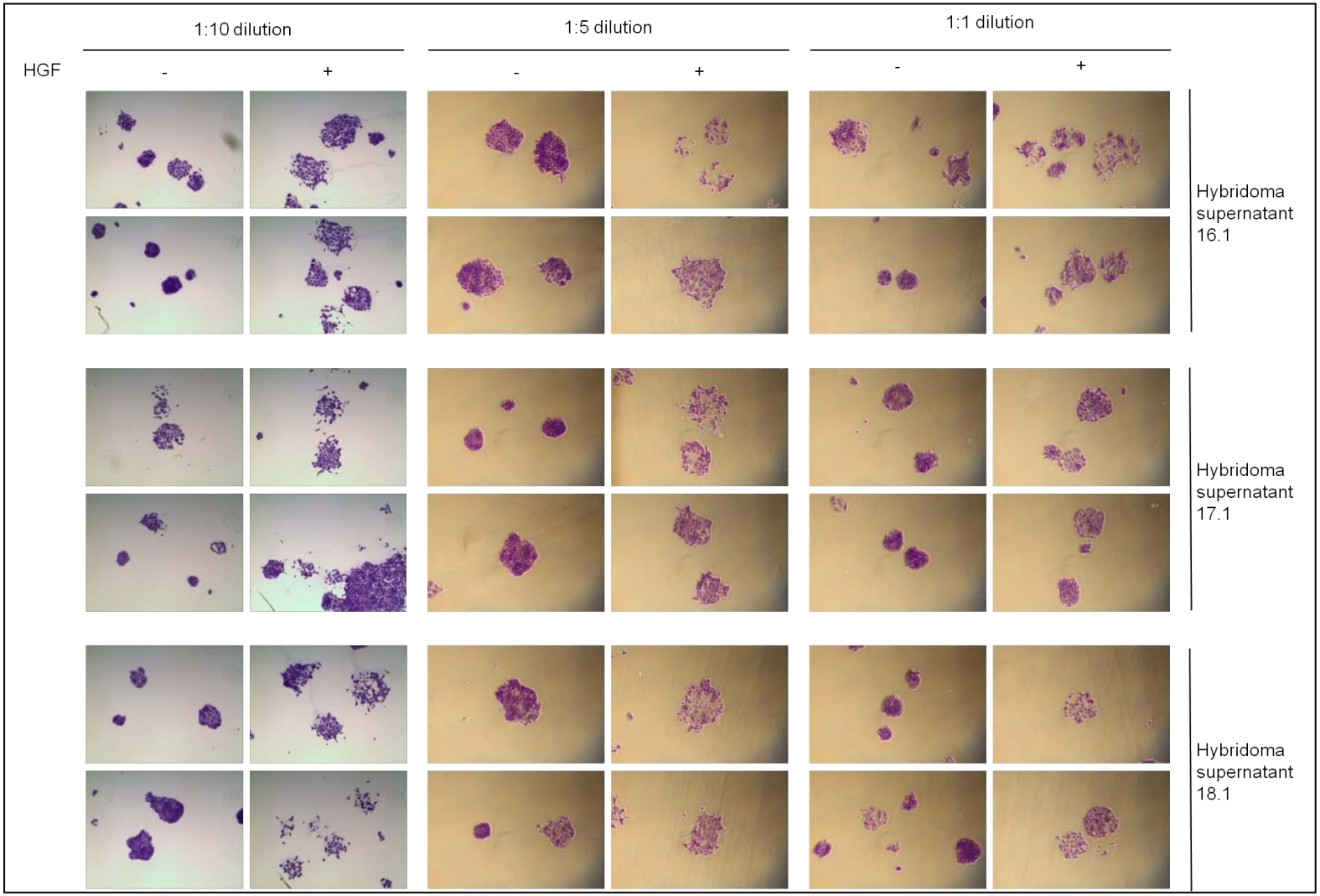

Figure 3.32F: Mab 16.1, 17.1 and 18.1 effects on cell scattering in HaCatT cells.
Crystal violet staining of HaCaT cells. HaCaT cells were seeded at low cell density and allowed to grow until colonies were formed. Cells were serum-starved for 24 hrs before incubating with cell supernatant containing monoclonal antibodies for an hour. Cell supernatants were diluted 1:10, 1:5 and 1:1 in serum-free media. HGF was added to the cells for 24 hrs before fixation in methanol and staining in crystal violet. Two fields are shown for each cell treatment condition.

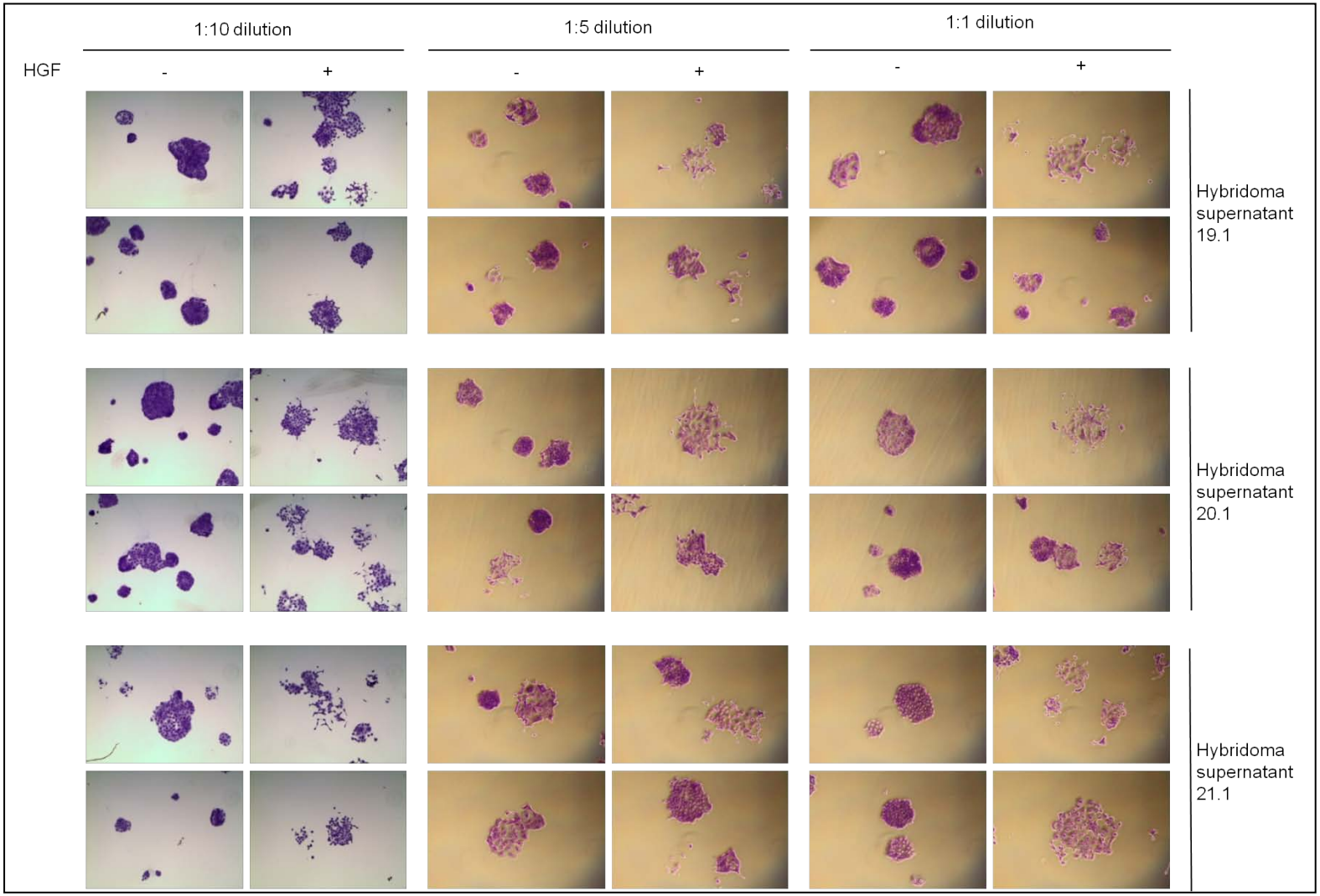

Figure 3.32G: Mab 19.1, 20.1 and 21.1 effects on cell scattering in HaCaT cells.
Crystal violet staining of HaCaT cells. HaCaT cells were seeded at low cell density and allowed to grow until colonies were formed. Cells were serum-starved for 24 hrs before incubating with cell supernatant containing monoclonal antibodies for an hour. Cell supernatants were diluted 1:10, 1:5 and 1:1 in serum-free media. HGF was added to the cells for 24 hrs before fixation in methanol and staining in crystal violet. Two fields are shown for each cell treatment condition.

Table 3.6: Result summary of monoclonal hybridoma cell supernatants in functional assays.

Monoclonal antibody	c-Met binding region	Total ERK/phosphorylated ERK[a]	Cell scatter[b]
1.1	7	S/S	–
2.1	7	S/S	–
3.1	5	S/↓	–
4.1	6	↓/↓	Inhibit
5.1	5	↓/↓	–
6.1	8	↓/↓	Activate
7.1	10	S/↓	–
8.1	9	S/↓	Inhibit
9.1	7	S/S	–
10.1	8	↓/↓	–
11.1	3	↓/↓	Inhibit
12.1	2	↓/↓	–
13.1	8	S/S	–
14.1	4	S/S	Inhibit
15.1	10	S/S	–
16.1	1	↓/↓	–
17.1	4 & 8	↓/↓	Inhibit
18.1	4	↓/↓	–
19.1	4	↓/↓	–
20.1	2	↓/↓	–
21.1	3	↓/↓	–

Results of hybridoma cell supernatant effects on ERK phosphorylation and cell scatter are compiled together. Antibody binding region are shown for comparison.

a) Levels of total ERK compared to levels of ERK phosphorylation, in the presence of HGF. Results were obtained from Table 3.5 where the levels of total ERK and phosphorylated ERK, in the presence of HGF, were compared to control cells treated in media containing 5% FCS. Hybridoma cell supernatant that have the same effects on ERK levels are highlighted in the same colour (i.e. colour coding was directly obtained from Table 3.5 whereby the hybridoma cell supernatants that were observed to give the same effects on total ERK and phosphorylated ERK levels were grouped according to colour.). For further details, refer to Table 3.5. (↑): increased levels compared to control; (↓): decreased levels compared to control; (S): levels remain the same as control.

b) Results of hybridoma cell supernatant on cell scatter (reference to Figures 3.32A to G in section 3.3.3). (Inhibit): antibodies have an inhibitory effect on cell scattering; (Activate): antibodies have an activating effect on cell scattering; (-): no clear effect.

3.3.4: Monoclonal antibodies effects on clustering of cells

It was demonstrated that the recognition of monoclonal antibodies directed against surface protein causes cell clustering (Zhang. *et al.*, 1998, Choo A.B. *et al.*, 2008). To examine the ability of our monoclonal antibodies to recognise and bind native c-Met, and cause cell clumping, c-Met expressing cells, growing in suspension culture were required (Figure 3.6). SNU-5 suspension cells were thus incubated in hybridoma cell supernatant, diluted 1:20, 1:10, 1:5 and 1:1 dilution in RPMI cell media, for 4 – 24 hrs before examining for cell clusters (Figures 3.33). As an antibody control, cell supernatant from 4B2 hybridoma cells was used which produce an anti-Mdm2 monoclonal antibody.

Results of cell cluster are summarised in Table 3.7. Cell clustering was only observed in hybridoma supernatants diluted at 1:1 (Figures 3.33). Mab 3.1, 5.1, 6.1, 16.1, 17.1 and 19.1 had no response, suggesting that they do not bind native c-Met. Mab 2.1, 11.1, 12.1, 13.1, and 8.1 were observed to induce a strong cell cluster response (more than 30 cells in a cluster). Mab 1.1, 10.1, 14.1 and 17.1 induced intermediate responses (20 – 30 cells in a cluster) and Mab 9.1, 18.1 and 20.1 induced weak response (10 – 20 cells in a cluster).

There is little understanding of the clustering of cells induced by monoclonal antibody recognition of cell surface proteins. Cell cluster induced by anti-Porimin *(P*ro-oncosis *r*eceptor *i*nducing *m*embrane *in*jury) monoclonal antibody results in lethal damage to cell membrane which eventually led to cell death (Zhang *et al.*, 1998). Interestingly, the mAb 84 antibody directed against PDOXL (Podocalyxin-Like Protein-1), is able to bind to PDOXL on undifferentiated human embryonic stem cells and cause cell killing in a similar fashion as the anti-Porimin antibodies. This form of cell killing is independent

of complement and shares no characteristic with apoptosis (no DNA fragmentation or apoptotic bodies observed). Cell killing induced by anti-Porimin and anti-PDOXL monoclonal antibodies, however, share similar characteristic with oncosis – initially proposed by von Reckling-hausen in 1910 to describe cell death caused by swelling (Majno and Joris, 1995). Beers *et al*. (2008) reported the classification of type I and II therapeutic monoclonal antibodies against the CD20 antigen. Type II antibodies are able to cause cell clustering (also known as homotypic adhesion) and were found to be more efficient in the elimination of malignant B-cells by programme cell (PCD) (Alduaji *et al*., 2011, Beers *et al.*, 2008). Alduaji *et al.* (2011) also reported that the induction of PCD is not mediated by effector functions of the anti-CD20 monoclonal antibody. It is intriguing that the clustering of cells, induced by antibody treatment, eventually led to cell death. Antibody-induced cell death is still debatable (whether oncosis is considered as PCD or it is two different cell death mechanisms) and more studies are required as apoptosis is clearly not the cause of cell death.

The ability to cause cell cluster may only reflect the ability of our antibodies to recognise native c-Met and the size of the cell cluster might not provide much information of our antibodies. However, it would be interesting to test if our antibodies, like the above mentioned antibodies, are able to induce cell death. In our study, although the use of an anti-Mdm2 monoclonal antibody was used to demonstrate that the cell clustering was mediated through c-Met, knocking down c-Met expression via siRNA in SNU-5 cells would have provided stronger evidence.

In this section, we attempted to characterise the functional activities of 21 monoclonal antibodies in the form of cell supernatants by ERK phosphorylation and cell scattering. It is observed that the presence of FCS in the cell media have an effect on the functional activities of the antibodies, resulting in contradictory results. Functional analysis of the

monoclonal antibodies could be more explicit if purified monoclonal antibodies were used. However, these tests were being carried out as a preliminary screen to identify potential therapeutic antibodies. Purification of all the monoclonal antibodies would be time-consuming and unnecessary. Since it was not possible to quantify the antibody concentration in these experiments, steps were therefore taken to test varying antibody concentration in each case, which can be viewed as no more than a preliminary screening process. In the next section, potential antibodies identified from this preliminary screen were selected for ascites production followed by antibody purification. Purified monoclonal antibodies were then subjected to further characterisation and analysis.

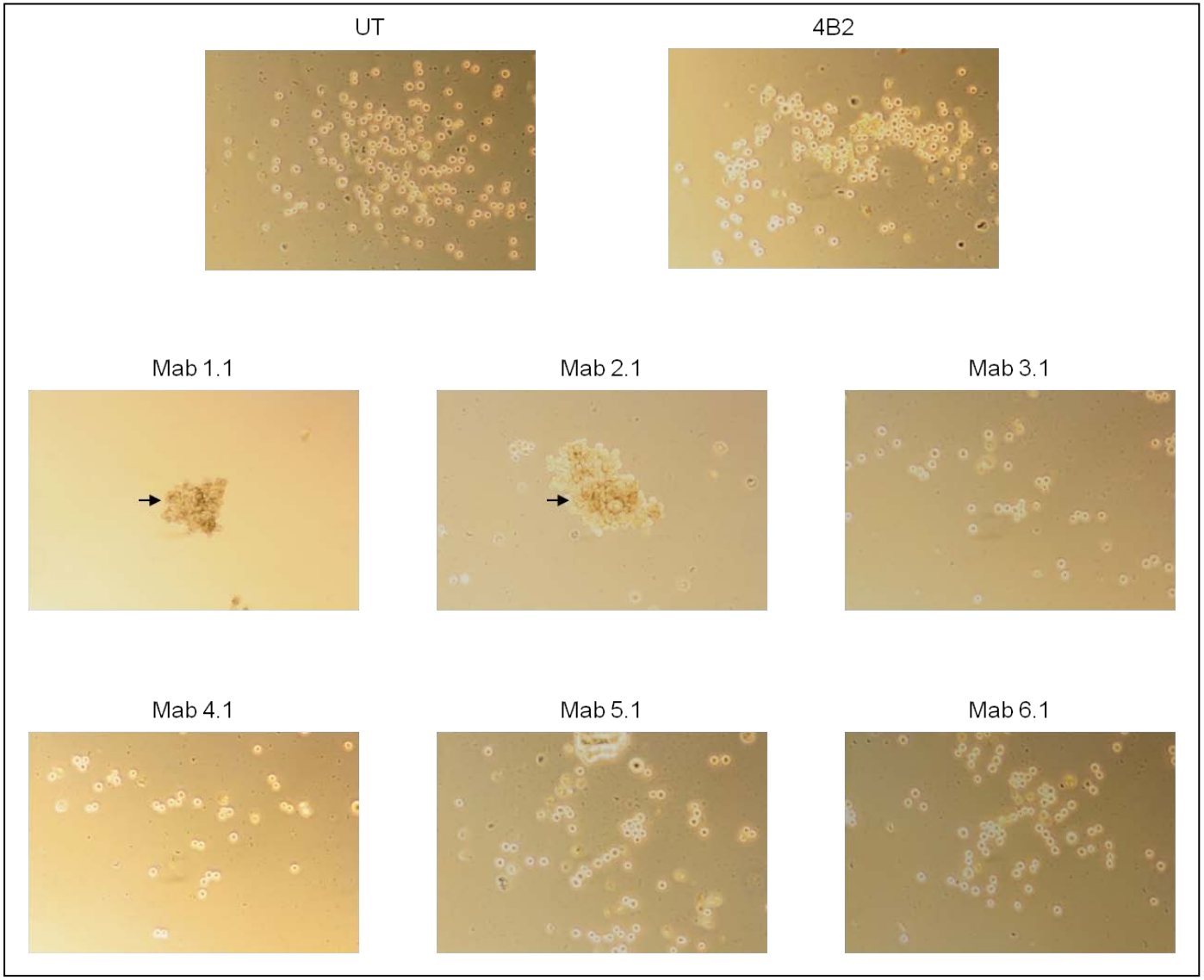

Figure 3.33A: Homotypic adhesion of SNU-5 cells. SNU-5 suspension cells were incubated with hybridoma cell supernatants (Mab 1.1 to 6.1). Cell supernatants were diluted 1:1 in RPMI cell media. Untreated (UT) cells were incubated in media containing 1:1 DMEM/RPMI. A hybridoma, clone 4B2, producing antibody to Mdm2 was used as a control. Cells were incubated for 4-24 hrs before examining for cell clusters. Arrows indicate cell clusters.

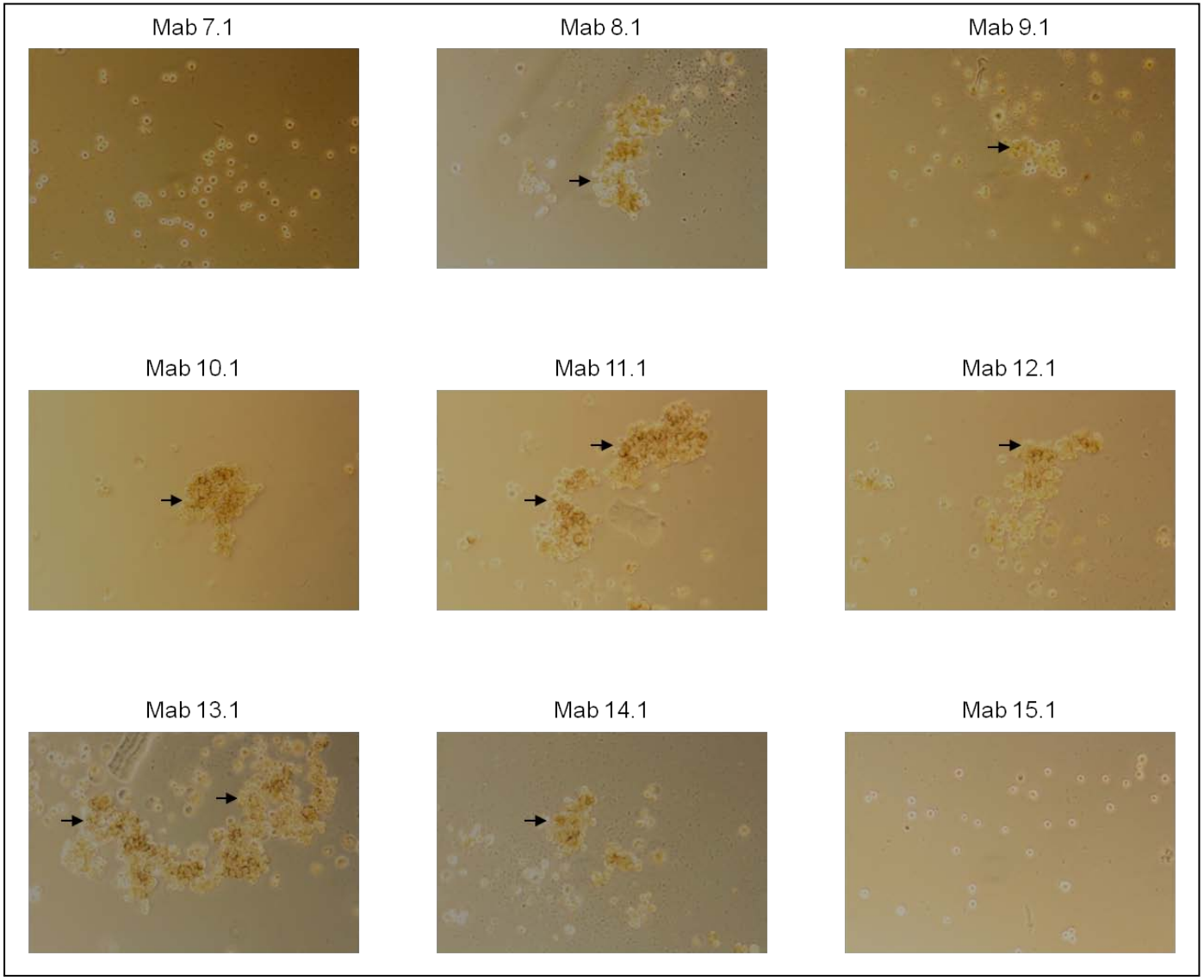

Figure 3.33B: Homotypic adhesion of SNU-5 cells. SNU-5 suspension cells were incubated with hybridoma cell supernatants (Mab 7.1 to 15.1). Cell supernatants were diluted 1:1 in RPMI cell media. Untreated (UT) cells were incubated in media containing 1:1 DMEM/RPMI. A hybridoma, clone 4B2, producing antibody to Mdm2 was used as a control. Cells were incubated for 4-24 hrs before examining for cell clusters. Arrows indicate cell clusters.

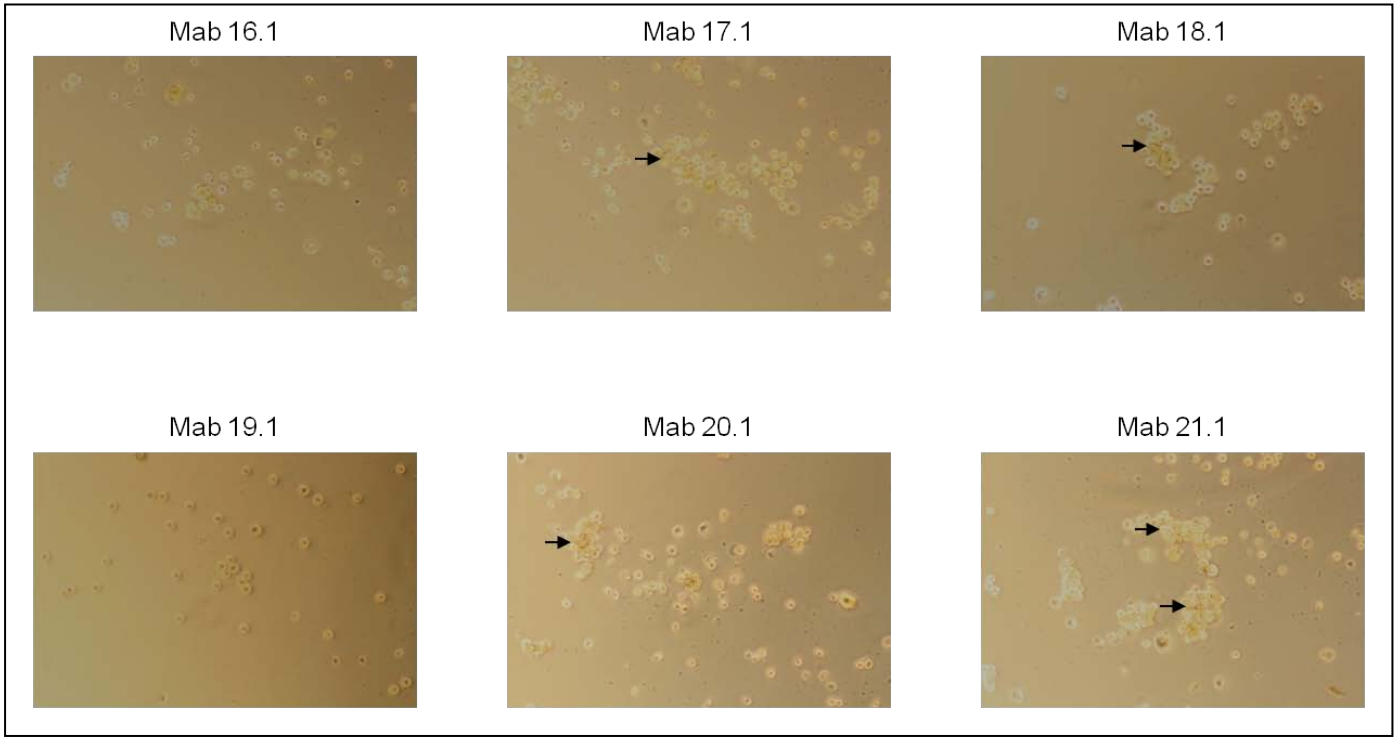

Figure 3.33C: Homotypic adhesion of SNU-5 cells.
SNU-5 suspension cells were incubated with hybridoma cell supernatants (Mab 16.1 to 21.1). Cell supernatants were diluted 1:1 in RPMI cell media. Untreated (UT) cells were incubated in media containing 1:1 DMEM/RPMI. A hybridoma, clone 4B2, producing antibody to Mdm2 was used as a control. Cells were incubated for 4-24 hrs before examining for cell clusters. Arrows indicate cell clusters.

Table 3.7: Summary of hybridoma cell supernatant results obtained from ERK phosphorylation, cell scattering and cell clustering assays.

Binding region[a]	Monoclonal Antibody	IgG subclass[a]	Total ERK/phosphorylated ERK[b]	HaCaT cell scatter[c]	Cell clustering[d]
1	16.1	IgG2A	↓/↓	-	-
2	12.1	IgG1	↓/↓	-	+++
	20.1		↓/↓	-	+
3	11.1	IgG1	↓/↓	Inhibit	+++
	21.1		↓/↓	-	++
4	14.1	IgG1	S/S	Inhibit	++
	18.1		↓/↓	-	+
	17.1		↓/↓	Inhibit	++
	19.1	IgG2B	↓/↓	-	-
5	3.1	IgG1	S/↓	-	-
	5.1		↓/↓	-	-
6	4.1	IgG2A	↓/↓	Inhibit	-
7	1.1	IgG1	S/S	-	++
	2.1		S/S	-	+++
	9.1		S/S	-	+
8	6.1	IgG1	↓/↓	Activate	-
	10.1		↓/↓	-	++
	13.1		S/S	-	+++
	17.1		↓/↓	-	++
9	8.1	IgG1	S/↓	Inhibit	+++
10	7.1	IgG1	S/↓	-	-
	15.1		S/S	-	-

Monoclonal hybridoma cell supernatants are being grouped according to their epitope binding region. Highlighted in blue are hybridoma clones selected for ascites production and antibody purification.

a) Characterisation of antibody binding regions and isotypes were obtained from Table 3.4.

b) Levels of total ERK levels were compared to levels of phosphorylated ERK in the presence of HGF (refer to Table 3.5 or 3.6 for further details). (↑): increased levels compared to no treatment control; (↓): decreased levels compared to no treatment control; (S): levels remain the same as no treatment control.

c) Effects of monoclonal hybridoma cell supernatants on cell scatter (refer to Table 3.6 or Figures 3.32A to G). (Inhibit): antibodies in cell supernatant have an inhibitory effect on cell scattering; (Activate): antibodies in cell supernatant have an activating effect on cell scattering; (-): no clear effect.

d) Results of cell clustering, in reference to Figures 3.33A to C, are scored accordingly. (-): no response; (+): weak response; (++): intermediate response; (+++): strong response.

3.4: Characterisation of purified monoclonal antibodies

3.4.1: Ascites production and purification of monoclonal antibodies

21 hybridoma clones were single cell cloned and the antibody they produce was characterised for their region of binding, recognition of c-Met on Western blotting, isotype and ability to block/activate c-Met in functional assays. Hybridoma clones expressing monoclonal antibodies in tissue culture produce approximately 0.05 mg/ml of antibodies when grown to confluence (Harlow and Lane, 1999). In order to characterise further the monoclonal antibodies describe here, a more efficient way of producing monoclonal antibodies was required. Hybridoma clones were therefore selected for ascites production which was performed by Moravian Biotechnology.

From the 21 hybridoma cell clones tested, eleven were selected for ascites production. Selection was based on several criteria: 1) Results from functional assays: monoclonal antibodies that inhibited c-Met activation were selected. 2) monoclonal antibodies that induced a strong cell cluster response were selected. 3) Analysis of antibody binding region (Section 3.2.7). Antibodies were grouped according to their binding region on c-Met. One antibody was selected from each binding region (except region 5) to represent the binding region. Region 5 is not repeated, but this lies within region 6. The eleven clones selected for ascites production were: Mab 2.1, 4.1, 8.1, 11.1, 12.1, 13.1, 14.1, 15.1, 16.1, 17.1 and 18.1. Ascites fluids, obtained from the peritoneal cavity of mice that were injected with hybridoma cells, were produced by Moravian Biotechnology.

We purified monoclonal antibodies from ascites fluid using protein A beads. Depending on the isotype of the monoclonal antibody (characterised in Section 3.2.6), high salt or low salt purification was performed. Purified monoclonal antibodies were dialysed in phosphate-buffered saline (PBS) except for Mab 4.1 which precipitated in PBS. 2 μg of

purified antibody was resolved on a SDS-PAGE gel and stained with Coomassie blue dye (Figure 3.34). Commercially-bought mouse IgG was used as a control.

An IgG antibody molecule is made up of two heavy and two light polypeptide chains held together by disulphide bonds. Two bands of approximately 51 kD and 25 kD were observed in each antibody sample (Figure 3.34). The bands correspond to an antibody's heavy chain (51 kD) and light chain (25 kD). The variations in molecular weight of the light chains observed in different antibodies samples were due to the different amino acid composition that makes up the antigen binding site in each antibody. Interestingly, two bands corresponding to the light chain were observed in Mab 17.1, suggesting that the Mab 17.1 molecule contains two different epitope binding sites. This is consistent with Mab 17.1 being a polyreactive monoclonal antibody, and binds to regions 4 and 8 of c-Met. Similarly, the variations in molecular weight of the heavy chains is due to differing amino acid composition of the antigen binding site and sequences specific to the antibody isotype. No other protein bands were observed in the Coomassie-stained gel, suggesting that the purification of the monoclonal antibodies was successful and the antibody samples have a high level of purity.

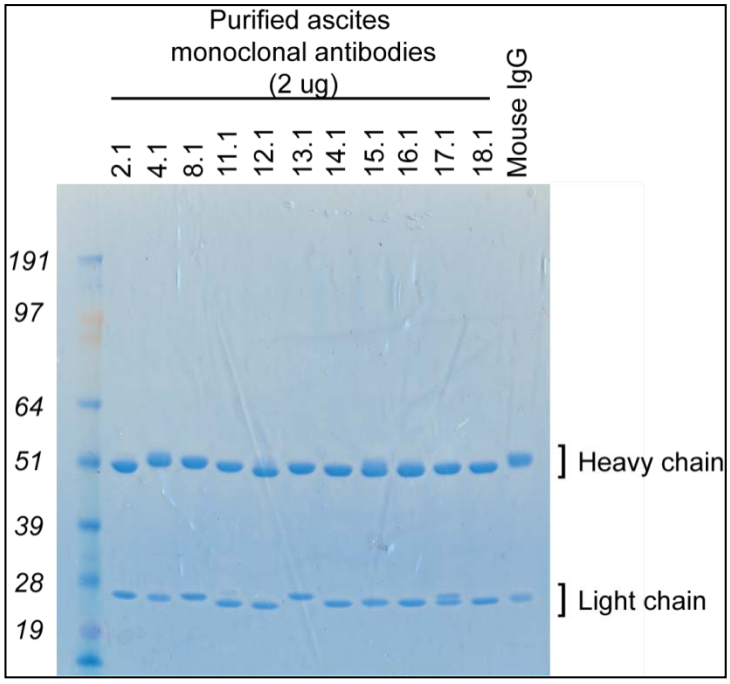

Figure 3.34: Purification of monoclonal antibodies from mouse ascites.
Coomassie-stained SDS-PAGE gel of monoclonal antibodies purified from mouse ascites. Monoclonal antibodies obtained from mouse ascites were purified using protein A beads. 2 µg of antibody was resolved on a SDS-PAGE gel and stained with Coomassie blue dye. Commercially-obtained mouse IgG (2 µg) was used as a control. Antibody heavy and light chain are indicated. Molecular weights are noted aside, in kilodaltons.

3.4.2: Purified monoclonal antibodies on Western blotting

To ensure that the monoclonal antibodies retained their anti-α-chain activity after ascites production and purification, purified monoclonal antibodies were characterised again by Western blotting (Figure 3.35). 1 μg/ml of purified monoclonal antibodies was used to detect purified c-Met α-chain, transfected and endogenous c-Met from whole cell lysates of NIH3T3 transfected cells and U-87MG cells respectively. All monoclonal antibodies, except Mab 13.1 and 15.1, successfully detected purified c-Met α-chain, transfected and endogenous human c-Met. Mab 13.1 and 15.1 had low specificity towards c-Met. Mab 13.1 only detected purified α-chain weakly and showed little or no reaction with endogenous or transfected c-Met samples. Mab 15.1 was able to detect purified α-chain but detected full length c-Met precursor weakly. Mab 2.1 and 14.1 were observed to have higher affinity towards c-Met, compared to Mab 13.1 and 15.1, however they also recognise other non-specific protein bands. Mab 4.1, 8.1, 16.1, 17.1 and 18.1 have affinity towards c-Met and fewer non-specific bands. Despite having different epitopes, most of the anti-α-chain monoclonal antibodies share the same patterns of band recognition with Mab 11.1 and 12.1. This suggests that the band profiles of Mab 11.1 and 12.1 are completely specific. Mab 11.1 and 12.1 are thus the best monoclonal antibodies to use on Western blots as they detected c-Met with good affinity and specificity. NIH3T3 cells transfected samples were observed to have more protein bands. This could be due to degradation of c-Met since the cell was expressing high levels of transfected protein. For some antibodies, non-specific binding was observed even though purified monoclonal antibodies were used. Lastly, protein bands observed at approximately 50 kD could possibility be the α-chain of c-Met.

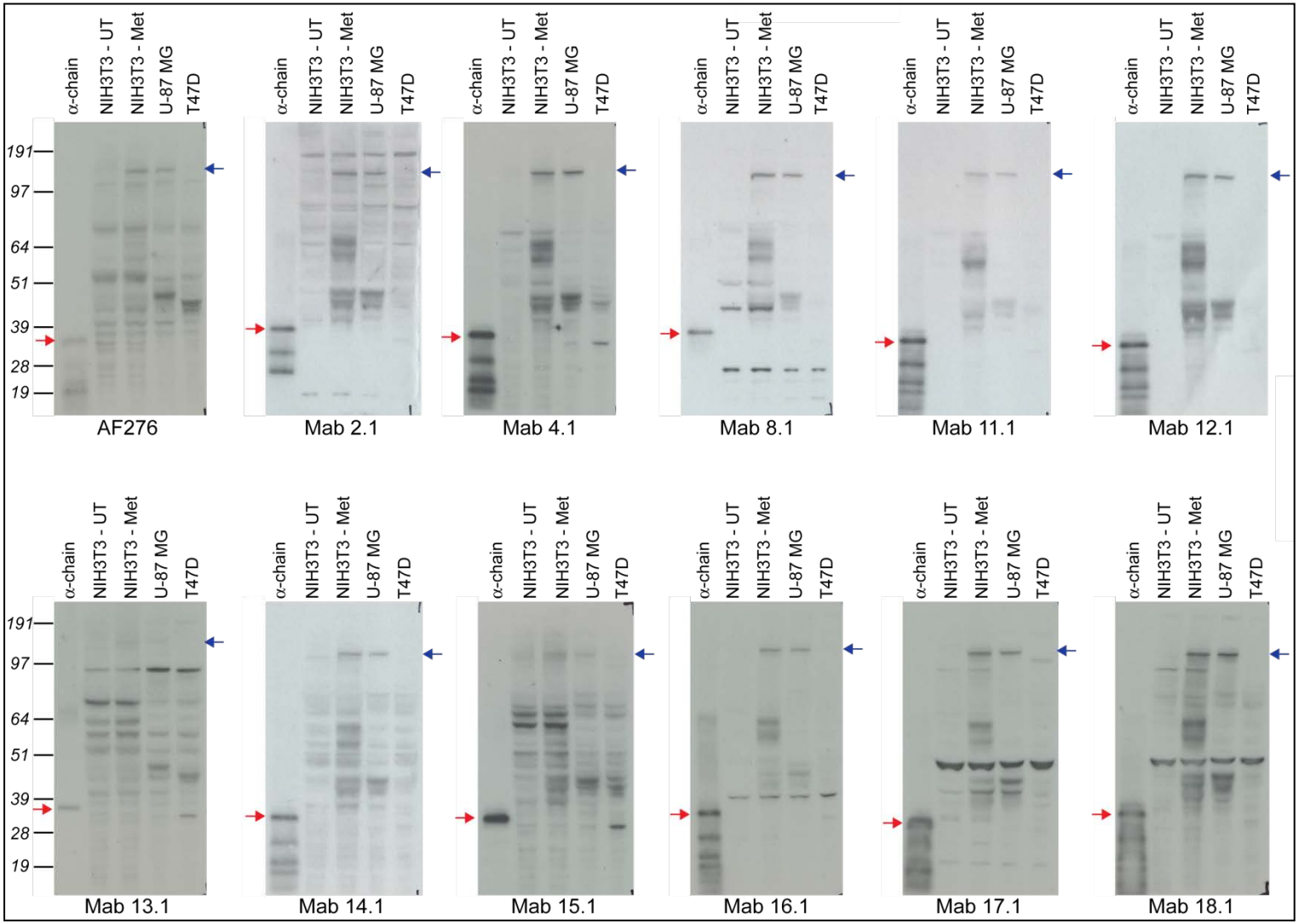

Figure 3.35: Purified monoclonal antibodies on Western blotting.
11 hybridoma clones were selected for ascites production. Monoclonal antibodies were purified from ascites and tested again for reactivity against full length c-Met in whole cell lysates. 50 µg of whole cell lysate was obtained from untransfected NIH3T3 cells (UT), NIH3T3 cells transfected with full length human c-Met (Met), U-87 MG cell lines and T47D cell lines. Monoclonal antibodies are used at concentration of 1 µg/ml. 10 ng of purified α-chain was used as positive control. AF276 antibody was used as control. Blue arrows indicate c-Met precursor (170 kD). Red arrows indicate purified α-chain. Mab: Monoclonal antibody. Molecular weights are noted aside, in kilodaltons.

3.4.3: Characterisation of purified monoclonal antibodies by immunofluorescence

Purified monoclonal antibodies were tested if they could be utilised as biological tools for the investigation of endogenous c-Met by immunofluorescence. SNU-5 cells were selected in this assay because it is a c-Met expressing cell line and gave the clearest staining, compared to HaCaT and U-87MG cells, when tested with AF276 antibody (data not shown). T47D, a low c-Met expressing cell line, was used in this assay as a control. Cells were fixed in methanol/acetone before incubation with 1 μg/ml of monoclonal antibody. FITC-conjugated anti-mouse secondary antibody was used to detect the bound monoclonal antibody. DAPI was used as a counterstain. Table 3.8 is a summary of the results obtained from immunofluorescence assay.

c-Met is a tyrosine receptor kinase expressed on the cell membrane. Immunofluorescence staining of endogenous c-Met would therefore localise to the plasma membrane of cells. We attempted to use phalloidin conjugated-rhodamine as a control for cell membrane staining. However, phalloidin, which stains F-actin, only worked on paraformaldehyde-fixed cells. Under methanol/acetone fixation conditions, phalloidin staining only worked in areas where cell densities were extremely high (data not shown). In these areas, staining of c-Met on the plasma membrane becomes unclear as the cells were overlapping. We therefore could not use phalloidin as a control to counterstain the plasma membrane. The lack of a plasma membrane control to use in both suspension (SNU-5 cells) and adherent (T47D cells) cell lines needs to be addressed in future.

Although the commercial antibody AF276 stained the cytoplasm, predominant staining was observed on the cell membrane (Figure 3.36). Mab 2.1, 8.1, 11.1 and 12.1 were observed to produce identical staining to AF276 antibody, thus it is assumed that these

antibodies are staining for c-Met localised on the cell membrane (Figures 3.36A and B). Weak staining localised to the plasma membrane was observed by Mab 13.1, 14.1, 16.1, 17.1 and 18.1 which suggests that these antibodies are not strong enough to detect c-Met by immunofluorescence (Figures 3.36B to D). Mab 15.1 detectably recognised transfected and endogenous c-Met by Western blotting (Figure 3.35) but failed to stain for endogenous c-Met by immunofluorescence (Figure 3.36C). Mab 4.1 worked well in Western blotting, but showed diffused cytoplasmic staining, suggesting that Mab 4.1 can be used as a biological tool for Western blotting but not in immunofluorescence assays (Figure 3.36A). Weak cytoplasmic staining was also observed in the SNU-5 cell treated controls (AF276 antibody and secondary-only antibody). The diffused cytoplasmic staining observed in our monoclonal antibody-treated samples in SNU-5 cells could be due to the antibody detecting precursor c-Met in the cytoplasm, as suggested by the AF276 antibody. Cytoplasmic staining could also be due to the non-specific effects of the secondary antibody. Background staining was observed in T47D cells stained with Mab 2.1, 12.1 and 17.1 which could be attributed to the antibodies recognising non-specific proteins in the cytoplasm. Antibody concentration was only tested at 1 μg/ml as this was only a preliminary test aimed to investigate if the anti-α-chain monoclonal antibodies function in immunofluorescence assays. As each antibody has an optimum working condition, an optimisation of antibody concentration is required for each monoclonal antibody. Exposure time varied in each sample. Stained cells were exposed until a signal was observed.

Table 3.8: Summary of immunofluorescence results using purified monoclonal antibodies.

Monoclonal antibody	Immunofluorescence staining of SNU-5 cells		Immunofluorescence staining of T47D cells (background staining)
	Membrane staining	Cytoplasmic staining	
2.1	+++	++	++
4.1	-	+	-
8.1	+++	++	-
11.1	+++	+	-
12.1	+++	+	+
13.1	+	+	-
14.1	++	+	-
15.1	-	-	-
16.1	++	++	-
17.1	+	++	+
18.1	++	++	-
Secondary alone	-	+	-

(-): no staining; (+): slight staining; (++): intermediate staining; (+++): intense staining.

Figure 3.36A: Immunofluorescence of endogenous c-Met in SNU-5 and T47D cells.
Detection of endogenous c-Met in SNU-5 and T47D cells by immunofluorescence using purified anti-α-chain monoclonal antibodies. 1 µg/ml of monoclonal antibody was used. Bound monoclonal antibodies were detected by anti-mouse FITC-conjugated secondary antibody. AF276 antibody and secondary-only were used as controls. Cells were counterstained with DAPI.

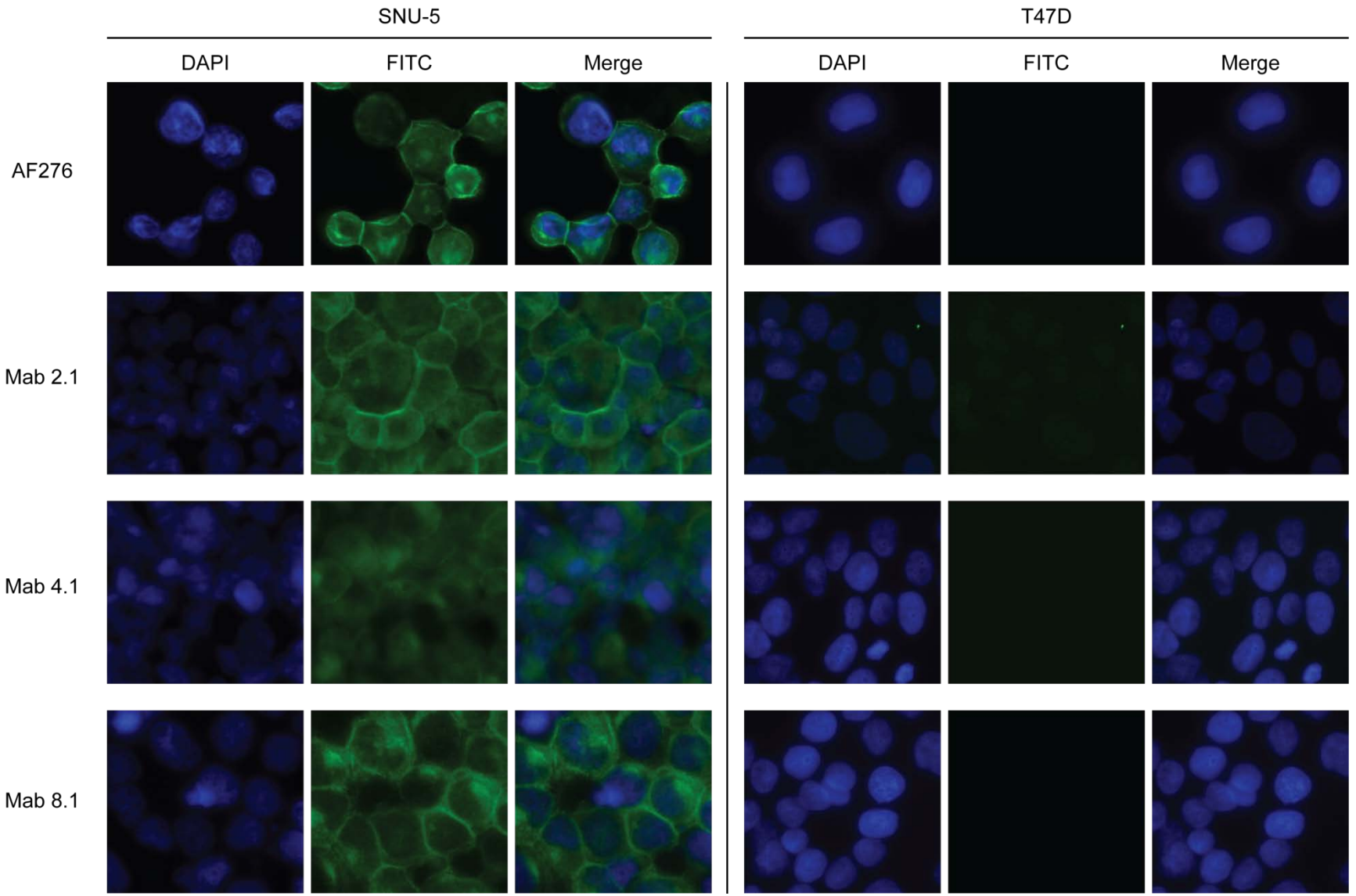
SNU-5
T47D
DAPI
FITC
Merge
DAPI
FITC
Merge
AF276
Mab 2.1
Mab 4.1
Mab 8.1

Figure 3.36B: Immunofluorescence of endogenous c-Met in SNU-5 and T47D cells.
Detection of endogenous c-Met in SNU-5 and T47D cells by immunofluorescence using purified anti-α-chain monoclonal antibodies. 1 µg/ml of monoclonal antibody was used. Bound monoclonal antibodies were detected by anti-mouse FITC-conjugated secondary antibody. AF276 antibody and secondary-only were used as controls. Cells were counterstained with DAPI.

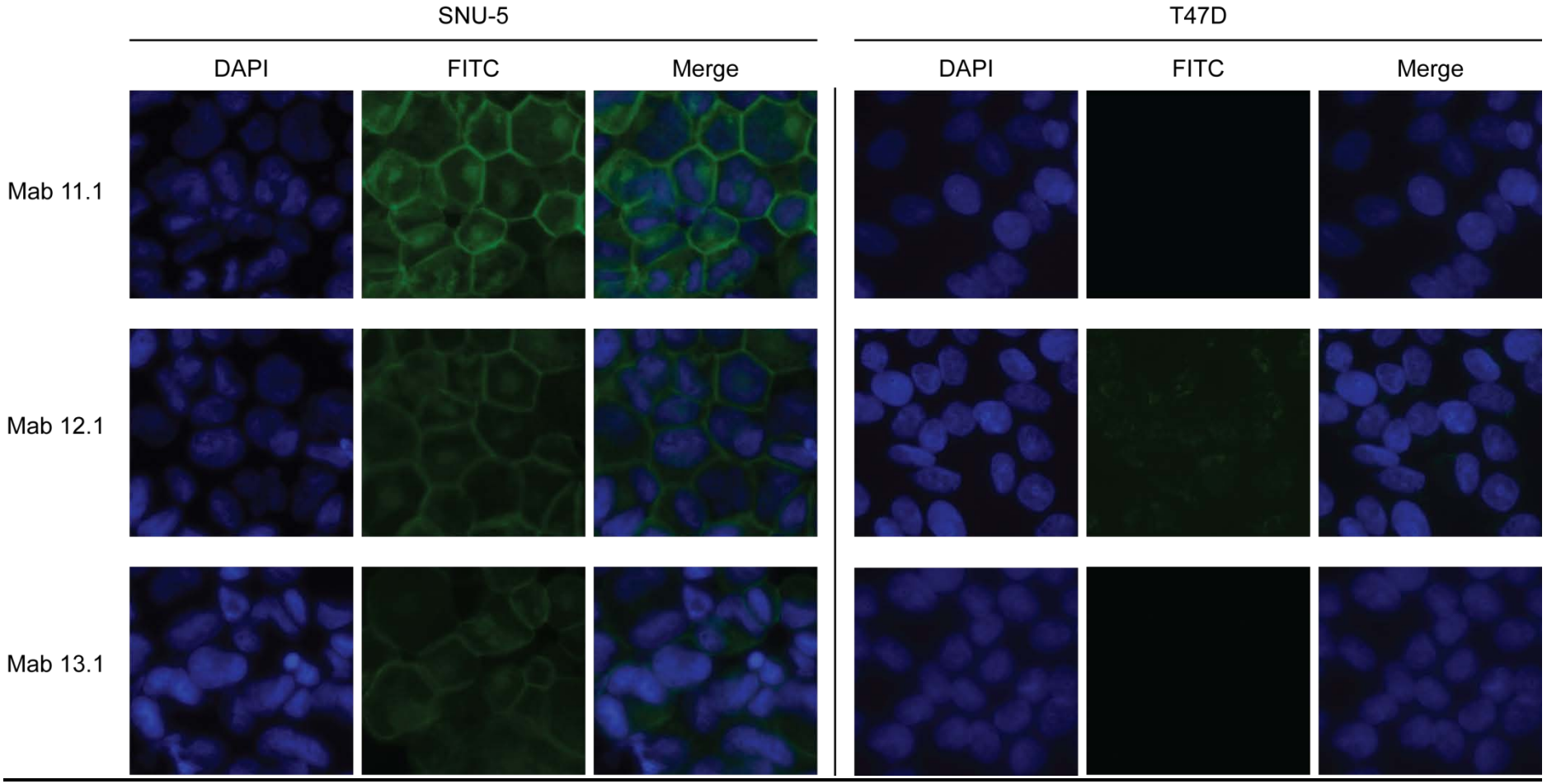
SNU-5
T47D
DAPI
FITC
Merge
DAPI
FITC
Merge
Mab 11.1
Mab 12.1
Mab 13.1

Figure 3.36C: Immunofluorescence of endogenous c-Met in SNU-5 and T47D cells.
Detection of endogenous c-Met in SNU-5 and T47D cells by immunofluorescence using purified anti-α-chain monoclonal antibodies. 1 µg/ml of monoclonal antibody was used. Bound monoclonal antibodies were detected by anti-mouse FITC-conjugated secondary antibody. AF276 antibody and secondary-only were used as controls. Cells were counterstained with DAPI.

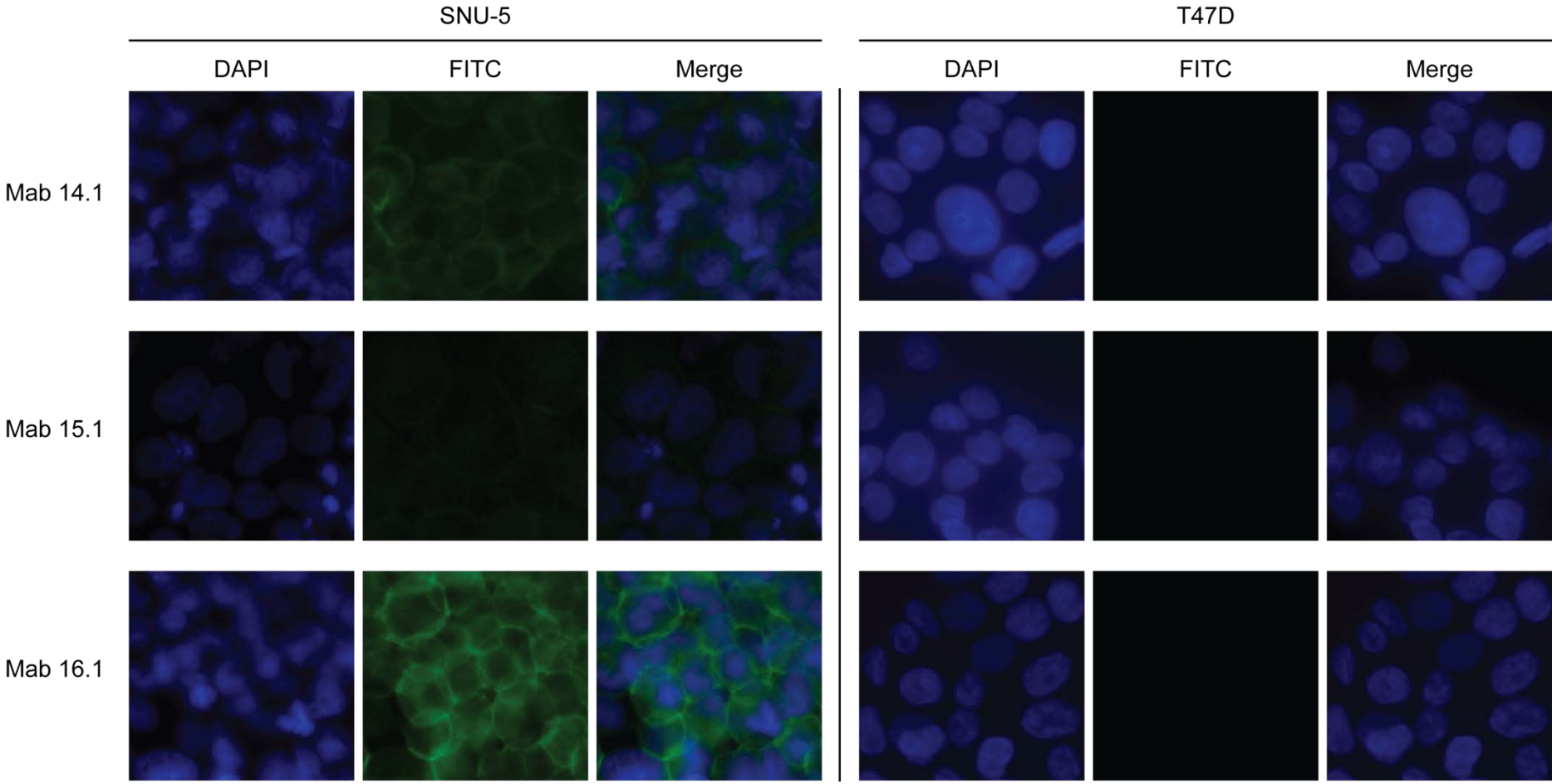
SNU-5
T47D
DAPI
FITC
Merge
DAPI
FITC
Merge
Mab 14.1
Mab 15.1
Mab 16.1

Figure 3.36D: Immunofluorescence of endogenous c-Met in SNU-5 and T47D cells.
Detection of endogenous c-Met in SNU-5 and T47D cells by immunofluorescence using purified anti-α-chain monoclonal antibodies. 1 µg/ml of monoclonal antibody was used. Bound monoclonal antibodies were detected by anti-mouse FITC-conjugated secondary antibody. AF276 antibody and secondary-only were used as controls. Cells were counterstained with DAPI.

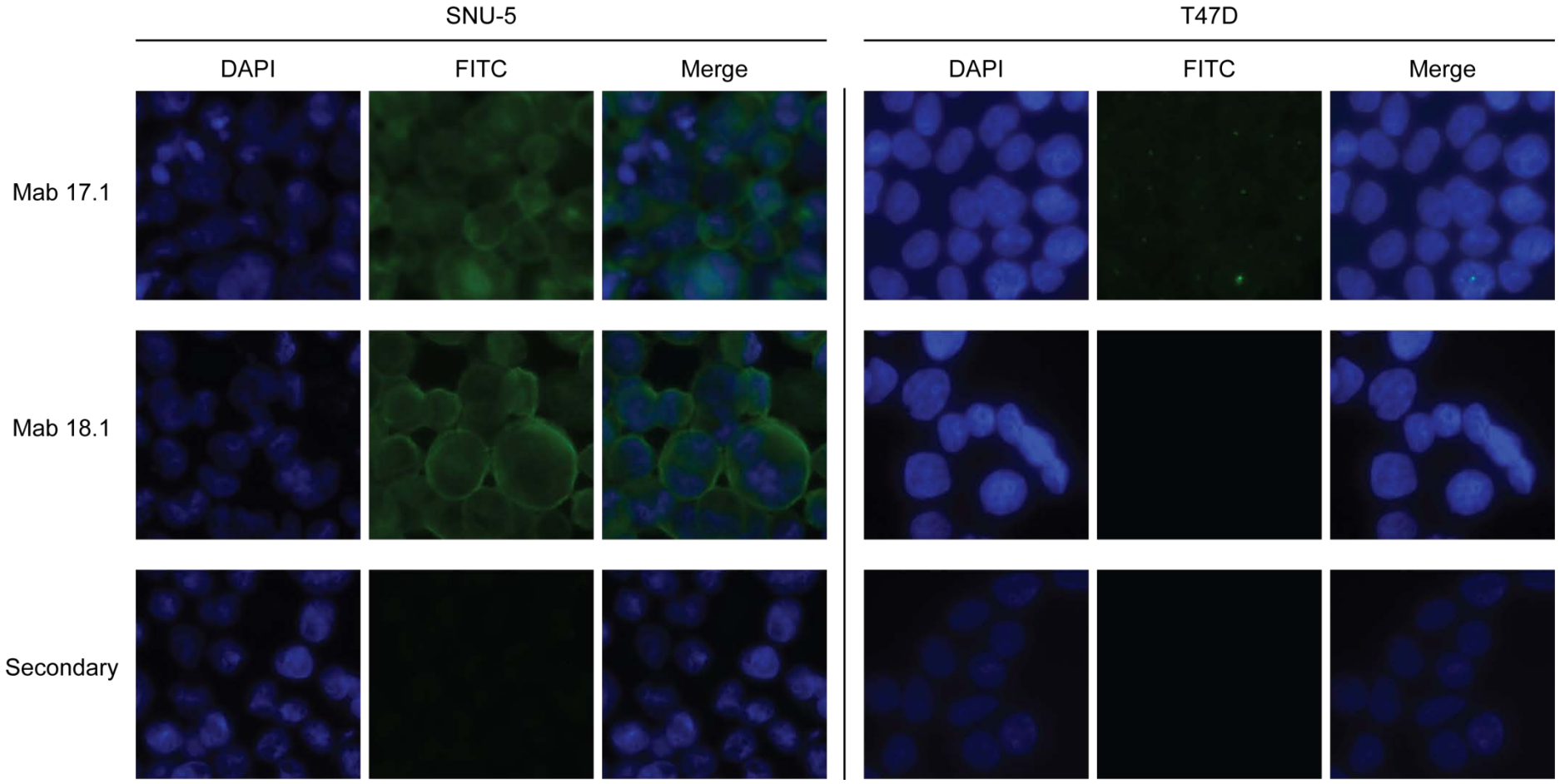
SNU-5
T47D
DAPI
FITC
Merge
DAPI
FITC
Merge
Mab 17.1
Mab 18.1
Secondary

3.4.4: Purified monoclonal antibody effects on ERK phosphorylation

In Section 3.3.2, ERK phosphorylation was used as an indicator to examine the effects of monoclonal hybridoma supernatant on HGF-induced c-Met activation. Due to the presence of FCS in cell supernatant, antibody concentration determination was not possible and it was difficult to differentiate between the effects of the antibodies and those of FCS. To avoid this issue, the effects of purified monoclonal antibody on c-Met activation were tested on HaCaT cells in serum-free media. HaCaT cells were serum-starved for 24 hrs before treatment with 1 μg/ml of monoclonal antibodies in serum-free media. The cells were incubated 1 hr with monoclonal antibodies before HGF was added to the cells. Cells were harvested in sample loading buffer and cell lysates were analysed by Western blotting (Figure 3.37). Commercially-obtained IgG, anti-HGF antibody and a small molecule inhibitor of c-Met (SU11274) were controls. Similarly to the ERK analysis in Section 3.3.2, phosphorylation of ERK was used as an indicator of c-Met activation status.

As previously, phosphorylation of ERK would indicate activation of c-Met by HGF or by the monoclonal antibodies. Untreated cells after serum starvation were observed to have undetectable phosphorylation of ERK even though total ERK levels were detectable. Increased ERK phosphorylation, particularly in ERK2 (lower band), was observed in serum-starved cells treated with 10 ng/ml of HGF alone, indicating the activation of c-Met. Total ERK levels were also observed to increase in these cells, suggesting that c-Met activation by HGF increases or stabilises ERK protein levels. The mechanism in which how c-Met activation affects ERK protein levels is unknown. To ensure that the antibodies do not have non-specific effects on ERK phosphorylation, cells were treated with mouse IgG. In the absence of HGF, these mouse IgG-treated cells were observed to have no ERK phosphorylation and total ERK levels were similar

to untreated cells. In the presence of HGF, these cells showed significant increase in ERK phosphorylation and protein levels. The c-Met small molecule inhibitor, SU11274, and the commercially-obtained anti-HGF antibody were used as controls to inhibit c-Met activation by HGF. While SU11274 prevents c-Met downstream signalling by binding to the catalytic domain of c-Met (Bellon *et al.*, 2008), anti-HGF antibody sequesters HGF present in the cell media and prevents HGF from binding to c-Met. As shown in Figure 3.37, SU11274 completely inhibited ERK phosphorylation while a slight phosphorylation of ERK2 was still observed in cells treated with the combination of anti-HGF antibody and HGF. SU11274 is a better c-Met inhibitor compared to anti-HGF antibody. Interestingly, regardless of the presence of HGF, total ERK levels in anti-HGF treated samples were identical to untreated cells while a decrease was observed in SU11274-treated samples. The SU11274 inhibitor showed constant levels of total ERK protein in both HGF induced and un-induced samples.

Purified monoclonal antibody treatment of HaCaT cells were compared to the mouse IgG control and results were tabulated in Table 3.9. As in the previous ERK assay (Section 3.3.2), our monoclonal antibodies fell into groups according to the levels of total ERK and phosphorylated ERK compared to mouse IgG. After induction with HGF, treatment with Mab 13.1, 14.1, 15.1 and 16.1 (Table 3.9, highlighted in green) resulted in a decrease in ERK phosphorylation while total ERK levels remained constant. This suggests that these antibodies are inhibiting ERK phosphorylation without affecting the total levels of ERK, thus are antagonist towards HGF-induced ERK phosphorylation. Mab 2.1 and 4.1 were observed to show an increase in ERK levels and ERK phosphorylation levels, in the absence of HGF. This suggests that Mab 2.1 and 4.1 could be inducing c-Met activation by dimerising c-Met molecules on the cell surface. Mab 12.1 and 17.1 did not affect the status of ERK and phosphorylated

ERK in the absence of HGF but they were able to decrease ERK and phosphorylated ERK levels in the presence of HGF. Mab 12.1 and 17.1 may affect ERK phosphorylation levels by decreasing ERK levels via an unknown pathway. Treatment with Mab 18.1 without HGF induction had no effect on ERK and phosphorylated ERK levels indicating that Mab 18.1 is not an activator of c-Met. No change was observed in the levels of ERK and phosphorylated ERK in samples treated with Mab 18.1 and HGF. Mab 18.1 might be blocking c-Met activation by HGF thus resulting in the constant levels of ERK protein and ERK phosphorylation levels. Finally, Mab 8.1 and 11.1 do not fall into any group and the results were unexpected. In the presence of HGF, total ERK levels and phosphorylation levels remained constant in Mab 8.1 treated cells. Mab 8.1 caused an unexplainable decrease in total ERK levels but an increase in phosphorylation levels in the absence of HGF. Similarly, Mab 11.1 caused an increase in ERK phosphorylation in the absence of HGF while total ERK and ERK phosphorylation levels remain constant in other treatment.

Table 3.9: Effects of purified monoclonal antibody on total ERK and phosphorylated ERK levels.

Mab	Total ERK		Phosphorylated ERK	
	No HGF	HGF	No HGF	HGF
2.1	↑	S	↑	↑
4.1	↑	S	↑	↑
8.1	↓	S	↑	S
11.1	S	S	↑	S
12.1	S	↓	S	↓
13.1	S	S	S	↓
14.1	S	S	S	↓
15.1	S	S	S	↓
16.1	S	S	S	↓
17.1	S	↓	S	↓
18.1	S	S	S	S

HaCaT cells were treated with 1 µg/ml of purified monoclonal antibody, in the presence or absence of HGF. Levels of ERK and phosphorylated ERK from these cells were compared to control cells treated with mouse IgG and tabulated. Antibodies that share the same results are highlighted. (↑): increased levels compared to control; (↓): decreased levels compared to control; (S): levels remain the same as control.

The effects of our purified anti-α-chain monoclonal antibodies were also tested at concentrations of 0.1 μg/ml, 0.5 μg/ml, 5 μg/ml, 10 μg/ml and 50 μg/ml (results not shown). Due to time constraints, these results were not reproduced and thus not discussed here. However, an in depth analysis of the antibodies effects on ERK activation has to be pursued in future. As ERK is involved in many signalling pathways, a slight change in growth condition might affect the outcome of this assay. Therefore, it would be ideal to determine c-Met activation by directly observing c-Met phosphorylation status. To do this, an antibody with better affinity toward phosphorylated c-Met than the commercial antibody is required. Moravian Biotechnology is presently developing this antibody.

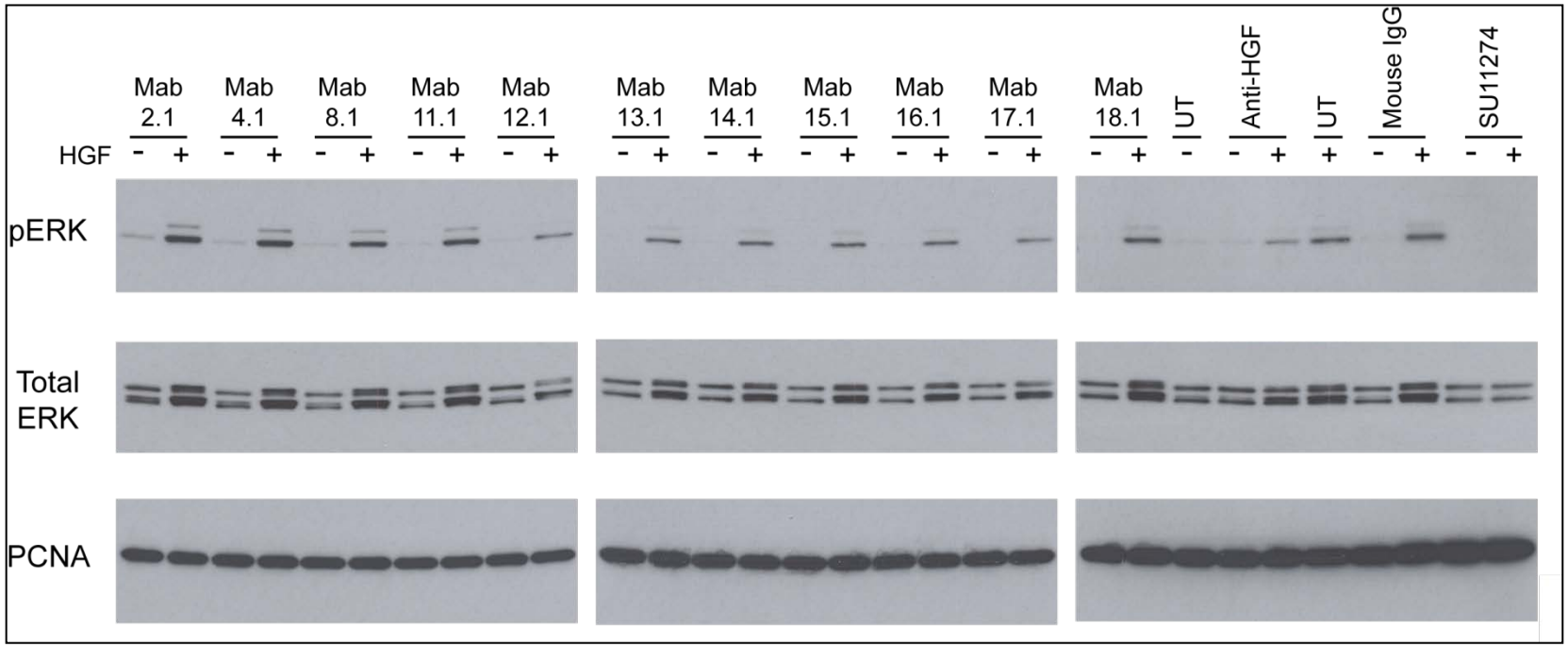

Figure 3.37: Western blot analysis of HaCaT cells treated with purified monoclonal antibodies.
HaCaT cells were serum-starved for 24 hrs. 1 µg/ml of purified monoclonal antibodies were added to cells and incubated for 1 hr before 10 ng/ml of HGF were added to the cells. Cells were incubated in the presence of HGF for 30 mins before the cells were directly lysed in sample buffer. 5 µg of cell lysate were analysed in each sample. Detection of phosphorylated ERK (pERK) was used to determine the effects of monoclonal antibodies on c-Met activation. The molecular weights of ERK1 (top band) and ERK2 (bottom band) are 44 kD and 42 kD respectively. Total ERK and PCNA were used as controls. Anti-HGF antibody (anti-HGF), commercial mouse immunoglobulin G (IgG) and the small molecule c-Met inhibitor SU11274 were used as controls at a final concentration of 5 µg/ml, 1 µg/ml and 5 µM. UT: Untreated.

3.4.5: Effects of purified monoclonal antibodies on cell scatter

Monoclonal antibodies produced in tissue culture were tested for their ability to block/induce cell scatter in Section 3.3.3. As discussed above, the presence of FCS and undetermined antibody concentration made these results difficult to interpret. Here, we examine the effects of purified monoclonal antibodies on cell scatter. HaCaT cells were seeded at low density and allowed to grow until colonies formed. Cells were serum-starved for 24 hrs before incubating with 1 μg/ml monoclonal antibodies. HGF was added, at a final concentration of 10 ng/ml, to the cells and cells were incubated for a further 24 hrs before fixing and crystal violet staining.

Cell scattering is one of the biological hallmarks of c-Met activation. Inhibition of HGF-induced c-Met activation by our purified monoclonal antibodies would result in the inhibition of cell scatter. Agonist monoclonal antibodies would activate c-Met and cause cells to become motile and disperse. As expected, cell scatter of HaCaT cells was induced by HGF (Figure 3.38). Presence of non-specific IgG (mouse IgG) did not affect scattering. Anti-HGF antibody and SU11274 were used as controls to inhibit HGF-induced cell scatter. Similarly to the results from the analysis of ERK phosphorylation, SU11274 was a better antagonist as compared to anti-HGF antibody. In the presence of HGF, SU11274-treated cell colonies remained circular while a slight scattering was observed in anti-HGF antibody-treated cell colonies. The differences observed between anti-HGF antibody and SU11274 may be due to their mechanism of action. SU11274 is c-Met kinase inhibitor that binds tightly and specifically to c-Met catalytic domain. It was identified as a competitive inhibitor of ATP. SU11274 competes with ATP for the c-Met catalytic domain, prevents c-Met from phosphorylating cytoplasmic proteins, thus blocking the downstream signalling cascade. Anti-HGF antibody, on the other hand, competes with c-Met from binding to HGF and prevents c-Met activation. The

binding of an antibody to its antigen is a dynamic process whereby the antibody, antigen and antibody-antigen complex is in equilibrium i.e. constantly associating and dissociating together. It is thus possible that when HGF is released from this interaction, it is free to bind and activate c-Met. This result in the slight scattering observed in cells treated with anti-HGF antibody and HGF combination.

Cell colonies treated with Mab 2.1 and 16.1 seems to scatter in the absence of HGF. However, increased magnification on these cell colonies indicate that the cells remain in tight clusters and this effect is due to variation in staining intensity. No cell scatter was thus observed in cells treated with monoclonal antibodies alone (Figure 3.39). This suggests that the monoclonal antibodies are not agonist towards c-Met activated cell scatter.

All monoclonal antibodies failed to completely inhibit HGF-induced cell scattering. To our surprise, Mab 12.1 which was observed to inhibit ERK phosphorylation in HGF-induced cells (Figure 3.37), failed to inhibit cell scattering. Binding of Mab 12.1 to c-Met might force c-Met into a structural conformation that resulted in inhibition of ERK phosphorylation only. For Mab 4.1, 8.1, 14.1, 15.1 and 17.1, it is clear that these antibodies do not inhibit HGF-induced cell scatter. Cell colonies treated with Mab 2.1, 11.1, 13.1, 16.1 and 18.1 were observed to scatter less as compared to the HGF-induced control. This suggests that these antibodies may be partially inhibiting c-Met and it would interestingly to test if a combination of these antibodies would be able to completely inhibit cell scatter. Cao *et al.* (2001) described the production of monoclonal antibodies against HGF and tested their ability to block HGF from binding to c-Met. None of the antibodies alone were capable of blocking c-Met activity. However, c-Met activity was blocked by combining three different monoclonal antibodies against HGF. van der Horst *et al.* (2009) reported that the ability of a combination of two anti-Met

Fab molecules to disrupt HGF-cMet binding was more potent than treatment with a single Fab on its own.

It should be noted that cell scatter was performed in media containing 1% FCS. It is ideal that no FCS should be used as FCS might contain motility stimulating or inhibitory factors. However in this assay, HGF-induced scattering failed in the absence of FCS (data not shown). Failure to induce cell motility in the absence of HGF was not seen during the initial optimisation process of cell scattering. Variations in batches of HGF might be the cause of this problem and further work is required to verify this issue. Cell scattering was also tested on antibody concentrations of 0.5 μg/ml, 5 μg/ml and 10 μg/ml. The results for cell scatter at these concentrations were extremely unclear due to the varied effects of HGF. Cell scattering tested at these antibody concentrations needs to be repeated.

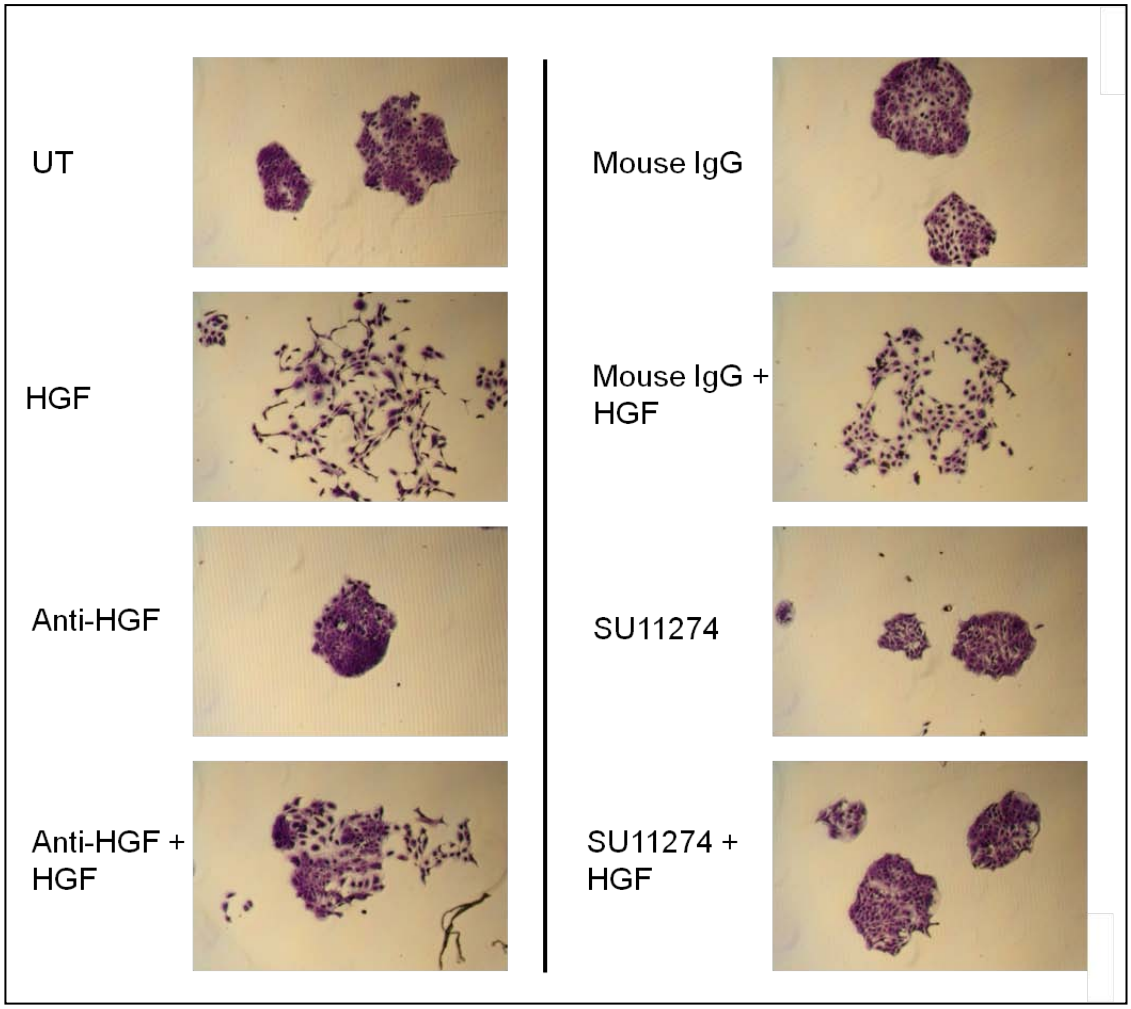

Figure 3.38: Analysis of effects of antibodies and a c-Met inhibitor on cell scatter in HaCaT cells. HaCaT cells were serum-starved for 24 hrs before treatment. Monoclonal antibodies (1 μg/ml), HGF (10 ng/ml), anti-HGF antibody (5 μg/ml) and SU11274 (5 μM) were added to the cells and incubated for 24 hrs before fixation. Cells were then stained with crystal violet for visualisation. Anti-HGF antibody (anti-HGF), commercially-obtained mouse immunoglobulin G (IgG), and c-Met small molecule inhibitor SU11274 were used as controls. UT: Untreated.

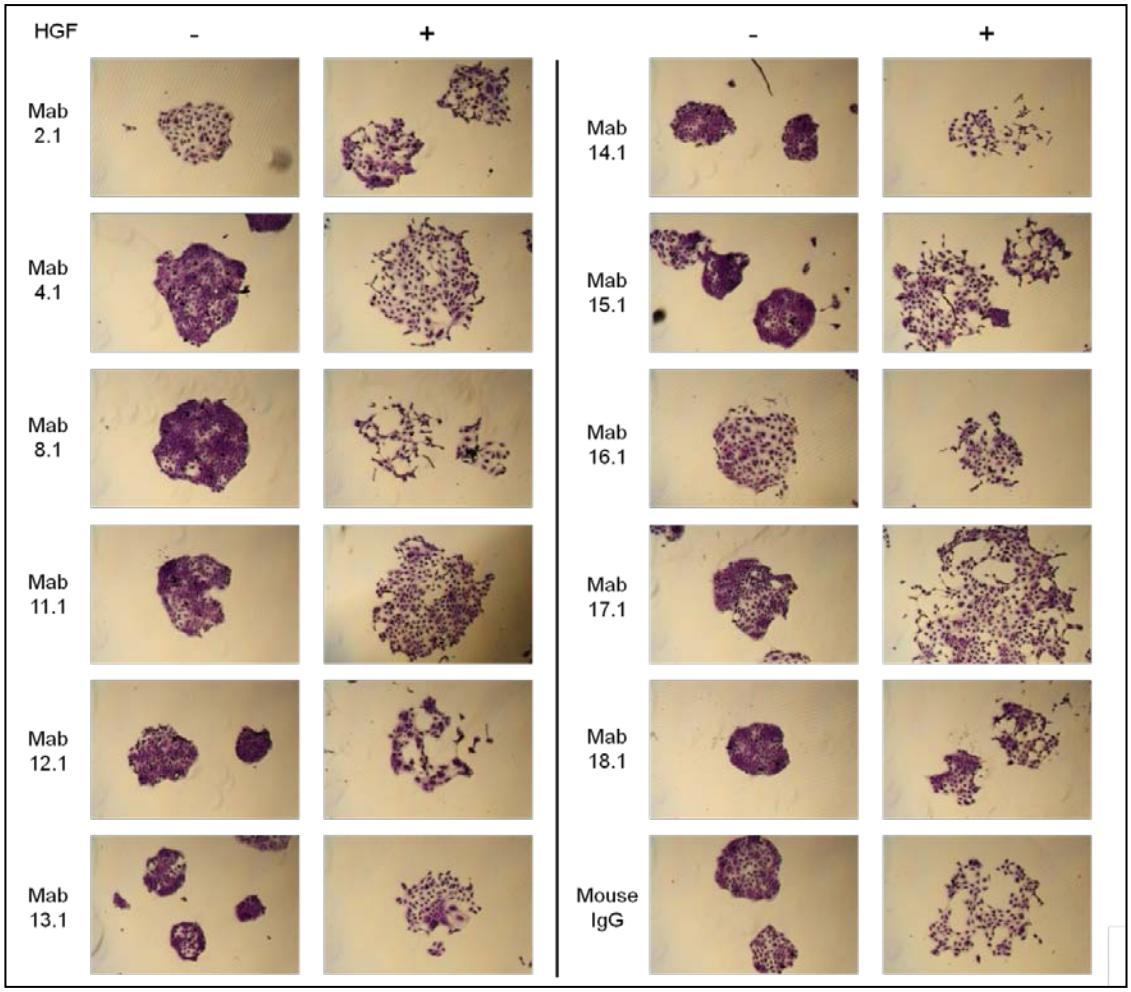

Figure 3.39: Effects of purified monoclonal antibodies on cell scatter.
HaCaT cells were serum-starved for 24 hrs before treatment. Monoclonal antibodies (1 μg/ml) and HGF (10 ng/ml) were added to the cells and incubated for 24 hrs before fixation. Cells were then stained with crystal violet for visualisation. Commercially-obtained mouse immunoglobulin G (IgG) was used as a control. UT: Untreated.

3.4.6: Purified monoclonal antibodies in flow cytometry

Failure to inhibit ERK phosphorylation and cell scattering could be due to the inability of monoclonal antibodies to recognise c-Met in its native conformation. We therefore decided to use flow cytometry to determine whether the antibodies described here could bind to c-Met in its native form using live cells. The cells chosen for this analysis were SNU-5 cells because they express high levels of c-Met (Section 3.1.4) and grow in suspension, making them ideal for flow cytometry analysis. Binding of anti-α-chain antibodies to native c-Met expressed on the cell surface of SNU-5 cells was detected using anti-mouse secondary antibody conjugated with Alexa Fluor® 488 dye. T47D, which expresses very low levels of c-Met, was used as a control to determine if the antibodies bind non-specifically to the cell surface.

The flow cytometry results of purified monoclonal antibody treated-T47D cells were indistinguishable from the negative control (secondary antibody only), indicating that monoclonal antibodies do not bind non-specifically to the cell surface (Figure 3.40). Flow cytometry results obtained with SNU-5 cells showed that the antibodies fell into three distinct groups with different fluorescence intensity towards native c-Met: strong fluorescence intensity, intermediate fluorescence intensity and weak fluorescence intensity (Figure 3.41). Mab 2.1 and 13.1 showed the strongest fluorescence intensity in this assay. Surprisingly, they both showed poor binding for c-Met by Western blotting (Figure 3.35). Mapping of the Mab 13.1 binding region (Section 3.2.7) suggests that Mab 13.1 may recognise small denatured regions in a peptide screen *in vitro*, but its epitope could be influenced by secondary structures making it able to recognise native c-Met. Mab 8.1, 11.1, 12.1 and 17.1 showed intermediate fluorescence intensity while Mab 4.1, 14.1, 15.1, 16.1 and 18.1 showed weak fluorescence intensity (as demonstrated by the small peak shift in Figure 3.41). Weak fluorescence intensity to

native c-Met might explain why some of the antibodies were unsuccessful in inhibiting HGF-induced ERK phosphorylation and/or cell scattering. However, analysis of the characterisation of the purified monoclonal antibodies listed in Table 3.10 indicates that there is no obvious correlation between the results obtained from the ERK phosphorylation assay, cell scatter assay and flow cytometry assay. Despite the use of T47D as a negative cell line to demonstrate the monoclonal non-specificity, it would be more appropriate to use the same cell line in both the negative and positive controls. It is thus possible to knock down the expression of c-Met in SNU-5 cells using siRNA to determine the non-specificities of the antibodies. Alternatively, we can use transiently express c-Met in T47D cells using other expression system (i.e. Lentiviral expression). Finally, the difference in antibody subclasses will affect the binding of the anti-mouse secondary antibody, thus affecting the fluorescence intensity in this assay. Other methods such as labelling of the antibodies with FITC (or other fluorescence molecules) will circumvent this issue. These are only preliminary findings and optimisation of antibody concentration is required to fully understand an antibody's functional activity.

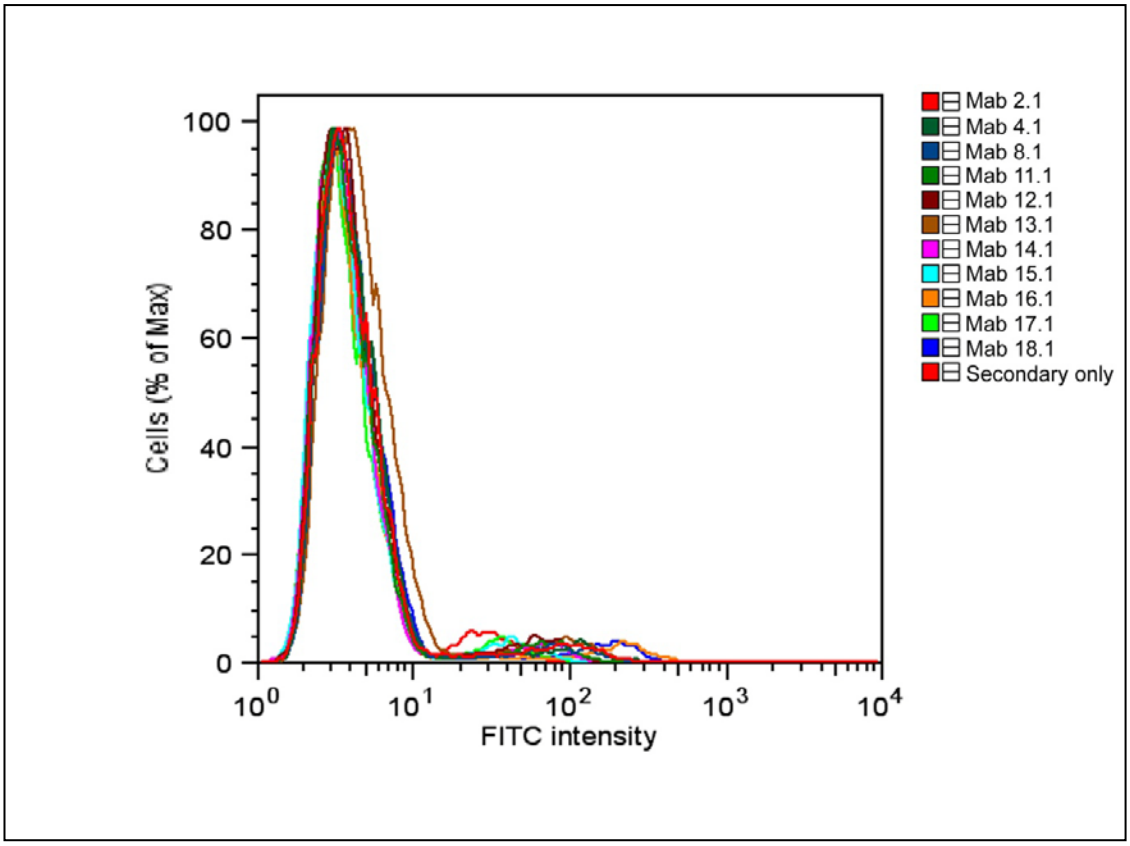

Figure 3.40: Flow cytometry analysis of T47D cells treated with monoclonal antibodies.
Purified monoclonal antibodies (1 µg/ml) were incubated with live T47D cells. Bound antibodies were detected using FITC-conjugated secondary antibodies before the cells were passed through a flow cytometer. A shift in FITC intensity would indicate monoclonal antibodies binding to T47D cells. Data analysis was assisted by Daniel Klotz.

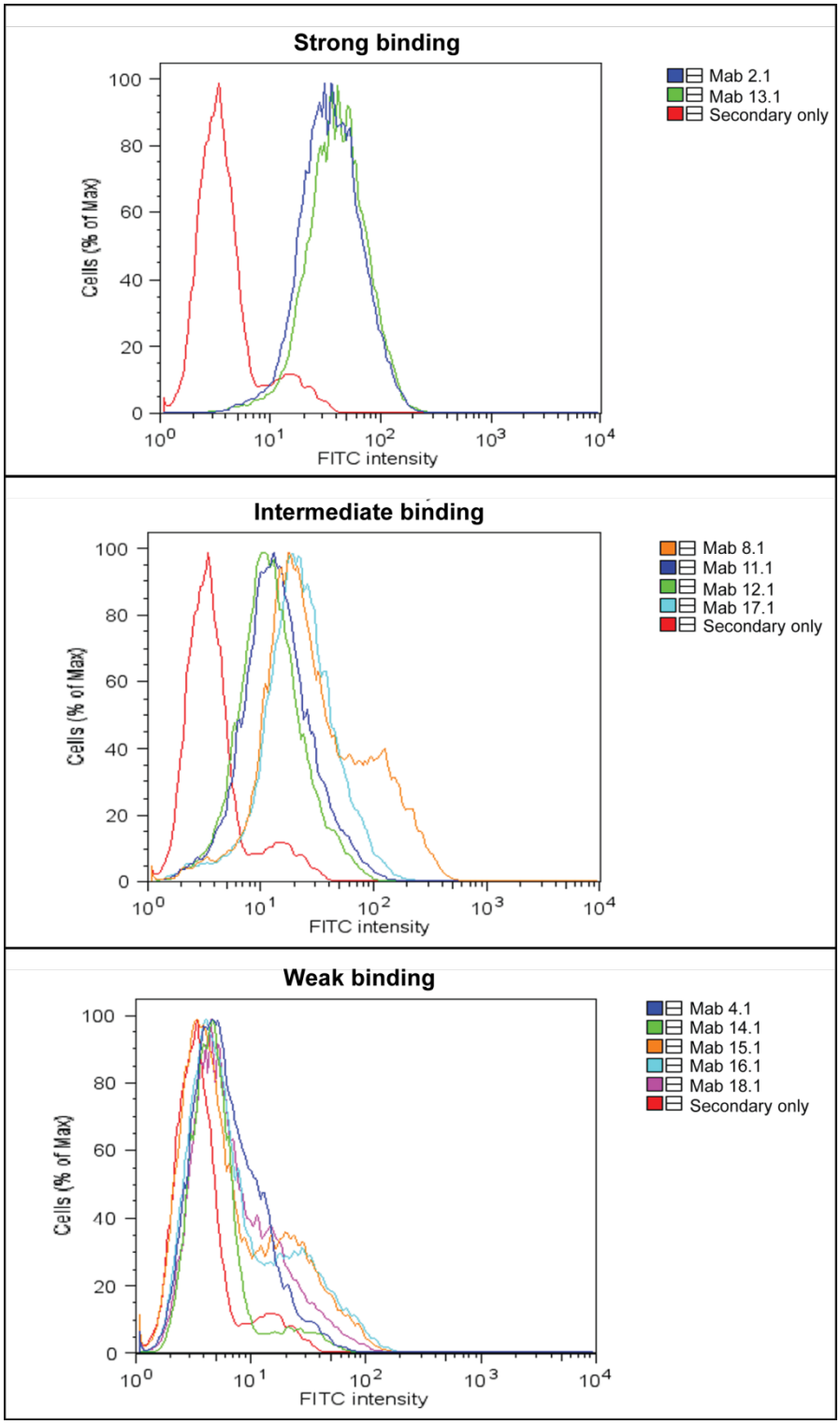

Figure 3.41: Flow cytometry analysis of SNU-5 cells treated with monoclonal antibodies.
Purified monoclonal antibodies (1 µg/ml) were incubated with live SNU-5 cells. Bound antibodies were detected using FITC-conjugated secondary antibodies before the cells were passed through a flow cytometer. A shift in FITC intensity indicates monoclonal antibodies binding to SNU-5 cells. Data analysis was assisted by Daniel Klotz.

Table 3.10: Summary of monoclonal antibody characterisation.

Monoclonal antibody	Western blotting[a]		Total ERK/Phosphorylated ERK[b]	Inhibition of cell scatter[c]	Flow cytometry[d]	Immunofluorescence staining[e]	Cell cluster[f]
	Affinity	Specificity					
2.1	++	+	S/↑	Partial	Strong	+++	+++
4.1	+++	++	S/↑	ND	Weak	-	-
8.1	+++	++	S/S	ND	Intermediate	+++	+++
11.1	++	+++	S/S	Partial	Intermediate	+++	+++
12.1	+++	+++	↓/↓	ND	Intermediate	+++	+++
13.1	-/+	+	S/↓	Partial	Strong	+	+++
14.1	++	+	S/↓	ND	Weak	++	++
15.1	+	+	S/↓	ND	Weak	-	-
16.1	++	++	S/↓	Partial	Weak	++	-
17.1	+++	++	↓/↓	ND	Intermediate	+	++
18.1	+++	++	S/S	Partial	Weak	++	+

*Table legends are noted on next page.

Table 3.10 summarises the results obtained using purified monoclonal antibodies in Western blotting, effect on ERK phosphorylation, ability to inhibit cell scatter, flow cytometry, immunofluorescence staining. Results of cell cluster using monoclonal antibody from cell supernatants have been included.

a) Affinity and specificity of monoclonal antibodies against c-Met in Western blots. Results were based on Figure 3.35. Highlighted in red are antibodies that work well in Western blotting. (-): no binding; (+): Low affinity/specificity; (++): intermediate affinity/specificity; (+++): strong affinity/specificity.

b) Effects of antibody treatment on ERK protein and phosphorylation levels following treatment with HGF. Results were obtained from Table 3.9, where the levels of total ERK and phosphorylated ERK, in the presence of HGF, were compared to mouse Ig-treated control cells. For further details, refer to Table 3.9 and Figure 3.37. (↑): increased levels compared to control; (↓): decreased levels compared to control; (S): levels remain the same as control.

c) Ability of monoclonal antibody to block HGF-induced c-Met cell scatter (Figure 3.39). (Partial): monoclonal antibody caused partial blockage of cell scatter; (ND): not determined as the effects of cell scatter was not clear.

d) Ability of monoclonal antibodies to bind to native c-Met was tested by flow cytometry. Refer to Figure 3.41. ‘Strong’, ‘intermediate’ and ‘weak’ was used to categorise the antibodies binding ability to native c-Met on cell surface.

e) Ability of monoclonal antibodies to stain the cell membrane of SNU-5 cells in immunofluorescence (IF). (-): no membrane staining; (+): weak membrane staining; (++): intermediate membrane staining; (+++): strong membrane staining.

f) Ability of monoclonal antibodies (from hybridoma cell supernatant) to cause cell cluster. Refer to Figures 3.33A to C. (-): no response; (+): weak response; (++): intermediate response; (+++): strong response.

CHAPTER 4: DISCUSSION AND FUTURE WORK

c-Met is a tyrosine kinase receptor involved in a wide spectrum of cellular activities such as cell proliferation, tubulogenesis, cell motility, angiogenesis and morphogenesis. The only known ligand for c-Met is the soluble cytokine, HGF. While c-Met is expressed in epithelial cells, HGF is differentially expressed in cells of mesenchymal origin. Together, signalling between c-Met and HGF form a cell-to-cell communication between epithelial cells and their neighbouring stromal cells. Activation of c-Met by HGF results in the activation of several signal transduction pathways, eventually leading to the various biological activities. The role of the c-Met/HGF axis in cancer development has been well documented: 1) expression of c-Met/HGF correlates with tumour grade, aggression and disease prognosis (Birchmeier *et al.*, 2003), 2) mutation in the kinase domain of c-Met was found in patients with sporadic and hereditary papillary renal tumours (Jeffers *et al.*, 1997), 3) gastric cell lines harbouring c-Met gene amplification demonstrated sensitivity to the c-Met small molecule inhibitor PHA-665752 (Smolen *et al.*, 2006), and 4) in xenograft models, tumours with abnormal c-Met active expression show inhibition of tumour growth and invasion upon treatment with anti-Met molecules such as the OA-5D5 antibody (Martens *et al.*, 2006), the c-Met small molecule inhibitor SU11274 (Sattler *et al.*, 2003) and the c-Met competitor decoy-Met (Michieli *et al.*, 2004).

c-Met is essential for embryonic and placental development. In adult tissues, c-Met is only required for wound healing and liver regeneration (Knudsen and Vande Woude, 2008). The dispensable nature of c-Met in adult tissues and the involvement of c-Met/HGF in tumourigenesis and tumour cell-acquired resistance towards EGFR drugs makes c-Met/HGF an attractive target for drug therapy. Many groups have used various mechanisms to inhibit c-Met activation. Small molecule kinase inhibitors such as the

PHA-665752, AM7 and SU11274 were extremely successful in inhibiting c-Met activation (Bellon *et al.*, 2008; Sattler *et al.*, 2003). However, toxicity issues due to off-target effects of the small molecule inhibitors are of major concern. In addition, SU11274 was reported to be ineffective against specific c-Met mutations (Berthou *et al.*, 2004). Abounader *et al.* (2001) reported the use of U1snRNA/ribozyme to downregulate the expression levels of c-Met/HGF. Although this method is novel and intriguing, at present it is not feasible to use this method for cancer treatment due to drug delivery issues. U1snRNA/ribozyme has to be efficiently delivered into every tumour cell to be expressed in order to be effective. The process of delivery will be a challenging problem. The use of HGF and c-Met fragments, such as NK4 and decoy-Met respectively, to compete for Met-HGF interactions has been examined. These competitive inhibitors show efficient inhibition of c-Met activation *in vivo* xenograft models, however, their clinical utility has yet to be determined (Brockmann *et al.*, 2003; Michieli *et al.*, 2004). Successful anti-cancer drugs in the field are largely represented by small molecule inhibitors and therapeutic antibodies (Ma and Adjei, 2009).

The success of using therapeutic monoclonal antibodies for cancer treatment is evident. Herceptin (Trastuzamab), a humanised IgG1 antibody targeted against the human epidermal growth factor receptor (Her2), is widely used for the treatment of breast cancer. Rituxan (Rituximab) targeting CD20 and Avastin (Bevaciumab) targeting vascular endothelial growth factor receptor (VEGFR), both chimeric IgG1 antibodies, have been successful in treatment of lymphomas and of colorectal and lung cancer respectively (Adams and Weiner, 2005). Therapeutic antibodies success in disease treatment can be attributed to their high affinity and specificity towards their target antigen. Antibody stability *in vivo* and their ability to recruit the host immune system to destroy tumour cells make this form of therapy clinically advantageous over other types

of c-Met/HGF inhibitors (De Souza *et al.*, 2009). In addition, advances in antibody engineering can improve the pharmacokinetiecs of a therapeutic antibody molecule.

The aims of this project is to develop monoclonal antibodies against c-Met and to use the antibodies as therapeutic molecules in cancer treatment/diagnostics. The first phase of this project was to develop and build bio-tools required for the screening and development of anti-Met antibodies. The commercial antibodies used in the thesis fall into two classes, those raised against synthetic peptides and those raised against recombinant protein fragments (AF276 was raised against the extracellular domain of c-Met which recognises endogenous c-Met precursor and c-Met β-chain while SC-10 was raised against a synthetic peptide in the C-terminal tail of c-Met). AF276 was shown to be the most reliable antibody to use as an antibody control as compared to other commercial anti-Met antibodies (SC-10 and EP1454Y) tested. We have shown that AF276 antibody detected purified α-chain weakly, but not endogenous α-chain. Both AF276 and SC-10 are polyclonal antibodies. While the epitope recognised by the SC-10 antibody is essentially defined by the immunogen (anti-peptide antibody) this is not the case for the AF276 antibody. It would have been possible to map the epitopes recognised by these antibodies using the pepscan library but this would not have provided information of much value. The antibodies will recognise both complex, conformational, and linear epitopes and the mapping data would therefore be incomplete. The results might have indentified dominant epitopes but this would not have affected our analysis. We used a new immunogen different from those used by the commercial suppliers and we used a complete scan of the protein fragment we immunised with successfully mapping all of the epitopes recognised by our large set of antibodies. How knowing what epitopes a commercial antibody recognises would help in this analysis is not clear. The key issue that comparison with the commercial

antibodies has revealed is the superior performance of our new reagents in both immunoblotting and immunoprecipitation analysis.

In order to characterise the monoclonal antibodies, expressing and non-expressing c-Met cell lines were required. The expression and phosphorylation status of endogenous c-Met was thus examined in a range of cell lines and SNU-5, U-87MG, HaCaT and T47D cells were chosen for further study. We have also exploited the adenoviral system and used various high-expression mammalian vectors in attempt to increase human c-Met transient expression in cell lines. By using the same c-Met expression vectors, it is also possible to *in-vitro* translating c-Met as a positive control for antibody characterisation. We developed the use of the novel SBP tag to purify c-Met from cell lines to a high purity, which could be used for future c-Met high-throughput processes. To develop antibodies against c-Met, the α-chain of c-Met was expressed in bacteria, purified and used as an immunogen for mouse immunisation. The α-chain of c-Met was expressed as inclusion bodies in bacteria and re-folding in 6M urea was required. Prokaryotic expression system allows for low cost, simple and high yield protein expression but lacks in eukaryotic post-translational medication and proper protein folding of eukaryotic proteins (e.g. proper formation of disulphide bonds). Other types of expression systems such as mammalian cells or insect cells could be utilise to produce soluble c-Met in the correct conformation for antibody immunisation. The mammalian cells and insect cell expression system have proper eukaryotic post-translational modification and are able to express protein in the right conformation but compromising on the yield of the expressed protein.

The second phase of this project was the production and screening of mouse monoclonal antibodies against the α-chain of c-Met. In total, 39 hybridoma cell lines were identified which stably express anti-α-chain antibodies. It is unusual to obtain such

large numbers of positive cell lines in antibody hybridoma fusion. The α-chain of c-Met must be highly immunogenic and the hybridoma cell fusion must have been extremely successful. 21 hybridoma cells lines were selected for single cell cloning and monoclonal antibody production. Monoclonal antibodies were characterised by identifying their epitope binding region as well as their isotype subclasses (Table 3.4). All 21 monoclonal antibodies were IgG antibodies, with a majority of them being IgG1. As a preliminary screen, the functional effects of the antibodies were characterised by analysing their effects on ERK phosphorylation and cell scatter. As the antibodies were produced as tissue culture supernatants, the presence of FCS interfered with these analyses. The antibodies were also analysed for their ability to cause cell clustering. Finally, eleven monoclonal antibodies were selected for ascites production and antibody purification. These antibodies were characterised in their pure form again by Western blotting, immunofluorescence staining, functional assays (ERK phosphorylation and cell scatter) and for their ability to recognise native c-Met by flow cytometry (Table 3.10).

Our antibodies are the first anti-α-chain c-Met antibodies developed. We have shown that our purified monoclonal antibodies are able to detect endogenous human c-Met by Western blotting and immunofluorescence staining. This is extremely beneficial to the research field of c-Met because we have shown that our antibodies have higher affinity and specificity compared to the currently available commercial antibodies in both Western blotting and immunofluorescence staining. Presently, we are optimising the use of our monoclonal antibodies in immunohistochemistry for the diagnostic purposes of examining c-Met expression in human tumour samples. Mab 11.1 and 12.1 were the best antibodies for Western blotting as they demonstrated good affinity and high specificity towards c-Met. Despite other anti-α-chain antibodies having different

epitopes, nearly all the anti-α-chain antibodies share similar band profiles with Mab 11.1 and 12.1, indicating that the protein bands observed between 40 kD and 70 kD genuinely represent the α-chain of c-Met. In addition, the absence of these bands in the T47D samples (low c-Met expressing cell line) further reinforces this hypothesis. No groups have specifically examined the expression of endogenous c-Met α-chain therefore there is no literature we could make reference to. There are many possibilities that could result in the varied molecular weight of c-Met α-chain. The α-chain is heavily glycosylated and differential glycosylation could lead to the varied molecular weight observed. The α-chain forms part of c-Met sema domain (Figure 1.1) which is an elliptical structure and could result in the α-chain running at a higher molecular weight on SDS-PAGE gels (Tolbert *et al.*, 2007). There have also been various reports of truncated forms of c-Met (Deheuninck *et al.*, 2008; Petrelli *et al.*, 2006; Prat *et al.*, 1998) which might also led to the variations in the molecular weight of c-Met α-chain. There has not been much study on the truncated forms of c-Met and it seems that the lack of good biological tools has hindered our further understanding of c-Met. Presently, we have yet to characterise how our antibodies are able to function in immunoprecipitation and ELISA. Having antibodies that are well-characterised in various biochemical techniques would be highly advantageous. Our antibodies will be valuable tools for c-Met further studies.

Our antibodies, in particular Mab 11.1 and 12.1, were shown to work well in detecting endogenous c-Met in immunofluorescence. This is an assumption based on comparisons with the immunofluorescence staining observed by AF276 antibody. A membrane marker will be an ideal control to ensure that the immunofluorescence staining was indeed localised to the cell membrane. However, because T47D cells are adherent cells and SNU-5 cells are suspension cells, it was difficult to select an appropriate membrane

marker to use in both cell types. In addition, our antibodies only work on methanol/acetone-fixed cells and not on paraformaldehyde-fixed cells. This makes the selection for an appropriate membrane marker harder. E-cadherin could be used as a marker for T47D cells and, since suspension cells would probably lose E-cadherin expression, carcinoembryonic antigen (CEA) could be used for SNU-5 cells. Alternatively, by designing siRNA against c-Met, expression of c-Met can be knock down in SNU-5 cells. This serves as a control to determine the specificity of our antibodies when compared to siRNA un-treated cells. Knock down of c-Met expression via siRNA could also be used as a control in other assays such as Western blotting and flow cytometry.

The alignment of the human and mouse c-Met sequences indicate that epitope binding regions 5 and 6 share exact amino acid sequence. This indicating that the antibodies in these regions might cross react with the mouse c-Met. It is possible to raise antibodies against self protein as immune tolerance to low abundant antigen lies at the T helper cell level. The autoreactive B cells are readily stimulated by injection across species. The most dramatic example of this derives from Silver and Lane (1975) where it was demonstrated that autoantibodies to the liver-specific F antigen could not be raised by autoimmunisation but by cross strain immunisation. The resulting antibodies however cannot distinguish between the F antigen of different strains. This is because self tolerance to this antigen rests entirely in the T cell compartment (Silver and Lane, 1975). Many other examples of this exist and closer to home, the extensive collection of murine monoclonal antibodies raised to human p53 that cross react with mouse p53 might be mentioned.

The epitope binding region of Mab 17.1 was the most interesting and unexpected as it recognises two binding regions (region 4 and 8) simultaneously. Although it is

theoretically not possible to obtain an antibody with two distinct paratopes, Monquet *et al*. (2010) reported the existence of polyreactive antibodies against HIV in humans. The genetic rearrangements of an antibody gene that occur when a naive B-cell differentiates into an antibody-producing cell would suggest that a hybridoma clone expressing polyreactive antibody is genetically unstable. This would explain the varied results of epitope binding analysis obtained from the second single-cell cloning of Mab 17.1. Colonies obtained from Mab 17.1 would continue to produce antibodies that recognise both regions. As the parental Mab 17.1 clone is unstable, some of these colonies might stabilise and produce antibodies recognising only one region. However, it is unclear why only antibodies that recognise region 4 was produced and not region 8. Mab 17.1, despite being able to bind to two epitopes, showed no significant inhibition/activation compared to the other antibodies in the functional assays tested. It is possible that binding to the two sites recognised by Mab 17.1 is not sufficient to block HGF from interacting with c-Met.

There are various ways in which our antibodies might be able to block c-Met activation. Through epitope mapping, we were able to predict if the binding sites of our antibodies lie within the HGF-interacting region of c-Met, phosphotyrosine residues and glycosylated residues. No phosphorylation sites were predicted on c-Met alpha chain. Four residues (Asp45, Asp106, Asp149 and Asp202) were predicted to be glycosylated with *N*-acetylglucosamine (*N*-linked GlcNAc), however, epitope mapping indicate that the glycosylated residues do not lie in the region of our monoclonal antibodies epitopes (Figure 3.22). The inability of our antibodies to recognise native c-Met, which was developed using bacterially-expressed c-Met α-chain as an immunogen, was not due to the blockage by the sugar molecule. Antibody binding regions 4, 7, 9 and 10 were found to lie within the HGF-Met interacting region (Figure 3.24). Binding of these antibodies

(Mab 1, 2, 8, 7, 9, 14, 15, 18 and 19) to c-Met could therefore block c-Met interaction with HGF and this would be effective against tumours in which c-Met is abnormally activated by HGF. Our antibodies might also block c-Met dimerisation which would affect both wild-type c-Met and c-Met activating mutants as dimerisation is required for c-Met activation (Jeffers, 1999). Binding of our antibodies to c-Met might also lock c-Met in an 'inactive' conformation thus preventing its interaction with HGF, or preventing c-Met dimerisation and activation. Alternatively, our antibodies could disrupt c-Met's crosstalk with other cell surface molecules such as EGFR, α6β4 integrin, plexins and CD44v6, thus affecting c-Met induced biological activity (Corso *et al.*, 2005).

The final aim of this project is to use the antibodies as therapeutic molecules in the treatment of human cancer. Since there is no clear understanding of how an antibody is able to efficiently recruit immune effector functions to destroy tumour cells, it is not possible to screen antibodies directly for this function. *In vitro* functional analysis of our antibodies is one of the best methods to identify antibodies that would exert their functional effects *in vivo*. We have chosen to test if our antibodies have an inhibitory effect on HGF-induced ERK phosphorylation and cell scatter. c-Met is known to be activated upon dimerisation. Due to the bivalent binding of an IgG antibody to its target antigen and based on several reports (Cioce *et al*., 1996; Michieli *et al*., 2004; Prat *et al*., 1998; Tolbert *et al*., 2007), we anticipated that some of our antibodies would be agonist towards c-Met activation. Although agonistic bivalent c-Met antibodies have little therapeutic use, we would know that these antibodies are eliciting their effects through c-Met binding. These antibodies can be used as bio-tools for further understanding of c-Met. Alternatively, these antibodies could also be engineered to be monovalent (scFv or Fab antibody fragments) for therapeutic purposes. An excellent

example is the anti-Met 5D5 antibody that was engineered to contain only a single Fab fragment is OA-5D5. OA-5D5 was shown to inhibit glioma growth in mouse models (Martens *et al.*, 2006).

To our surprise, some of our antibodies affected total ERK levels through an unknown pathway. This makes the analysis of the effects of our antibody on ERK phosphorylation difficult to interpret. Due to the subtle changes in ERK levels, it would be preferable to compare the changes in ERK levels/phosphorylation levels by quantifying the band intensity rather than by visual comparison. This can be done by densitometric scanning, or using the image analysis softwares such as Image J or Photoshop. We could also employ more sensitive assay such as the AlphaScreen®SureFire® p-ERK1/2(Thr202/Tyr204) from PerkinElmer to measure the phosphorylation of ERK. As ERK is central to many growth signalling pathways, minor changes in growth conditions will affect ERK levels/phosphorylation levels which, in turn, will affect antibody analysis. To overcome this problem, the analysis of the effect of our antibodies on ERK phosphorylation should be repeated more comprehensively. We could also analyse the functional effects of our antibodies through other signalling pathways such as AKT activation/phosphorylation. Analysing pathways downstream of c-Met may not be a good indicator of c-Met activation/inhibition because these pathways are usually shared by other tyrosine receptors/signal transduction pathways. Non-specific interactions of the antibodies or interactions of other inhibitors/activators might separately affect these downstream pathways and influence the analysis of the effects of our antibodies. Therefore, directly analysing the phosphorylation status of c-Met by Western blotting will be the best method to determine c-Met activation/inhibition. However, this is presently not possible due to the poor affinity and specificity of current commercial anti-phospho-Met antibodies. Moravian

Biotechnology is presently developing anti-phospho-Met antibodies which were shown to have high affinity and specificity for phosphorylated c-Met in Western blotting. These anti-phospho-Met antibodies will be vital tools for c-Met analysis. Finally, the effects of our antibodies on ERK phosphorylation should be tested on other cells lines, such as SNU-5 and U-87MG cells, that have aberrant c-Met expression. This is because the biological activity induced by c-Met is dependent on the cell type and extracellular matrix, suggesting that different signalling pathways are activated in different cell lines to bring about the varied biological changes. HaCaT cells may not be the ideal cell line in which to study the effects of our antibodies on ERK phosphorylation as, in these cells, the major signal transduction pathway of c-Met activation may not be through ERK pathway. In addition, Christensen *et al*. (2003) demonstrated that the small molecule c-Met inhibitor PHA-665752 drastically inhibited c-Met activation in cells expressing high levels of c-Met, but had little effect on BxPC-3 cells which express moderate levels of c-Met. HaCaT cells used in our assay express lower levels of c-Met expression compared to SNU-5 and U-87MG cells and are not dependent on c-Met activation for survival. Therefore, similar to the BxPC-3 cells, inhibition of c-Met in HaCaT cells using our antibodies might have resulted in the subtle changes in ERK phosphorylation observed.

Similarly to ERK phosphorylation, the effects of our antibodies on cell scatter were difficult to interpret. This was partly due to the inconsistent effects of varying batches of commercially-obtained HGF. In addition, each cell colony (in the same well) responded differently to the same treatment resulting in a variation of scatter response observed. Although the effects of the antibodies on cell scatter were analysed according to the majority effects, it is sometimes difficult to interpret the overall result. The varied response of the cell colonies could be due to the size of the colony where more cells

result in more complicated cell-to-cell communication among the colony. Presence of neighbouring cell colonies might also affect cell scatter as cell colonies can communicate with each other to grow closer together. Individually growing and treating a cell colony in a 96-well might be more ideal for analysing the effects of our antibodies on cell scatter.

The results from flow cytometry provide the strongest and direct evidence that some of our antibodies bind and recognise native c-Met. These antibodies (especially Mab 2.1 and 13.1) can be useful tools for the study of c-Met on the cell surface. It would also be tempting to further engineer and improve these antibodies for imaging of tumour cells *in vivo*. Interestingly, results from flow cytometry correlate with the ability of the cells to cause cell cluster; Mab 2.1, 8.1, 11.1, 12.1 and 13.1 were strongly positive for cell cluster and showed intense fluorescence staining in flow cytometry. These antibodies must be able to recognise native c-Met on the cell surface so as to cause cell cluster. This suggests that the result of cell cluster is real and could be used as a high-throughput, quick and simple assay to screen for antibodies that bind to native protein on the cell surface.

Interestingly, Mab 13.1, which showed very poor affinity and specificity to c-Met by Western blotting and immunofluorescence, was, along with Mab 2.1, produced the highest fluorescence staining determined by flow cytometry. Through the binding of Mab 2.1 or 13.1 to c-Met, these antibodies may be able to elicit a functional effect on c-Met. It is interesting that the some antibodies affect ERK signalling but not cell scatter. This might be due to the binding of our antibodies to different epitopes on c-Met. Both Mab 2.1 and 13.1 could be partial antagonists of c-Met as Mab 2.1 causes ERK phosphorylation, but is able to partially inhibit cell scatter, while Mab 13.1 inhibits ERK phosphorylation and partially inhibit cell scatter. Partial inhibition of c-Met-

induced biological activities using monoclonal anti-Met antibodies has also been described by Prat *el al*. (1998). The anti-Met antibody, DN-30, inhibits other c-Met-induce biological activities, but not cell motility. In the same study, another monoclonal antibody (DO-24) developed from the same immunisation as DN-30, was a full agonist capable of eliciting full c-Met activity. From another study, it also demonstrated that more than three monoclonal antibodies are required to completely inhibit c-Met binding (Cao *et al.*, (2001). The molecular mechanisms of c-Met activation by HGF are still unclear. This interaction is more complex than previously thought and from these antibodies studies, it is obvious that there are critical interaction sites that are responsible for eliciting various c-Met activities. It is possible that binding of our monoclonal antibodies to c-Met might interfere with c-Met conformation, thus affecting c-Met binding to downstream signalling molecules such as Gab1 and p85 (subunit of PI3K) and influencing the biological activity of the cell. As mentioned above, c-Met was demonstrated to cross talk with other receptors and cell surface molecules causing an amplification of downstream signals that led to cancer progression. Our antibodies could bind to c-Met, inhibit c-Met cross talk and shut down the signalling pathways responsible for abnormal growth.

In contrast to Mab 2.1 and 13.1, Mab 11.1 and 12.1 demonstrated good affinity and high specificity towards c-Met in Western blotting and immunofluorescence staining, but only bound to native c-Met with intermediate affinity. The difference in the affinity of the antibodies to recognise native and denatured c-Met is likely due to the antibody's epitope. Mab 2.1 and 13.1 epitope recognition is partially dependent upon secondary structure while for Mab 11.1 and 12.1 epitope can be denatured. Mab 2.1 and 13.1 are the most interesting antibodies as they have the most potential to be developed into

therapeutic antibodies while Mab 11.1 and 12.1 will be useful tools for c-Met expression studies that require the detection of antigen in Western blot methods.

There is high potential for developing our panel of anti-α-chain antibodies for clinical purposes. However, at present, more work is required to further characterise our anti-α-chain antibodies. As every antibody works differently, an antibody concentration will have a significant effect of the antibody's ability to inhibit/activate c-Met. More work is thus required to optimise the antibody concentration in the functional assays for each antibody. We can also characterise the effects of our antibodies on other c-Met-induced functional assays such as Matrigel gel invasion assays and proliferation assays. As shown by Cao *et al*. (2001) and van der Horst *et al*. (2009), combinations of monoclonal antibodies demonstrated the best inhibition of c-Met interaction with HGF. It would be interesting to test the different combinations of our antibodies to determine if c-Met inhibition could be improved. We might also need to develop scFv or Fab fragments of our antibodies for therapeutic purposes. The next step would to bring the antibodies into xenograft models and to test if the antibodies are able to function *in vivo*. Humanising potential antibodies for therapeutic/diagnostic purposes and testing these engineered antibodies again for their functional activity will be the next step of developing therapeutic antibodies. Our humanised anti-Met antibodies will also be tested for effector functions such as binding abilities to various FcγR to mediate ADCC, binding abilities to C1q component to induce CDC or ability of antibodies to cause cell death in chromium pre-loaded cells.

REFERENCES

Abounader, R., B. Lal, C. Luddy, G. Koe, B. Davidson, E.M. Rosen, and J. Laterra. 2002. In vivo targeting of SF/HGF and c-met expression via U1snRNA/ribozymes inhibits glioma growth and angiogenesis and promotes apoptosis. *Faseb J*. 16:108-10.

Abounader, R., and J. Laterra. 2005. Scatter factor/hepatocyte growth factor in brain tumor growth and angiogenesis. *Neuro Oncol*. 7:436-51.

Adams, G.P., and L.M. Weiner. 2005. Monoclonal antibody therapy of cancer. *Nat Biotechnol*. 23:1147-57.

Bardelli, A., C. Ponzetto, and P.M. Comoglio. 1994. Identification of functional domains in the hepatocyte growth factor and its receptor by molecular engineering. *J Biotechnol*. 37:109-22.

Beers, S.A., C.H. Chan, S. James, R.R. French, K.E. Attfield, C.M. Brennan, A. Ahuja, M.J. Shlomchik, M.S. Cragg, and M.J. Glennie. 2008. Type II (tositumomab) anti-CD20 monoclonal antibody out performs type I (rituximab-like) reagents in B-cell depletion regardless of complement activation. *Blood*. 112:4170-7.

Bellon, S.F., P. Kaplan-Lefko, Y. Yang, Y. Zhang, J. Moriguchi, K. Rex, C.W. Johnson, P.E. Rose, A.M. Long, A.B. O'Connor, Y. Gu, A. Coxon, T.S. Kim, A. Tasker, T.L. Burgess, and I. Dussault. 2008. c-Met inhibitors with novel binding mode show activity against several hereditary papillary renal cell carcinoma-related mutations. *J Biol Chem*. 283:2675-83.

Berthou, S., D.M. Aebersold, L.S. Schmidt, D. Stroka, C. Heigl, B. Streit, D. Stalder, G. Gruber, C. Liang, A.R. Howlett, D. Candinas, R.H. Greiner, K.E. Lipson, and Y. Zimmer. 2004. The Met kinase inhibitor SU11274 exhibits a selective inhibition pattern toward different receptor mutated variants. *Oncogene*. 23:5387-93.

Bertotti, A., M.F. Burbridge, S. Gastaldi, F. Galimi, D. Torti, E. Medico, S. Giordano, S. Corso, G. Rolland-Valognes, B.P. Lockhart, J.A. Hickman, P.M. Comoglio, and L. Trusolino. 2009. Only a subset of Met-activated pathways are required to sustain oncogene addiction. *Sci Signal*. 2:er11.

Birchmeier, C., W. Birchmeier, E. Gherardi, and G.F. Vande Woude. 2003. Met, metastasis, motility and more. *Nat Rev Mol Cell Biol*. 4:915-25.

Birchmeier, C., and E. Gherardi. 1998. Developmental roles of HGF/SF and its receptor, the c-Met tyrosine kinase. *Trends Cell Biol*. 8:404-10.

Brockmann, M.A., A. Papadimitriou, M. Brandt, R. Fillbrandt, M. Westphal, and K. Lamszus. 2003. Inhibition of intracerebral glioblastoma growth by local treatment with the scatter factor/hepatocyte growth factor-antagonist NK4. *Clin Cancer Res*. 9:4578-85.

Burton, D.R., and R.A. Dwek. 2006. Immunology. Sugar determines antibody activity. *Science*. 313:627-8.

Cao, B., Y. Su, M. Oskarsson, P. Zhao, E.J. Kort, R.J. Fisher, L.M. Wang, and G.F. Vande Woude. 2001. Neutralizing monoclonal antibodies to hepatocyte growth factor/scatter factor (HGF/SF) display antitumor activity in animal models. *Proc Natl Acad Sci U S A*. 98:7443-8.

Chan, A.C., and P.J. Carter. Therapeutic antibodies for autoimmunity and inflammation. *Nat Rev Immunol*. 10:301-16.

Chmielowiec, J., M. Borowiak, M. Morkel, T. Stradal, B. Munz, S. Werner, J. Wehland, C. Birchmeier, and W. Birchmeier. 2007. c-Met is essential for wound healing in the skin. *J Cell Biol*. 177:151-62.

Choo, A.B., H.L. Tan, S.N. Ang, W.J. Fong, A. Chin, J. Lo, L. Zheng, H. Hentze, R.J. Philp, S.K. Oh, and M. Yap. 2008. Selection against undifferentiated human embryonic stem cells by a cytotoxic antibody recognizing podocalyxin-like protein-1. *Stem Cells*. 26:1454-63.

Christensen, J.G., J. Burrows, and R. Salgia. 2005. c-Met as a target for human cancer and characterization of inhibitors for therapeutic intervention. *Cancer Lett*. 225:1-26.

Christensen, J.G., R. Schreck, J. Burrows, P. Kuruganti, E. Chan, P. Le, J. Chen, X. Wang, L. Ruslim, R. Blake, K.E. Lipson, J. Ramphal, S. Do, J.J. Cui, J.M. Cherrington, and D.B. Mendel. 2003. A selective small molecule inhibitor of c-Met kinase inhibits c-Met-dependent phenotypes in vitro and exhibits cytoreductive antitumor activity in vivo. *Cancer Res*. 63:7345-55.

Cioce, V., K.G. Csaky, A.M. Chan, D.P. Bottaro, W.G. Taylor, R. Jensen, S.A. Aaronson, and J.S. Rubin. 1996. Hepatocyte growth factor (HGF)/NK1 is a naturally occurring HGF/scatter factor variant with partial agonist/antagonist activity. *J Biol Chem*. 271:13110-5.

Conrotto, P., D. Valdembri, S. Corso, G. Serini, L. Tamagnone, P.M. Comoglio, F. Bussolino, and S. Giordano. 2005. Sema4D induces angiogenesis through Met recruitment by Plexin B1. *Blood*. 105:4321-9.

Correia I.R. 2010. Stability of IgG isotypes in serum. *mAbs*. 2(3):221-32.

Cooper, C.S., P.R. Tempest, M.P. Beckman, C.H. Heldin, and P. Brookes. 1986. Amplification and overexpression of the met gene in spontaneously transformed NIH3T3 mouse fibroblasts. *Embo J*. 5:2623-8.

Corso, S., P.M. Comoglio, and S. Giordano. 2005. Cancer therapy: can the challenge be MET? *Trends Mol Med*. 11:284-92.

Daugherty, A.L., and R.J. Mrsny. 2003. Emerging technologies that overcome biological barriers for therapeutic protein delivery. *Expert Opin Biol Ther*. 3:1071-81.

De Souza, E.B., S.T. Cload, P.S. Pendergrast, and D.W. Sah. 2009. Novel therapeutic modalities to address nondrugable protein interaction targets. *Neuropsychopharmacology*. 34:142-58.

Deheuninck, J., B. Foveau, G. Goormachtigh, C. Leroy, Z. Ji, D. Tulasne, and V. Fafeur. 2008. Caspase cleavage of the MET receptor generates an HGF interfering fragment. *Biochem Biophys Res Commun*. 367:573-7.

Deheuninck, J., G. Goormachtigh, B. Foveau, Z. Ji, C. Leroy, F. Ancot, V. Villeret, D. Tulasne, and V. Fafeur. 2009. Phosphorylation of the MET receptor on juxtamembrane tyrosine residue 1001 inhibits its caspase-dependent cleavage. *Cell Signal*. 21:1455-63.

Engelman, J.A., K. Zejnullahu, T. Mitsudomi, Y. Song, C. Hyland, J.O. Park, N. Lindeman, C.M. Gale, X. Zhao, J. Christensen, T. Kosaka, A.J. Holmes, A.M. Rogers, F. Cappuzzo, T. Mok, C. Lee, B.E. Johnson, L.C. Cantley, and P.A. Janne. 2007. MET amplification leads to gefitinib resistance in lung cancer by activating ERBB3 signaling. *Science*. 316:1039-43.

Fresno Vara, J.A., E. Casado, J. de Castro, P. Cejas, C. Belda-Iniesta, and M. Gonzalez-Baron. 2004. PI3K/Akt signalling pathway and cancer. *Cancer Treat Rev*. 30:193-204.

Furlan, A., C. Vercamer, X. Desbiens, and A. Pourtier. 2008. Ets-1 triggers and orchestrates the malignant phenotype of mammary cancer cells within their matrix environment. *J Cell Physiol*. 215:782-93.

Gandino, L., P. Longati, E. Medico, M. Prat, and P.M. Comoglio. 1994. Phosphorylation of serine 985 negatively regulates the hepatocyte growth factor receptor kinase. *J Biol Chem*. 269:1815-20.

Gessner, J.E., H. Heiken, A. Tamm, and R.E. Schmidt. 1998. The IgG Fc receptor family. *Ann Hematol*. 76:231-48.

Gherardi, E., M.E. Youles, R.N. Miguel, T.L. Blundell, L. Iamele, J. Gough, A. Bandyopadhyay, G. Hartmann, and P.J. Butler. 2003. Functional map and domain structure of MET, the product of the c-met protooncogene and receptor for hepatocyte growth factor/scatter factor. *Proc Natl Acad Sci U S A*. 100:12039-44.

Giordano, S., Z. Zhen, E. Medico, G. Gaudino, F. Galimi, and P.M. Comoglio. 1993. Transfer of motogenic and invasive response to scatter factor/hepatocyte growth factor by transfection of human MET protooncogene. *Proc Natl Acad Sci U S A*. 90:649-53.

Glennie, M.J., and J.G. van de Winkel. 2003. Renaissance of cancer therapeutic antibodies. *Drug Discov Today*. 8:503-10.

Hammond, D.E., S. Urbe, G.F. Vande Woude, and M.J. Clague. 2001. Down-regulation of MET, the receptor for hepatocyte growth factor. *Oncogene*. 20:2761-70.

Harlow, E., and D. Lane. 1999. Using Antibodies: A laboratory manual. Cold Spring Harbour Laboratory Press, Cold Spring Harbour, New York. 495 pp.

Hartmann, G., L. Naldini, K.M. Weidner, M. Sachs, E. Vigna, P.M. Comoglio, and W. Birchmeier. 1992. A functional domain in the heavy chain of scatter factor/hepatocyte growth factor binds the c-Met receptor and induces cell dissociation but not mitogenesis. *Proc Natl Acad Sci U S A*. 89:11574-8.

Hay, R.V., B. Cao, R.S. Skinner, L.M. Wang, Y. Su, J.H. Resau, B.S. Knudsen, M.F. Gustafson, H.M. Koo, G.F. Woude, and M.D. Gross. 2003. Radioimmunoscintigraphy of human met-expressing tumor xenografts using met3, a new monoclonal antibody. *Clin Cancer Res*. 9:3839S-44S.

Jain, M., N. Kamal, and S.K. Batra. 2007. Engineering antibodies for clinical applications. *Trends Biotechnol*. 25:307-16.

Jefferis, R. 2009. Recombinant antibody therapeutics: the impact of glycosylation on mechanisms of action. *Trends Pharmacol Sci*. 30:356-62.

Jefferis, R. 2007. Antibody therapeutics: isotype and glycoform selection. *Expert Opin. Biol. Ther.* 7(9):1401-1413.

Jeffers, M., S. Rong, and G.F. Woude. 1996. Hepatocyte growth factor/scatter factor-Met signaling in tumorigenicity and invasion/metastasis. *J Mol Med*. 74:505-13.

Jeffers, M., L. Schmidt, N. Nakaigawa, C.P. Webb, G. Weirich, T. Kishida, B. Zbar, and G.F. Vande Woude. 1997a. Activating mutations for the met tyrosine kinase receptor in human cancer. *Proc Natl Acad Sci U S A*. 94:11445-50.

Jeffers, M., G.A. Taylor, K.M. Weidner, S. Omura, and G.F. Vande Woude. 1997b. Degradation of the Met tyrosine kinase receptor by the ubiquitin-proteasome pathway. *Mol Cell Biol*. 17:799-808.

Jeffers, M.F. 1999. Activating mutations in the Met receptor overcome the requirement for autophosphorylation of tyrosines crucial for wild type signaling. *Oncogene*. 18:5120-5.

Jiao, Y., P. Zhao, J. Zhu, T. Grabinski, Z. Feng, X. Guan, R.S. Skinner, M.D. Gross, R.V. Hay, H. Tachibana, and B. Cao. 2005. Construction of human naive Fab library and characterization of anti-met Fab fragment generated from the library. *Mol Biotechnol*. 31:41-54.

Jun, H.T., J. Sun, K. Rex, R. Radinsky, R. Kendall, A. Coxon, and T.L. Burgess. 2007. AMG 102, a fully human anti-hepatocyte growth factor/scatter factor neutralizing antibody, enhances the efficacy of temozolomide or docetaxel in U-87 MG cells and xenografts. *Clin Cancer Res*. 13:6735-42.

Keefe, A.D., D.S. Wilson, B. Seelig, and J.W. Szostak. 2001. One-step purification of recombinant proteins using a nanomolar-affinity streptavidin-binding peptide, the SBP-Tag. *Protein Expr Purif*. 23:440-6.

Knudsen, B.S., and G. Vande Woude. 2008. Showering c-MET-dependent cancers with drugs. *Curr Opin Genet Dev*. 18:87-96.

Kong-Beltran, M., J. Stamos, and D. Wickramasinghe. 2004. The Sema domain of Met is necessary for receptor dimerization and activation. *Cancer Cell*. 6:75-84.

Lane DP, Stephen CW, Midgley CA, Sparks A, Hupp TR, Daniels DA, Greaves R, Reid A, Vojtesek B, Picksley SM. 1996. Epitope analysis of the murine p53 tumour suppressor protein. *Oncogene*. 12(11):2461-6.

Lietha, D., D.Y. Chirgadze, B. Mulloy, T.L. Blundell, and E. Gherardi. 2001. Crystal structures of NK1-heparin complexes reveal the basis for NK1 activity and enable engineering of potent agonists of the MET receptor. *Embo J*. 20:5543-55.

Ma, W.W., and A.A. Adjei. 2009. Novel agents on the horizon for cancer therapy. *CA Cancer J Clin*. 59:111-37.

Martens, T., N.O. Schmidt, C. Eckerich, R. Fillbrandt, M. Merchant, R. Schwall, M. Westphal, and K. Lamszus. 2006. A novel one-armed anti-c-Met antibody inhibits glioblastoma growth in vivo. *Clin Cancer Res*. 12:6144-52.

Matzke, A., P. Herrlich, H. Ponta, and V. Orian-Rousseau. 2005. A five-amino-acid peptide blocks Met- and Ron-dependent cell migration. *Cancer Res*. 65:6105-10.

Michieli, P., M. Mazzone, C. Basilico, S. Cavassa, A. Sottile, L. Naldini, and P.M. Comoglio. 2004. Targeting the tumor and its microenvironment by a dual-function decoy Met receptor. *Cancer Cell*. 6:61-73.

Migliore, C., and S. Giordano. 2008. Molecular cancer therapy: can our expectation be MET? *Eur J Cancer*. 44:641-51.

Mondino, A., S. Giordano, and P.M. Comoglio. 1991. Defective posttranslational processing activates the tyrosine kinase encoded by the MET proto-oncogene (hepatocyte growth factor receptor). *Mol Cell Biol*. 11:6084-92.

Mouquet, H., J.F. Scheid, M.J. Zoller, M. Krogsgaard, R.G. Ott, S. Shukair, M.N. Artyomov, J. Pietzsch, M. Connors, F. Pereyra, B.D. Walker, D.D. Ho, P.C. Wilson, M.S. Seaman, H.N. Eisen, A.K. Chakraborty, T.J. Hope, J.V. Ravetch, H. Wardemann, and M.C. Nussenzweig. Polyreactivity increases the apparent affinity of anti-HIV antibodies by heteroligation. *Nature*. 467:591-5.

Naka, D., T. Ishii, Y. Yoshiyama, K. Miyazawa, H. Hara, T. Hishida, and N. Kidamura. 1992. Activation of hepatocyte growth factor by proteolytic conversion of a single chain form to a heterodimer. *J Biol Chem*. 267:20114-9.

Naldini, L., K.M. Weidner, E. Vigna, G. Gaudino, A. Bardelli, C. Ponzetto, R.P. Narsimhan, G. Hartmann, R. Zarnegar, G.K. Michalopoulos, and et al. 1991. Scatter factor and hepatocyte growth factor are indistinguishable ligands for the MET receptor. *Embo J*. 10:2867-78.

Nicholson, K.M., and N.G. Anderson. 2002. The protein kinase B/Akt signalling pathway in human malignancy. *Cell Signal*. 14:381-95.

Nimmerjahn, F., and J.V. Ravetch. 2007. Antibodies, Fc receptors and cancer. *Curr Opin Immunol*. 19:239-45.

Ohashi, K., P.L. Marion, H. Nakai, L. Meuse, J.M. Cullen, B.B. Bordier, R. Schwall, H.B. Greenberg, J.S. Glenn, and M.A. Kay. 2000. Sustained survival of human hepatocytes in mice: A model for in vivo infection with human hepatitis B and hepatitis delta viruses. *Nat Med*. 6:327-31.

Park, M., M. Dean, C.S. Cooper, M. Schmidt, S.J. O'Brien, D.G. Blair, and G.F. Vande Woude. 1986. Mechanism of met oncogene activation. *Cell*. 45:895-904.

Pennacchietti, S., P. Michieli, M. Galluzzo, M. Mazzone, S. Giordano, and P.M. Comoglio. 2003. Hypoxia promotes invasive growth by transcriptional activation of the met protooncogene. *Cancer Cell*. 3:347-61.

Peruzzi, B., and D.P. Bottaro. 2006. Targeting the c-Met signaling pathway in cancer. *Clin Cancer Res*. 12:3657-60.

Peschard, P., T.M. Fournier, L. Lamorte, M.A. Naujokas, H. Band, W.Y. Langdon, and M. Park. 2001. Mutation of the c-Cbl TKB domain binding site on the Met receptor tyrosine kinase converts it into a transforming protein. *Mol Cell*. 8:995-1004.

Petrelli, A., P. Circosta, L. Granziero, M. Mazzone, A. Pisacane, S. Fenoglio, P.M. Comoglio, and S. Giordano. 2006. Ab-induced ectodomain shedding mediates hepatocyte growth factor receptor down-regulation and hampers biological activity. *Proc Natl Acad Sci U S A*. 103:5090-5.

Ponzetto, C., A. Bardelli, Z. Zhen, F. Maina, P. dalla Zonca, S. Giordano, A. Graziani, G. Panayotou, and P.M. Comoglio. 1994. A multifunctional docking site mediates signaling and transformation by the hepatocyte growth factor/scatter factor receptor family. *Cell*. 77:261-71.

Prat, M., T. Crepaldi, S. Pennacchietti, F. Bussolino, and P.M. Comoglio. 1998. Agonistic monoclonal antibodies against the Met receptor dissect the biological responses to HGF. *J Cell Sci*. 111 (Pt 2):237-47.

Rong, S., M. Bodescot, D. Blair, J. Dunn, T. Nakamura, K. Mizuno, M. Park, A. Chan, S. Aaronson, and G.F. Vande Woude. 1992. Tumorigenicity of the met proto-oncogene and the gene for hepatocyte growth factor. *Mol Cell Biol*. 12:5152-8.

Rong, S., S. Segal, M. Anver, J.H. Resau, and G.F. Vande Woude. 1994. Invasiveness and metastasis of NIH 3T3 cells induced by Met-hepatocyte growth factor/scatter factor autocrine stimulation. *Proc Natl Acad Sci U S A*. 91:4731-5.

Rosario, M., and W. Birchmeier. 2003. How to make tubes: signaling by the Met receptor tyrosine kinase. *Trends Cell Biol*. 13:328-35.

Ruco, L.P., T. Ranalli, A. Marzullo, P. Bianco, M. Prat, P.M. Comoglio, and C.D. Baroni. 1996. Expression of Met protein in thyroid tumours. *J Pathol*. 180:266-70.

Salfeld J.G. 2007. Isotype selection in antibody engineering. *Nat Biotechnol.* 25(12):1369-72.

Sattler, M., Y.B. Pride, P. Ma, J.L. Gramlich, S.C. Chu, L.A. Quinnan, S. Shirazian, C. Liang, K. Podar, J.G. Christensen, and R. Salgia. 2003. A novel small molecule met inhibitor induces apoptosis in cells transformed by the oncogenic TPR-MET tyrosine kinase. *Cancer Res*. 63:5462-9.

Schmidt, C., F. Bladt, S. Goedecke, V. Brinkmann, W. Zschiesche, M. Sharpe, E. Gherardi, and C. Birchmeier. 1995. Scatter factor/hepatocyte growth factor is essential for liver development. *Nature*. 373:699-702.

Schmidt, R.E., and J.E. Gessner. 2005. Fc receptors and their interaction with complement in autoimmunity. *Immunol Lett*. 100:56-67.

Shawver, L.K., D. Slamon, and A. Ullrich. 2002. Smart drugs: tyrosine kinase inhibitors in cancer therapy. *Cancer Cell*. 1:117-23.

Shen, Y., M. Naujokas, M. Park, and K. Ireton. 2000. InIB-dependent internalization of Listeria is mediated by the Met receptor tyrosine kinase. *Cell*. 103:501-10.

Silver, D.M. and Lane, D.P. 1975. Dominant nonresponsiveness in the induction of autoimmunity to liver-specific F antigen. *J Exp Med.* 142(6):1455-61.

Smolen, G.A., R. Sordella, B. Muir, G. Mohapatra, A. Barmettler, H. Archibald, W.J. Kim, R.A. Okimoto, D.W. Bell, D.C. Sgroi, J.G. Christensen, J. Settleman, and D.A. Haber. 2006. Amplification of MET may identify a subset of cancers with extreme sensitivity to the selective tyrosine kinase inhibitor PHA-665752. *Proc Natl Acad Sci U S A*. 103:2316-21.

Stella, M.C., and P.M. Comoglio. 1999. HGF: a multifunctional growth factor controlling cell scattering. *Int J Biochem Cell Biol*. 31:1357-62.

Teeling, J.L., W.J. Mackus, L.J. Wiegman, J.H. van den Brakel, S.A. Beers, R.R. French, T. van Meerten, S. Ebeling, T. Vink, J.W. Slootstra, P.W. Parren, M.J. Glennie, and J.G. van de Winkel. 2006. The biological activity of human CD20 monoclonal antibodies is linked to unique epitopes on CD20. *J Immunol*. 177:362-71.

Tempest, P.R., M.R. Stratton, and C.S. Cooper. 1988. Structure of the met protein and variation of met protein kinase activity among human tumour cell lines. *Br J Cancer*. 58:3-7.

Thiery, J.P. 2002. Epithelial-mesenchymal transitions in tumour progression. *Nat Rev Cancer.* 2(6):442-54.

Tolbert, W.D., J. Daugherty, C. Gao, Q. Xie, C. Miranti, E. Gherardi, G.V. Woude, and H.E. Xu. 2007. A mechanistic basis for converting a receptor tyrosine kinase agonist to an antagonist. *Proc Natl Acad Sci U S A*. 104:14592-7.

Tremmel, M., A. Matzke, I. Albrecht, A.M. Laib, V. Olaku, K. Ballmer-Hofer, G. Christofori, M. Heroult, H.G. Augustin, H. Ponta, and V. Orian-Rousseau. 2009. A CD44v6 peptide reveals a role of CD44 in VEGFR-2 signaling and angiogenesis. *Blood*. 114:5236-44.

Trusolino, L., A. Bertotti, and P.M. Comoglio. 2001. A signaling adapter function for alpha6beta4 integrin in the control of HGF-dependent invasive growth. *Cell*. 107:643-54.

van der Horst, E.H., L. Chinn, M. Wang, T. Velilla, H. Tran, Y. Madrona, A. Lam, M. Ji, T.C. Hoey, and A.K. Sato. 2009. Discovery of fully human anti-MET monoclonal antibodies with antitumor activity against colon cancer tumor models in vivo. *Neoplasia*. 11:355-64.

Wang, X., P. Le, C. Liang, J. Chan, D. Kiewlich, T. Miller, D. Harris, L. Sun, A. Rice, S. Vasile, R.A. Blake, A.R. Howlett, N. Patel, G. McMahon, and K.E. Lipson. 2003. Potent and selective inhibitors of the Met [hepatocyte growth factor/scatter factor (HGF/SF) receptor] tyrosine kinase block HGF/SF-induced tumor cell growth and invasion. *Mol Cancer Ther*. 2:1085-92.

Xiao, G.H., M. Jeffers, A. Bellacosa, Y. Mitsuuchi, G.F. Vande Woude, and J.R. Testa. 2001. Anti-apoptotic signaling by hepatocyte growth factor/Met via the phosphatidylinositol 3-kinase/Akt and mitogen-activated protein kinase pathways. *Proc Natl Acad Sci U S A*. 98:247-52.

Ye, M., D. Hu, L. Tu, X. Zhou, F. Lu, B. Wen, W. Wu, Y. Lin, Z. Zhou, and J. Qu. 2008. Involvement of PI3K/Akt signaling pathway in hepatocyte growth factor-induced migration of uveal melanoma cells. *Invest Ophthalmol Vis Sci*. 49:497-504.

Zhao, P., T. Grabinski, C. Gao, R.S. Skinner, T. Giambernardi, Y. Su, E. Hudson, J. Resau, M. Gross, G.F. Vande Woude, R. Hay, and B. Cao. 2007. Identification of a met-binding peptide from a phage display library. *Clin Cancer Res*. 13:6049-55.

Appendix

Appendix 1

c-Met and HGF relevance in human cancer.
Adapted from adapted from Birchmeier *et al.*, 2003.

Hepatocyte growth factor/scatter factor, Met and cancer references

COMMENTS? - Bookmark - Print

Click on Y to view the references.

Category	Cancer Type	HGF/SF expression	Met expression	Poor Prognosis	Mutation of Met	In vitro studies	Animal model	Therapeutic Development	Review
Carcinomas								Y	Y
	Bladder	Y	Y	Y	..N.	Y	Y	Y	..N.
	Breast	Y	Y	Y	Y	Y	Y	Y	..N.
	Cervical	Y	Y	Y	..N.	Y	..N.	Y	..N.
	Cholangiocarcinoma	Y	Y	..N.	..N.	Y	Y	Y	Y
	Colorectal	Y	Y	Y	..N.	Y	Y	Y	Y
	Endometrial	Y	Y	..N.	..N.	Y	Y	Y	..N.
	Esophogeal	Y	Y	Y	..N.	Y	..N.	Y	..N.
	Gastric	Y	Y	Y	Y	Y	Y	Y	Y
	Head and Neck	Y	Y	Y	Y	Y	Y	Y	Y
	Kidney	Y	Y	Y	Y	Y	Y	Y	Y
	Liver	Y	Y	Y	Y	Y	Y	Y	Y
	Lung	Y	Y	Y	Y	Y	Y	Y	Y
	Nasopharyngeal	Y	Y	Y	..N.	Y	..N.	..N.	..N.
	Ovarian	Y	Y	Y	Y	Y	Y	Y	Y
	Pancreas/Gall Bladder	Y	Y	..N.	..N.	Y	Y	Y	..N.
	Prostate	Y	Y	Y	..N.	Y	Y	Y	Y
	Thyroid	Y	Y	Y	Y	Y	..N.	Y	..N.
Musculoskeletal sarcomas		Y	Y			Y			
	Osteosarcoma	Y	Y	..N.	Y	Y	Y	Y	..N.
	Rhabdomyosarcoma	Y	Y	Y	..N.	Y	Y	Y	..N.
	Synovial Sarcoma	Y	Y	Y	..N.	Y	..N.	..N.	..N.
Soft tissue sarcomas					Y		Y		
	Kaposi's Sarcoma	Y	Y	Y	..N.	Y	Y	..N.	..N.
	Leiomyosarcoma	Y	Y	Y	..N.	Y	Y	Y	..N.
	MFH/Fibrosarcoma	Y	Y	..N.	..N.	Y	Y	Y	..N.
Hematopoietic Malignancies									
	Acute Myelogenous Leukemia	Y	..N.	..N.	..N.	Y	..N.	..N.	..N.
	Adult T Cell Leukemia	Y	Y	Y	..N.	Y	..N.	Y	..N.
	Chronic Myeloid Leukemia	Y	..N.	Y	..N.	..N.	..N.	..N.	..N.
	Lymphomas	Y	Y	Y	Y	Y	Y	Y	Y
	Multiple Myeloma	Y	Y	Y	..N.	Y	Y	Y	Y
Other Neoplasms		Y							
	Glioblastomas/Astrocytomas	Y	Y	Y	Y	Y	Y	Y	Y
	Melanoma	Y	Y	..N.	..N.	Y	Y	Y	..N.
	Mesothelioma	Y	Y	Y	..N.	Y	..N.	Y	Y
	Wilms' Tumor	Y	Y	..N.	..N.	..N.	Y	Y	..N.

The table shows significant references relating to the roles of HGF/SF or Met in the types of cancer indicated. For each cancer type, headings correspond to studies showing: HGF/SF expression in tumour biopsies; Met expression in tumour biopsies; expression of HGF/SF or Met correlating with poor prognosis; sporadic or germline-activating mutations in Met; tumour cells in vitro expressing Met or HGF/SF, some with correlation to in vitro neoplastic-like activities; and animal models supporting the role of Met and HGF/SF in cancer, including human tumour xenografts in immunecompromised mice, mice with HGF/SF or Met transgenes, or other animal models displaying dependence on HGF/SF or Met in cancer development. A, autocrine; MFH, malignant fibrous histiocytoma; %, percentage of tumours examined that are positive; N, no report.

27985

Appendix 2

Full length alignment of human (P08581) and mouse (P16056) c-Met.

```
Human           MKAPAVLAPGILVLLFTLVQRSNGECKEALAKSEMNVNMKYQLPNFTAETPIQNVILHEH 60
Mouse           MKAPTVLAPGILVLLLSLVQRSHGECKEALVKSEMNVNMKYQLPNFTAETPIQNVVLHGH 60
                ****:**********::*****:*******.************************:** *

Human           HIFLGATNYIYVLNEEDLQKVAEYKTGPVLEHPDCFPCQDCSSKANLSGGVWKDNINMAL 120
Mouse           HIYLGATNYIYVLNDKDLQKVSEFKTGPVLEHPDCLPCRDCSSKANSSGGVWKDNINMAL 120
                **:***********::*****:*:***********:**:******* *************

Human           VVDTYYDDQLISCGSVNRGTCQRHVFPHNHTADIQSEVHCIFSPQIEEPSQCPDCVVSAL 180
Mouse           LVDTYYDDQLISCGSVNRGTCQRHVLPPDNSADIQSEVHCMFSPE-EESGQCPDCVVSAL 179
                :************************:* :::*********:***: **..**********

Human           GAKVLSSVKDRFINFFVGNTINSSYFPDHPLHSISVRRLKETKDGFMFLTDQSYIDVLPE 240
Mouse           GAKVLLSEKDRFINFFVGNTINSSYPPGYSLHSISVRRLKETQDGFKFLTDQSYIDVLPE 239
                ***** * ***************** *.::************:*** *************

Human           FRDSYPIKYVHAFESNNFIYFLTVQRETLDAQTFHTRIIRFCSINSGLHSYMEMPLECIL 300
Mouse           FLDSYPIKYIHAFESNHFIYFLTVQKETLDAQTFHTRIIRFCSVDSGLHSYMEMPLECIL 299
                * *******:******:********:*****************::***************

Human           TEKRKKRSTKKEVFNILQAAYVSKPGAQLARQIGASLNDDILFGVFAQSKPDSAEPMDRS 360
Mouse           TEKRRKRSTREEVFNILQAAYVSKPGANLAKQIGASPSDDILFGVFAQSKPDSAEPVNRS 359
                ****:****::****************:**:***** .******************::**

Human           AMCAFPIKYVNDFFNKIVNKNNVRCLQHFYGPNHEHCFNRTLLRNSSGCEARRDEYRTEF 420
Mouse           AVCAFPIKYVNDFFNKIVNKNNVRCLQHFYGPNHEHCFNRTLLRNSSGCEARSDEYRTEF 419
                *:********************************************** *******

Human           TTALQRVDLFMGQFSEVLLTSISTFIKGDLTIANLGTSEGRFMQVVVSRSGPSTPHVNFL 480
Mouse           TTALQRVDLFMGRLNQVLLTSISTFIKGDLTIANLGTSEGRFMQVVLSRTAHLTPHVNFL 479
                ************:::*******************************:**:.  *******

Human           LDSHPVSPEVIVEHTLNQNGYTLVITGKKITKIPLNGLGCRHFQSCSQCLSAPPFVQCGW 540
Mouse           LDSHPVSPEVIVEHPSNQNGYTLVVTGKKITKIPLNGLGCGHFQSCSQCLSAPYFIQCGW 539
                **************. ********:*************** ************ *:****

Human           CHDKCVRSEECLSGTWTQQICLPAIYKVFPNSAPLEGGTRLTICGWDFGFRRNNKFDLKK 600
Mouse           CHNQCVRFDECPSGTWTQEICLPAVYKVFPTSAPLEGGTVLTICGWDFGFRKNNKFDLRK 599
                **::*** :** ******:*****:*****.******** ***********:******:*

Human           TRVLLGNESCTLTLSESTMNTLKCTVGPAMNKHFNMSIIISNGHGTTQYSTFSYVDPVIT 660
Mouse           TKVLLGNESCTLTLSESTTNTLKCTVGPAMSEHFNVSVIISNSRETTQYSAFSYVDPVIT 659
                *:**************** **********.:***:*:****.: *****:*********

Human           SISPKYGPMAGGTLLTLTGNYLNSGNSRHISIGGKTCTLKSVSNSILECYTPAQTISTEF 720
Mouse           SISPRYGPQAGGTLLTLTGKYLNSGNSRHISIGGKTCTLKSVSDSILECYTPAQTTSDEF 719
                ****:*** **********:**********************:********** * **

Human           AVKLKIDLANRETSIFSYREDPIVYEIHPTKSFISGGSTITGVGKNLNSVSVPRMVINVH 780
Mouse           PVKLKIDLANRETSSFSYREDPVVYEIHPTKSFISGGSTITGIGKTLNSVSLPKLVIDVH 779
                .************* *******:******************:**.*****:*::**:**

Human           EAGRNFTVACQHRSNSEIICCTTPSLQQLNLQLPLKTKAFFMLDGILSKYFDLIYVHNPV 840
Mouse           EVGVNYTVACQHRSNSEIICCTTPSLKQLGLQLPLKTKAFFLLDGILSKHFDLTYVHNPV 839
                *.* *:*********************:**.***********:*******:*** ******

Human           FKPFEKPVMISMGNENVLEIKGNDIDPEAVKGEVLKVGNKSCENIHLHSEAVLCTVPNDL 900
Mouse           FEPFEKPVMISMGNENVVEIKGNNIDPEAVKGEVLKVGNQSCESLHWHSGAVLCTVPSDL 899
                *:***************:*****:***************:***.:* ** *******.**

Human           LKLNSELNIEWKQAISSTVLGKVIVQPDQNFTGLIAGVVSISTALLLLLGFFLWLKKRKQ 960
Mouse           LKLNSELNIEWKQAVSSTVLGKVIVQPDQNFAGLIIGAVSISVVVLLLSGLFLWMRKRK- 958
                **************:***************:*** *.****..:*** *:***::***

Human           IKDLGSELVRYDARVHTPHLDRLVSARSVSPTTEMVSNESVDYRATFPEDQFPNSSQNGS 1020
Mouse           HKDLGSELVRYDARVHTPHLDRLVSARSVSPTTEMVSNESVDYRATFPEDQFPNSSQNGA 1018
                 ******************************************************:

Human           CRQVQYPLTDMSPILTSGDSDISSPLLQNTVHIDLSALNPELVQAVQHVVIGPSSLIVHF 1080
Mouse           CRQVQYPLTDLSPILTSGDSDISSPLLQNTVHIDLSALNPELVQAVQHVVIGPSSLIVHF 1078
                **********:************************************************
```

```
Human           NEVIGRGHFGCVYHGTLLDNDGKKIHCAVKSLNRITDIGEVSQFLTEGIIMKDFSHPNVL 1140
Mouse           NEVIGRGHFGCVYHGTLLDNDGKKIHCAVKSLNRITDIEEVSQFLTEGIIMKDFSHPNVL 1138
                ********************************** ********************

Human           SLLGICLRSEGSPLVVLPYMKHGDLRNFIRNETHNPTVKDLIGFGLQVAKGMKYLASKKF 1200
Mouse           SLLGICLRSEGSPLVVLPYMKHGDLRNFIRNETHNPTVKDLIGFGLQVAKGMKYLASKKF 1198
                ************************************************************

Human           VHRDLAARNCMLDEKFTVKVADFGLARDMYDKEYYSVHNKTGAKLPVKWMALESLQTQKF 1260
Mouse           VHRDLAARNCMLDEKFTVKVADFGLARDMYDKEYYSVHNKTGAKLPVKWMALESLQTQKF 1258
                ************************************************************

Human           TTKSDVWSFGVLLWELMTRGAPPYPDVNTFDITVYLLQGRRLLQPEYCPDPLYEVMLKCW 1320
Mouse           TTKSDVWSFGVLLWELMTRGAPPYPDVNTFDITIYLLQGRRLLQPEYCPDALYEVMLKCW 1318
                *********************************:**************.*********

Human           HPKAEMRPSFSELVSRISAIFSTFIGEHYVHVNATYVNVKCVAPYPSLLSSEDNADDEVD 1380
Mouse           HPKAEMRPSFSELVSRISSIFSTFIGEHYVHVNATYVNVKCVAPYPSLLPSQDNIDGEGN 1378
                *****************:*****************************.*:** *.* :

Human           TRPASFWETS 1390
Mouse           T--------- 1379
                *
```

Appendix 3

Mab (diluted 1:5) effects on ERK phosphorylation in HaCaT cells.

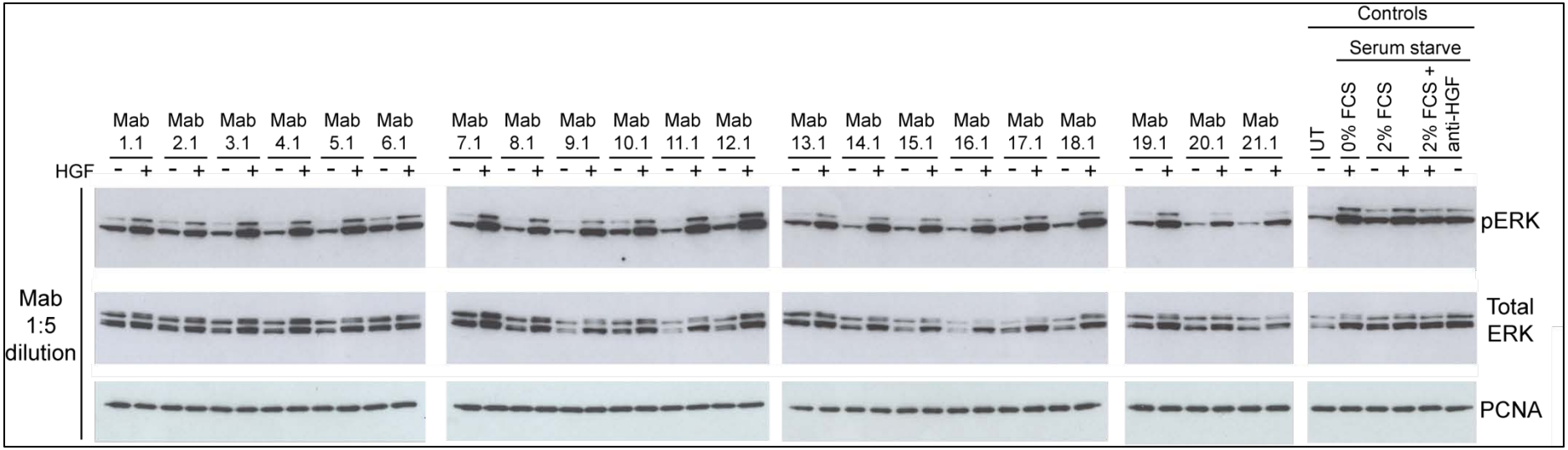

HaCaT cells were treated with anti-α-chain c-Met antibodies. HaCaT cells were grown to 90% confluency before serum starvation. Monoclonal antibody cell supernatants were diluted 1:5 in serum-free media and incubated with HaCaT cells for an hour. 10 ng/ml of HGF was added to the cells for 30 mins before harvesting in hot sample buffer. 10 µg of total cell lysate was analysed in each sample by SDS-PAGE. Western blotting was performed using anti-phospho-ERK, anti-ERK and PC10 antibodies to detect phosphorylated ERK, total ERK and PCNA levels respectively. Activation of c-Met was determined by phosphorylation of ERK. PCNA levels were used as loading control. All controls were serum-starved, except for untreated (UT) samples. Controls with media containing 0% and 5% FCS were performed to examine the effect of FCS on ERK phosphorylation. Antibody against HGF (5 µg/ml) was used as a control to block HGF from binding to c-Met. pERK: Phosphorylated ERK. Anti-HGF: Antibody against HGF.